

Interagency Ecological Program

Synthesis of data and studies relating to Delta Smelt
biology in the San Francisco Estuary, emphasizing water
year 2017

By Flow Alteration - Management, Analysis, and Synthesis Team (FLOAT-MAST)

IEP Technical Report 95



Interagency
Ecological Program
COOPERATIVE ECOLOGICAL
INVESTIGATIONS SINCE 1970



— BUREAU OF —
RECLAMATION



Suggested citation:

FLOAT-MAST (Flow Alteration - Management, Analysis, and Synthesis Team). 2020. Synthesis of data and studies relating to Delta Smelt biology in the San Francisco Estuary, emphasizing water year 2017. IEP Technical Report 95. Interagency Ecological Program, Sacramento, CA

Any use of trade, product, or firm names is for descriptive purposes only and does not imply endorsement by the U.S. Government or the State of California.

Although this report is in the public domain, permission must be secured from the individual copyright owners to reproduce any copyrighted material contained within this report.

Contents

Contents iii

Figures..... iv

Appendices xiii

Membership..... xv

Conversion Factors..... xvi

Executive Summary..... 18

Introduction..... 22

Purpose and Scope 29

Background 30

 Study area..... 30

 Delta Smelt 33

 Conceptual models 40

 Predictions 51

Methodology 55

Evaluations of Predictions 57

 Dynamic abiotic habitat components..... 58

 Dynamic biotic habitat components 82

 Phytoplankton and Chlorophyll-*a*..... 82

 Harmful algal blooms..... 106

 Zooplankton 118

 Clam Biomass, Grazing Rate and Recruitment 128

 Aquatic Vegetation 136

 Fish Assemblage..... 144

Delta Smelt responses.....	149
Growth Rate.....	149
Conclusion	158
Life History Diversity	161
Conclusion	175
Health Metrics.....	176
Conclusion	184
Feeding Success	186
Conclusion	199
Delta Smelt Range and Distribution	199
Survival and Population Growth.....	207
Discussion	229
Next Steps.....	238
References Cited.....	240

Figures

Figure 1. Map of the San Francisco Estuary (from IEP-MAST 2015). Inset shows a selection of X2 locations.	23
Figure 2. Delta outflow from 1979 through 2017.....	26
Figure 3. Abundance indices for the four major IEP fish monitoring programs.	29
Figure 4. Map of the upper San Francisco Estuary (from IEP-MAST 2015).	32
Figure 5. Abundance indices from the FMWT for species associated with the pelagic organism decline.....	36
Figure 6. Linear regression between bottom water temperature (Y) and surface water temperature (X).....	39
Figure 7. Illustration showing estuarine habitat conceptual model (modified from Peterson 2003).....	41
Figure 8. Spatially explicit conceptual model for the western reach of the modern Delta Smelt range in the fall....	42
Figure 9. Delta Smelt general life cycle conceptual model (IEP-MAST 2015).	46

Figure 10.	Conceptual model of drivers affecting the transition from Delta Smelt adults to larvae.....	47
Figure 11.	Conceptual model of drivers affecting the transition from Delta Smelt larvae to juveniles.	48
Figure 12.	Conceptual model of drivers affecting the transition from Delta Smelt juveniles to subadults.....	49
Figure 13.	Conceptual model of drivers affecting the transition from Delta Smelt subadults to adults.....	50
Figure 14.	Delta outflow and X2 computed using DAYFLOW.....	58
Figure 15.	Salinity in A) July and August collected by Summer Townet Survey and B) in September-December collected by FMWT.....	60
Figure 16.	Salinity by water type for A) July and August collected by Summer Townet Survey and B) in September-December collected by FMWT.....	61
Figure 17.	Water temperature at sites with salinity <1, 1-6, and ≤ 6 for A) July and B) August.....	63
Figure 18.	Water temperature at sites with salinity <1, 1-6, and ≤ 6 for A) September and B) October.	63
Figure 19.	Secchi depth (cm) in A) July and August collected by California Department of Fish and Wildlife Summer Townet Survey and B) in September-December.....	65
Figure 20.	Secchi depth (cm) by water type for A) July and August B) in September-December.....	67
Figure 21.	Predicted 2-week-average depth-averaged salinity for 2017.....	68
Figure 22.	Predicted 2-week-average depth-averaged temperature for 2017.....	70
Figure 23.	Emmaton and Jersey Point continuous monitoring locations.....	71
Figure 24.	Observed hourly water temperature at Emmaton (top) and Jersey Point (bottom) from May through December 2017 (black lines).....	72
Figure 25.	Observed hourly water temperature at Emmaton from April through December for 2006 (top), 2011, (middle), and 2017 (bottom).	73
Figure 26.	Cumulative time in days that the observed water temperature exceeded 20, 22, 24, and 26°C.....	74
Figure 27.	Cumulative time in days that the predicted water temperature exceeded 22°C.....	75
Figure 28.	Daily averaged wind speed and direction over Suisun Bay.....	77

Figure 29.	Predicted 2-week-average surface turbidity for 2017 2-week EDSM sampling periods.....	79
Figure 30.	Predicted Delta Smelt station index (SI_H) for 2-week EDSM sampling periods.....	80
Figure 31.	Predicted depth-averaged temperature averaged over 2-week EDSM sampling periods.....	82
Figure 32.	Region map of Environmental Monitoring Program (EMP) discrete phytoplankton, chlorophyll- <i>a</i> , and continuous water quality monitoring stations.	86
Figure 33.	Mean chlorophyll- <i>a</i> concentration ($\mu\text{g L}^{-1}$) and anomalies by region and season for post-POD years 2003-2017..	87
Figure 34.	Environmental Monitoring Program chlorophyll- <i>a</i> concentration for 2017 by region and month.	88
Figure 35.	Environmental Monitoring Program phytoplankton taxa groups (total organisms mL^{-1}) by region and month.	89
Figure 36.	Environmental Monitoring Program phytoplankton taxa total biovolume by group and % of taxa making up $\geq 3\%$ of total biovolume by region and month.	90
Figure 37.	Mean concentration of A) ammonium (NH_4) and B) nitrate + nitrite ($\text{NO}_3 + \text{NO}_2$) for 2017 by region and month.	92
Figure 38.	Lower Sacramento River region monthly mean concentration of ammonium (NH_4) and nitrate + nitrite ($\text{NO}_3 + \text{NO}_2$) for 2011 - 2017.	93
Figure 39.	Suisun Bay region monthly mean ammonium (NH_4) and nitrate + nitrite ($\text{NO}_3 + \text{NO}_2$) concentrations for 2011 - 2017.	94
Figure 40.	California Department of Water Resources North Delta Special Study region monthly mean chlorophyll- <i>a</i> ($\mu\text{g L}^{-1}$) for A) 2016 and B) 2017.....	96
Figure 41.	California Department of Water Resources North Delta Special Study 2016 and 2017 continuous total chlorophyll fluorescence $\mu\text{g L}^{-1}$ and daily average flow at site LIS	97
Figure 42.	California Department of Water Resources North Delta Special Study region phytoplankton taxa total mean biovolume by taxa group.....	99

Figure 43.	Region map for California Department of Water Resources and San Francisco State University and Low Salinity Zone Special Study water quality, nutrients, and chlorophyll- <i>a</i> sampling transects.....	101
Figure 44.	California Department of Water Resources and San Francisco State University Fall Low Salinity Zone Special Study chlorophyll- <i>a</i> concentration in A) 2011 and B) 2017.	102
Figure 45.	California Department of Water Resources and San Francisco State University Low Salinity Zone Special Study 2011 and 2017 A) water temperature (°C) and B) Secchi depth (m).	103
Figure 46.	California Department of Water Resources and San Francisco State University Low Salinity Zone Special Study 2011 and 2017 A) NO ₃ + NO ₂ (µM) and B) NH ₄ (µM).	104
Figure 47.	Map of Environmental Monitoring Program stations utilized in this analysis.....	108
Figure 48.	Mean surface <i>Microcystis</i> bloom visual index values collected during the Summer Townet and Fall Midwater Trawl surveys.....	109
Figure 49.	Mean biovolume and median absolute deviation of surface <i>Microcystis</i> colonies greater than 0.75 µm in diameter sampled with a surface net tow between June and November 2017 by month (a) and by station (b).	111
Figure 50.	Mean abundance of total <i>Microcystis</i> cells, toxic <i>Microcystis</i> cells, and total cyanobacteria	112
Figure 51.	Comparison of the abundance of total <i>Microcystis</i> cells, toxic <i>Microcystis</i> cells, and total cyanobacteria cells.	114
Figure 52.	Herbivorous calanoid copepod anomalies 2003 through 2017.	121
Figure 53.	Mysid anomalies 2003 through 2017.	122
Figure 54.	Herbivorous calanoid copepod (<i>Eurytemora</i> , <i>Pseudodiaptomus</i> , and <i>Sinocalanus</i> adults and juveniles) mean catch per unit effort (CPUE±SE) from 2003 through 2017	125
Figure 55.	Mysid mean catch per unit effort (CPUE±SE) from 2003 through 2017.	126
Figure 56.	Ash-free-dry mass of <i>Potamocorbula</i> and <i>Corbicula</i> in the upper San Francisco Estuary.....	132
Figure 57.	Grazing rate of <i>Potamocorbula</i> and <i>Corbicula</i> in the upper San Francisco Estuary	135

Figure 58.	Delineation of Delta regions for comparison of aquatic vegetation coverage, 2014 – 2017.....	138
Figure 59.	(A) Estimated coverage of Water Hyacinth and Water Primrose, from Center for Spatial Technologies and Remote Sensing (CSTARS) classification of hyperspectral imagery collected in the fall of each year. (B) Total acres treated (across entire Delta) for floating aquatic vegetation (FAV) by California Department of Boating and Waterways, 2014 – 2017.....	140
Figure 60.	(A) Estimated coverage of submerged aquatic vegetation, from CSTARS classification of hyperspectral imagery collected in the fall of each year. (B) Total acres of SAV treated (across entire Delta) by California Department of Boating and Waterways, 2014 – 2017.....	141
Figure 61.	Average monthly outflow, April 2014– October 2017. (B) Boxplots of dissolved ammonium, nitrate + nitrite, conductivity, turbidity, and water temperature for each month, April 2014 – October 2017.	143
Figure 62.	Annual mean biomass per tow for the 20-mm Survey in the summer (survey 7 to 9) with marine fish species removed.	146
Figure 63.	Annual mean biomass per tow for the Summer Townet with marine fish species excluded.	146
Figure 64.	Annual average biomass per tow for the Fall Midwater Trawl with marine fish species excluded.	147
Figure 65.	Annual mean biomass per volume for the Delta littoral fish assemblage.....	148
Figure 66.	Mean catch per cubic meter (m ³) at the 22 index beach seine stations.....	148
Figure 67.	Somatic growth rates of Delta Smelt collected from surveys conducted from 2011 to 2017.....	153
Figure 68.	Boxplots of somatic growth rates of Delta Smelt by month collected from surveys conducted from 2011 to 2017.....	154
Figure 69.	Intrinsic effect of age (days post-hatch) on marginal otolith growth (zero-centered 14-day mean otolith growth rate in microns/d) rate from 2011-2017 (modified from Hobbs et al. 2019c).	155
Figure 70.	Age corrected marginal otolith growth rate (zero-centered 14-day mean otolith growth rate in microns/d corrected for age post-hatch).....	156

Figure 71.	Three-dimensional plots for associations of water temperature (temp), salinity (sal) and Secchi depth (secchi) at capture	157
Figure 72.	Age and water quality (WQ) corrected marginal otolith growth rate (14-day age and water-corrected zero-centered marginal otolith growth rate) by year, EDSM region and EDSM strata for 2011-2017 (modified from Hobbs et al. 2019c).	158
Figure 73.	Heatmap of daily mean water temperature from five continuous water quality sondes, 2011-2017 ..	159
Figure 74.	Conceptual model describing the relationship between water temperature, timing and duration of the maturation window and hatching window for Delta Smelt.	163
Figure 75.	Julian hatch-date distributions (black vertical bars) for Delta Smelt from 2011-2017.....	166
Figure 76.	Cumulative distribution of -Date (dotted line) and dispersal date (solid line) for Delta Smelt from 2011 to 2017.....	168
Figure 77.	Boxplots of Julian date (A), age (B) and length (C) when Delta Smelt dispersed from freshwater to the LSZ from 2011-2017 (modified from Hobbs et al. 2019b).....	170
Figure 78.	Trends in hatch-date duration and phenology.....	172
Figure 79.	Natal origins (strontium isotope ratios) for Delta Smelt from 2011-2017.....	173
Figure 80.	Heatmap of Julian hatch date and natal origins ($^{87}\text{Sr}/^{86}\text{Sr}$).....	174
Figure 81.	The proportion of different life history phenotypes contributing to adult abundance in the California Department of Fish and Wildlife's Spring Kodiak Trawl Survey	175
Figure 82.	Partial residuals (lesion scores) from the selected liver lesion model by A) region B) year class.	180
Figure 83.	The partial residuals for the top-ranked gill lesion score model by A) fork length, B) salinity, and C) year class.	181
Figure 84.	The partial residuals (liver glycogen scores) for the top-ranked liver glycogen score model by fork length (A), region (B), and X2 (C)..	183

Figure 85.	Mean (\pm SE) Delta Smelt gut fullness (% body weight, BW) by A) year, B) salinity, C) season, and D) hour of collection.	197
Figure 86.	Condition factor plotted against gut fullness (% body weight, BW) for Delta Smelt (N = 1925).....	198
Figure 87.	Delta Smelt distribution in river kilometers in the upper Estuary from Summer Townet Survey (STN) catch at index stations in July and August during 2003-2017.....	200
Figure 88.	Delta Smelt distribution in river kilometers in the upper Estuary from Fall Midwater Trawl Survey (FMWT) catch at index stations in September and October during 2003-2017.	201
Figure 89.	Scatterplot of median Delta Smelt distribution based on river kilometers in the upper Estuary from Summer Townet Survey (STN) CPUE at index stations and the average location of X2 during July and August.	202
Figure 90.	Scatterplot of median Delta Smelt distribution based on river kilometers in the upper Estuary from Fall Midwater Trawl Survey (FMWT) catch and the average location of X2 during September-October.....	203
Figure 91.	20-mm Survey Delta Smelt catch per 10,000 m ³ (CPUE) since 2002 (post-POD).	204
Figure 92.	20-mm Survey Delta Smelt catch per 10,000 m ³ (CPUE) in 2006, 2011, and 2017 grouped by region across the upper San Francisco Estuary.....	205
Figure 93.	Mean CPUE of Delta Smelt by year class collected by CDFW 20-mm, Summer Townet (STN), Fall Midwater Trawl (FMWT) and Spring Kodiak Trawl during routine surveys at stations in the North Delta.	207
Figure 94.	Spring to summer survival index (STN/20-mm) for Delta Smelt based on the ratio of the Summer Townet (STN) to 20-mm Survey (20-mm) relative abundance indices.....	209
Figure 95.	Anomalies of spring to summer survival indices (STN/20-mm) for Delta Smelt based on the ratio of the Summer Townet (STN) to 20-mm Survey (20-mm) relative abundance indices.....	210
Figure 96.	Summer to fall survival index (FMWT/STN) for Delta Smelt based on the ratio of the Fall Midwater Trawl (FMWT) to Summer Townet (STN) relative abundance indices.....	211

Figure 97.	Anomalies of summer to fall survival index (FMWT/STN) for Delta Smelt based on the ratio of the Fall Midwater Trawl (FMWT) to Summer Townet (STN) relative abundance indices.....	212
Figure 98.	Least squares linear regression ($y = 0.3674x + 13.161$; $R^2 = 0.9115$) of the FMWT and SKT relative abundance indices for Delta Smelt year classes 2003-2017.....	212
Figure 99.	Fall to winter survival index (SKT/FMWT) for Delta Smelt based on the ratio of the Spring Kodiak Trawl (SKT) to Fall Midwater Trawl (FMWT) relative abundance indices.....	213
Figure 100.	Anomalies of fall to winter survival index (SKT/FMWT) for Delta Smelt based on the ratio of the Spring Kodiak Trawl (SKT) to Fall Midwater Trawl (FMWT) relative abundance indices.....	214
Figure 101.	Summer to fall survival index (FMWT/STN) for Delta Smelt versus the average position of X2 during September-October during the period 1969-2017.....	215
Figure 102.	Summer to fall survival index for Delta Smelt (Y) versus the average position of X2 (X) during September-October for the period 2002-2014.....	216
Figure 103.	Relative abundance index for Delta Smelt during fall (Y) versus the average position of X2 during September-October for the period 1967-2017 (X).....	217
Figure 104.	Relative abundance index for Delta Smelt during fall (Y) versus the average position of X2 during September-October for the period 2002-2017 (X).....	218
Figure 105.	Catch per unit effort of juvenile, sub-adult, and adult Delta Smelt across 10 strata sampled by the Enhanced Delta Smelt Monitoring Kodiak trawl between December 2016 and December 2017.....	220
Figure 106.	Estimated abundance (mean \pm SE) of juvenile-subadult Delta Smelt between July and December 2017 across 10 Enhanced Delta Smelt Monitoring strata.....	221
Figure 107.	Catch per unit effort of larval-juvenile Delta Smelt across 10 strata sampled by the 20 mm Enhanced Delta Smelt Monitoring survey between April and July 2017.....	222
Figure 108.	Delta Smelt conceptual life history model from Bennett (2005).....	223

Figure 109. Conceptual model of variability in production of a new year class of Delta Smelt based on 1-3 clutches per female..... 224

Figure 110. Relationship between potential population fecundity from adult Delta Smelt population estimates and CDFW 20-mm Survey Delta Smelt annual indices of young for the period 2002-2017. 225

Figure 111. Non-linear regression (power function) relationship between potential population fecundity (number of eggs) and adult abundance estimates for Delta Smelt year classes 2002-2017 (blue line), 2015-2016 (red line), and 2017 (dashed line). 227

Figure 112. Spring recruitment index (20-mm/SKT) for larval and juvenile Delta Smelt based on the ratio of the 20-mm Survey (20-mm) and Spring Kodiak Trawl (SKT) relative abundance indices..... 228

Figure 113. Fall recruitment index (FMWT/FWMT_{previous year}) for subadult Delta Smelt based on the ratio of the Fall Midwater Trawl (FMWT) relative abundance indices. 229

Figure 114. Variation in water temperature (hourly data) at Emmaton on the Sacramento River for a two-week period in July 2017, when the two-week average exceeded 22°C. 233

Tables

Table 1. Water year designations for water years 1979-2017. 24

Table 2. Assessments of predicted qualitative and quantitative outcomes for September to October of the fall Reasonable and Prudent Alternative action based on 3 levels of the action 52

Table 3. Predictions regarding the effects of high flows on Delta Smelt and Delta Smelt habitat. 54

Table 4. Selected data sources used in this report. 55

Table 5. Spearman correlation coefficients computed between environmental variables and surface *Microcystis* biovolume and subsurface *Microcystis* abundance..... 115

Table 6. Spearman correlation coefficients computed for surface *Microcystis* biovolume and subsurface *Microcystis* abundance. 116

Table 7.	Spearman correlation coefficients computed for 10 stations sampled monthly at 1m depth between July and November of 2017.....	116
Table 8.	Summary of statistically significant comparisons of wet years (2006, 2011, 2017) against other years by region and season for herbivorous calanoid copepods and mysids.	124
Table 9.	Summary of model coefficients and fit for all models $<2 \Delta AICc$ away from the best ranked model. * $p < 0.05$; ** $p < 0.01$, *** $p < 0.001$	149
Table 10.	Summary of Delta Smelt hatching from 2011-2017. Hatch range was calculated both as the interquartile range (IQR) and as the percentile range (95%-5%) (modified from Hobbs et al. 2019b).....	166
Table 11.	Summary of thermal phenology from 2011-2017 (modified from Hobbs et al. 2019b).....	167
Table 12.	Summary of dispersal phenology from 2011-2017 (modified from Hobbs et al. 2019b).....	171
Table 13.	Diet by percent number of major prey categories in stomachs of Delta Smelt collected in salinity <0.5 for months June-August (J-A), September-November (S-N), and December-May (D-M) among years 2011-2017. 190	
Table 14.	Diet by percent number of major prey categories in stomachs of Delta Smelt collected in salinity 0.5-6. 191	
Table 15.	Diet by percent number of major prey categories in stomachs of Delta Smelt collected in salinity >6	192
Table 16.	Diet by percent weight of major prey categories in stomachs of Delta Smelt collected in salinity <0.5 ..	193
Table 17.	Diet by percent weight of major prey categories in stomachs of Delta Smelt collected in salinity 0.5-6.	194
Table 18.	Diet by percent weight of major prey categories in stomachs of Delta Smelt collected in salinity >6	195
Table 19.	Outcomes for predictions regarding the effects of high flows on Delta Smelt and Delta Smelt habitat..	230

Appendices

Appendix 1: Enhanced Delta Smelt Monitoring

Denise Barnard, U.S. Fish and Wildlife Service

Appendix 2: Modeling of Physical Habitat

Michael MacWilliams and Aaron Bever, Anchor QEA, LLC

Appendix 3: Environmental Variables

Steven Slater, California Department of Fish and Wildlife

Appendix 4: Phytoplankton

Jared Frantzich and Peggy Lehman, California Department of Water Resources

Appendix 5: Cyanobacteria Harmful Algal Blooms

Peggy Lehman, California Department of Water Resources

Appendix 6: Zooplankton

April Hennessy, California Department of Fish and Wildlife

Appendix 7: Clams

Janet Thompson, U.S. Geological Survey

Appendix 8: Aquatic Vegetation

Louise Conrad, Delta Science Program, and Shruti Khanna, California Department of Fish and Wildlife

Appendix 9: Fish Assemblages

Brian Mahardja, U.S. Fish and Wildlife Service

Appendix 10: Mississippi Silversides

Brian Mahardja, U.S. Fish and Wildlife Service

Appendix 11: Survival and Population Growth

Steven Slater, California Department of Fish and Wildlife and Gonzalo Castillo, U.S. Fish and Wildlife Service

Membership

Shawn Acuña, Metropolitan Water District

Randy Baxter, California Department of Fish and Wildlife

Aaron Bever, Anchor QEA

Larry R. Brown, U.S. Geological Survey

Christina Burdi, California Department of Fish and Wildlife

Gonzalo Castillo, U.S. Fish and Wildlife Service

Louise Conrad, California Department of Water Resources (currently Delta Stewardship Council)

Steven Culberson, Delta Stewardship Council

Lauren Damon, California Department of Fish and Wildlife

Jared Frantzich, California Department of Water Resources

Lenny Grimaldo, ICF International

Bruce Hammock, University of California Davis

April Hennessy, California Department of Fish and Wildlife

James Hobbs, University of California Davis

Shruti Khanna, California Department of Fish and Wildlife

Peggy Lehman, California Department of Water Resources

Michael MacWilliams, Anchor QEA

Brian Mahardja, U.S. Fish and Wildlife Service

Andrew Schultz, U.S. Bureau of Reclamation

Steven B. Slater, California Department of Fish and Wildlife

Ted Sommer, California Department of Water Resources

Swee Teh, University of California Davis

Janet Thompson, U.S. Geological Survey

Conversion Factors

SI to Inch/Pound

Multiply	By	To obtain
Length		
centimeter (cm)	0.3937	inch (in.)
millimeter (mm)	0.03937	inch (in.)
meter (m)	3.281	foot (ft)
kilometer (km)	0.6214	mile (mi)
Area		
square meter (m ²)	0.0002471	acre
hectare (ha)	2.471	acre
square kilometer (km ²)	247.1	acre
square centimeter (cm ²)	0.001076	square foot (ft ²)
hectare (ha)	0.003861	square mile (mi ²)
square kilometer (km ²)	0.3861	square mile (mi ²)
Volume		
liter (L)	1.057	quart (qt)
liter (L)	0.2642	gallon (gal)
cubic meter (m ³)	35.31	cubic foot (ft ³)
cubic kilometer (km ³)	0.2399	cubic mile (mi ³)
cubic meter (m ³)	0.0008107	acre-foot (acre-ft)
Flow rate		
cubic meter per second (m ³ /s)	70.07	acre-foot per day (acre-ft/d)
meter per second (m/s)	3.281	foot per second (ft/s)
meter per minute (m/min)	3.281	foot per minute (ft/min)
cubic meter per second (m ³ /s)	35.31	cubic foot per second (ft ³ /s)
cubic meter per day (m ³ /d)	35.31	cubic foot per day (ft ³ /d)
Mass		
gram (g)	0.03527	ounce, avoirdupois (oz)
kilogram (kg)	2.205	pound avoirdupois (lb)
megagram (Mg)	1.102	ton, short (2,000 lb)
megagram (Mg)	0.9842	ton, long (2,240 lb)

metric ton per day	1.102	ton per day (ton/d)
megagram per day (Mg/d)	1.102	ton per day (ton/d)
megagram per year (Mg/yr)	1.102	ton per year (ton/yr)
metric ton per year	1.102	ton per year (ton/yr)

- Temperature in degrees Celsius ($^{\circ}\text{C}$) may be converted to degrees Fahrenheit ($^{\circ}\text{F}$) as follows:
- $^{\circ}\text{F}=(1.8\times^{\circ}\text{C})+32$
- Temperature in degrees Fahrenheit ($^{\circ}\text{F}$) may be converted to degrees Celsius ($^{\circ}\text{C}$) as follows:
- $^{\circ}\text{C}=(^{\circ}\text{F}-32)/1.8$
- Specific conductance is given in microsiemens per centimeter at 25 degrees Celsius ($\mu\text{S}/\text{cm}$ at 25°C).
- Salinity has been expressed without units in this report, which is the current convention. However, readers should be aware that salinity is measured with various instruments and methods among the monitoring programs and studies referenced in this report and has been reported as ppt, psu or without units. Refer to the methods of the specific monitoring program or study for details. Any differences are likely small with no effect on the conclusions of this report.
- Concentrations of chemical constituents in water are given either in milligrams per liter (mg/L), micrograms per liter ($\mu\text{g}/\text{L}$) or micromolar ($\mu\text{M}/\text{L}$).

Synthesis of data and studies relating to Delta Smelt biology in the San Francisco Estuary, emphasizing water year 2017

By: Flow Alteration - Management, Analysis, and Synthesis Team (FLOAT-MAST)

Executive Summary

In the San Francisco Estuary (SFE), the effects of freshwater flow on the aquatic ecosystem have been studied extensively over the years and remains a contentious management issue. It is especially contentious with regards to the Delta Smelt (*Hypomesus transpacificus*), a species endemic to the SFE that has been listed as threatened under the Federal Endangered Species Act and endangered by the State of California. Early studies of Delta Smelt distribution within the SFE suggested that Delta Smelt habitat is determined largely by freshwater flow; however, the exact mechanisms and processes producing such benefits remained unclear. In the summer of 2017, the Flow Alteration Management, Analysis, and Synthesis Team (FLOAT-MAST) was established to analyze, synthesize, and summarize the data collected from the various flow-related monitoring and special studies occurring in 2017 (see Table Intro 4). This report will focus on the 2017 summer-fall status of Delta Smelt and its habitat following a record wet year.

There has been a long-term decline in the abundance of Delta Smelt associated with a decline in other pelagic fishes. Investigators concluded that the decline has likely been caused by the interactive effects of several causes, including changes in both physical and biotic habitats, many of which are tied to amount and timing of freshwater flow. For this report, we formulated a number of

basic predictions about the likely effects of high flows in 2017 on Delta Smelt and their habitat (Table 3). We use a qualitative weight of evidence approach to evaluate whether these predictions were supported by available data. Data sources included a variety of long-term monitoring surveys conducted by Interagency Ecological Program (IEP) agencies, as well as model outputs.

The spring of 2017 was wet, with high outflows that resulted in the Low Salinity Zone (LSZ) being located at the western border of Suisun Bay. The position of X2 (the horizontal distance from the Golden Gate up the axis of the estuary to where tidally averaged near-bottom salinity is 2) remained between 74 and 81 km through December. The basic prediction is that physical habitat conditions are better for Delta Smelt when the LSZ (indexed by X2) is located in Suisun Bay. Dynamic abiotic habitat components responded to the high flows partially as predicted. Salinity reacted as expected with decreased salinity in wet years; however, water temperature and Secchi depth (i.e., turbidity) did not exhibit a clear pattern with regard to water year type.

Dynamic biotic habitat components did not always respond as predicted to high flows. The Suisun Bay region had elevated phytoplankton biomass in 2017 compared to other post-Pelagic Organism Decline (POD) years, but there was no consistent pattern between high or low outflow water years. The increased biomass was explained by a higher biovolume of cyanobacteria, green algae, and cryptophytes rather than diatoms. There was a relatively small *Microcystis* bloom in the wet year of 2017; however, the responses of *Microcystis* to outflow and X2 were not consistent from year to year. Similarly, our prediction of high abundances of herbivorous calanoid copepods in the LSZ in 2017 was supported; however, not all wet years had similarly high abundances of zooplankton. Bivalves responded mostly as predicted, with lower *Potamocorbula* biomass and grazing rates in the LSZ during wet years, though there were less pronounced differences in *Corbicula* biomass and grazing rates. Water Hyacinth was generally reduced, while Water Primrose increased and submerged aquatic vegetation (SAV) increased slightly or stayed the same; however, the importance of the high flows in the observed differences relative to other factors was not clear. There were apparent effects of flow on the pelagic fish assemblage, where the wet year of 2006 was similar to 2017 but both those years were different from 2011; however, there have not been enough wet years recently to make firm conclusions.

Delta Smelt population, health, and life history metrics rarely responded as predicted. Water temperature appears to have a stronger effect on Delta Smelt growth rate and some metrics of life history diversity than outflow or X2 position. Other life history diversity attributes varied but did not appear to be driven by outflow or temperature. Health status was difficult to interpret. Low prevalence of lesions and improved nutritional condition during the drought was contradicted by declining overall population levels. Because of the sparse catches of Delta Smelt in the post-POD years, we consider the data insufficient to reach firm conclusions about the predictions concerning range and distribution of Delta Smelt, especially in the fall. The prediction of high survival was not supported. The 2017 Delta Smelt year class began with poor recruitment in spring of 2017 and below average survival for spring to summer and summer to fall. Thus, low production and low survival led to low abundance of all life stages. During the fall to winter period survival improved, yet the resulting adults were low in number. Foraging success of the fish captured, as measured by stomach fullness, was high for juveniles and adults in 2017 relative to recent years associated with the higher densities of common zooplankton prey that occurred in 2017.

The long periods of higher than normal water temperatures in July and August had a major negative effect on Delta Smelt in 2017, and temperature is likely a primary factor in the lack of response of the Delta Smelt population to the high flows. The data suggest that high flows set up favorable salinity conditions for survival of Delta Smelt but the benefits of high flows may be contingent on other physical factors, particularly water temperature. Dynamic biotic habitat components were somewhat better in 2017; however, the lack of response of the Delta Smelt population suggests that any benefits of changes in the habitat were minimal. Increased abundance of zooplankton combined with the low biomass and grazing rates for clams and low incidence of harmful algal blooms (HABs) in 2017 would suggest more food available for planktivorous fishes. Biomass of other planktivorous fishes did increase in 2017, but any response of Delta Smelt was undetectable, and survival was poor. This suggests some mismatch of timing or geographic area, such that increased production of food was unavailable to Delta Smelt for some life stages.

The conclusion of this report is that high fall outflow alone is not sufficient to provide favorable conditions for Delta Smelt. This conclusion poses difficult challenges for managers and policy makers. We currently have practical management tools for managing outflow, but tools have not been

developed for managing turbidity or water temperature. It may be possible to decrease temperature slightly by greatly increasing outflow. However, adjusting flows for this purpose must be considered in the context of overall water management for multiple threatened species and uses.

Suggestions for future directions:

1. Establish a group of scientists and managers dedicated to the development and implementation of a science plan for Delta Smelt.
2. The Delta Smelt Science Plan should consider all aspects of Delta Smelt Science from monitoring to modeling and should consider all factors potentially affecting the species.
3. We suggest an initial effort to better understand how water temperature varies across the Delta in different water year types.
4. Focused studies of lower trophic levels and development of models to better understand production of Delta Smelt food to determine appropriate management actions.
5. Conduct large mesocosm studies or field experiments using caged hatchery fish to better understand responses of Delta Smelt to variation in ambient conditions within the upper estuary.

Introduction

The amount and variability of freshwater outflow are among the most important environmental drivers in estuarine ecosystems. In the San Francisco Estuary (SFE, Figure 1), the effects of freshwater flow on the aquatic ecosystem have been studied extensively over the years and remain a contentious management issue. This is especially true relative to Delta Smelt (*Hypomesus transpacificus*), a species endemic to the SFE that has been listed as threatened under the Federal Endangered Species Act and as endangered under the California Endangered Species Act. Early studies of Delta Smelt distribution within the SFE suggested that Delta Smelt habitat is determined largely by freshwater flow, because Delta Smelt are often found in the low salinity portion of the SFE during the summer and fall period (Moyle et al. 1992). Subsequent studies also demonstrated that higher freshwater flow into the estuary along with other water quality and hydrodynamic factors could improve the abiotic habitat for Delta Smelt (Feyrer et al. 2007, Feyrer et al. 2011, Bever et al. 2016), reduce the extent and intensity of harmful algal blooms (Lehman et al. 2005, Lehman et al. 2013), and increase food availability (Miller et al. 2012, Kimmerer et al. 2019). However, the exact mechanisms and processes producing such benefits remained unclear, and subsequent studies have shown that individual Delta Smelt can show a wide range of life history variation with respect to salinity inhabited at different life stages (e.g., completing entire life cycle in freshwater) (Moyle et al. 2016, Bush 2017, Hobbs et al. 2019a).

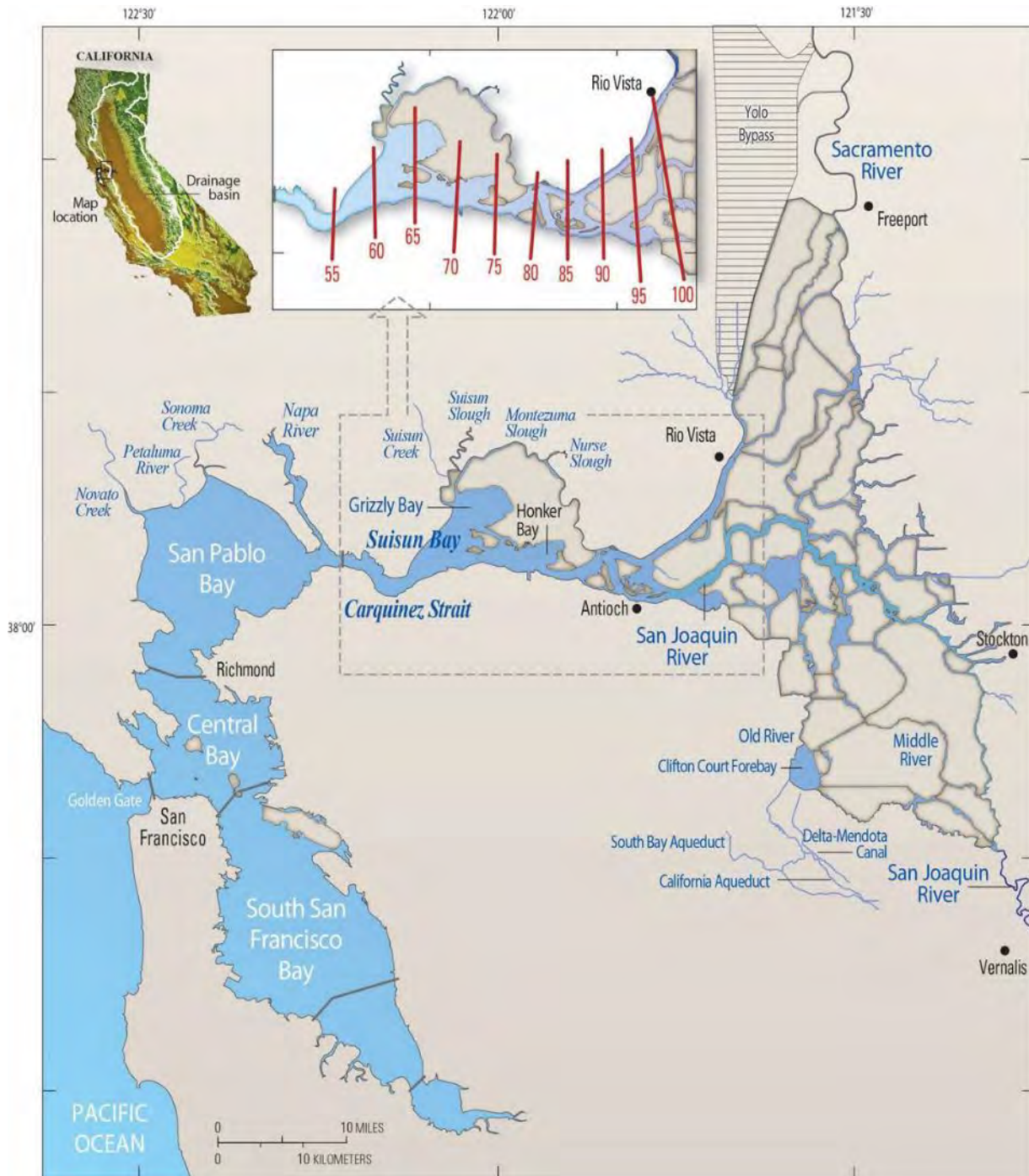


Figure 1. Map of the San Francisco Estuary (from IEP-MAST 2015). Inset shows a selection of X2 locations.

In 2008, the U.S. Fish and Wildlife Service (USFWS) issued a Biological Opinion (BiOp) on Central Valley Project (CVP) and State Water Project (SWP) operations in relation to Delta Smelt (U.S. Fish and Wildlife Service 2008). The BiOp concluded that aspects of the CVP and SWP operations jeopardize the continued existence of Delta Smelt and adversely modify Delta Smelt critical habitat. In the BiOp, the

USFWS issued a Reasonable and Prudent Alternative (RPA) action that requires the adaptive management of Sacramento-San Joaquin Delta (Delta) outflow in the fall following a wet year. More specifically this RPA action stipulates that during water years classified as “above normal” or “wet” (as defined by the Sacramento Basin index), the low salinity habitat (LSH) should be managed so that monthly mean X2 is no greater than 74 km in a wet year and no greater than 81 km in above normal years in September and October (the index, X2, is the horizontal distance in kilometers from the Golden Gate up the axis of the estuary to where tidally averaged near-bottom salinity is 2; Jassby et al. 1995). However, because there is considerable uncertainty regarding the fall low-salinity habitat component of the RPA, the RPA also stipulates that this action is subject to adaptive management. Note that LSH refers to all habitat variables within the low salinity zone (LSZ). The low salinity zone has been defined as the region with salinity ranging from 1 to 6 or from 0.5 to 6, depending on the specific study.

The first “wet” or “above normal” water year since the publication of the BiOp occurred in 2011 (see https://www.waterboards.ca.gov/waterrights/water_issues/programs/bay_delta/wq_control_plans/1995wqcp/docs/1995wqcpb.pdf for definitions of water year types) (Figure 2; Table 1). Operations in 2011 resulted in the low-salinity habitat being located close to the range listed in the RPA during the fall of 2011, specifically that monthly average X2, during September and October, is no greater than 74 km. To provide a summary of the results from this first year of the fall low-salinity habitat RPA action and help guide its future implementation, the U.S. Bureau of Reclamation in collaboration with the Interagency Ecological Program (IEP) sponsored a fall low-salinity habitat investigations (FLaSH) report that was completed in 2014 (Brown et al. 2014).

Table 1. Water year designations for water years 1979-2017, where W=Wet, AN=Above normal, BN=Below normal, D=Dry, C=Critical. Data and explanations for calculations of indices available at <http://cdec.water.ca.gov/cgi-progs/ioidir/wsihist>.

Year	Sacramento Valley Index	San Joaquin Valley Index
1979	BN	AN
1980	AN	W

1981	D	D
1982	W	W
1983	W	W
1984	W	AN
1985	D	D
1986	W	W
1987	D	C
1988	C	C
1989	D	C
1990	C	C
1991	C	C
1992	C	C
1993	AN	W
1994	C	C
1995	W	W
1996	W	W
1997	W	W
1998	W	W
1999	W	AN
2000	AN	AN
2001	D	D
2002	D	D
2003	AN	BN
2004	BN	D
2005	AN	W
2006	W	W
2007	D	C
2008	C	C
2009	D	BN
2010	BN	AN
2011	W	W
2012	BN	D
2013	D	C
2014	C	C
2015	C	C
2016	BN	D
2017	W	W

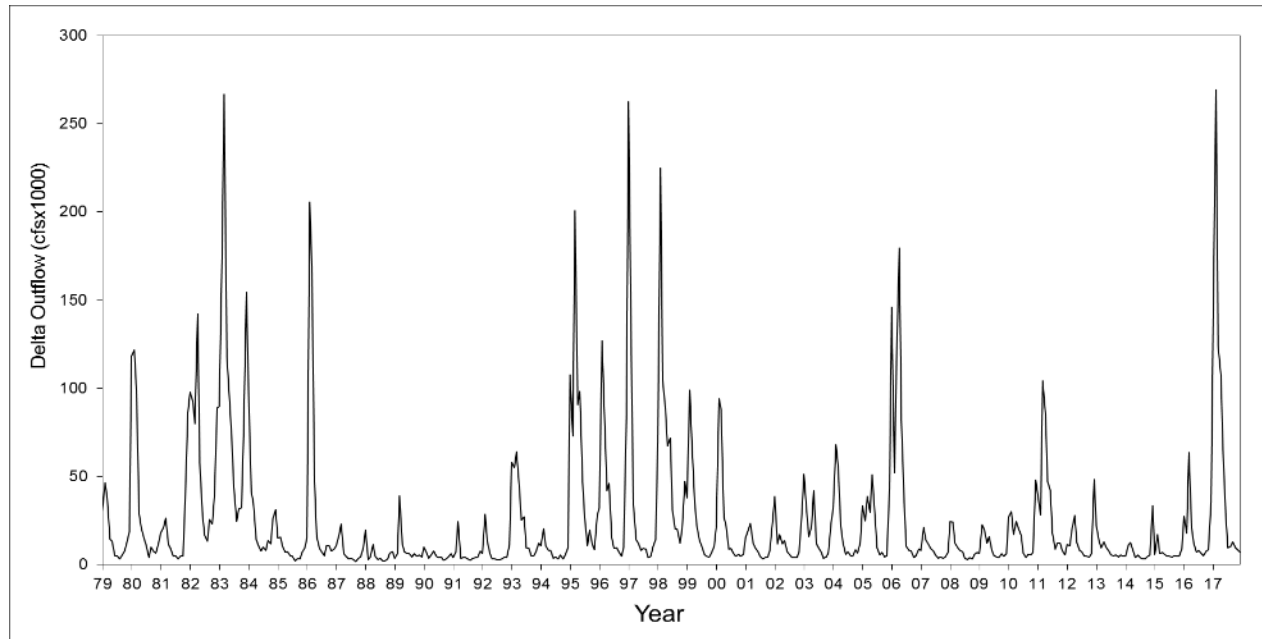


Figure 2. Delta outflow from 1979 through 2017.

The cool, wet year of 2011 was associated with an increase in Delta Smelt abundance in summer, fall, and the following winter compared to previous years since the pelagic organism decline (POD) in about 2002 (see, Sommer et al. 2007, Thomson et al. 2010) (Figure 3); however, the increase was short lived and Delta Smelt declined after 2011 to historically low levels (Figure 3) in association with an extended drought (2012-2016) (Figure 3, Table 1). The decline of Delta Smelt numbers in these drought years led to the issuance of the Delta Smelt Resiliency Strategy, which listed various management actions to be taken to improve the status of Delta Smelt (California Natural Resources Agency 2016). A number of actions listed in the Delta Smelt Resiliency Strategy involve altering flow to some extent in the San Francisco Bay-Delta ecosystem: summer outflow augmentation to the Sacramento-San Joaquin Delta to improve overall Delta Smelt habitat; flow augmentation to the Yolo Bypass Toe Drain to promote food production for the species; and changes in the operations of the Suisun Marsh Salinity Control Gates to provide low-salinity habitat in Suisun Marsh during the summer. These potential flow actions were a topic of discussion within the Collaborative Science and Adaptive Management Program (CSAMP; a policy level group) and associated Collaborative Adaptive Management Team (CAMT; upper management and technical level), leading to a request from CAMT for the IEP to establish a Project Work Team (PWT) to provide a more public venue for the discussion

and evaluation of these actions. The Flow Alteration Project Work Team (FLOAT-PWT) was established in late 2016 and, like all IEP PWTs, is open to all interested parties (see, <https://www.water.ca.gov/Programs/Environmental-Services/Interagency-Ecological-Program>).

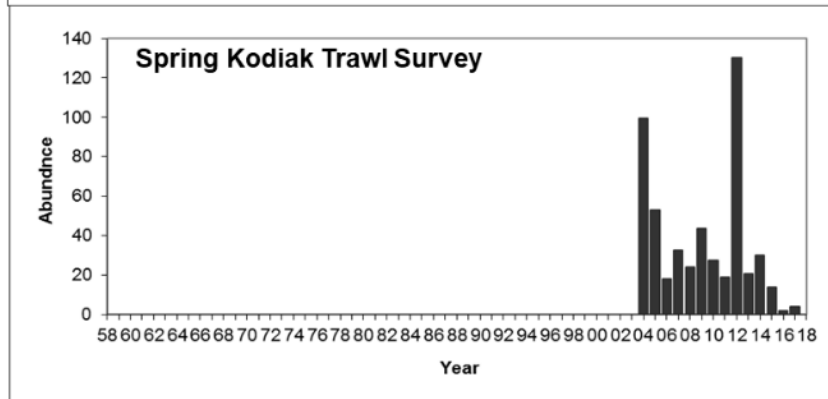
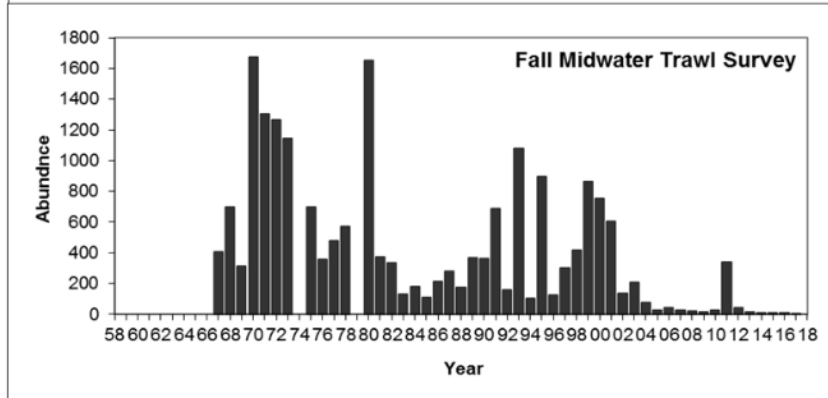
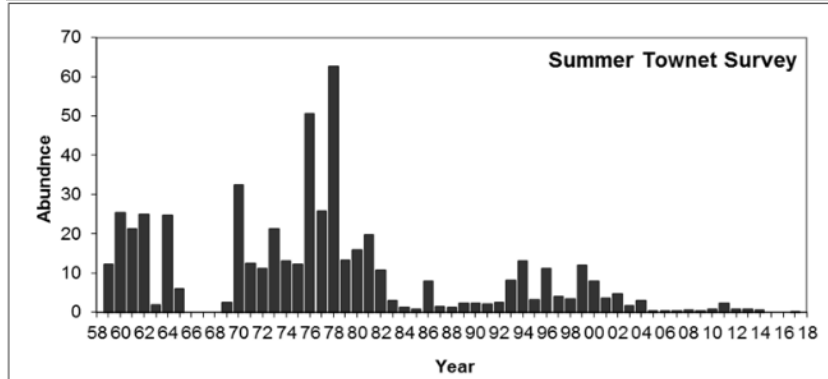
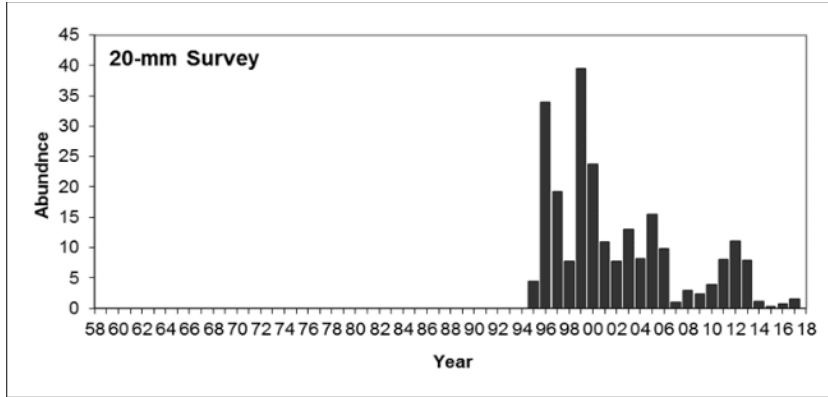


Figure 3. Abundance indices for the four major IEP fish monitoring programs, the 20-mm survey, summer townet, fall midwater trawl and the spring kodiak trawl. Note that the adults of the 2011 cohort are sampled in the spring of 2012 by the kodiak trawl survey.

Subsequent to the establishment of the FLOAT-PWT, a record wet year occurred in 2017 (Figure 2), triggering the fall low-salinity zone component of the RPA for the second time (U.S. Fish and Wildlife Service 2008). However, as in 2011, there was not a standing body of scientists tasked with evaluating the effects of this unusual flow event on the Delta Smelt population or the ecosystem in general. In the summer of 2017, the FLOAT Management, Analysis, and Synthesis Team (MAST) was established as a subgroup of the FLOAT-PWT to analyze, synthesize, and summarize the data collected from the various flow-related monitoring and special studies occurring in 2017 and produce a report similar to the FLaSH effort (Brown et al. 2014). This report constitutes the first FLOAT-MAST effort, which will focus on the 2017 summer-fall status of Delta Smelt and its habitat resulting from a record wet year.

Purpose and Scope

This report has three main objectives. The first is to summarize data collected from FLOAT-related special studies and long-term monitoring programs for the water year of 2017, with an emphasis on data relevant to the fall low-salinity habitat component of the RPA. Because some studies and monitoring program require time-intensive sample processing and/or analysis, this report will simply document the status of ongoing study elements that were not completed in time for inclusion in this report. Similarly, new avenues of analysis identified during the preparation of this report were not necessarily pursued given time constraints but were identified for exploration in future years by FLOAT-MAST or other entities. The second main objective of this report is to provide synthesis of new and previous data (such as the FLaSH report; Brown et al. 2014) to further assess the validity of some of the hypotheses underlying the fall low-salinity habitat component of the RPA (U.S. Fish and Wildlife Service 2008) and to provide a baseline for future evaluations. Any new findings from this FLOAT-MAST effort may also be used to update the current conceptual models for Delta Smelt (Brown et al. 2014, IEP-MAST 2015, Moyle et al. 2016). The final objective of this report is to put results from the FLOAT-related studies into the context of the overall body of knowledge on Delta Smelt (Moyle et al. 2016) and the Delta food web (Brown et al. 2016a) and improve the scientific basis for adaptively managing

Delta outflow in the future. It is important to note that this report generally covers information available through about 2018. Because monitoring, studies, and analyses of SFE and Delta Smelt ecology are ongoing, it is possible that information will be updated by the time this report is published. Readers are advised to consult the most recent information available on their topic of interest.

The overall spatiotemporal scope of the report is broad; however, this report will focus on certain regions and time periods that are most relevant to understanding the effects of high flows in 2017. Because Delta Smelt is the study species of primary concern, we will focus on the low-salinity zone and freshwater portion of the SFE where Delta Smelt are generally found in summer and fall. The low-salinity zone for Delta Smelt is defined here as the area of the upper SFE where salinity ranges from 1 to 6 (Bennet 2005, Brown et al. 2014, IEP-MAST 2015). This report will also attempt to incorporate information from all years in which data are available; however, the primary focus will be on years that are the most comparable to the wet year of 2017. As such, the water years 2006 and 2011 will receive considerable attention because these were the only two other wet years that have been observed after the pelagic organism decline (POD) that began in the early 2000s (Sommer et al. 2007, Baxter et al. 2010; Thomson et al. 2010). The persistent low abundance of Delta Smelt suggests that the post-POD period provides a better baseline for assessing the benefits of management actions.

Background

Study area

The SFE (Figure 1) is the largest estuary on the West Coast of North America, and it has been characterized as one of the best studied estuaries in the world (for example, Conomos 1979, Hollibaugh 1996, Feyrer et al. 2004). Like other estuaries around the world, the SFE has been highly modified by human development and extraction of resources (Nichols et al. 1986, Lotze et al. 2006). The most notable changes are the loss of wetlands, inputs of contaminants, alterations of hydrodynamics for diversion of water, and both accidental and deliberate introductions of species (Bennett and Moyle 1996, Brown and Moyle 2005, Baxter et al. 2010, National Research Council 2012). These changes and others have been implicated in declines of terrestrial and aquatic resources, including fishes. Many of these anthropogenic changes took place before the advent of modern

regulations and management, when the primary focus of resource development was providing human benefits.

This report focuses on the upper SFE, principally the Delta and Suisun region (Figure 4). Historically, the northern portion of the Delta was dominated by the Sacramento River and associated floodplains, flood basins, low natural levees, and seasonal and permanent wetlands (Whipple et al. 2012). The southern portion of the Delta was dominated by the smaller San Joaquin River, associated distributary channels, and dead-end sloughs. As development progressed in the Delta, higher levees were constructed to protect farmlands. Formerly isolated larger channels were connected, while many smaller channels were disconnected from historical channel networks. Deep new channels were dredged to facilitate shipping to and from the ports of Stockton and Sacramento. State-wide water development by federal (CVP, Central Valley Project) state (SWP, State Water Project) and more local entities (e.g., irrigation districts), resulted in further changes, most-notably the installation and operation of large water-diversion facilities in the southern Delta by the CVP and SWP (Figure 4).

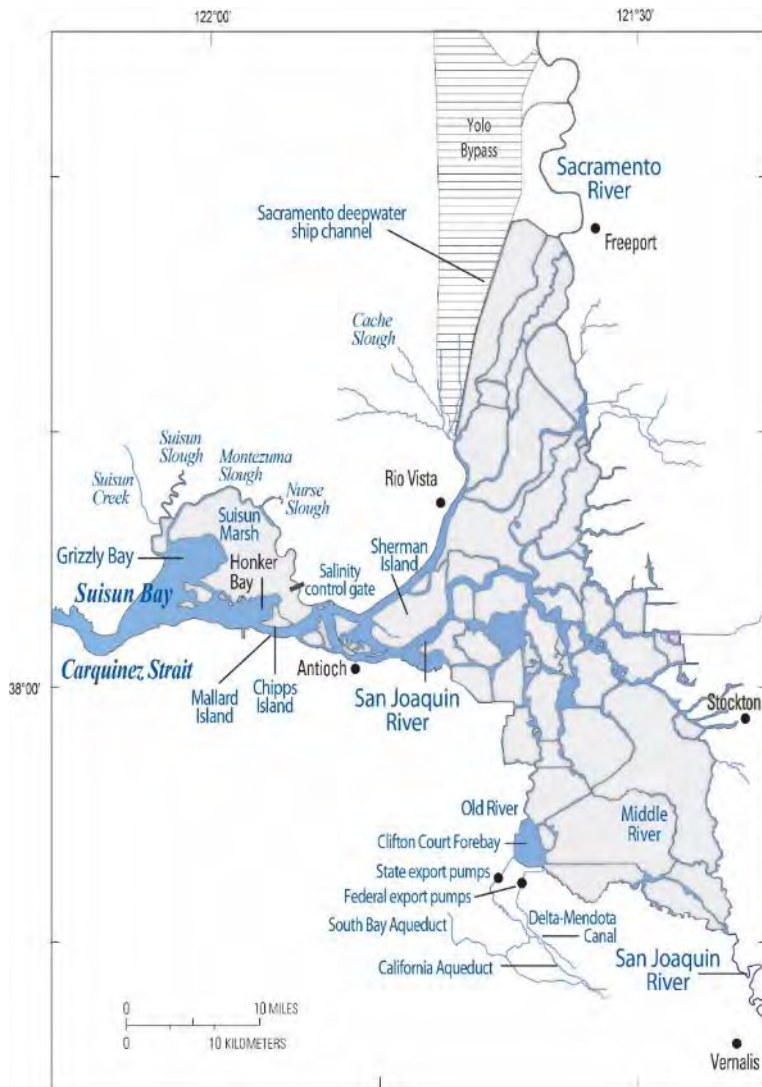


Figure 4. Map of the upper San Francisco Estuary (from IEP-MAST 2015).

The current configuration of the Delta includes a complex network of interconnected channels between leveed islands (Figure 4). A few such islands have flooded, leaving pockets of open water within the Delta. Most of the channels are relatively shallow, except for the dredged, deepwater ship channel in the San Joaquin River to the Port of Stockton and a similar channel in the Sacramento River to the Port of West Sacramento (Sacramento River deepwater ship channel, SRDWSC). The SRDWSC splits from the main Sacramento River just upstream of the town of Rio Vista and follows the lower portion of Cache Slough north, through the Yolo Basin, to the port (Figure 4). Cache Slough continues northwest and is associated with Liberty Island, which is now flooded, and several tributary creeks and sloughs; it also serves as the connection between the Yolo Bypass and the Sacramento River (Figure 4).

The Yolo Bypass is a flood bypass located in the historical Yolo flood basin (Whipple et al. 2012). It diverts high flows associated with winter storms from the Sacramento River around the City of Sacramento and also provides important floodplain habitat for Chinook Salmon, Splittail, and other native fishes (Sommer et al. 2001, Sommer et al. 2003, Feyrer et al. 2006, Goertler et al. 2018).

The region where the Sacramento and San Joaquin Rivers join (confluence region) was once dominated by sinuous sloughs and low, tidally inundated islands and wetlands (Whipple et al. 2012). Today, the waterways of this region are disconnected from most of the former wetland areas and are generally deep and uniform in bathymetry with relatively narrow channels compared to the Suisun region (Figure 4). The Suisun region includes Suisun, Grizzly, and Little Honker Bays. This region is also connected to Suisun Marsh, to the north, through Suisun and Montezuma Sloughs. The Suisun region then connects to San Pablo and San Francisco Bays through Carquinez Strait.

Delta Smelt

Early information on the Delta Smelt population was collected as part of sampling and monitoring programs related to water development and management of the sport fishery for introduced Striped Bass, *Morone saxatilis* (e.g., Erkkila et al. 1950, Radtke 1966, Stevens and Miller 1983). These early fish monitoring activities, combined with subsequent water quality monitoring and research activities (largely under the auspices of the IEP), provided sufficient information on the decline of Delta Smelt (Moyle et al. 1992) to support a petition for listing under the Federal Endangered Species Act. Delta Smelt was listed as threatened under the Federal Endangered Species Act in 1993 (U.S. Fish and Wildlife Service 1993). The species was listed as threatened under the state endangered species statute in 1993, and the status was changed from threatened to endangered in 2009 (California Fish and Game Commission 2009). In 2010, federal reclassification of Delta Smelt from threatened to endangered was determined to be warranted but was precluded by other higher priority listing actions (U.S. Fish and Wildlife Service 2010). Subsequent declines in the Delta Smelt population, in concert with three other pelagic fishes (Figure 5), increased concern for achieving recovery of Delta Smelt. These declines are often referred to as the POD (Sommer et al. 2007, Baxter et al. 2008, 2010). Continued concern over status of the population has resulted in periodic reviews of Delta Smelt

biology as continued research provides new information (see Brown et al. 2014, IEP-MAST 2015, Moyle et al. 2016).

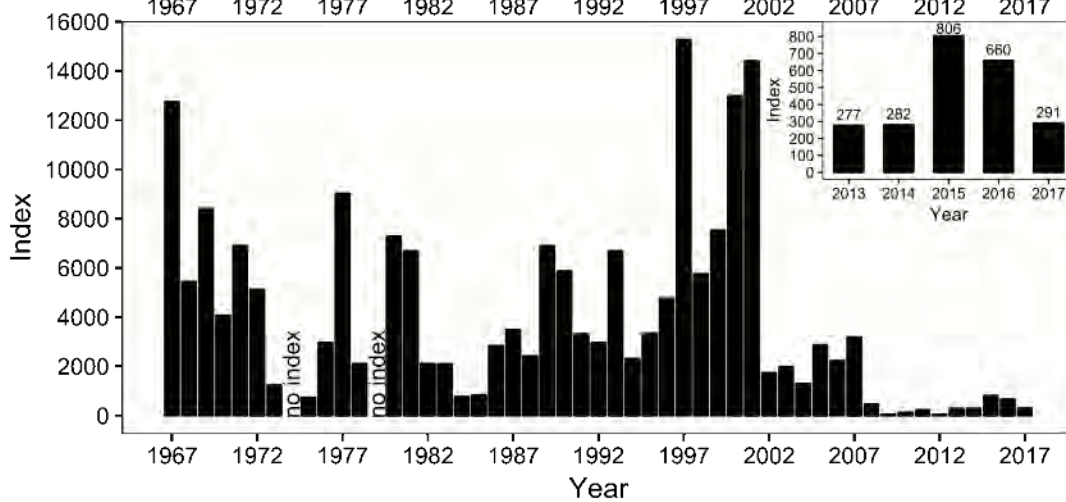
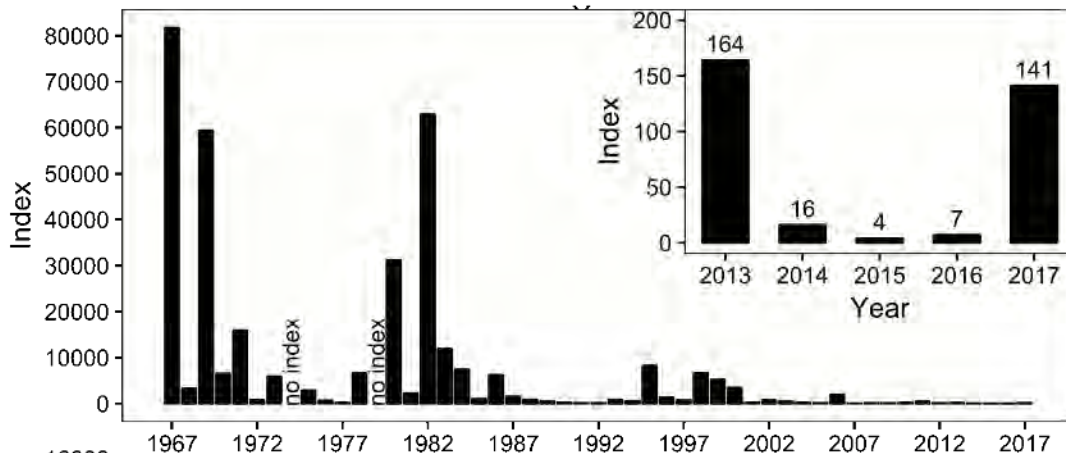
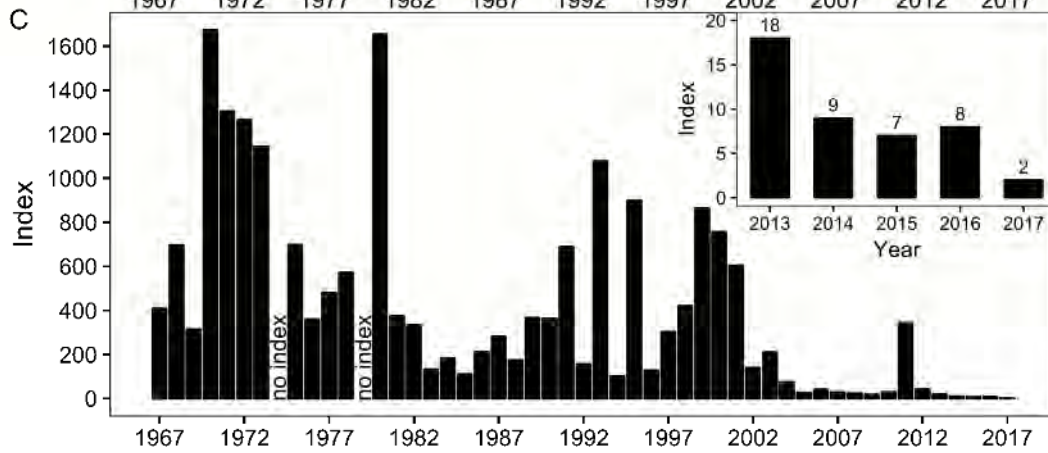
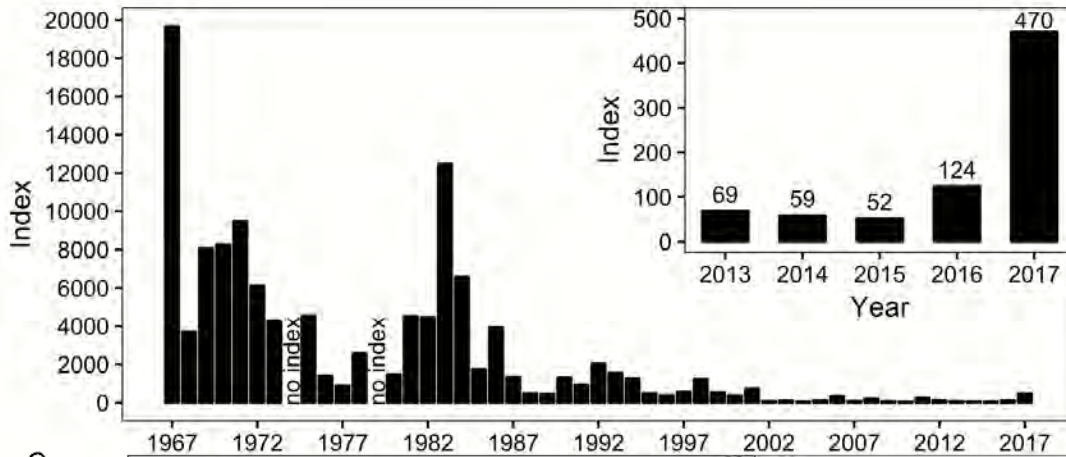


Figure 5. Abundance indices from the fall midwater trawl for species associated with the pelagic organism decline: age-0 Striped Bass, Delta Smelt, Longfin Smelt, and Threadfin Shad. The insets show index values during the most recent drought (2012-2016) and the wet year of 2017.

The Delta Smelt is endemic to the SFE and is the most estuary-dependent of the native fish species (Moyle et al. 1992, Bennett 2005). Delta Smelt are slender-bodied fish typically reaching 60–70 millimeters (mm) standard length (SL) with a maximum size of about 120 mm SL. Delta Smelt is primarily an annual species, reproducing at the end of their first year with a small percentage reproducing in their second year (Bennett 2005, Damon et al. 2016, Moyle et al. 2016). Delta Smelt feed primarily on planktonic copepods, mysids, amphipods, and cladocerans (Lott 1998, Nobriga 2002, Slater and Baxter 2014). Fisch et al. (2011) determined that there is a single, panmictic Delta Smelt population in the estuary.

It was originally believed that all Delta Smelt completed the majority of their life cycle in the LSZ of the upper estuary and used the freshwater portions of the upper estuary primarily for spawning and rearing of larval and early post-larval fish (Dege and Brown 2004, Bennett 2005); however, recent studies have shown that Delta Smelt actually display a continuum of life history types (Bush 2017, Hobbs et al. 2019a). The majority express the originally described life cycle but the transition from freshwater to brackish water is not restricted to a single age or life stage. However, some Delta Smelt complete their entire life cycle in either freshwater or brackish water.

The current range of juvenile and sub-adult Delta Smelt includes the Cache Slough area, the SRDWSC and Sacramento River in the northern Delta, the confluence region in the western Delta, and the Suisun region (Merz et al. 2011). Historically, juvenile and sub-adult Delta Smelt also inhabited the central and southern Delta during the summer and fall months (Erkkila et al. 1950), but they are now particularly rare in those areas during that time period (Bennett 2005, Nobriga et al. 2008, Sommer et al. 2011). Delta Smelt occur sporadically in the Napa River and San Pablo Bay, especially during high outflow years (Merz et al. 2011, Moyle et al. 2016); however, it has not been determined if those regions make a significant contribution to the spawning population in the following winter.

Juvenile and sub-adult Delta Smelt are most abundant at salinity 1–2 (Bennett 2005, Sommer et al. 2011). Recent analyses and expansion of sampling into the north Delta suggest that the freshwater region also contains a significant presence of Delta Smelt. Delta Smelt are generally not found above salinity 14 (Swanson et al. 2000); however, recent studies have shown that, under

laboratory conditions, Delta Smelt can survive in seawater (salinity ~ 33) for a short period of time (Komoroske et al. 2014). Although several laboratory studies have shown that salinities greater than 6 did not cause a significant stress (Hasenbein et al. 2013, Hammock et al. 2015, Komoroske et al. 2016) on the fish, Delta Smelt appear to be limited in their selected salinity range as they are less often observed at salinities above 6 (Sommer et al. 2011). Interactions with multiple stressors such as prey densities and water temperature may increase Delta Smelt's sensitivity to salinity stress.

Dispersal of maturing adults rearing in brackish waters to freshwater generally begins in the late fall or early winter, and most spawning takes place from early April through mid-May of the following year (Bennett 2005, Sommer et al. 2011). Active movement of adult fish into freshwater areas has been documented (Bennett and Burau 2015), but it is also possible that some fish maintain geographic position in relation to suitable habitat and experience changes in salinity as a result of changes in flow altering the position of the salinity field (Murphy and Hamilton 2013, Hobbs et al. 2019a). Many larval Delta Smelt move into the LSZ with the tides (Dege and Brown 2004), but the date of dispersal can vary widely and is influenced by water temperature (Hobbs et al. 2019a,b). As noted earlier, some fish remain in upstream reaches year-round, including the Cache Slough region, the SRDWSC, and the central Delta region (Sommer et al. 2011, Bush 2017). A small percentage of Delta Smelt are spawned in the brackish region and remain there (Bush 2017, Hobbs et al. 2019a). As noted earlier, Delta Smelt is primarily an annual species, with a very small percentage of the species surviving into a second year and potentially spawning in one or both years (Bennett 2005, Damon et al. 2016, Moyle et al. 2016). Additional studies by Sommer et al. (2011), Merz et al. (2011), Murphy and Hamilton (2013), and Manly et al. (2015) examined the habitat associations, geographic distribution, and dispersal patterns of Delta Smelt for each of the major IEP fish-monitoring surveys. Overall, these studies demonstrated that many Delta Smelt utilize freshwater during winter and spring months for spawning and early development and then reside in the LSZ, which may correspond with geographic affinities, in the summer and fall.

Summer physical habitat has been described by Nobriga et al. (2008). The summer (June–July) distribution of Delta Smelt is associated with areas that have appropriate salinity, but also have appropriate turbidity and temperature (Nobriga et al. 2008). Similarly, Feyrer et al. (2007, 2011) found the distribution of Delta Smelt to be associated with salinity and turbidity during fall months

(September through mid-December). Recent laboratory studies and analysis of field observations have better characterized temperature and turbidity conditions appropriate for Delta Smelt (e.g., Hasenbein et al. 2013, Komoroske et al. 2014, 2015). We have little information on the direct effects of temperature on Delta Smelt in the field; however, there are laboratory data on thermal physiology and some observational data that suggest some thresholds for interpreting temperature data. Growth experiments in the laboratory (see Bennett 2005) and evidence from otoliths (see Hobbs et al. 2019c, and Growth Rate section below) suggest that optimal temperature for Delta Smelt growth is $\leq 20^{\circ}\text{C}$. Other studies have demonstrated physiological stress of Delta Smelt, including increased metabolism (Jeffries et al. 2016) and expression of genes involved in heat stress responses at temperatures greater than 20°C (Komoroske et al. 2015, Jeffries et al. 2016). Hobbs et al. (2019a) found evidence that temperatures above 20°C stimulated Delta Smelt to disperse. Temperatures above around 24°C appear to be associated with physiological markers of heat stress (Komoroske et al. 2015) and temperatures above 26°C are likely chronically or acutely fatal to juvenile or sub adult Delta Smelt (Komoroske et al. 2014). Water temperatures greater than 20°C have also been associated with changes in behavior in laboratory experiments, including individual swimming behavior, grouping behaviors, responses to predator presence and susceptibility to predation (Davis et al. 2019). Such behavioral changes could be important to wild fish in the context of predator avoidance.

Based on the above information, we divided water temperature range between 20°C and 24°C into an initial phase of moderately reduced growth and beginning of behavioral avoidance from 20 to 22°C and a second phase between 22 and 24°C characterized by poor growth, behavioral avoidance, and onset of heat stress. For these reasons we consider water temperatures $\geq 22^{\circ}\text{C}$ as undesirable for Delta Smelt for the remainder of this report.

We also note here that there is little evidence of thermal stratification in the Delta or Suisun region that would provide refuge for Delta Smelt. Based on concurrently collected surface and bottom water temperatures in the 20-mm Enhanced Delta Smelt Monitoring (EDSM) survey, the observed differences between surface and bottom water temperatures in spring-summer 2017 suggests that vertical temperature gradients are too small to provide any local thermal refugia to larval and juvenile Delta Smelt when surface water temperatures are above 20°C (Figure 6). Similarly, Brown et al. (2016b) did vertical profiles in the North Delta and found minimal differences between top and bottom

water temperatures (S1 Appendix to Brown et al. 2016b). In 104 of 116 profiles, the difference was less than 1°C and was never greater than 2°C. Vroom et al. (2017) found similar results from analysis of empirical data and modeled water temperatures. Nevertheless, small temperature differences can be important when species are at their thermal limits, so the concept of thermal refuges should be explored further in habitats where water temperatures reach stressful levels.

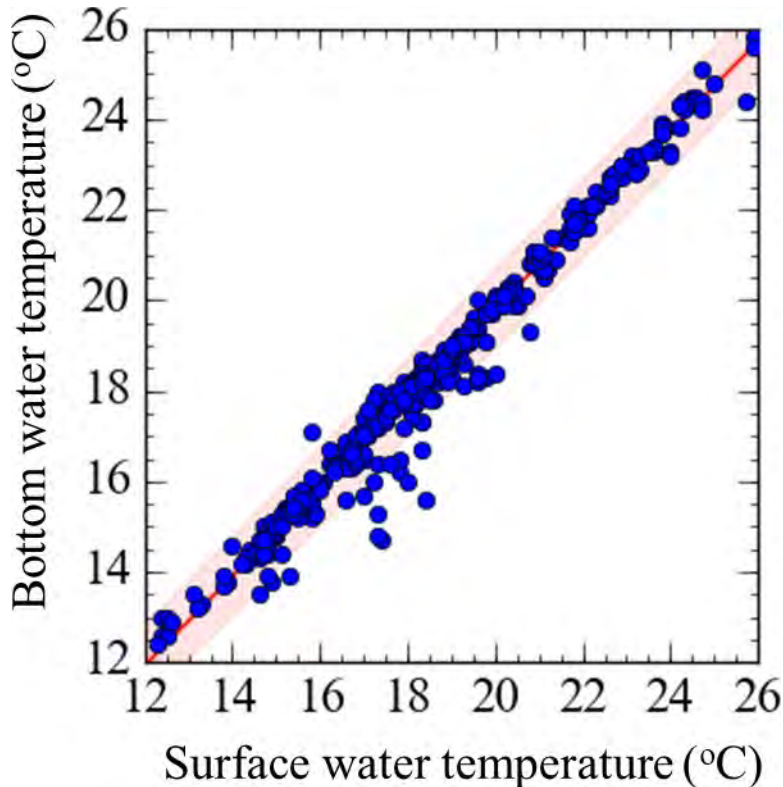


Figure 6. Linear regression between bottom water temperature (Y) and surface water temperature (X) in the upper San Francisco Estuary during April-July 2017 (data from Enhanced Delta Smelt Monitoring 20-mm tows). $Y = 0.12 + 0.98X$ ($R^2 = 0.98$, $P < 0.05$, 400 df).

Although abundance of Delta Smelt has been highly variable over the course of monitoring studies, many analyses have identified a long-term decline in abundance (Figure 3; Manly and Chotkowski 2006, Sommer et al. 2007, U.S. Fish and Wildlife Service 2008, Thomson et al. 2010). The decline spans the entire period of survey records from the completion of the major reservoirs in the Central Valley through the POD (Baxter et al. 2010). Statistical analyses also confirm that a step decline in pelagic fish abundance marks the transition to the POD period (Manly and Chotkowski 2006, Moyle and Bennett 2008, Mac Nally et al. 2010, Moyle et al. 2010, Thomson et al. 2010) and could signal a rapid ecological regime shift in the upper estuary (Baxter et al. 2010, Moyle et al. 2010). The decline of

Delta Smelt was intensively studied as part of an IEP effort to understand the POD (Sommer et al. 2007, Baxter et al. 2010). The POD investigators concluded that the decline has likely been caused by the interactive effects of several causes, including both changes in physical habitat (e.g., salinity and turbidity fields) and the biotic habitat (e.g., food web). This conclusion was generally supported by an independent review panel (National Research Council 2012). Such interactive effects were also consistent with the reported alteration of the salinity habitat of Delta Smelt and several other pelagic species and their population trends (Castillo et al. 2018).

Delta Smelt abundance has remained at a low level since their abrupt decline in the POD years (Sommer et al. 2007, Thomson et al. 2010). However, in 2011, the last wet year prior to 2017, the species' catch numbers from various surveys recovered to a level unseen since the pre-POD years (Brown et al. 2014). Following 2011, a five year-long drought occurred and Delta Smelt numbers declined to below post-POD levels (Figure 3; Castillo et al. 2018). Given the consistently low abundance of the species in the last decade, there was hope that the record wet year of 2017 would lead to another substantial increase in Delta Smelt abundance indices, similar to 2011 (Moyle et al. 2018). Yet, in contrast to 2011, Delta Smelt catch numbers from the various long-term monitoring surveys did not improve. Similarly, there was no response of Delta Smelt in 2006, another post-POD wet year (IEP-MAST 2015). There was a slight increase in the spring (20-mm Survey) index compared to low flow years (2014–2016), but that increase was not sustained through the summer and fall (Summer Townet Survey and Fall Midwater Trawl; Figures 3 and 5). By 2018, larval production was so low an index was incalculable (20-mm Survey; Tempel 2018a,b).

Conceptual models

There have been several conceptual models applied to the SFE and Delta Smelt over time and those conceptual models have been reviewed elsewhere (Brown et al. 2014, IEP-MAST 2015). In this section, we briefly review three conceptual models that are relevant to this report: Peterson (2003), Brown et al. (2014), and IEP-MAST (2015).

The estuarine habitats conceptual model (Figure 7) was an important element in developing the FLaSH conceptual model (Figure 8). The general model, developed by Peterson (2003), proposes an ecosystem-based view of estuarine habitats. In this view, the environment of an estuary consists of

two integral parts: 1) a stationary topography with distinct physical features that produce different levels of support and stress for organisms in the estuary; and 2) a dynamic regime of flows and salinities where organisms passively transported by flow or actively searching for a suitable salinity are exposed to the different levels of support and stress that are fixed in space in the stationary topography. Together, these stationary and dynamic habitat features are hypothesized to control the survival, health, growth, fecundity, and, ultimately, the reproductive success of estuarine pelagic species (Figure 7).

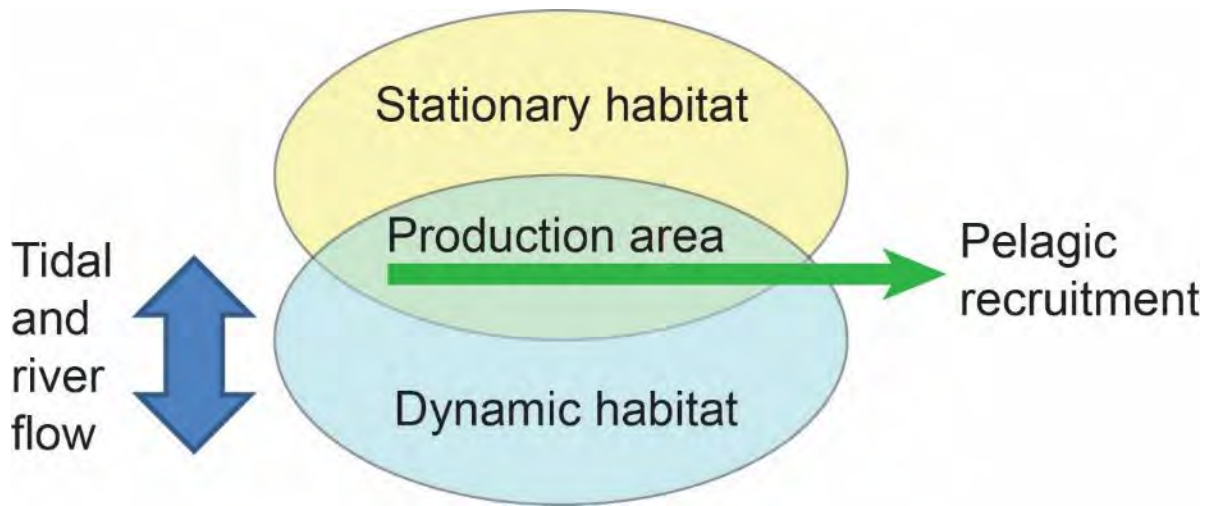


Figure 7. Illustration showing estuarine habitat conceptual model (modified from Peterson 2003).

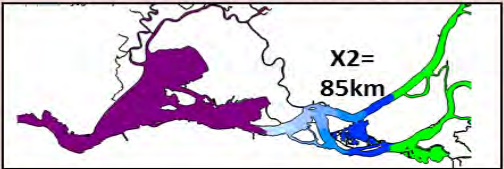
<i>Suisun Region</i>	Stationary Abiotic Habitat Components	<i>River Confluence</i>
<i>Higher</i>	Bathymetric Complexity	<i>Lower</i>
<i>Higher</i>	Erodible Sediment Supply	<i>Lower</i>
<i>Many in South, Fewer in North</i>	Contaminant Sources	<i>Many</i>
<i>Fewer</i>	Entrainment Sites	<i>More</i>
Variable Fall Outflow Regime Dynamic Abiotic Habitat Components		
<i>Higher After Wet Springs</i>	Net Total Delta Fall Outflow	<i>Always Low</i>
<i>Higher After Wet Springs</i>	San Joaquin River Contribution to Fall Outflow	<i>Always Low</i>
<i>After Wet Springs, Broad Fall LSZ Overlaps Suisun Region</i>	Location and Extent of the Fall LSZ (1-6 psu)	<i>Narrow Fall LSZ In River Channels, Never Overlaps Suisun Region</i>
		
<i>Higher After Wet Springs</i>	Hydrodynamic Complexity in the Fall LSZ	<i>Always Lower</i>
<i>Higher After Wet Springs</i>	Wind speed in the Fall LSZ	<i>Always Lower</i>
<i>More Variable, Higher After Wet Springs</i>	Turbidity in the Fall LSZ	<i>Always Less Variable, Lower</i>
<i>More Variable, Maybe Lower After Wet Springs</i>	Contaminant Concentrations in the Fall LSZ	<i>Less Variable, Maybe Higher</i>
<i>LSZ Overlaps Suisun Region</i>	Dynamic Biotic Habitat Components	<i>LSZ Overlaps River Confluence</i>
<i>Higher</i>	Food Availability and Quality	<i>Lower</i>
<i>Variable</i>	Predator Abundance	<i>Higher</i>
<i>LSZ Overlaps Suisun Region</i>	Delta Smelt Responses	<i>LSZ Overlaps River Confluence</i>
<i>Broad, Westward</i>	Distribution	<i>Constricted, Eastward</i>
<i>Higher</i>	Growth, Survival, Fecundity	<i>Lower</i>
<i>Better</i>	Health and Condition	<i>Worse</i>
<i>May be Higher</i>	Recruitment in the next Spring	<i>Lower</i>

Figure 8. Spatially explicit conceptual model for the western reach of the modern Delta Smelt range in the fall: interacting stationary and dynamic habitat features drive Delta Smelt responses. The location of the low-salinity zone (LSZ) is related to the value of X2, which is the horizontal

distance in kilometers (km) from the Golden Gate up the axis of the estuary to where tidally averaged near-bottom salinity is 2. Symbols: \leq , less than or equal to; and $>$, greater than. (from Brown et al. 2014).

For the Delta, this dynamic and interactive view of estuarine ecology captures several important elements. First, the interactions of outflow, and subsequent position of the LSZ (dynamic habitat), with the physical configuration of the Delta (stationary habitat) encompasses all of the concepts from earlier conceptual models, including the anticipated outcomes for estuarine organisms (for example, Jassby et al. 1995; recruitment) (see Brown et al. 2014, Bever et al. 2016). Second, variability in the dynamic habitat in daily, seasonal, annual, and longer time scales produces habitat complexity and variability, which can be important in promoting species diversity. Moyle et al. (2010) highlighted the extensive literature documenting the significant roles of habitat complexity and variability in promoting abundance, diversity, and persistence of species in a wide array of ecosystems, including the SFE. They concluded that ecological theory strongly supports the idea that an estuarine landscape that is heterogeneous in salinity and geometry (depth, the configuration of flooded islands, tidal sloughs, floodplains, and so on) is most likely to have high overall productivity, high species richness, and high abundances of desired species (Moyle et al. 2010).

The Peterson model (2003) provided the framework for the FLASH conceptual model that was specifically formulated to understand how the position of the low-salinity zone affects Delta Smelt habitat and the population (Figure 8). The stationary abiotic habitat components (Figure 8) are associated with the physical orientation and connections of the component waterbodies and the bathymetry of those waterbodies in the SFE. The dynamic abiotic habitat components are associated with hydrodynamic conditions and position of the salinity gradient associated with fall outflow. The interactions of stationary and dynamic abiotic habitat components determine the position and characteristics of LSH available for Delta Smelt (Figure 8). With respect to the RPA, interest is focused on two generalized flow regimes within the fall range of Delta Smelt. In the “low outflow” regime, LSH is located near the confluence of the Sacramento and San Joaquin Rivers (referred to as the “river confluence” in Figure 8). In the “high outflow” regime, LSH is located in the Suisun region, which extends seaward from the river confluence to the west and includes Suisun Bay, Grizzly Bay, Honker Bay, and Suisun Marsh (Figure 8). A central idea in the FLASH conceptual model is that the LSZ represents the optimal region for Delta Smelt production and represents the abiotic portion of the production area (Figure 7), which is the dynamic outcome of the interaction between stationary and

dynamic habitat components. The LSZ can be considered a dynamic, abiotic habitat component because its extent (for example, surface area) and location vary with net freshwater outflow from the Delta. Delta Smelt and other organisms that seek salinity levels within the LSZ range or are transported by hydrodynamic processes into the area, likely respond differently to the dynamic and stationary habitat features of the fall high- and low-outflow regimes. In other words, conditions for the different outflow regimes potentially do or do not correspond to those necessary for successful recruitment.

The IEP-MAST (2015) conceptual model was developed in response to comments on the FLaSH conceptual model from an independent review panel (FLaSH Panel 2012). The panel suggested that such a new conceptual model, in written and schematic form, should continue to stress processes and mechanisms, should be as complex as needed, and should extend both upstream and downstream of the LSZ (FLaSH Panel 2012). The basic approach of IEP-MAST was to develop a new conceptual model framework for Delta Smelt and to use this framework to synthesize new scientific information and update and integrate existing conceptual models. The resulting model consists of a general overview model (Figure 9) and four life stage transition models (Figures 10-13).

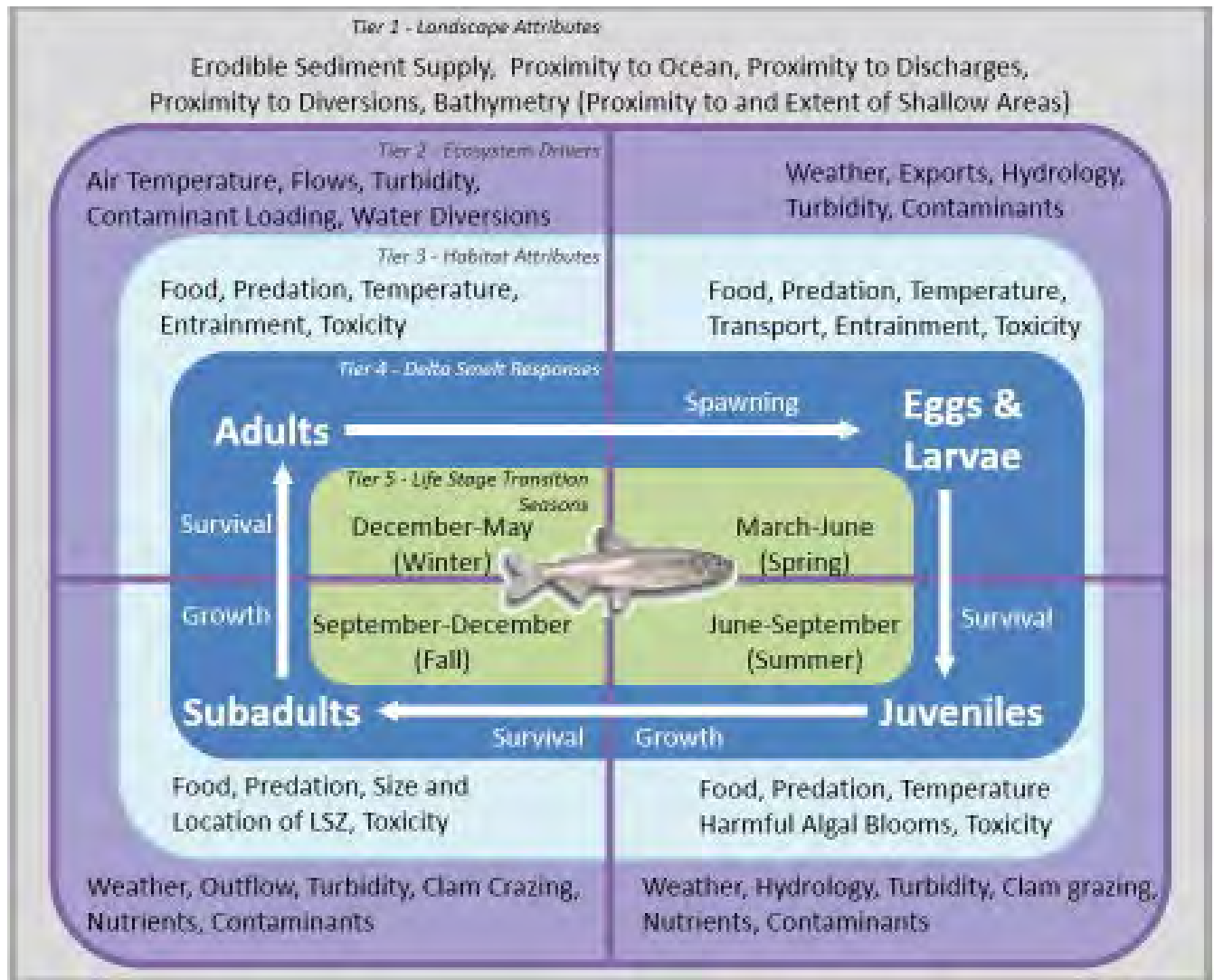


Figure 9. Delta Smelt general life cycle conceptual model (IEP-MAST 2015).

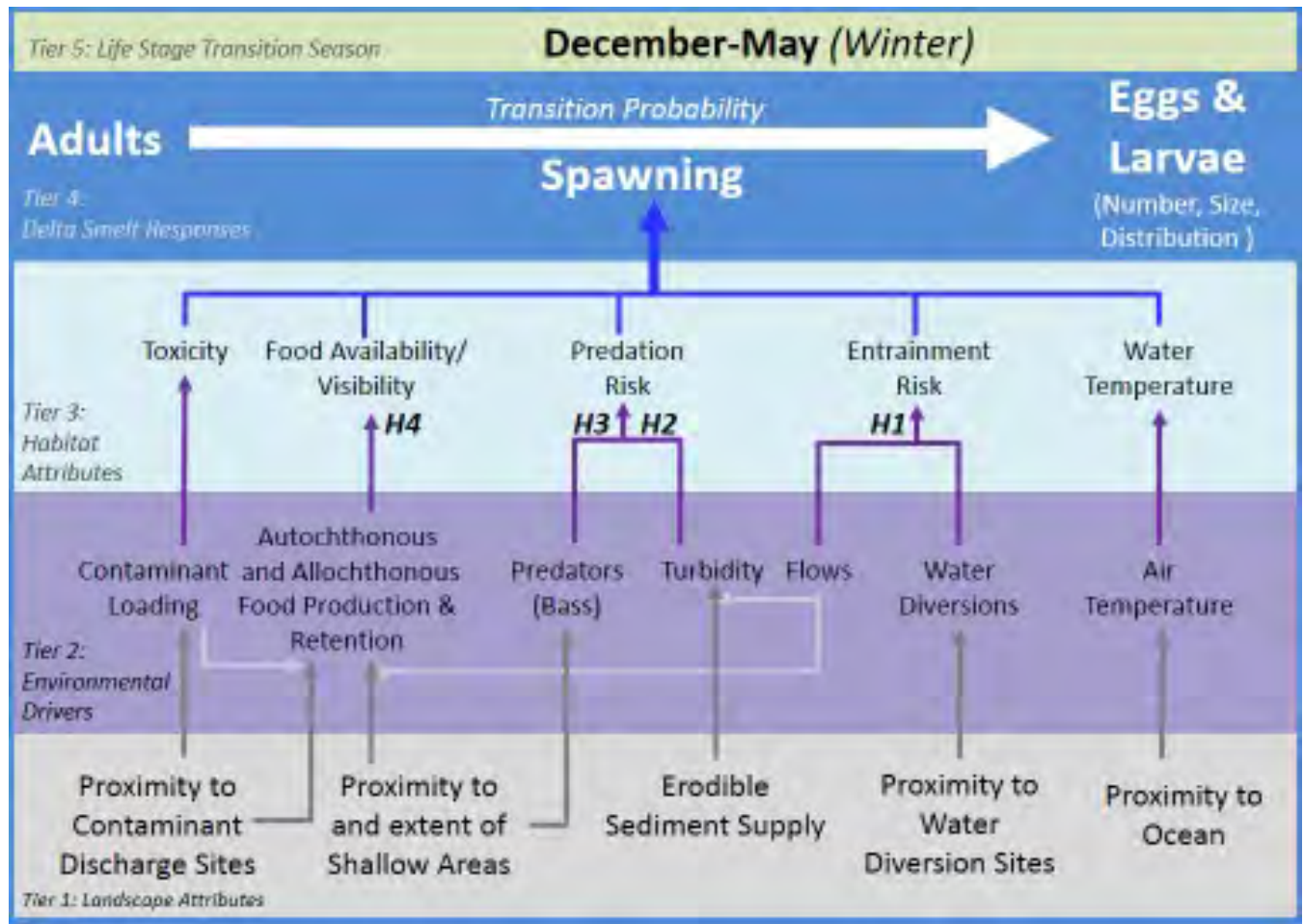


Figure 10. Conceptual model of drivers affecting the transition from Delta Smelt adults to larvae. Hypotheses addressed in IEP-MAST (2015) are indicated by the “H-number” combinations.

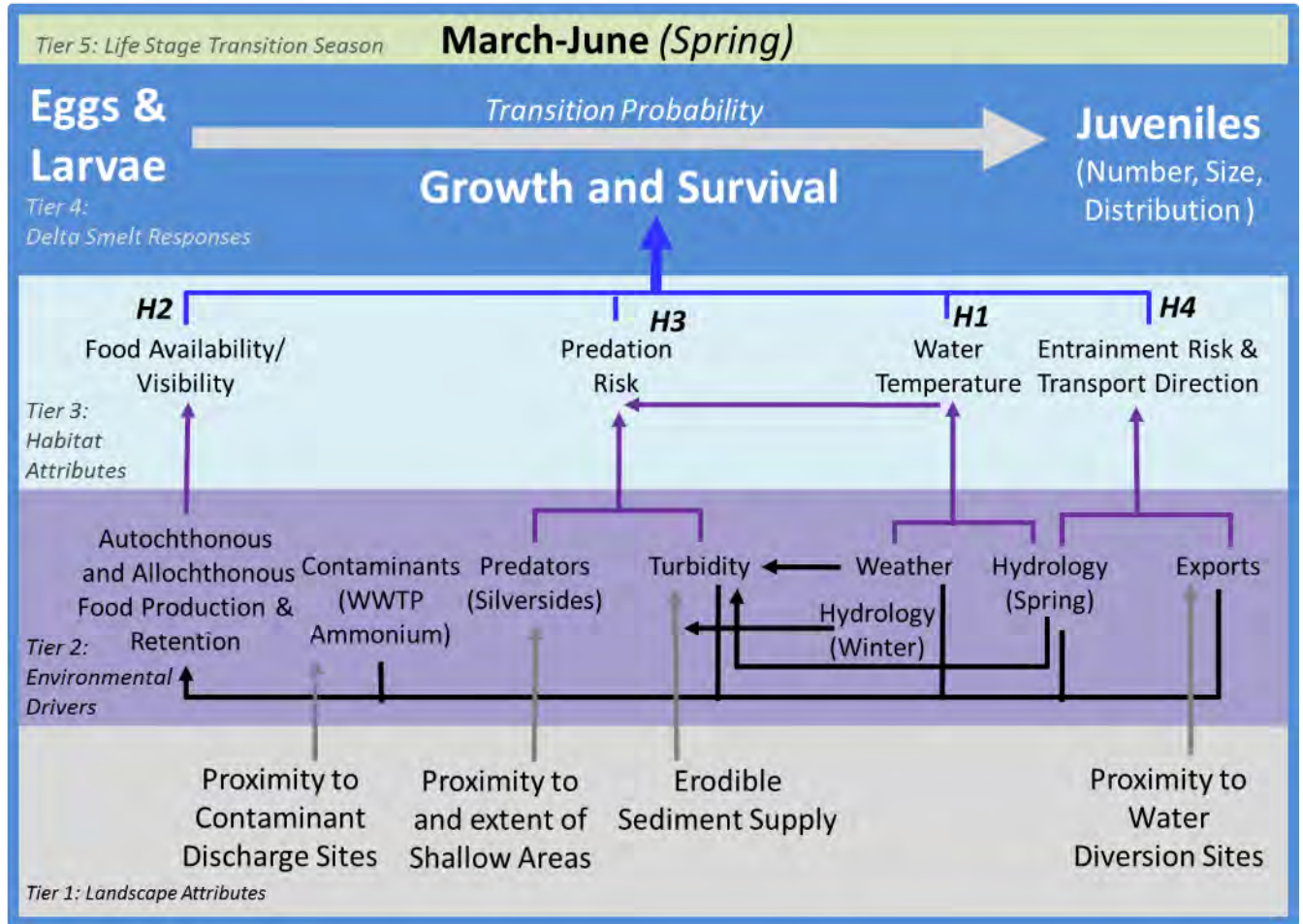


Figure 11. Conceptual model of drivers affecting the transition from Delta Smelt larvae to juveniles. Hypotheses addressed in IEP-MAST (2015) are indicated by the “H-number” combinations.

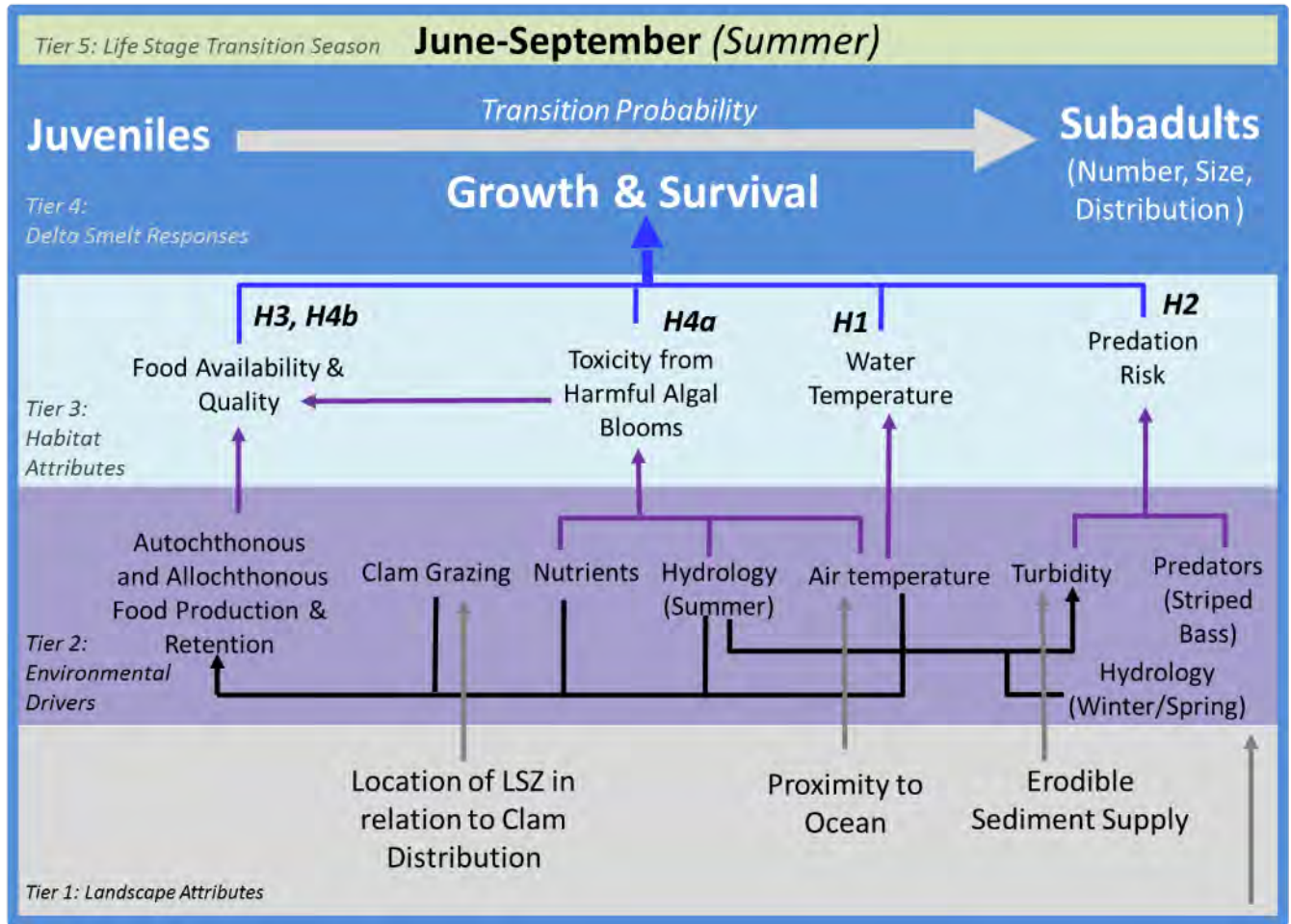


Figure 12. Conceptual model of drivers affecting the transition from Delta Smelt juveniles to subadults. Hypotheses addressed in IEP-MAST (2015) are indicated by the “H-number” combinations.

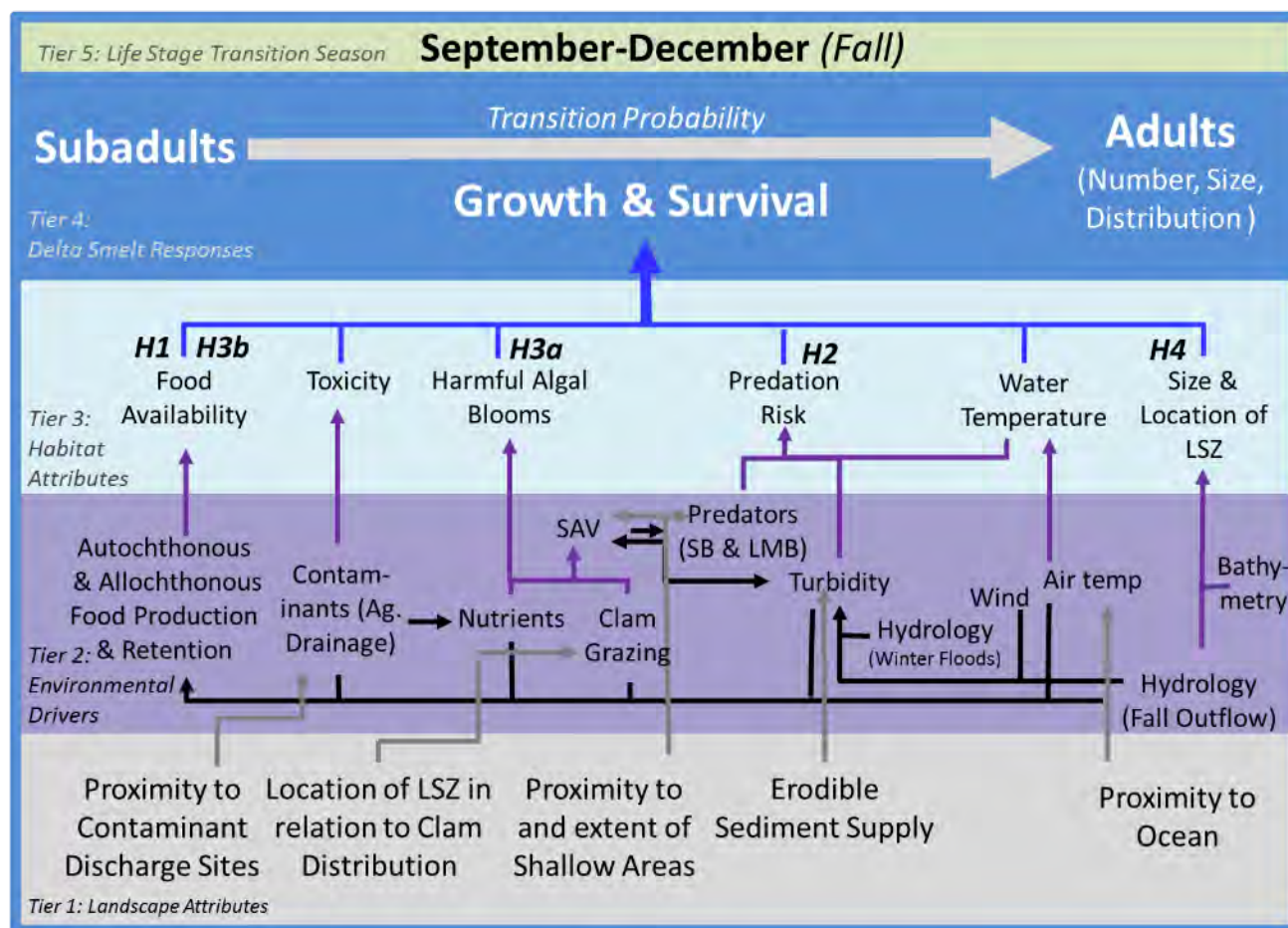


Figure 13. Conceptual model of drivers affecting the transition from Delta Smelt subadults to adults. Hypotheses addressed in IEP-MAST (2015) are indicated by the “H-number” combinations.

Growth and survival are the foundation of these life stage specific conceptual models. The 2015 IEP-MAST report focused on a subset of the linkages including water temperature, food availability, entrainment risk, predation, harmful algal blooms, and the size and location of the LSZ (Figures 10-13). The important linkages vary from season to season based on the relative importance of environmental drivers. These linkages form the basis for the predictions below. High flows in winter and spring are expected to transport fine sediments from upstream areas, increasing the erodible sediment supply for resuspension in summer and fall, providing turbidity. High outflow moves LSH into Suisun Bay (X2<74 km), which may indirectly influence Delta Smelt growth and survival via several linkages in the conceptual model. Water temperatures tend to be cooler in western Suisun Bay compared to the Delta in summer and fall so fish movement toward low-salinity habitat in those seasons may limit exposure of Delta Smelt to stressful water temperatures. Lower temperatures and higher flows also inhibit the

formation of harmful algal blooms. Production of phytoplankton and zooplankton is hypothesized to be higher in Suisun Bay because of the greater area of shoals available. Also, there is often a large difference between the spring and summer-fall distribution of invasive clams, which can interact with clam life history to reduce clam recruitment and subsequent grazing rates on phytoplankton and zooplankton. Note that detailed explanations and supporting information for the linkages and processes contained in Figures 9-13 are available in IEP-MAST (2015).

Predictions

The FLASH conceptual model (Figure 8) was used to generate a number of predictions (Table 2) related to the possible effects of 2011 high flows on low-salinity habitat for Delta Smelt and Delta Smelt response to those conditions. Available data were then used to assess whether the predictions about the effects of the high flows of 2011 were upheld. Unfortunately, few of the predictions could be evaluated based on the data available. In some cases, this was because certain variables were not monitored. In other cases, samples collected in 2011 were not processed and the data interpreted in time to be included in the assessment. Also, the predictions were focused on the low-salinity zone rather than the entirety of Delta Smelt habitat.

Table 2. Assessments of predicted qualitative and quantitative outcomes for September to October of the fall Reasonable and Prudent Alternative action based on 3 levels of the action (modified from U.S. Bureau of Reclamation 2012). The years considered representative of the 3 levels of action are indicated. Green means that data supported the prediction and red means the prediction was not supported. Gray indicates that data were not yet available to support a conclusion. No shading indicates there were no data to assess. From Brown et al. (2014). Refer to Brown et al. (2014) for details of prediction assessments.

	Predictions for X2 scenarios		
	85 km	81 km	74 km
		Year used to test prediction	
	2010	2005, 2006	2011
Variable (Sep-Oct)	(X2=85)	(X2=83,82)	(X2=75)
Dynamic Abiotic Habitat Components			
Average Daily Net Delta Outflow	~5000 cfs	~8000 cfs	11400
Surface area of the fall LSZ	~ 4000 ha	~ 5000 ha	~ 9000 ha
Delta Smelt Abiotic Habitat Index	3523	4835	7261
San Joaquin River Contribution to Fall Outflow	0	Very Low	Low
Hydrodynamic Complexity in LSZ	Lower	Moderate	Higher
Average Wind Speed in the LSZ	Lower	Moderate	Higher
Average Turbidity in the LSZ	Lower	Moderate	Higher
Average Secchi Depth in the LSZ	Higher	Moderate	Lower
Average Ammonium Concentration in the LSZ	Higher	Moderate	Lower
Average Nitrate Concentration in the LSZ	Moderate	Moderate	Higher
Dynamic Biotic Habitat Components			
Average Phytoplankton Biomass in the LSZ (excluding Microcystis)	Lower	Moderate	Higher
Contribution of Diatoms to LSZ Phytoplankton Biomass	Lower	Moderate	Higher
Contribution of Other Algae to LSZ Phytoplankton biomass at X2	Higher	Moderate	Lower
Average Floating Microcystis Density in the LSZ	Higher	Moderate	Lower
Phytoplankton biomass variability across LSZ	Lower	Moderate	Higher
Calanoid copepod biomass in the LSZ	Lower	Moderate	Higher
Cyclopoid copepod biomass in the LSZ	Lower	Moderate	Moderate
Copepod biomass variability across LSZ	Lower	Moderate	Higher
<i>Potamocorbula</i> biomass in the LSZ	Higher	Moderate	Lower
Predator Abundance in the LSZ	Lower	Moderate	Higher
Predation Rates in the LSZ	Lower	Moderate	Higher
Delta Smelt (DS) Responses			

DS caught at Suisun power plants	0	0	Some
DS in fall SWP & CVP salvage	Some	0	0
DS center of distribution (km)	85 (77-93)	82 (75-90)	78 (70-85)
DS growth, survival, and fecundity in fall ^a	Lower	Moderate	Higher
DS health and condition in fall	Lower	Moderate	Higher
DS Recruitment the next year	Lower	Moderate	Higher
DS Population life history variability	Lower	Moderate	Higher

^a Only survival from summer to fall as the ratio of the fall midwater-trawl survey population index to the summer townet survey population index was assessed.

The IEP-MAST (2015) conceptual model covers the entire range of Delta Smelt habitat and also identifies hypotheses about how abiotic and biotic habitat can affect Delta Smelt and the probability of individuals transitioning from one life stage to the next (Figures INTRO 10-13). However, the IEP-MAST (2015) model was not formulated to address specific flow conditions, so does not directly lead to predictions. Also, the IEP-MAST (2015) model contains many hypotheses about how certain processes work in the environment. Many of these hypotheses were supported with available data; however, other hypotheses could benefit from additional scrutiny.

For this report, we formulated a number of basic predictions about the likely effects of high flows in 2017 on Delta Smelt and their habitat (Table 3) based largely on the IEP-MAST (2015) model but also considering the results from the FLaSH studies (Brown et al. 2014). In addition to evaluating these predictions, additional information addressing processes and mechanisms in the IEP-MAST (2015) model or considered important to management of Delta Smelt may also be presented.

Table 3. Predictions regarding the effects of high flows on Delta Smelt and Delta Smelt habitat. The comparisons are relative (i.e., higher or lower) and based on position of X2, either near the confluence of the Sacramento and San Joaquin Rivers or near Suisun Bay.

2017 FloAT MAST Prediction Table		
Variable (September-October)	Fall X2 location	
	Sac-San Joaquin confluence	Suisun region
<i>Dynamic abiotic habitat components</i>		
Delta Smelt physical habitat	Lower	Higher
Low-salinity habitat	Smaller area	Larger area
Turbidity	Lower	Higher
Delta Smelt habitat index (based on turbidity, salinity, and hydrodynamic complexity in the Suisun Region)	NA	Similar among post-POD wet years
Water temperature in low-salinity habitat	Higher	Lower
<i>Dynamic biotic habitat components</i>		
Phytoplankton - food availability for zooplankton	Lower	Higher
Harmful algal blooms	Increase	Decrease
Zooplankton - food availability for Delta Smelt	Lower	Higher
Clam biomass and grazing rate	Higher	Lower
Aquatic Vegetation (floating and submerged aquatic vegetation)	Increase in Water Hyacinth, unknown for other species	Decrease in Water Hyacinth, unknown for other species
Fish assemblage – biomass of pelagic fishes	Lower	Higher
<i>Delta Smelt responses</i>		
Growth rate	Lower	Higher
Life history diversity (freshwater vs. LSZ); timing of migration to brackish water	Lower	Higher
Health metrics (liver and gill condition)	Poor	Good
Feeding success (diet); prey composition	Poor	Good
Delta Smelt range/distribution	More constricted	Wider distribution
Delta Smelt survival in the fall months	Lower	Higher

Methodology

We used a qualitative weight of evidence approach to evaluate each of the predictions (i.e., lines of evidence) listed in Table 3. For each prediction, we reviewed the available information and made a judgment about whether the prediction was supported by the available data. Note that we evaluated the predictions based on other years in addition to 2017. It is possible that a prediction is upheld, for example, in one wet year but not another. This prediction would be considered unsupported because the response is not consistent with regard to the effect of flow. Methods of analysis ranged from simple graphical and statistical comparisons of monitoring data to evaluation of model outputs from complex hydrodynamic models and statistical analyses. The data sources and methods used to evaluate each prediction are included in the text if the information is relatively simple or in Appendices if the material is complex or requires extensive explanation and is not available in a published source. Appendices for topics differ in content and complexity. The main purpose of the Appendices is to provide a place for details about data, methods, and results that will mainly be of interest to technical specialists. This allows us to provide a more succinct presentation of results relevant to the evaluation of the prediction. In many cases, there was only one data stream appropriate for evaluating the prediction. When more than one data stream was available, the results from each data stream were qualitatively weighted based on best professional judgement.

For the purposes of this report, we defined fall as the months of the fall midwater-trawl (FMWT) survey (September-December), which generally begins in September and ends by mid-December. Our evaluation of predictions relied heavily on agency collected monitoring data (Table 4) because those were the data available at the time, but this does not reflect any preference for those data. Note that data can include actual measurements, calculations from measurements, or the output of models (Table 4). Details of agency monitoring programs were previously described by Brown et al. (2014) and are not repeated here. Previously undescribed agency monitoring programs include Enhanced Delta Smelt Monitoring (Table 4, see Appendix 1 for details) and the Delta Juvenile Fish Monitoring Program seining survey (see Mahardja et al. 2017 for a description).

Table 4. Selected data sources used in this report. More detailed methods can be found in appendices associated with specific topics. Abbreviations: CDFW, California Department of Fish and Wildlife; DWR, California

Department of Water Resources; X2, the horizontal distance in kilometers up the axis of the estuary to where tidally averaged near-bottom salinity is 2; CDEC, California Data Exchange Center.

Data source			
Type of data	Responsible agency	Data type	
DayFlow			
Delta average daily outflow	DWR	Calculation	
X2	DWR	Calculation	
CDEC			
Continuous water temperature	DWR	Measurement	
ANCHOR QEA, LLC			
Maps of Delta salinity	ANCHOR QEA, LLC	Model output	
Maps of Delta water temperature	ANCHOR QEA, LLC	Model output	
Maps of Delta turbidity	ANCHOR QEA, LLC	Model output	
Maps of Delta Smelt habitat suitability	ANCHOR QEA, LLC	Model output	
Fall Midwater Trawl			
Delta Smelt abundance index	CDFW	Calculation	
Water temperature	CDFW	Measurement	
Specific conductance	CDFW	Measurement	
Secchi depth	CDFW	Measurement	
Turbidity	CDFW	Measurement	
<i>Microcystis</i> occurrence	CDFW	Measurement	
Diet data	CDFW	Measurement	
Center of distribution	CDFW	Calculation	
Environmental Monitoring Program			
Phytoplankton	DWR	Measurement	
Chlorophyll- <i>a</i>	DWR	Measurement	
Zooplankton abundance	CDFW	Measurement	
CDFW fish sampling			
Spring Kodiak Trawl Delta Smelt abundance index	CDFW	Calculation	
20-mm survey Delta Smelt abundance index	CDFW	Calculation	
Summer Townet survey Delta Smelt abundance index	CDFW	Calculation	
USFWS fish sampling			
Enhanced Delta Smelt Monitoring	USFWS	Measurement	
Delta Juvenile Fish Monitoring Program, seine survey	USFWS	Measurement	
UC Davis necropsy and tissue analysis			
Otolith microchemistry	UC Davis	Instrumentation	
Morphometric data	UC Davis	Measurement	
Histopathology	UC Davis	Microscopy	

We included analyses of data from other years besides 2017 because our approach is comparative. We included 2006 and 2011 because they are the most recent wet years preceding 2017. As already noted, we recognized that preceding habitat conditions can have important implications for the response of Delta Smelt to fall conditions during any particular year; therefore, we also considered data from other seasons, primarily summer, and other years.

The data analyses focused on calendar years rather than water years. A water year begins on October 1 of the preceding year and ends on September 30. Thus, for analysis of a selected calendar year, we included data from January 1 to September 30, which is the overlap of water year and calendar year, plus the first 3 months of the following water year, October 1 to December 31. We mainly focus on the POD period that started when fish abundances of Delta Smelt and three other pelagic species in the SFE suddenly dropped in about 2002 and have remained very low (Baxter et al. 2010, Thomson et al. 2010). In contrast to Brown et al. (2014), we did not stratify all analyses by salinity because freshwater residence is now recognized as an important aspect of Delta Smelt life history diversity (IEP-MAST 2015, Bush 2017, Hobbs et al. 2019a). Results from other ongoing research efforts were included as appropriate. When such data were not yet available from publicly available interim or final reports, the data will be included in an Appendix.

Evaluations of Predictions

The spring of 2017 was wet, with high outflows that resulted in the LSZ being located at the western border of Suisun Bay ($X2 < 55$ km) (Figure 14). Delta outflow dropped rapidly in June and $X2$ increased to about 75 km by the end of July (Figure 14). $X2$ remained between 74 and 81 km through December.

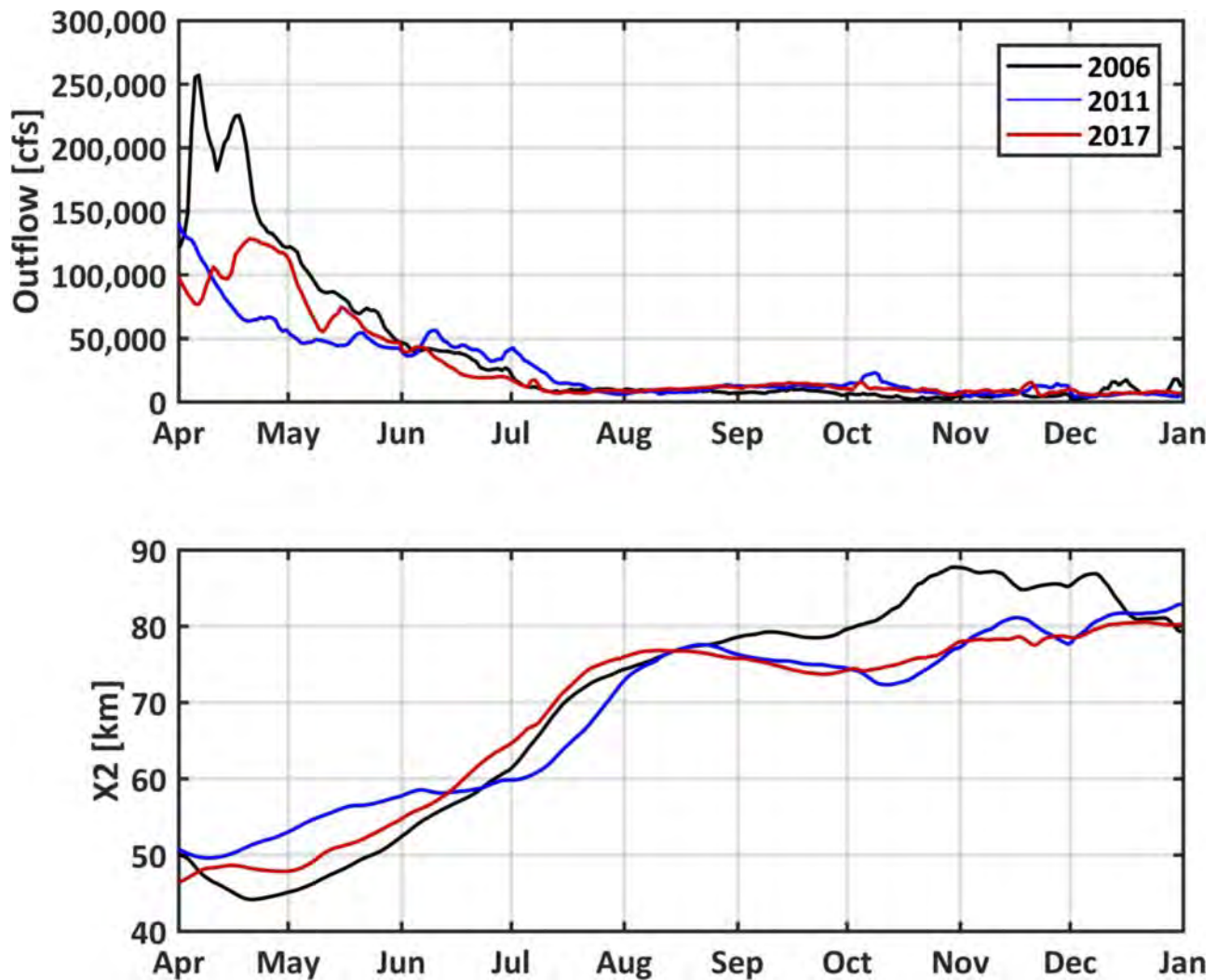


Figure 14. Delta outflow and X2 computed using the DAYFLOW X2 equation for April through December 2006, 2011, and 2017.

Dynamic abiotic habitat components

In this section, we address the distribution of physical habitat conditions in the estuary. The basic prediction is that physical habitat conditions are better for Delta Smelt when the low-salinity zone (indexed by X2) is located in Suisun Bay (Brown et al. 2014) during the fall. We specifically address this prediction for salinity, water temperature, and turbidity. We also calculate the Delta Smelt physical habitat index (habitat index) from Bever et al. (2016). The habitat index considers salinity, turbidity, and depth averaged maximum daily water velocity, as a measure of hydrodynamic conditions.

We assessed the predictions using simple analyses of environmental data collected during the Summer Townet (STN) and FMWT surveys. We analyzed data by month for July and August from STN data and for September-December from FMWT data (graphs and Kruskal-Wallis comparisons among years, water year types, and salinity zones; see Appendix 3). For salinity, we expected lower values across the sampling area in wetter years when the LSZ was located in Suisun Bay. For turbidity, we expected higher values in wetter years because of increases in erodible sediment supply resulting from increased sediment deposition in winter and spring, assuming other important factors, particularly wind, are the same. For water temperature, we expected lower values as the LSZ moved westward toward cooler temperatures in western Suisun Bay. In graphical analysis of water temperature, we separated freshwater from the LSZ. For some statistical analysis we combined freshwater with the low salinity zone to encompass habitat for freshwater resident Delta Smelt.

We also conducted detailed comparisons of the three wet years during the post-POD period to determine if there were differences in physical habitat that might account for differences in response of the Delta Smelt population. The UnTRIM Bay-Delta model (MacWilliams et al. 2015) was used to predict salinity, temperature, and turbidity during the period from June 1 through December 31, 2017, and for the same months in 2006 and 2011 (see Appendix 2 for details). The UnTRIM Bay-Delta model is a three-dimensional hydrodynamic model of San Francisco Bay and the Sacramento-San Joaquin Delta (MacWilliams et al. 2015) developed using the UnTRIM hydrodynamic model (Casulli 2009). The UnTRIM Bay-Delta model has been calibrated using water level, flow, salinity, and turbidity data collected in San Francisco Bay and the Delta in numerous previous studies (e.g., MacWilliams et al. 2008, MacWilliams and Gross 2010, MacWilliams et al. 2015, Bever et al. 2018).

Salinity tended to be lowest in wetter years in July, August, and September (Figure 15). October was somewhat variable. In November and December there appeared to be no obvious patterns among years and differences were small (all differences significantly different among years $P < 0.001$). The same patterns were visible when data were analyzed by water year type (Figure 16). The system is freshest during wet years and most saline during critically dry years (all differences significantly different among water year types $P < 0.001$).

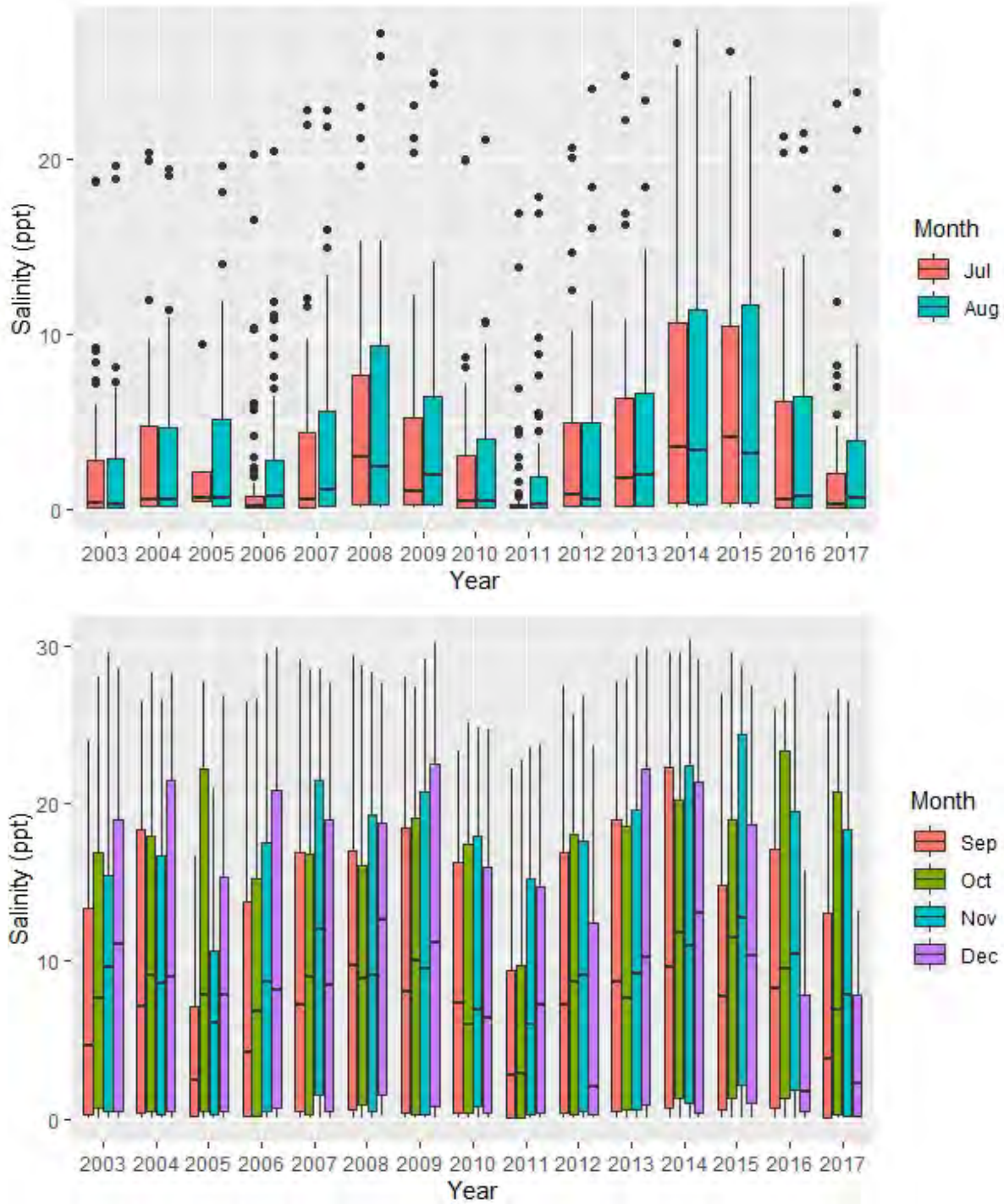


Figure 15. Salinity in A) July and August collected by California Department of Fish and Wildlife Summer Towntnet Survey and B) in September-December collected by California Department of Fish and Wildlife FMWT at index stations during 2003-2017. Water Year Type per Sac Valley Index across top of figure.

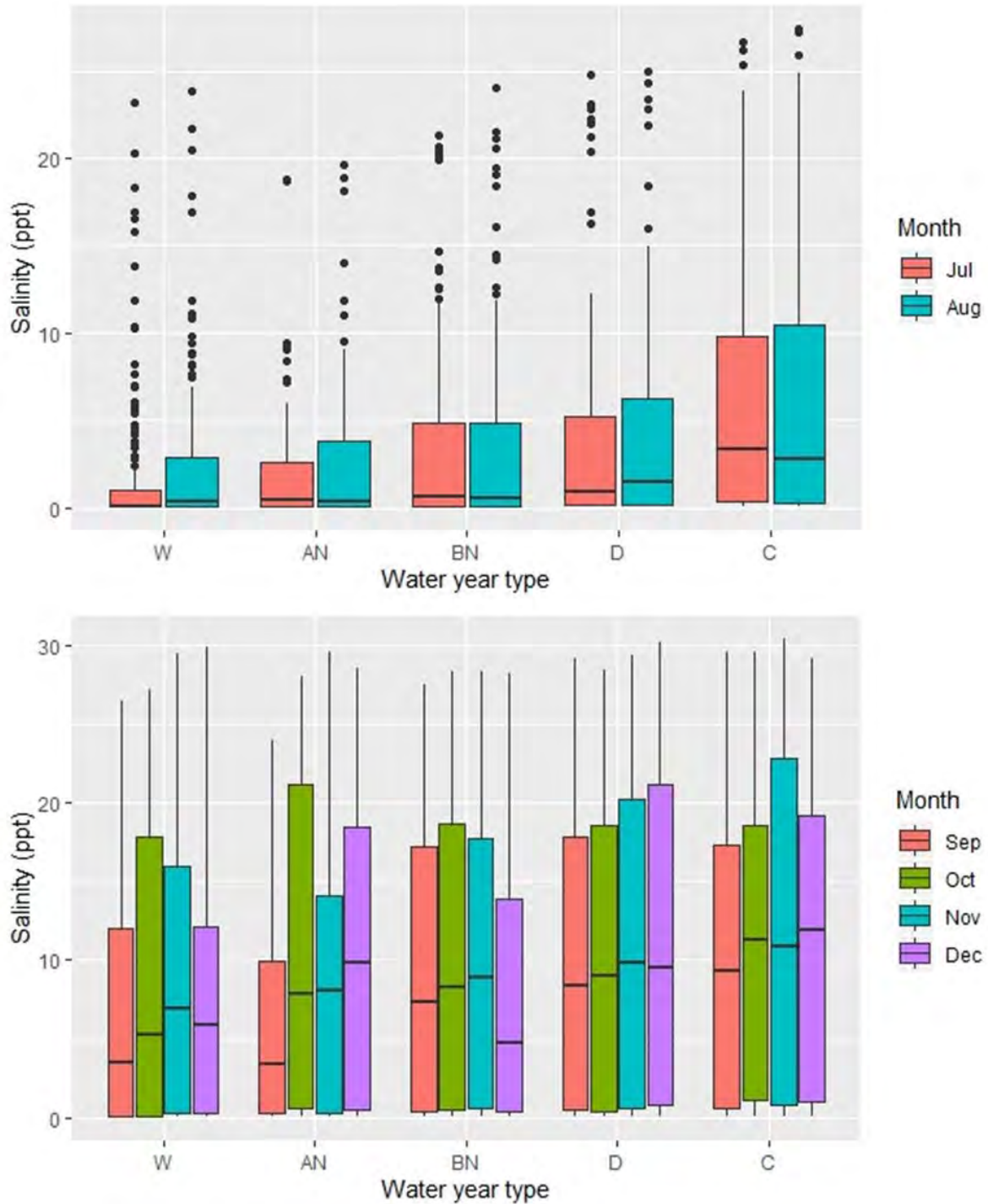


Figure 16. Salinity by water type for A) July and August collected by California Department of Fish and Wildlife Summer Townet Survey and B) in September-December collected by California Department of Fish and Wildlife FMWT at index stations during 2003-2017. Water Year Type per Sac Valley Index.

Water temperatures in waters less than salinity 6 were significantly different among years for all months (all $P < 0.001$); however, there were no clear patterns among years (Figures 17 and 18). Wet years could be warm (July 2006 and July and August 2017) or cool (2011) compared to other years. Water temperatures were highest in July in freshwater. Differences among years and salinity zones decreased through October (Figures 17 and 18). There was a consistent gradient from warm freshwater to cooler brackish water for July to September (Figures 17 and 18). All measured water temperatures were below 20°C in November and December (Appendix 3), indicating no potential for temperature stress.

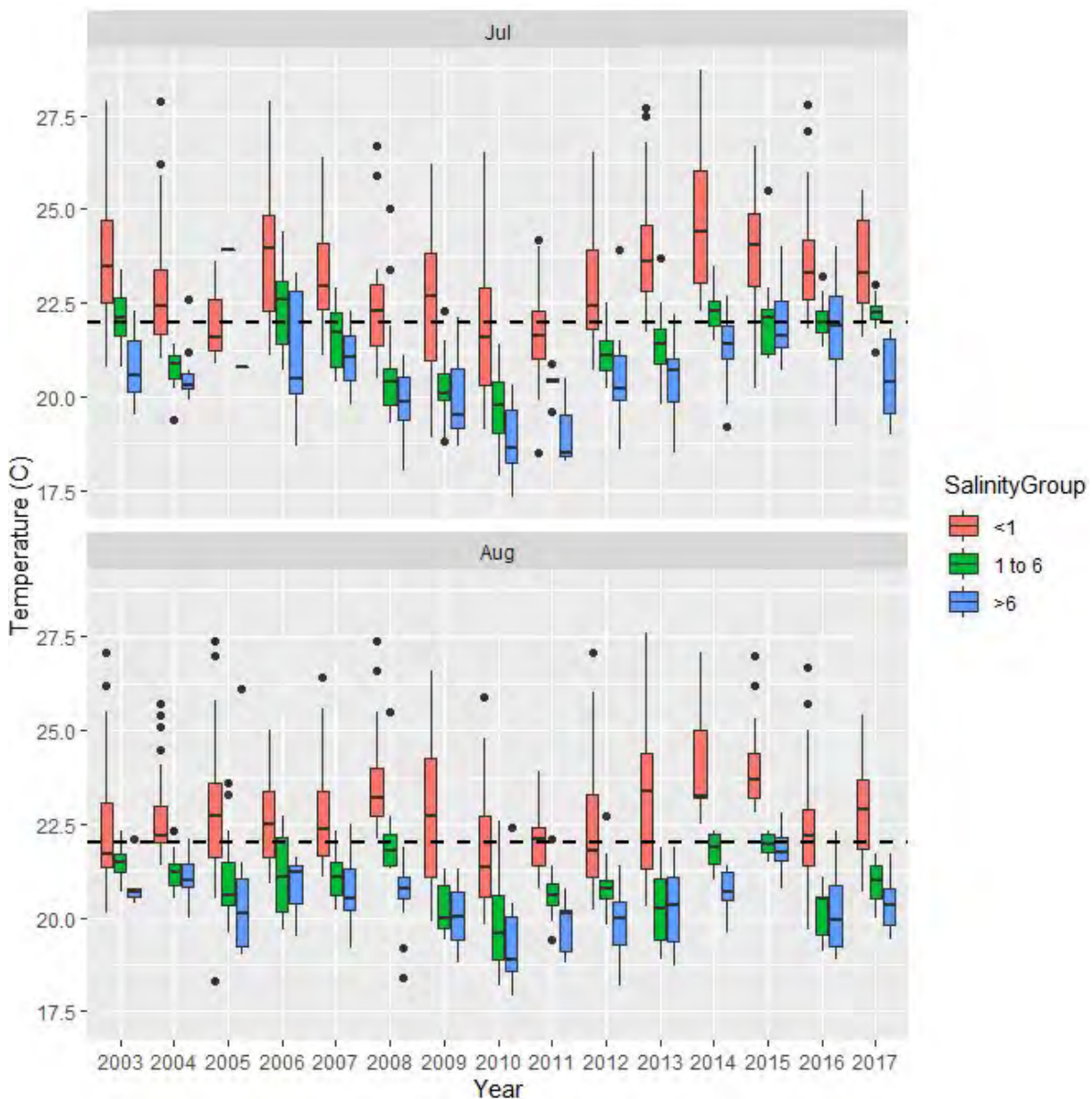


Figure 17. Water temperature at sites with salinity <1, 1-6, and ≤ 6 for A) July and B) August collected by California Department of Fish and Wildlife Summer Towntnet Survey at index stations during 2003-2017. Water Year Type per Sac Valley Index across top of figure. The dashed line designates 22°C.

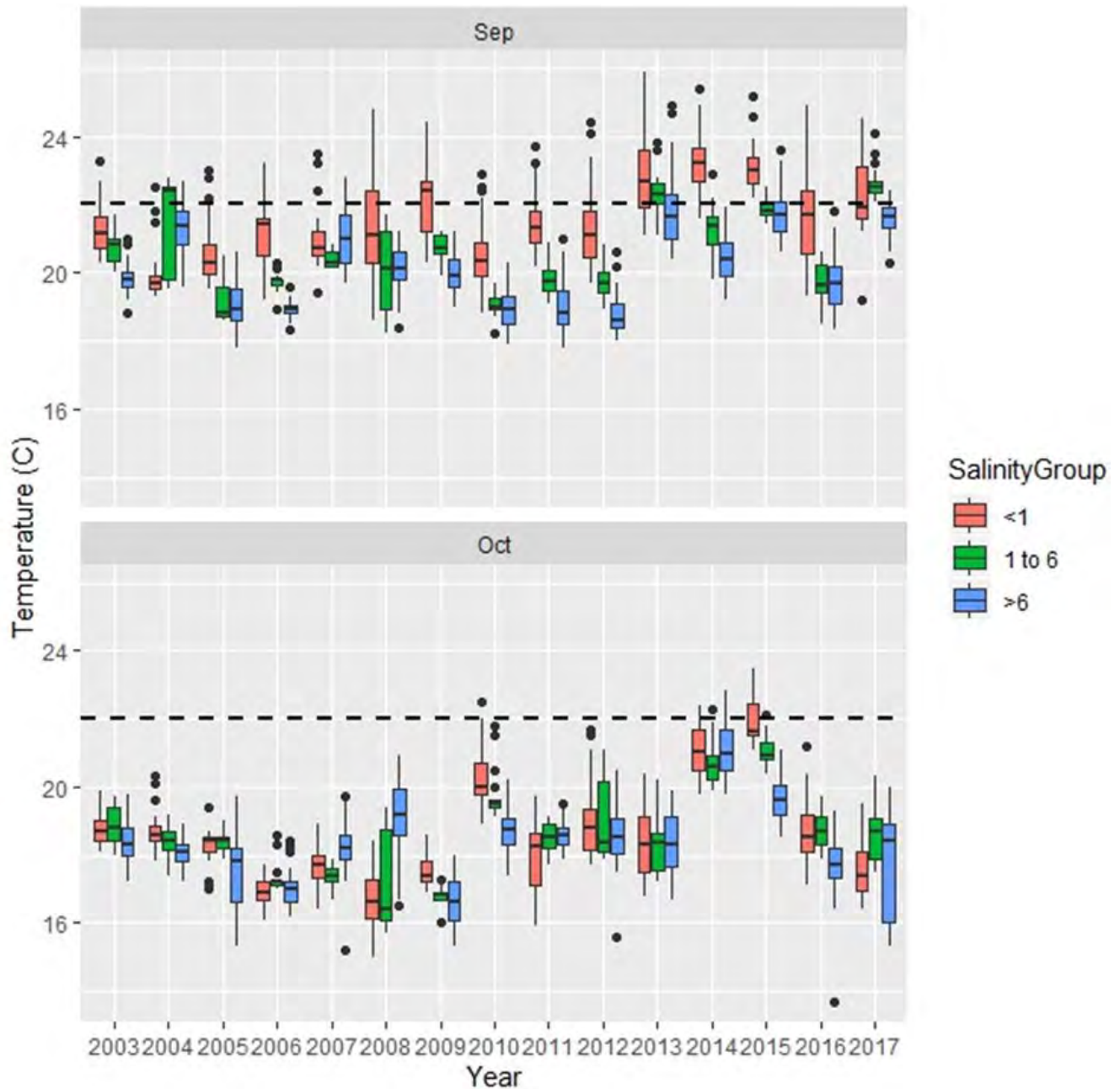


Figure 18. Water temperature at sites with salinity <1, 1-6, and ≤ 6 for A) September and B) October collected by California Department of Fish and Wildlife Fall Midwater Trawl Survey at index stations during 2003-2017. Water Year Type per Sac Valley Index across top of figure. The dashed line designates 22°C.

Secchi depths were statistically different among years for all months (all $P < 0.001$; Appendix 3); however, there did not appear to be any obvious pattern among years or water year type (Figures 19

and 20). There did seem to be a general pattern for greater Secchi depth measurements over time, but this is somewhat complicated by limited ability to measure Secchi depths greater than 2 m for 2009-2013 during the STN and 2005-2012 during the FMWT survey (Appendix 3). July 2017 Secchi depths were lower than the recent drought years but similar to a variety of water year types from 2003-2008 (except 2007) (Figure 19). When considered on a water year type basis, wet and above normal years appear to be more turbid than other year types in July, August, and September. Above normal years appear to be marginally more turbid than wet years.

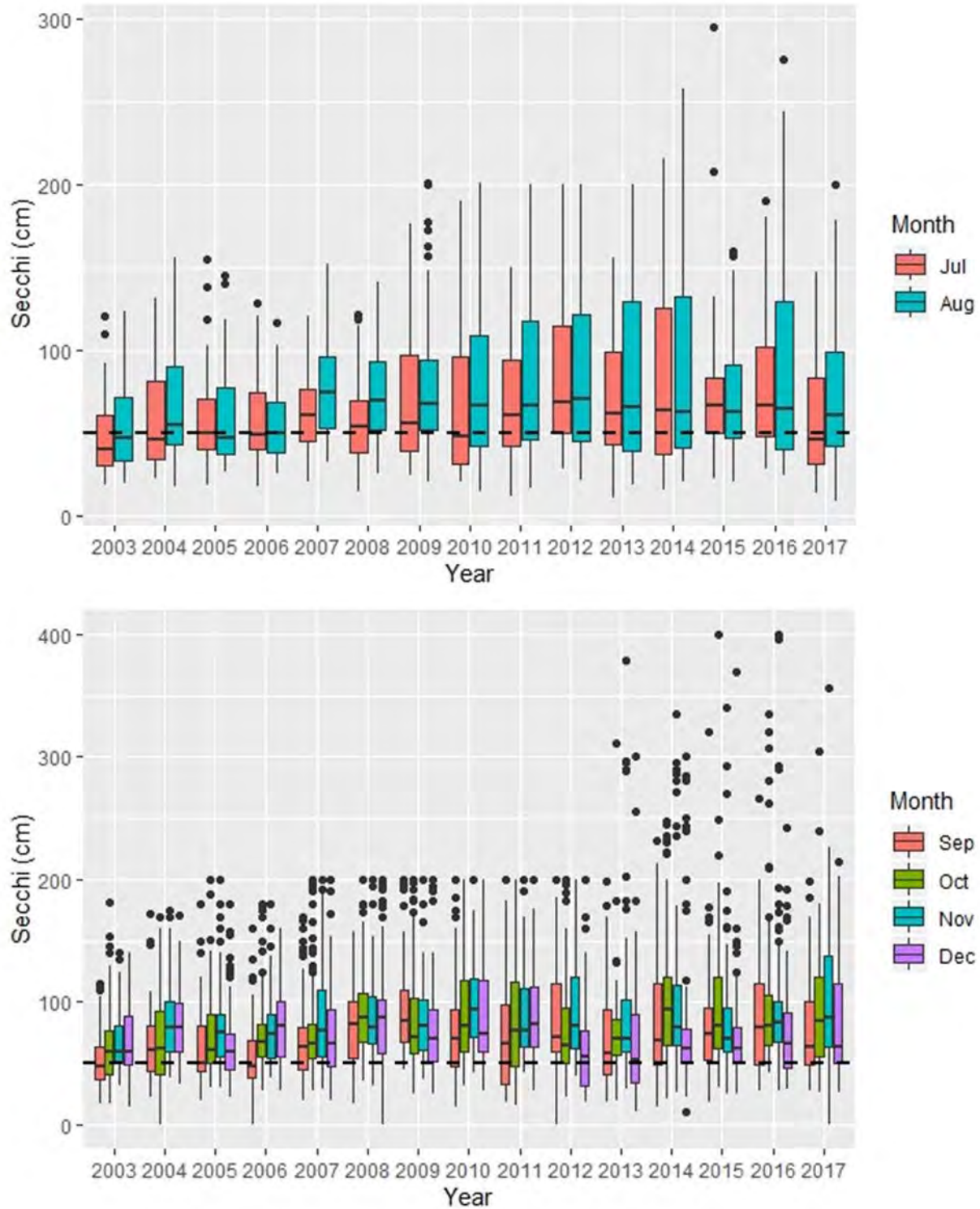


Figure 19. Secchi depth (cm) in A) July and August collected by California Department of Fish and Wildlife Summer Townet Survey and B) in September-December collected by CDFW Fall Midwater Trawl at index stations during 2003-2017. Dotted line denotes 50 cm. Water Year Type per Sac Valley Index across top of figure. Secchi depths were recorded at a maximum value of 200 cm during 2009-2013 for the Summer Townet

Survey and 2005-2012 for the Fall Midwater Trawl. Depth measures >200 cm were possible but occurred infrequently (<3% STN stations and <5% of FMWT samples) and so annual Secchi depths might be biased slightly low these years.

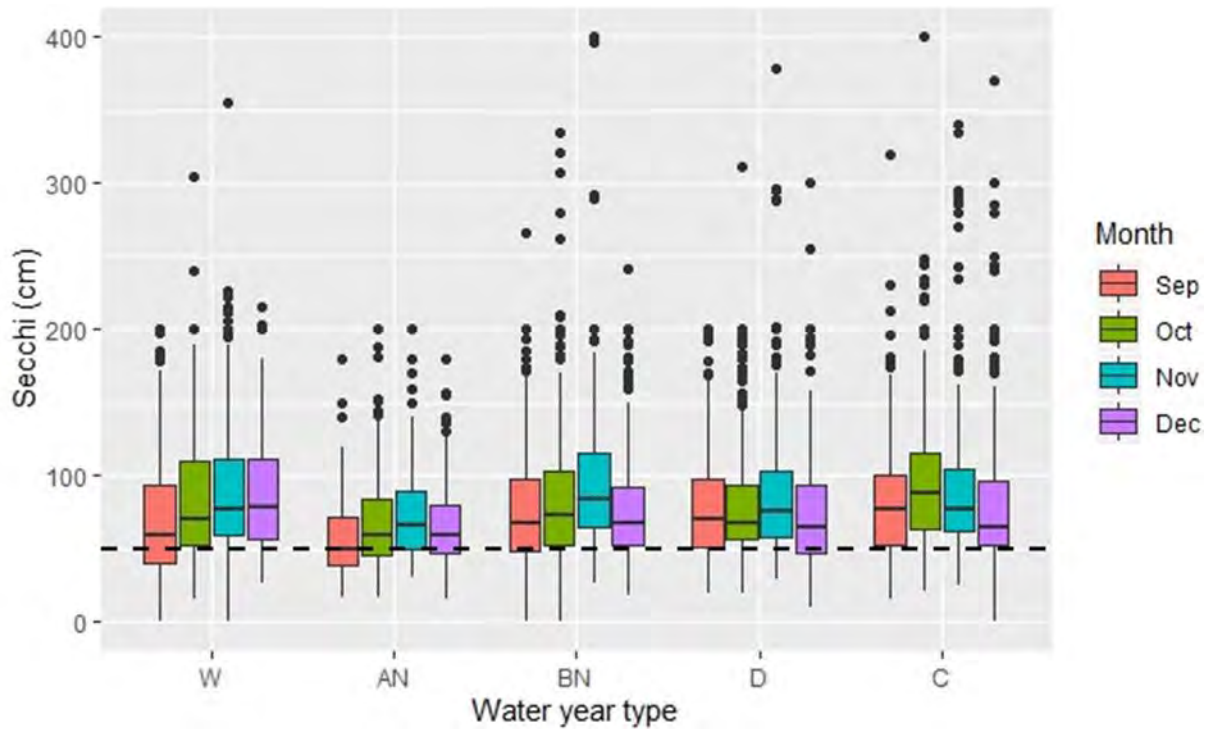
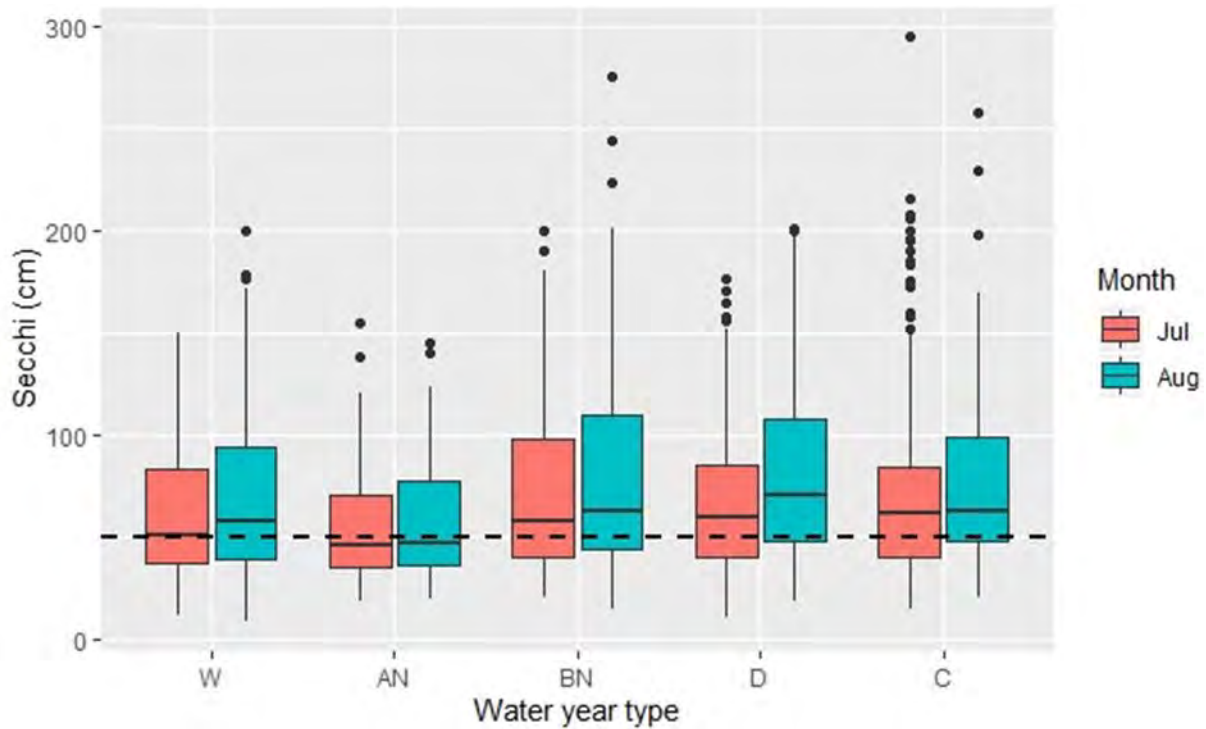


Figure 20. Secchi depth (cm) by water type for A) July and August collected by California Department of Fish and Wildlife Summer Townet Survey and B) in September-December collected by California Department of Fish and Wildlife Fall Midwater Trawl at index stations during 2003-2017. Dotted line denotes Secchi depth of 50 cm. Water Year Type per Sac Valley Index. Secchi depths were recorded at a maximum value of 200 cm during 2009-2013 for the Summer Townet Survey and 2005-2012 for the Fall Midwater Trawl. Depth measures >200 cm were possible but occurred infrequently (<3% STN stations and <5% of FMWT samples) and so annual Secchi depths might be biased slightly low these years.

Overall, the broad spatial and temporal patterns in salinity were similar for the wet years of 2011 and 2017 with 2006 having some differences based on the modeling results (see Appendix 2). Salinity throughout Suisun Bay and the confluence region was less than 6 through mid-July for all 3 years. During July through mid-October 2017, the salinity conditions in Suisun Bay and the confluence region were generally favorable for Delta Smelt, with salinity less than 6 in Grizzly Bay, Honker Bay, Montezuma Slough, and the confluence region (Figure 21). In 2017 and 2006, salinity in the western portion of Suisun Bay increased above 6 from mid-July to late July. In 2011, this increase in salinity in the western portion of Suisun Bay occurred later in the year, from the beginning to the middle of August. The later increase in salinity above 6 in 2011 resulted because Delta outflow in June and July was higher in 2011 than in 2006 and 2017 (Figure 14). Grizzly Bay, Honker Bay, and Montezuma Slough are historically favorable locations for catching Delta Smelt in the FMWT (Bever et al. 2016). The predicted salinity in these areas remained less than 6 until mid-October in 2017, late October in 2011, and until the beginning of October in 2006. Delta outflow in October was lower in 2006 than in the other 2 years, resulting in increased salinity intrusion at the beginning of October 2006 relative to 2017 and 2011 (see Figure 14 for similar response of X2). Salinity during November and December was predicted to be greater than 6 throughout Suisun Bay in each of the 3 wet water years simulated (see Appendix 2).

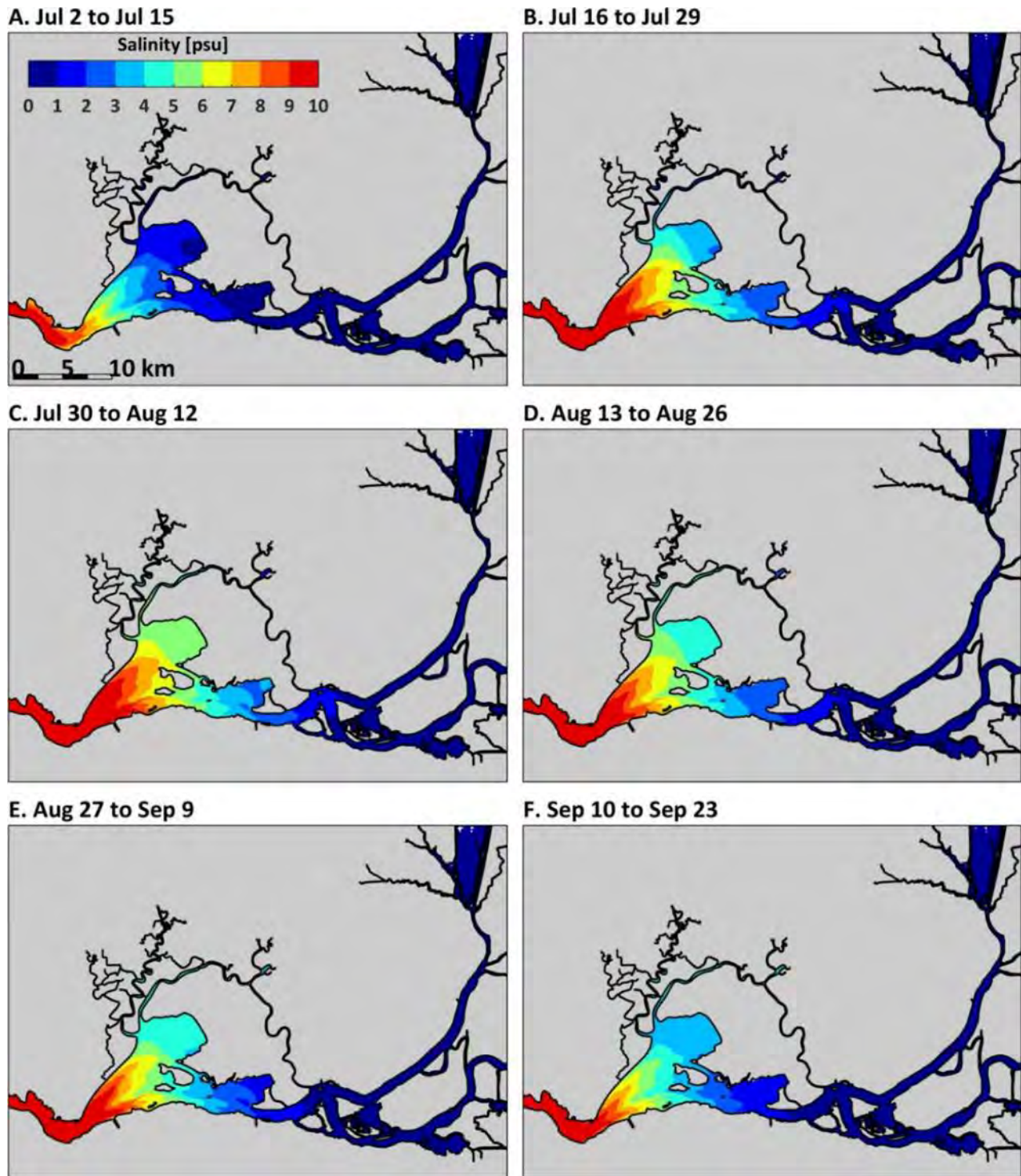


Figure 21. Predicted 2-week-average depth-averaged salinity for 2017 2-week EDSM sampling periods between A) July 2 and July 15; B) July 16 and July 29; C) July 30 to August 12; D) August 13 to August 26; E) August 27 to September 9; and F) September 10 to September 23.

Modeled water temperatures in 2017 were above 20°C for much of the period between mid-June and mid-September, especially near the confluence and upstream areas (Figure 22). The observed temperature at both Emmaton and Jersey Point (Figure 23) indicated that the observed daily averaged temperature at both locations was above 22°C between mid-June and mid-September 2017, with the exception of a short period of about a week towards the end of August (Figure 24). Maximum observed water temperatures at Emmaton were almost always less than 22°C during 2011 (Figure 25). During 2017, the maximum observed water temperatures were less than during 2006 (Figure 25); however, the duration of temperatures above 22°C was much longer in 2017. Based on the observed temperatures, the duration of time in days that the observed temperature exceeded 20, 22, 24, and 26°C was computed (Figure 26). The cumulative time that the water temperature exceeded 20°C was similar for 2011 and 2017 and both were greater than observed in 2006; however, the duration of time that the observed temperature exceeded 22°C was much longer in 2017 compared to 2011 and somewhat longer compared to 2006 (Figure 26). Temperature only exceeded 24°C in 2006 (Figure 26). Similarly, maps developed based on the modeled temperature for these same 3 years indicated a much larger geographic area where temperatures remained above 22°C for greater than 50 to 60 days in 2017 than in either 2006 or 2011 (Figure 27).

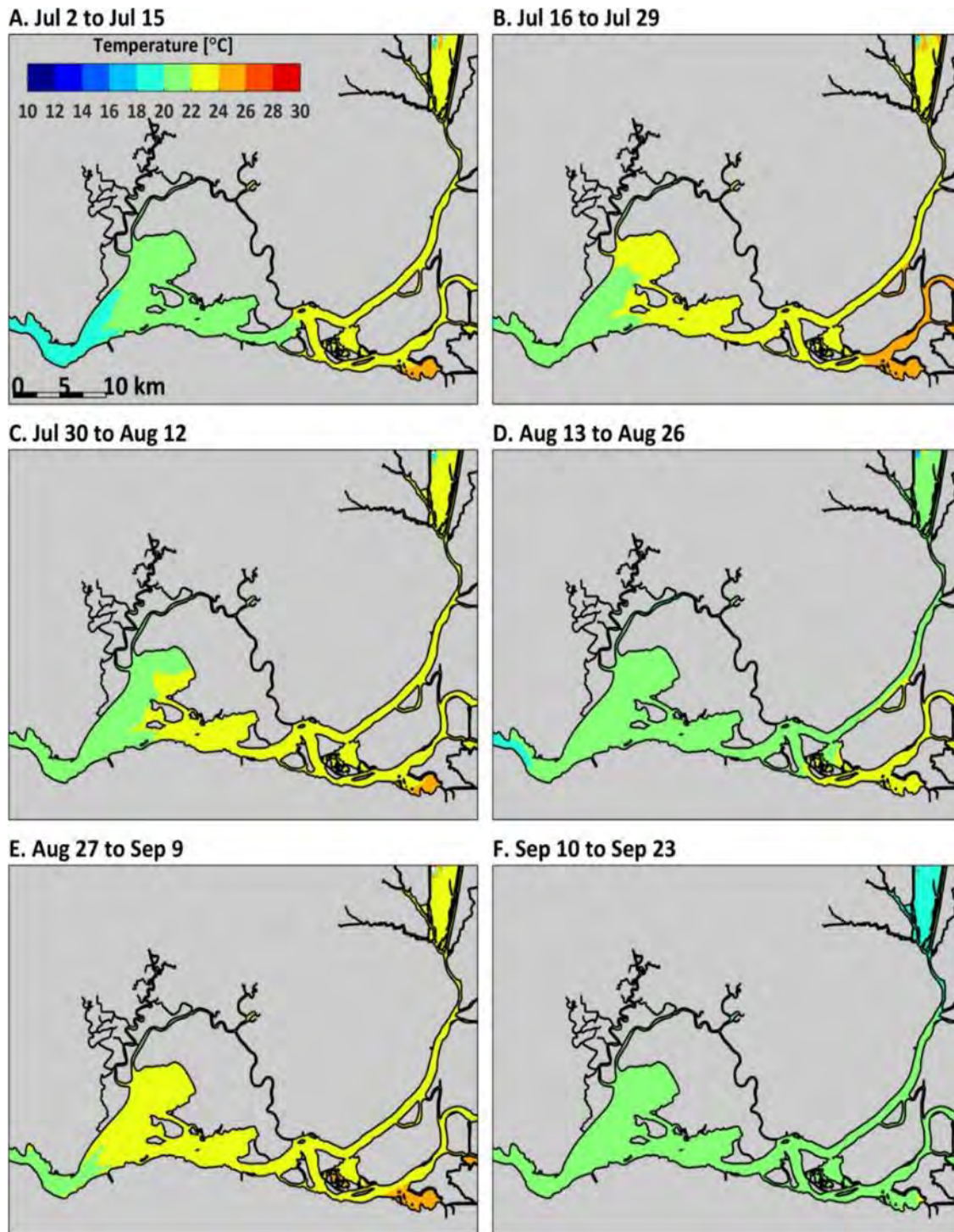


Figure 22. Predicted 2-week-average depth-averaged temperature for 2017 2-week Enhanced Delta Smelt Monitoring sampling periods between A) July 2 and July 15; B) July 16 and July 29; C) July 30 to August 12; D) August 13 to August 26; E) August 27 to September 9; and F) September 10 to September 23.

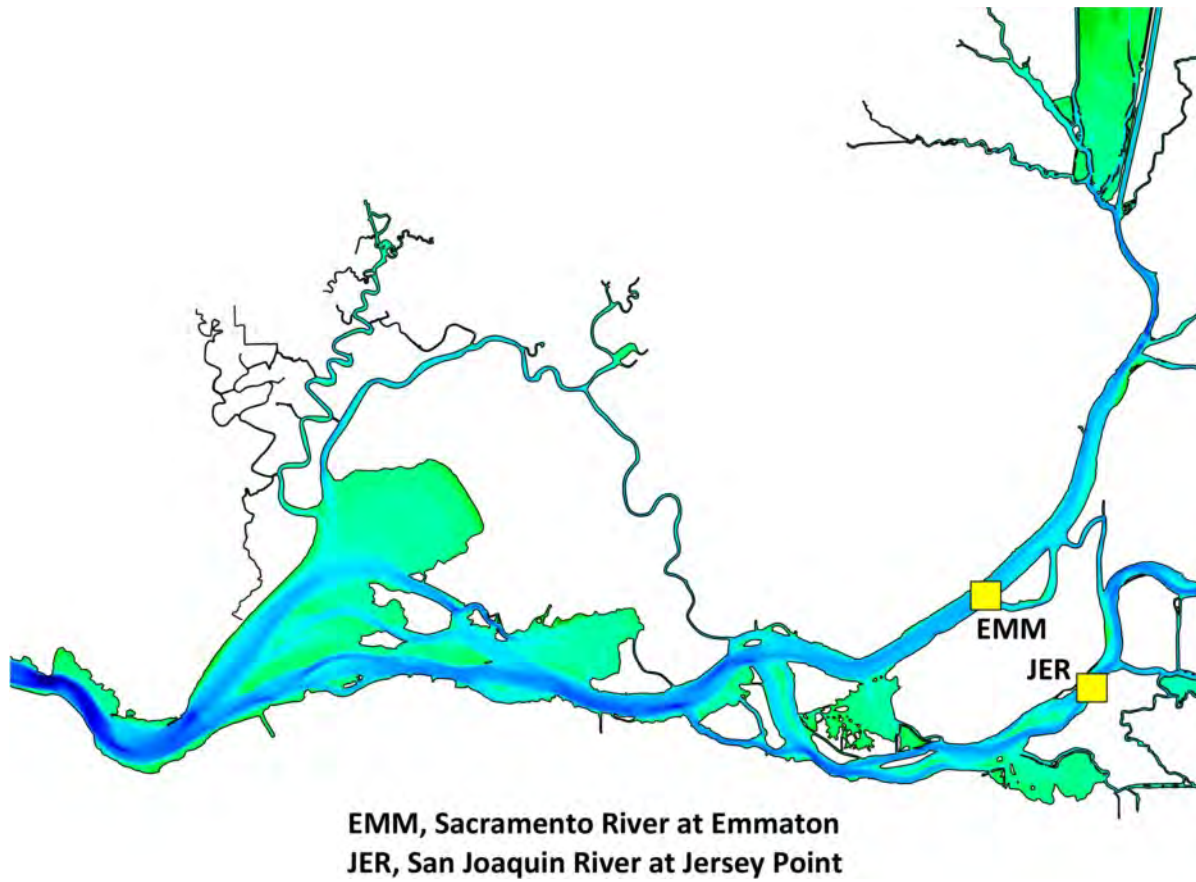


Figure 23. Emmaton and Jersey Point continuous monitoring locations.

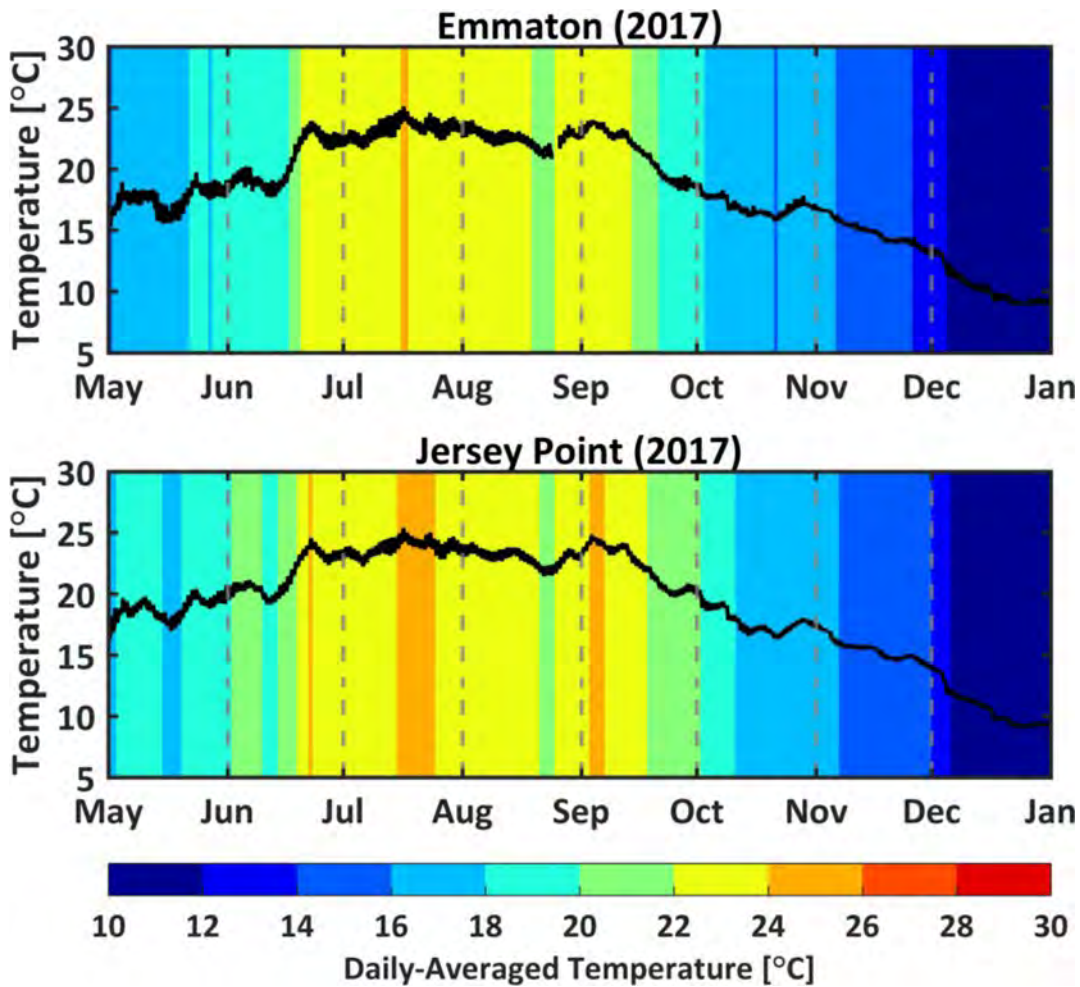


Figure 24. Observed hourly water temperature at Emmaton (top) and Jersey Point (bottom) from May through December 2017 (black lines). Color shading indicates observed daily averaged temperature.

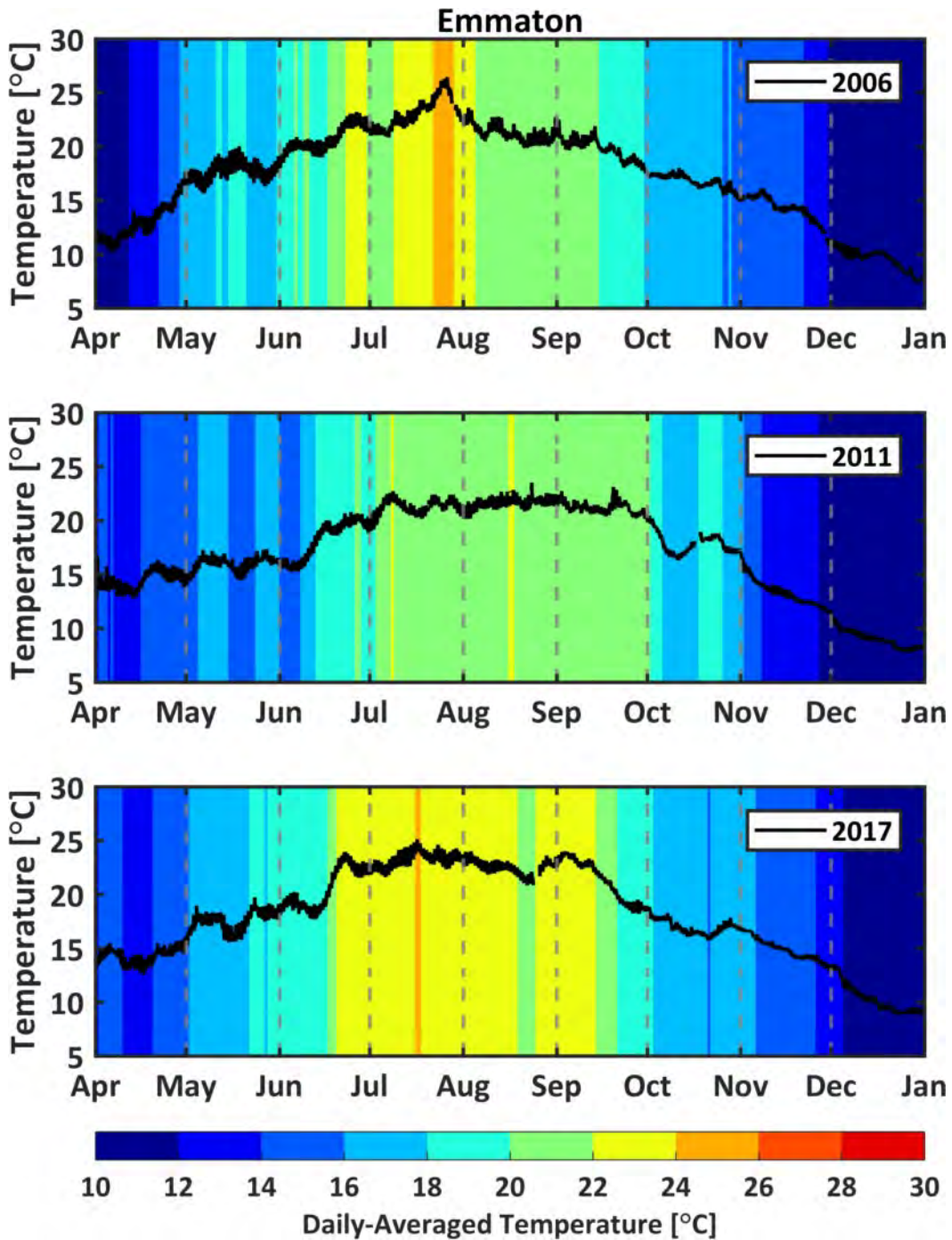


Figure 25. Observed hourly water temperature at Emmaton from April through December for 2006 (top), 2011, (middle), and 2017 (bottom). Color shading indicates observed daily averaged temperature.

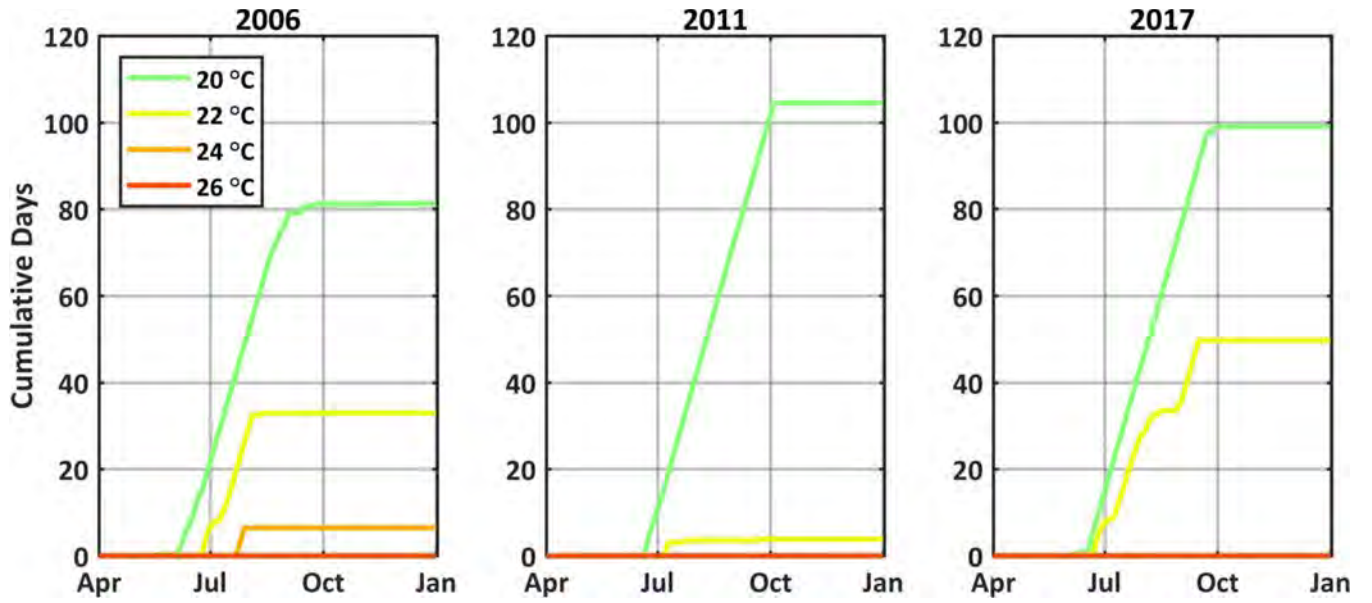


Figure 26. Cumulative time in days that the observed water temperature exceeded 20, 22, 24, and 26°C at Emmaton from April through December for 2006 (left), 2011, (middle), and 2017 (right).

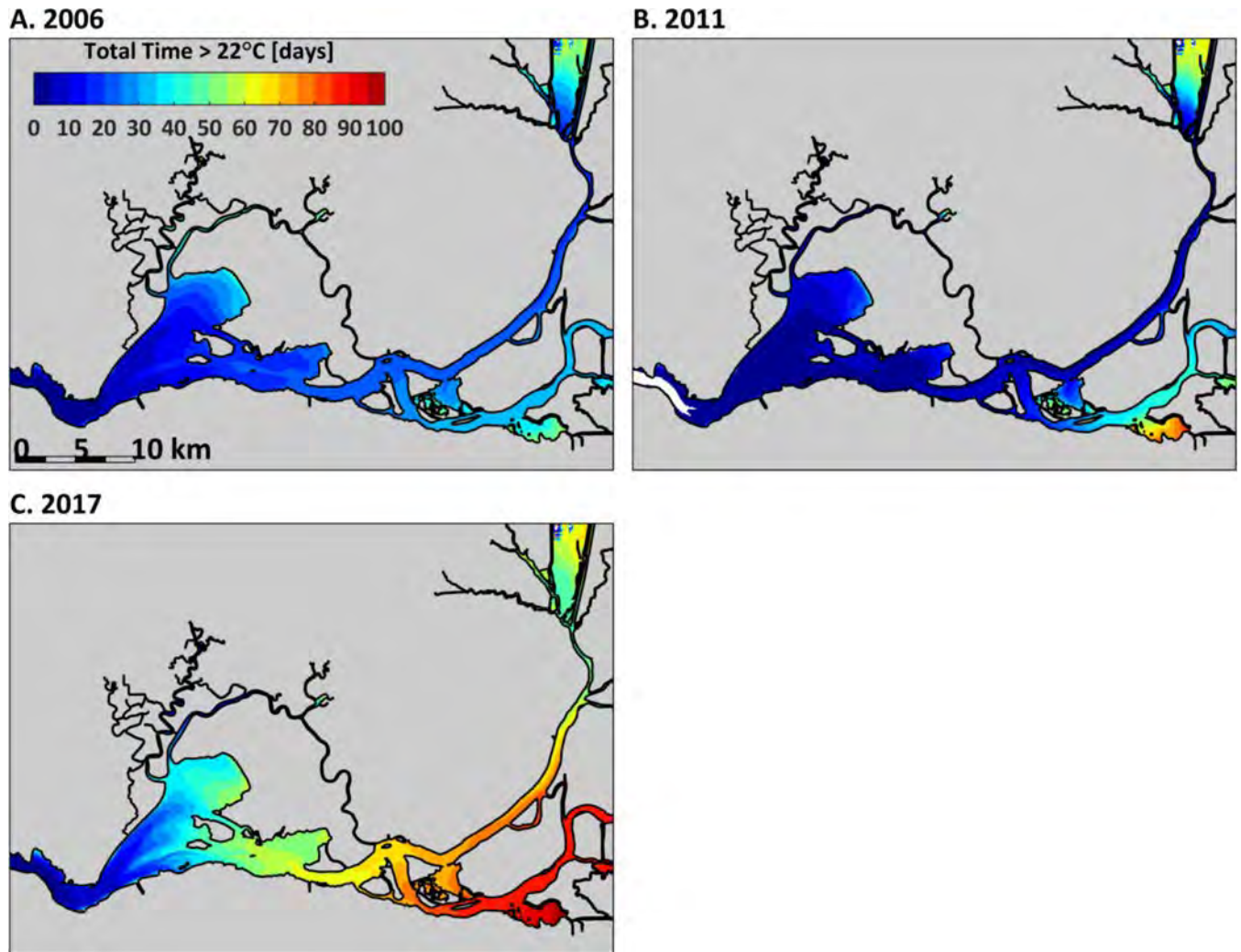


Figure 27. Cumulative time in days that the predicted water temperature exceeded 22°C from April through December for A) 2006; B) 2011; and C) 2017. White areas indicate the predicted water temperature never exceeded 22°C.

Previous studies have documented that Delta Smelt catch is often correlated to Secchi depth and turbidity (Feyrer et al. 2007, Sommer and Mejia 2013, Mahardja et al. 2017), with Delta Smelt generally not present when turbidity is less than about 12 NTU (Grimaldo et al. 2009, Sommer and Mejia 2013, Castillo et al. 2018). In the SFE, turbidity is correlated to the amount of sediment suspended in the water column. During the summer and fall, turbidity in Suisun Bay and the confluence region is driven by wind-wave resuspension of fine sediment from shallow areas and resuspension and transport by tidal currents in the deeper channels (Ruhl and Schoellhamer 1999, 2004, Bever et al. 2018). It is expected that differences in summer to fall turbidity between the wet

years of 2006, 2011, and 2017 will be more strongly influenced by differences in environmental conditions (i.e., wind) than by long-term changes to the sediment bed or tributary sediment supply within the post-POD period. Wind speed and direction over Suisun Bay varied seasonally and by year (Figure 28). Wind speeds were higher during the summer than in the fall. In summer 2017, wind blew predominantly toward the northeast, with winds slower and more variable in the fall than in the summer. Winds during 2006 and 2011 were more variable than during 2017 and blew predominantly toward the northeast to southeast. Winds blowing toward the northeast and east will have the longest fetch in which to generate wind-waves in Suisun Bay and the Grizzly and Honker subembayments. Thus, winds blowing toward the northeast or east should result in the most sediment resuspension and the highest turbidity in Suisun Bay.

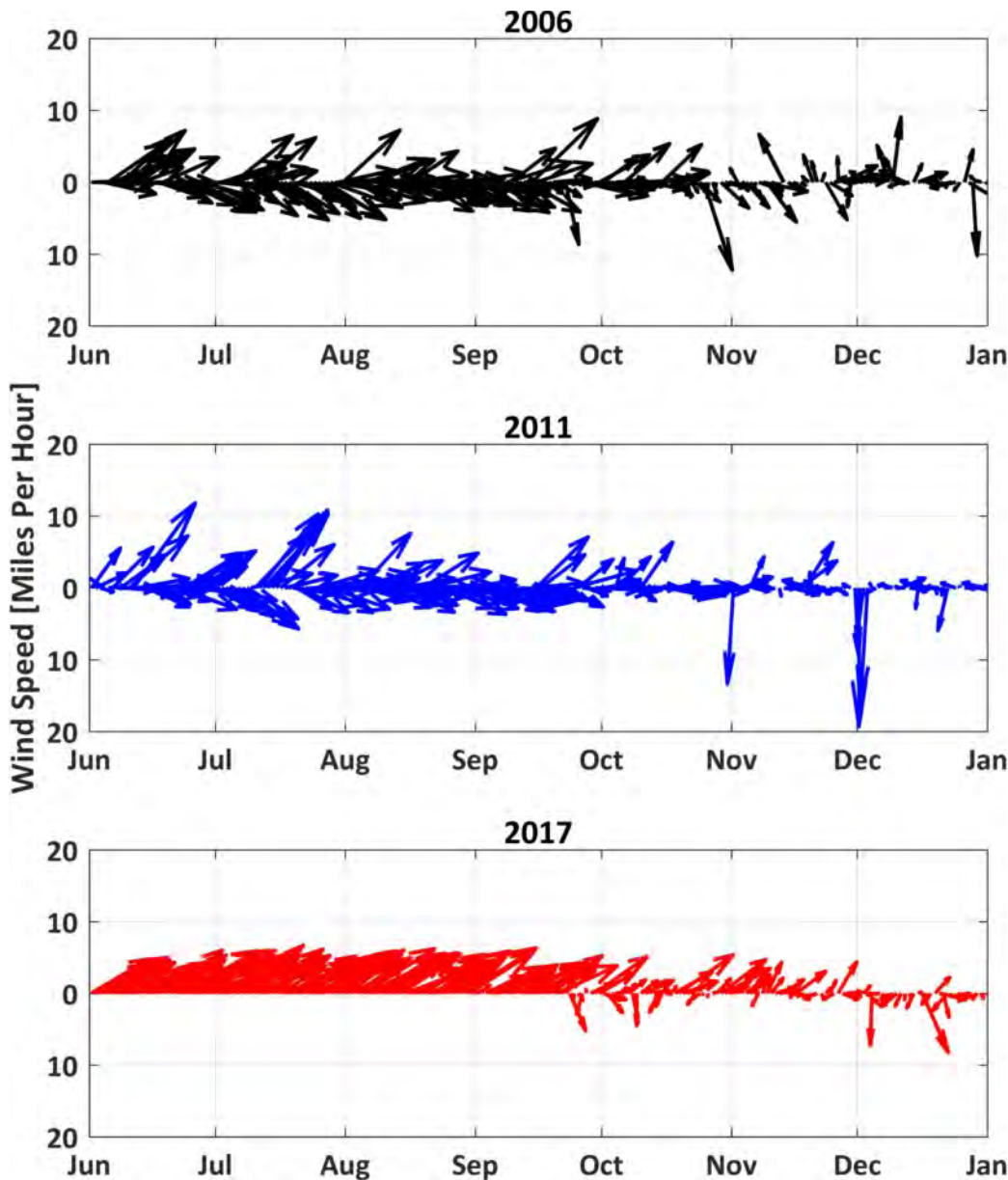


Figure 28. Daily averaged wind speed and direction over Suisun Bay used for hydrodynamic and sediment transport modeling.

All 3 years modeled had the same seasonal pattern of modeled turbidity in Suisun Bay, with higher turbidity predicted in the summer and decreasing into the fall (see Appendix 2). Modeled turbidity in Suisun Bay remained relatively high through the beginning of September. In 2017, modeled turbidity was highest in Grizzly Bay, Honker Bay, and the shallow shoals between the Suisun Bay channels (Figure 29). Modeled turbidity was generally low in the Delta. These temporal and spatial turbidity patterns resulted from the seasonally varying wind speed and the relatively low summer and

fall sediment loads from the Sacramento and San Joaquin Rivers. The overall highest modeled summer turbidity in Suisun Bay was in 2017, followed by 2006; 2011 had the lowest modeled turbidity (see Appendix 2). Notably, observed turbidity does not show any major differences between the 3 wet years (Figure 19), and there are still aspects of turbidity modeling that need improvement (Appendix 2).

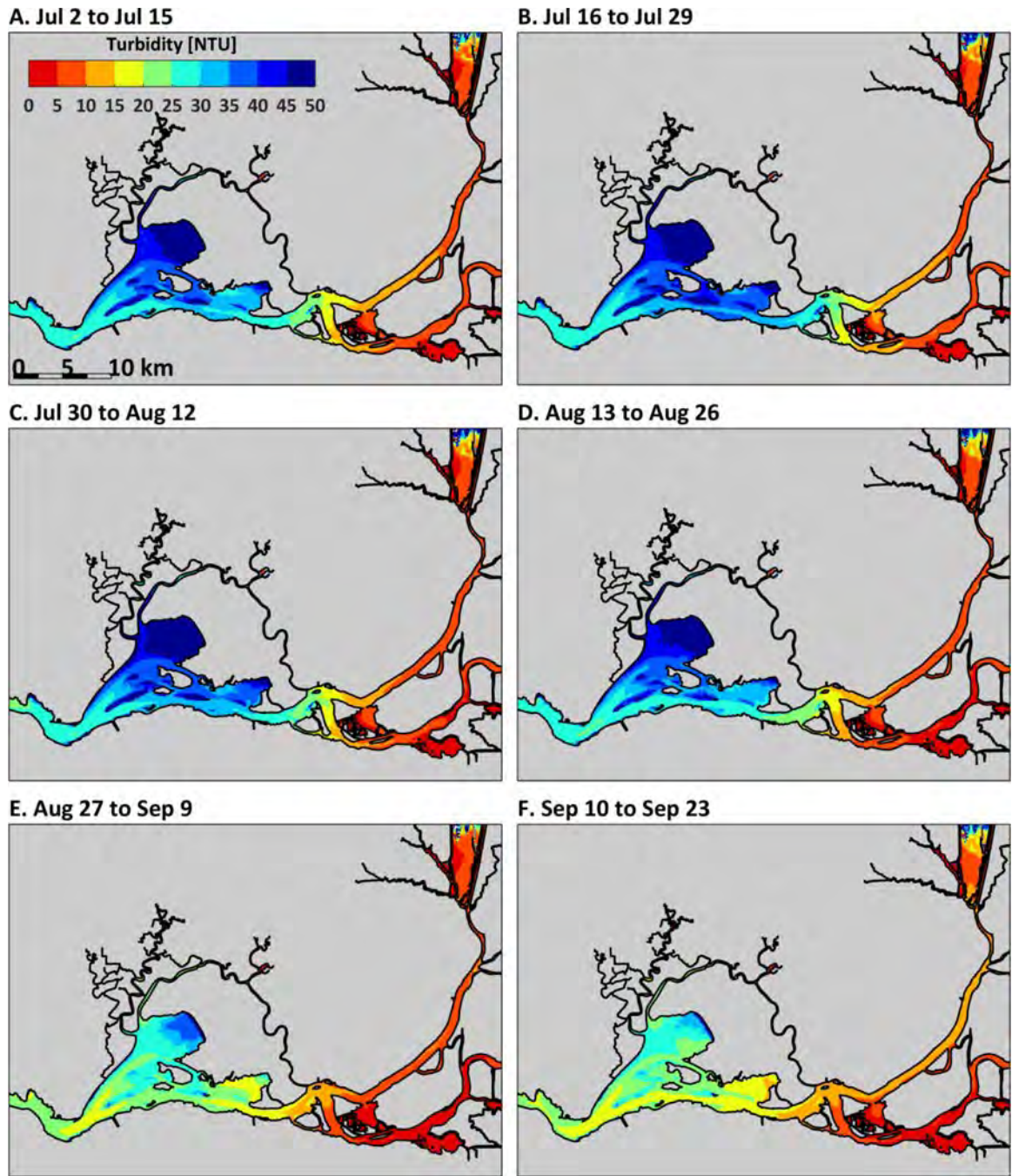


Figure 29. Predicted 2-week-average surface turbidity for 2017 2-week Enhanced Delta Smelt Monitoring sampling periods between A) July 2 and July 15; B) July 16 and July 29; C) July 30 to August 12; D) August 13 to August 26; E) August 27 to September 9; and F) September 10 to September 23.

Bever et al. (2016) developed a metric that uses the percent of time salinity was less than 6, maximum depth-averaged current speed, and Secchi depth to calculate an index that characterizes whether those environmental conditions were historically good or poor for Delta Smelt catch. The index ranges from 0 to 1, with 0 representing historically very poor conditions and 1 representing historically very good conditions for Delta Smelt catch. This station index (SI_H) is calculated using the following equation:

$$SI_H = C_1S + C_2V \quad \text{if } T < \text{cutoff}$$

$$SI_H = (C_1S + C_2V) * C_3 \quad \text{if } T > \text{cutoff}$$

where:

S = the Station Index computed from the percent time salinity is less than 6

V = the Station Index computed from maximum depth-averaged current speed

T = the Secchi depth, with a cutoff value of 0.5 meter

C_1 = 0.76

C_2 = 0.33

C_3 = 0.42

The value of SI_H was calculated throughout Suisun Bay for each 2-week EDSM sampling period to evaluate how SI_H varied during summer and fall of 2017. The percent of the time salinity was less than 6 was calculated at each model grid cell for each scenario for each 2-week period between July 2 and December 30. The spatially varying maximum depth-averaged current speed was determined by averaging the maximum depth-averaged current speeds from fall 2010 and fall 2011 (the 2 years analyzed in Bever et al. (2016)) and was thus constant for all periods. Secchi depth for each 2-week period was estimated by converting predicted turbidity at each model grid cell into predicted Secchi depth. Over the entire Suisun Bay and confluence region, the predicted SI_H had similar seasonal and

spatial patterns in each of the 3 years (Appendix 2). SI_H showed a general decreasing trend from June through December when averaged over the entire area (Figure 30), because of the combined influences of increasing salinity and increasing Secchi depth (decreasing turbidity) from June through December. SI_H in June and July was highest in 2017. From August to December, SI_H in 2011 and 2017 were quite similar, while in 2006 SI_H was predicted to be higher. Based on SI_H , habitat conditions for Delta Smelt in 2017 were predicted to be favorable in Grizzly Bay from July through August (Figure 30), with habitat quality predicted to decline through September and October due to higher salinity and Secchi depth (lower turbidity) (Figure 30D).

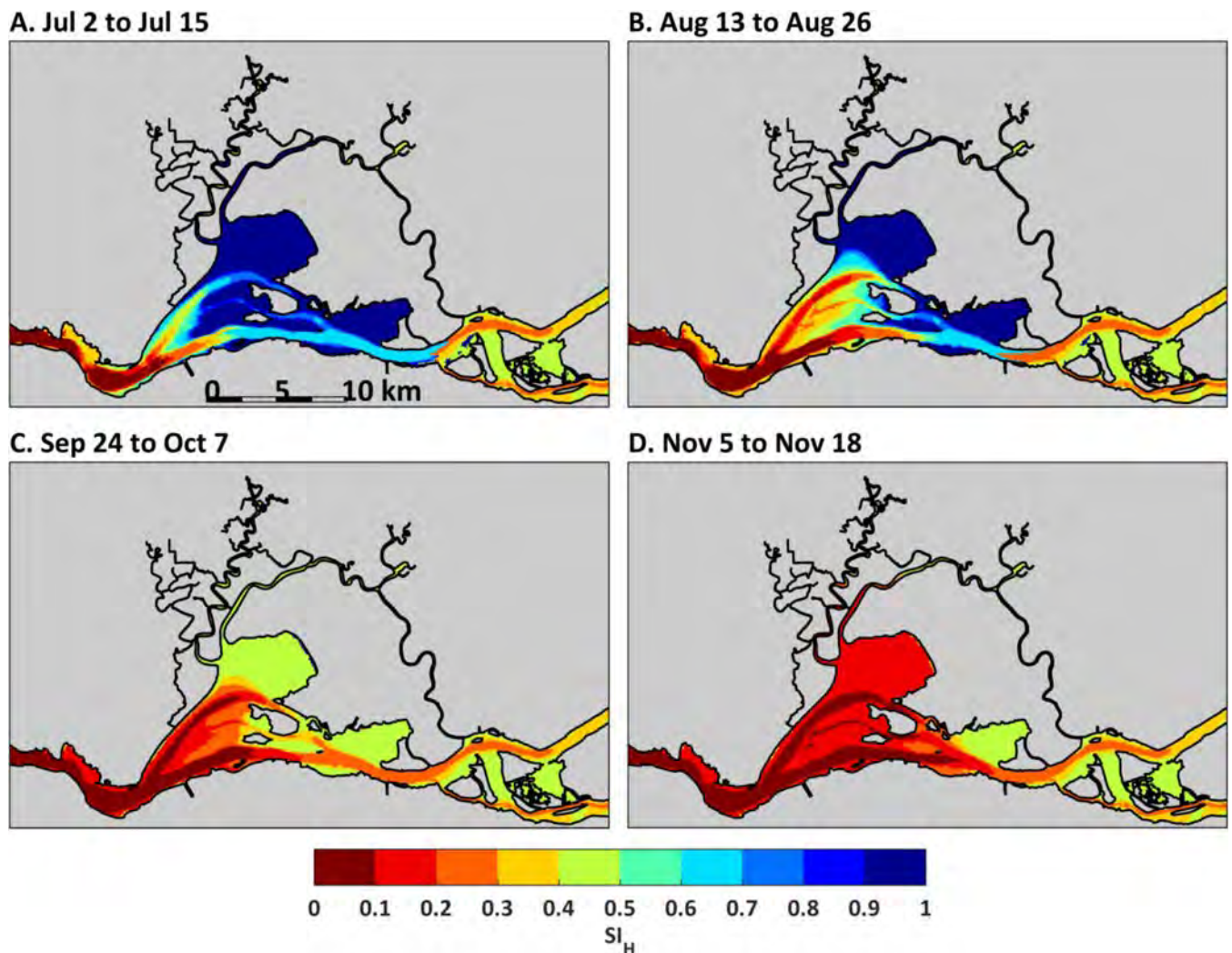


Figure 30. Predicted Delta Smelt station index (SI_H) for 2-week Enhanced Delta Smelt Monitoring sampling periods in 2017: A) July 2 to July 15; B) August 13 to August 26; C) September 24 to October 7; and D) November 5 to November 18.

Our overall prediction for abiotic habitat was only partially correct. Across all years, salinity reacted as expected with decreased salinity in wet years when the low-salinity habitat was located in Suisun Bay in the fall. Water temperature in summer and fall did not exhibit a clear pattern with regard to water year type. Wet years could be warm or cool. Similarly, Secchi depth showed no clear pattern with water year type. With respect to the wet years of 2006, 2011, and 2017, salinity conditions were considered favorable for Delta Smelt during the summer and early fall in all 3 wet years and turbidity conditions were also similar among the years. This resulted in similar values of the habitat suitability index in the Suisun Bay region for all three years. Water temperature conditions were very different for the three years for both observed and modeled temperatures. Water temperature was not included in the habitat suitability index because the index was developed for the fall period, using data from two cool years (2010 and 2011 see Bever et al. 2016; Figure 18). Consequently, the model development process did not recognize water temperature as a potentially important variable in warmer years or warmer summer months. Water temperatures in summer 2011 mainly stayed below 22°C in the lower Sacramento River but were much more stressful in 2006 and 2017 (Figures 25 and 26). High temperatures in the northern Delta, specifically the Sacramento Deepwater Ship Channel, were associated with the eventual absence of Delta Smelt from the area (Figure 31) with fish not returning to the northern Delta until December 2017.

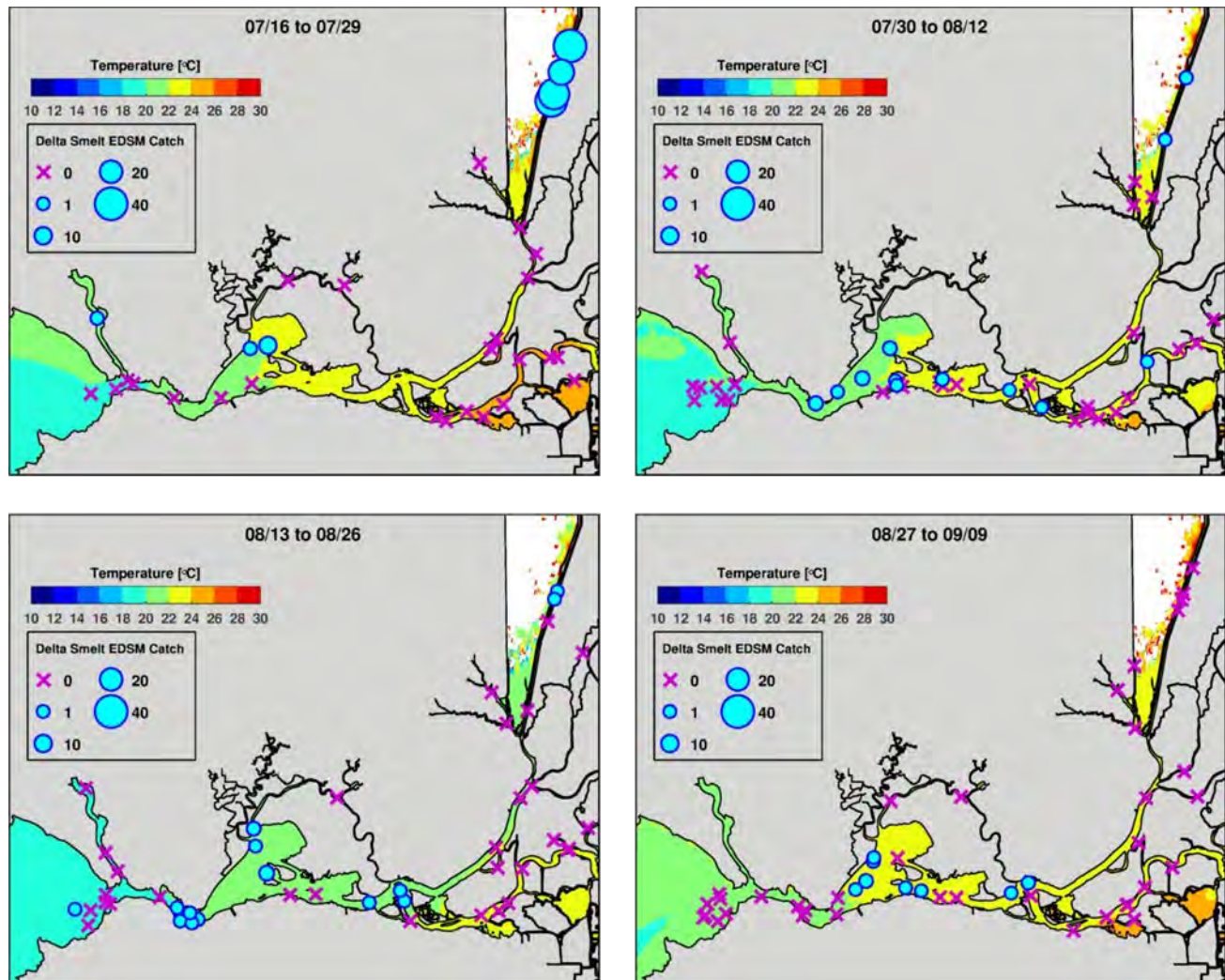


Figure 31. Predicted depth-averaged temperature averaged over 2-week Enhanced Delta Smelt Monitoring sampling periods in 2017, with Enhanced Delta Smelt Monitoring catch as bubbles.

Dynamic biotic habitat components

Phytoplankton and Chlorophyll-*a*

Phytoplankton are a very important part of the pelagic food web in the Delta and directly (i.e., direct consumption) or indirectly (i.e., consumption of intermediate consumers) support many of the organisms at higher trophic levels (Brown 2009, Jassby et al. 1993, Mueller-Solger et al. 2002, Sobczak et al. 2002). The SFE as compared to other estuaries throughout the world has low pelagic biomass

and primary productivity (Cloern and Jassby 2008). Further, phytoplankton biomass and primary productivity have exhibited a long-term downward trend since the mid-1970s (Jassby 2008). When monitoring began in the Delta, phytoplankton species composition was dominated by diatoms but more recently species composition is often dominated by smaller flagellates and cyanobacteria. This change has significant implications for the health of higher trophic levels (Brown 2009, Lehman et al. 2013).

The growth and loss of phytoplankton biomass can be controlled by various abiotic and biotic factors, and changes in these factors can alter the transport of phytoplankton throughout a given aquatic ecosystem (Lucas et al. 2009). Two changes have likely been particularly important in understanding current phytoplankton dynamics. Invasions of two clams have significantly altered the benthic clam community. *Corbicula fluminea* (hereafter *Corbicula*) is now the dominant freshwater benthic organism within the Delta (Peterson and Vayssieres 2010) and *Potamocorbula amurensis* (hereafter, *Potamocorbula*), a brackish water benthic clam, is also abundant. These clams are capable of greatly reducing phytoplankton biomass via grazing (Alpine and Cloern 1992, Jassby 2008, Jassby et al. 2002, Lucas et al. 2002). In addition, there has been a long-term shift in nutrient concentrations and ratios within the Delta, primarily due to increasing concentrations of ammonium associated with waste water treatment plant discharges (Dugdale et al. 2007, Glibert 2010, Wilkerson et al. 2006). Although there is sufficient dissolved inorganic nitrogen to support high phytoplankton biomass, it has been hypothesized that the high ammonium concentration may partially inhibit diatoms, which grow best on nitrate (Cloern and Dufford 2005, Dugdale et al. 2007, Wilkerson et al. 2006).

We predicted that having X2 located in Suisun Bay as a result of higher flows throughout the spring, summer, and fall of 2017 would result in higher total phytoplankton biovolume and

chlorophyll-*a* concentration (chlorophyll-*a* is used as a measure of phytoplankton biomass) throughout the upper SFE compared to when fall X2 is located toward the confluence (chlorophyll-*a* concentrations greater than $10 \mu\text{gL}^{-1}$ is generally considered a “bloom” under current conditions). High flows would also be expected to reduce toxic cyanobacteria (see Harmful Algal Bloom section) and increase both the growth and transport of high-quality diatom food resources into the western Delta and Suisun Bay regions of the SFE. We also might expect that high flows would initially export additional nutrients downstream from upper tributaries, but the subsequent downstream concentrations of nitrate + nitrite ($\text{NO}_3 + \text{NO}_2$) and ammonium (NH_4) may be diluted as high flows persist and loadings from upstream are reduced or depleted. If there is dilution of NH_4 we may also expect higher availability of $\text{NO}_3 + \text{NO}_2$, which may benefit phytoplankton growth and biomass. This would depend on the sources of mobilized nutrients such as runoff or discharge. It has been found that high flow conditions following a drought led to increased nutrient load (Van Metre et al. 2016) and prolonged flushing may reduce nutrient concentrations.

To test the prediction of increased phytoplankton biomass in 2017, we compared the Environmental Monitoring Program (EMP) data collected in 2017 to other post-POD years 2003-2016. Phytoplankton biomass data collected in 2016 and 2017 in the Yolo Bypass and Cache Slough Complex as part of California Natural Resources Agency Delta Smelt Resiliency Strategy (DSRS) was also compared to determine differences with (2016) and without (2017) North Delta outflow augmentation (Jared Frantzich, California Department of Water Resources Division of Environmental Services). In addition, high frequency phytoplankton biomass and associated environmental data, including nutrient data, collected during the fall of 2017 from lower Cache Slough into the LSZ was compared to 2011 data to determine differences between the two high outflow years (Frances Wilkerson and Dick

Dugdale, San Francisco State University; Jared Frantzich, California Department of Water Resources Division of Environmental Services). Detailed methods and additional results can be found in Appendix 4.

The EMP phytoplankton, chlorophyll-*a* and nutrient data for this analysis was grouped into four regions, representing different habitat types (Figure 32): Upper Sacramento River Region (site C3A), Lower Sacramento River Region (site D22 and D4), Lower San Joaquin River Region (D12 and D16), and Suisun Bay Region (site D6, D7, and D8). The DWR special study 2016 and 2017 phytoplankton and chlorophyll-*a* data for the Yolo Bypass and Cache Slough Complex was also grouped into four regions (Figure 32; upper Yolo Bypass (RD22, I80), lower Yolo Bypass (LIS, STTD), Cache Slough Complex (BL5, LIB, RYI), and lower Sacramento River (RVB, SDI)).

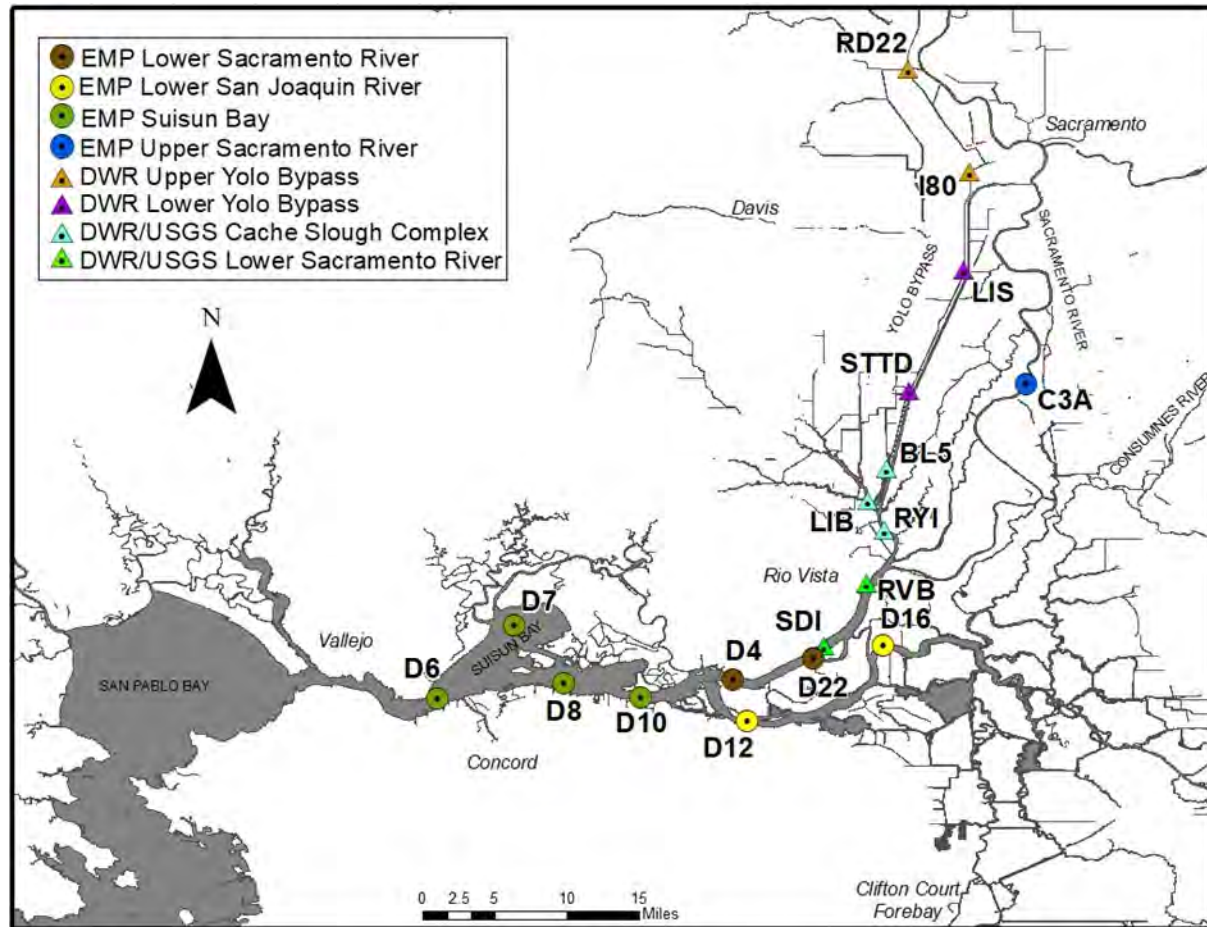


Figure 32. Region map of Environmental Monitoring Program (EMP) discrete phytoplankton, chlorophyll-*a*, and continuous water quality monitoring stations (circles); SDI, RYI, and LIB; and California Department of Water Resources (DWR) special study stations (triangles).

In 2017, the Lower Sacramento River and San Joaquin River regions had low spring chlorophyll-*a* concentration when compared to other post-POD years (2003-2016) (Figure 33). The lower San Joaquin River mean chlorophyll-*a* in spring 2017 was significantly lower than water years 2004 and 2016 (ANOVA, Tukey Test $p < 0.05$). Both regions had elevated chlorophyll-*a* levels in the summer (Figures 33 and 34). The lower San Joaquin River summer mean chlorophyll-*a* concentration was significantly higher in 2017 than in 2005, 2007, 2009 and the high outflow year 2011.

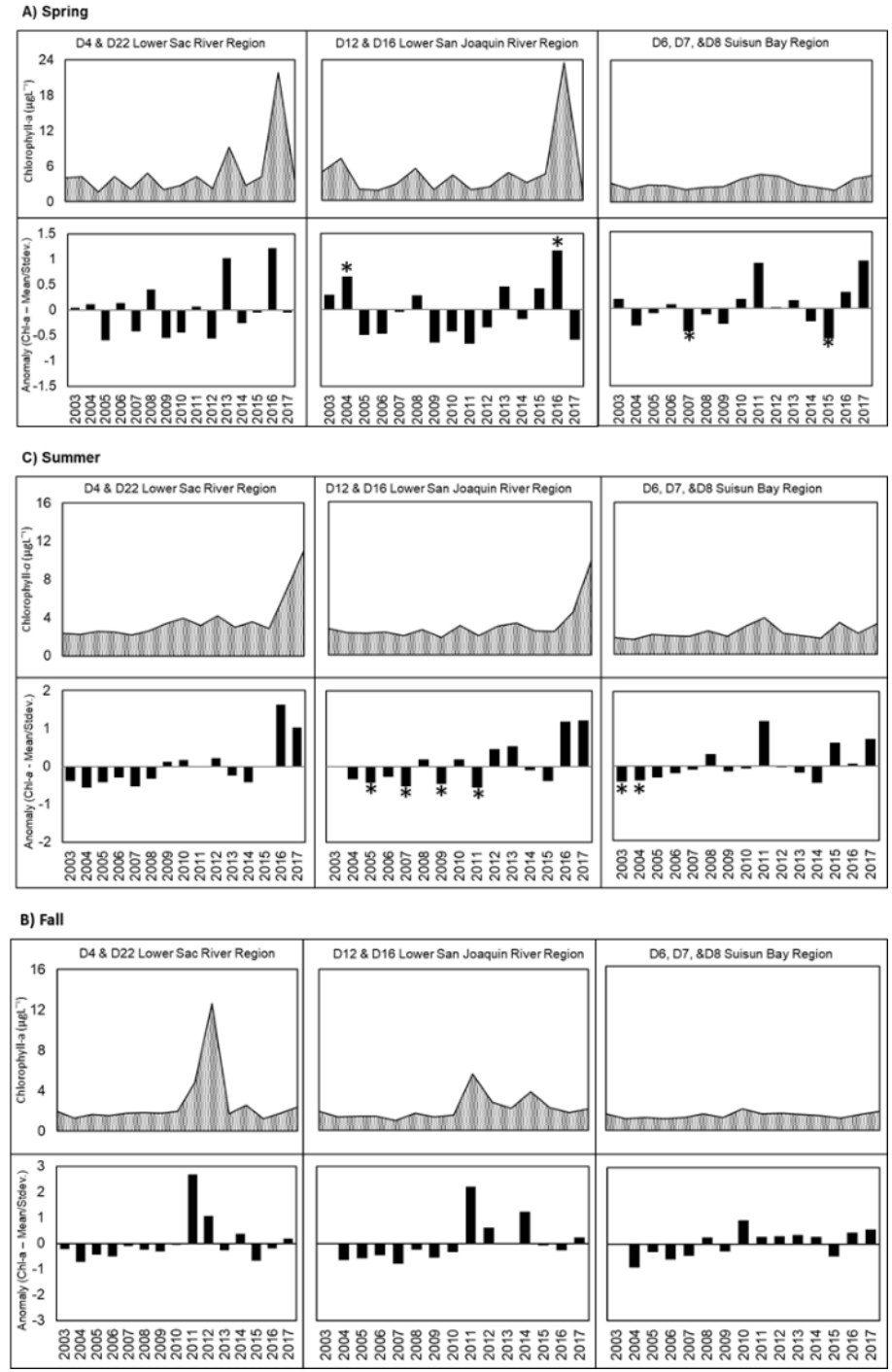


Figure 33. Mean chlorophyll-a concentration ($\mu\text{g}\text{L}^{-1}$) and anomalies by region and season for post-POD years 2003-2017. Asterisk denotes years that have significantly different mean chlorophyll-a concentration from 2017 (ANOVA and Tukey Test). Anomalies are calculated as: (annual value subtracted from the 2003-2017 mean)/standard deviation).

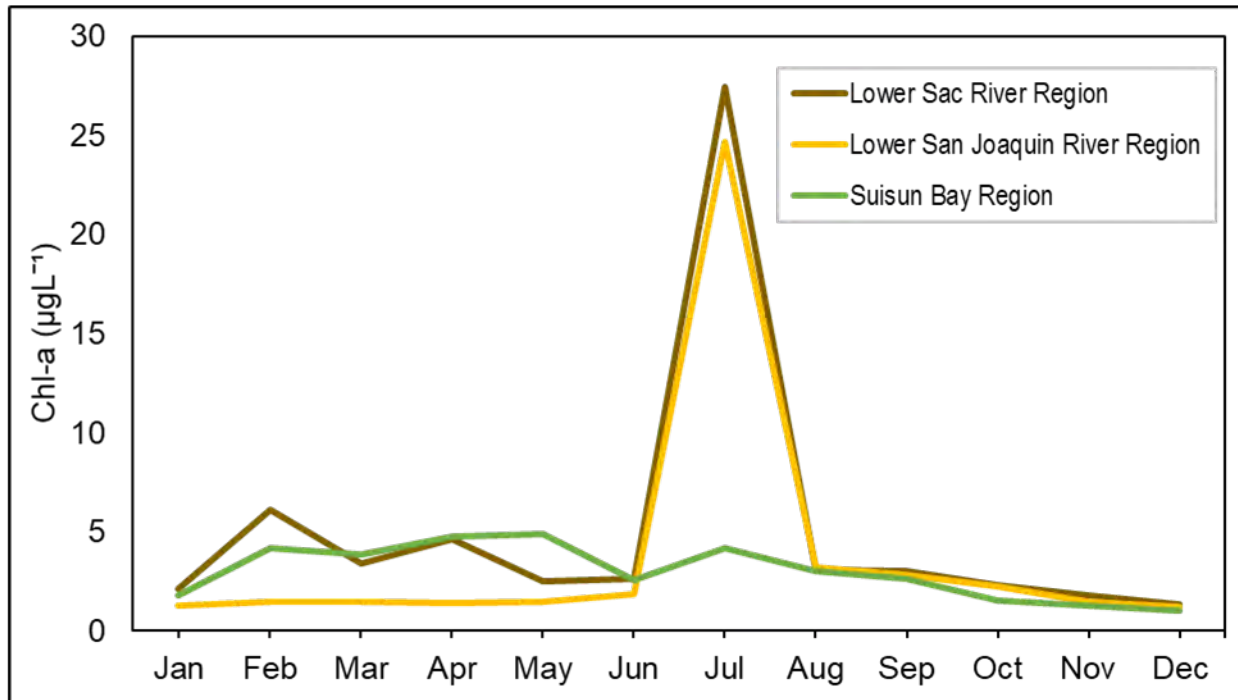


Figure 34. Environmental Monitoring Program chlorophyll-*a* concentration for 2017 by region and month.

The Suisun Bay region in 2017 had elevated mean chlorophyll-*a* concentration in the spring, summer, and fall compared to other post-POD years (Figure 33). In spring 2017, the mean chlorophyll-*a* concentration was significantly higher (ANOVA, Tukey Test $p > 0.05$) than the low outflow water years of 2007 and 2015. Summer chlorophyll-*a* mean concentration was elevated and similar to levels measured in both the high outflow year 2011 and the low outflow, critically dry year 2015. The fall mean chlorophyll-*a* levels in 2017 were not significantly different from other post-POD years, but were at similar levels as measured in 2010, which was not a wet year. Variability among years was low in the Suisun Bay Region compared to the other regions, particularly in the fall (Figure 33).

In 2017, the lower Sacramento River and lower San Joaquin River phytoplankton as total organisms mL⁻¹ and total biovolume (µm³mL⁻¹) were both high in the months between February and April, with a large peak in total biovolume in July (Figures 35A,B and 36A,B). Green algae and

cyanobacteria were the most abundant taxa throughout much of the year (Figures 35A,B and 36A,B), with diatoms making up a majority of the total biovolume in July (Figure 36A,B). This peak in diatom biovolume in both regions was composed primarily (>90%) of the centric diatom *Aulacoseira sp.* (Figure 36A, B), which is a good food source for zooplankton.

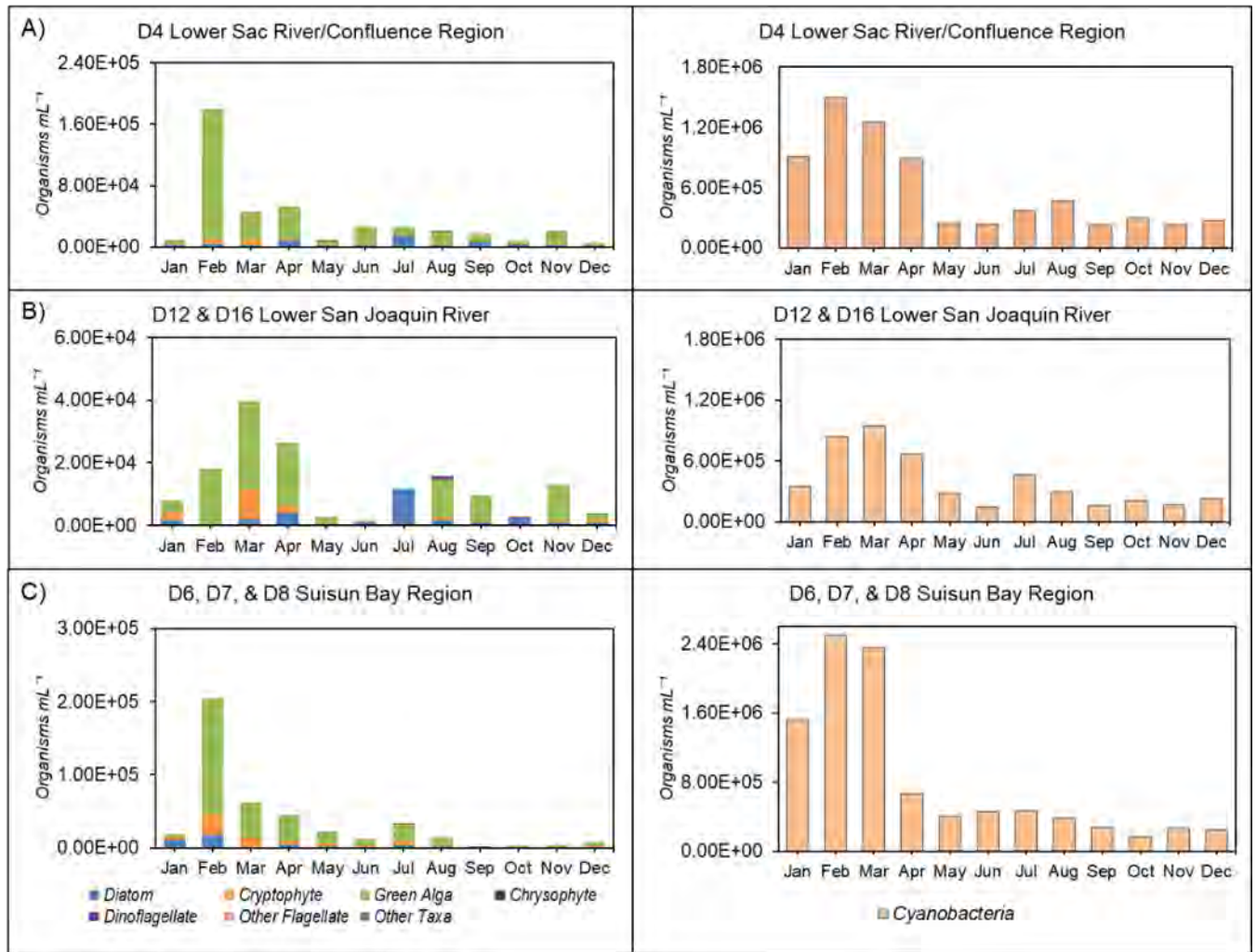


Figure 35. Environmental Monitoring Program phytoplankton taxa groups (total organisms mL⁻¹) by region and month. Regions: A) Lower Sacramento River, B) Lower San Joaquin River, and C) Suisun Bay.

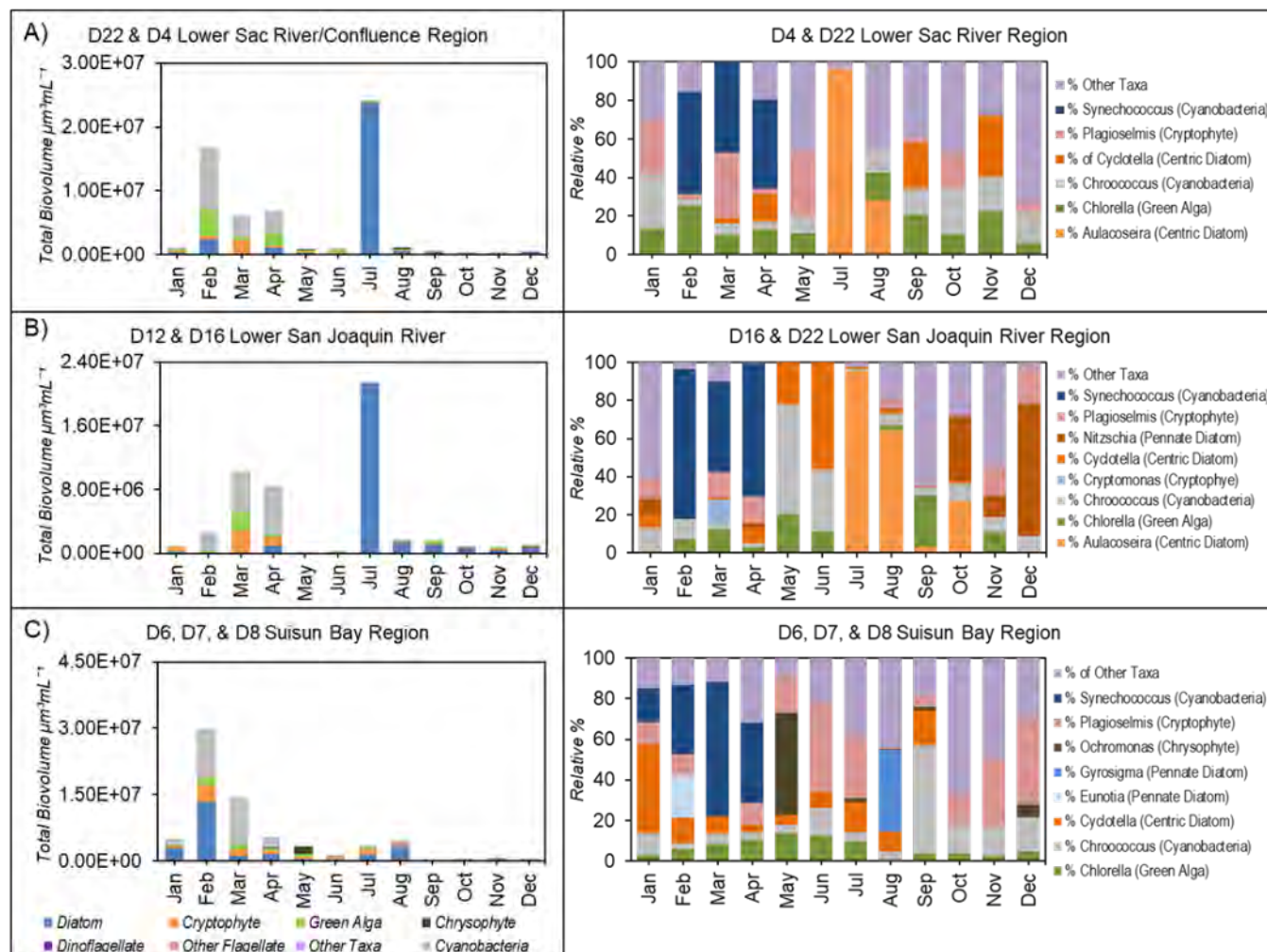


Figure 36. Environmental Monitoring Program phytoplankton taxa total biovolume by group and % of taxa making up $\geq 3\%$ of total biovolume by region and month. Regions: A) Lower Sacramento River, B) Lower San Joaquin River, and C) Suisun Bay.

In the Suisun Bay region phytoplankton abundance and total biovolume peaked in February (Figures 35C and 36C), with cyanobacteria and green algae comprising most of the phytoplankton taxa as organisms mL^{-1} . The February peak in phytoplankton total biovolume was primarily due to the cyanobacteria *Synechococcus sp.* (Figure 36C), a cyanobacteria known to bloom in warmer summer water temperature conditions (Kim et al. 2018) and predicted to increase in cell abundance with climate change (Flombaum et al. 2013).

The nitrogen concentrations throughout the three regions in 2017 followed similar seasonal trends, with highest concentrations of both ammonium (NH_4) and nitrate + nitrite (NO_3+NO_2) in winter and late fall and lower concentrations in summer (Figures 37-39). Mean NO_3+NO_2 concentrations in the lower Sacramento and lower San Joaquin Rivers in the summer months of June and July reached low levels ($\leq 1 \mu\text{M}$), that could have reduced phytoplankton growth. Regionally, the NH_4 and NO_3+NO_2 concentrations in the lower Sacramento River in 2017 were not significantly different (ANOVA, Tukey Test $p > 0.05$) compared to previous high outflow year of 2011. The lower Sacramento River in 2017 did have significantly lower NO_3+NO_2 concentrations (ANOVA, Tukey Test $p < 0.05$) in summer and fall compared to lower outflow years of 2014 and 2015 (fall only).

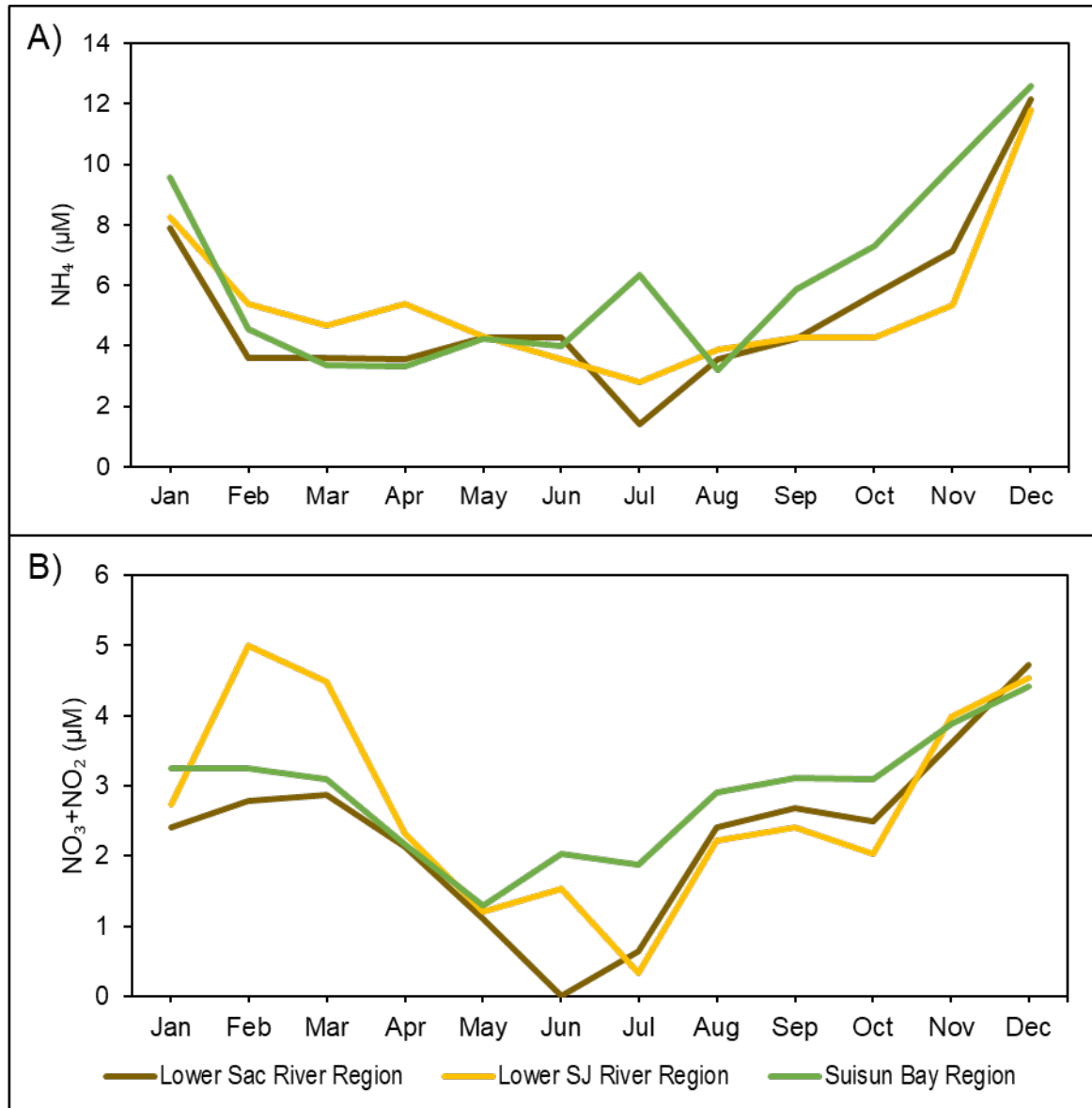


Figure 37. Mean concentration of A) ammonium (NH₄) and B) nitrate + nitrite (NO₃+NO₂) for 2017 by region and month.

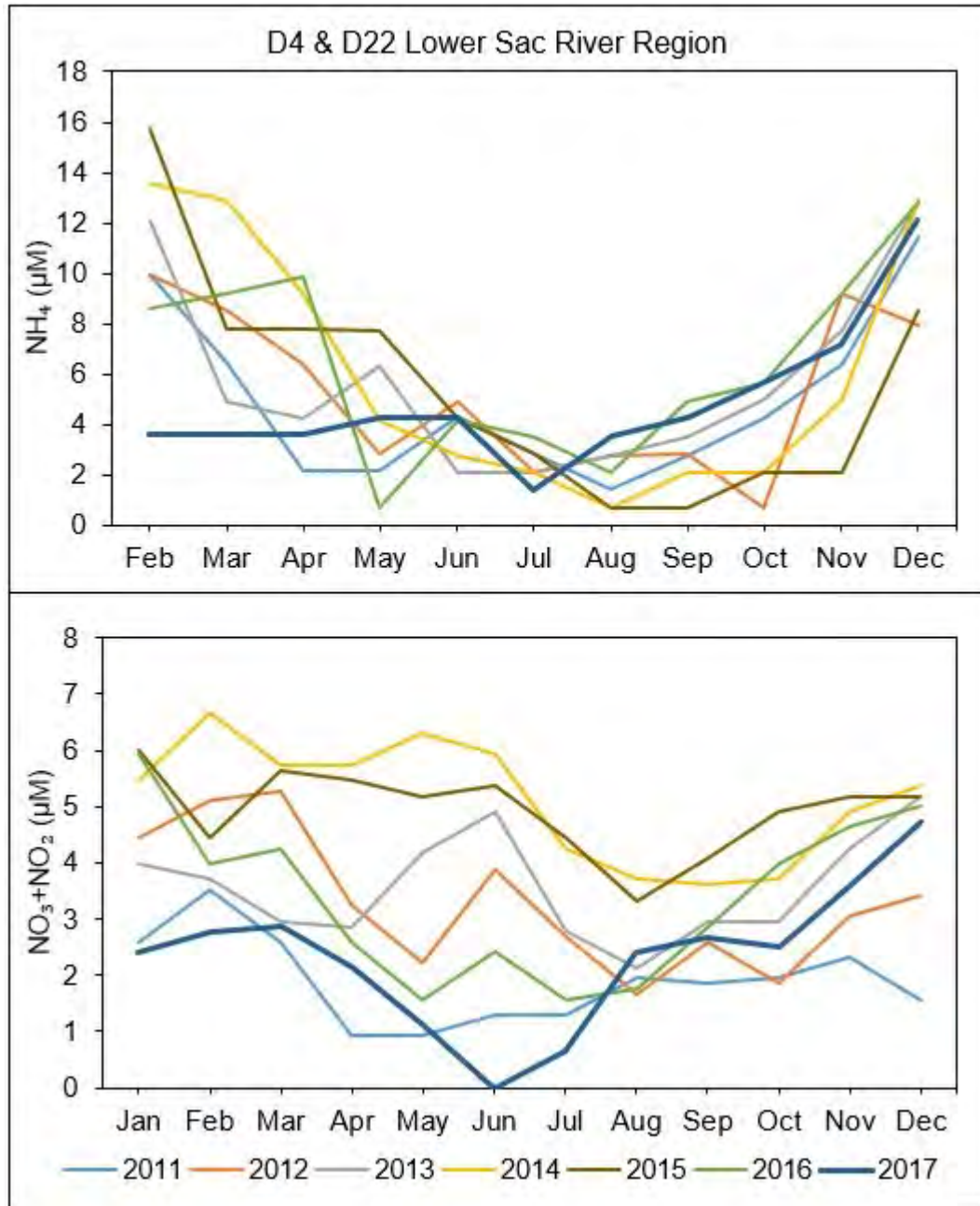


Figure 38. Lower Sacramento River region monthly mean concentration of ammonium (NH_4) and nitrate + nitrite ($\text{NO}_3 + \text{NO}_2$) for 2011 - 2017.

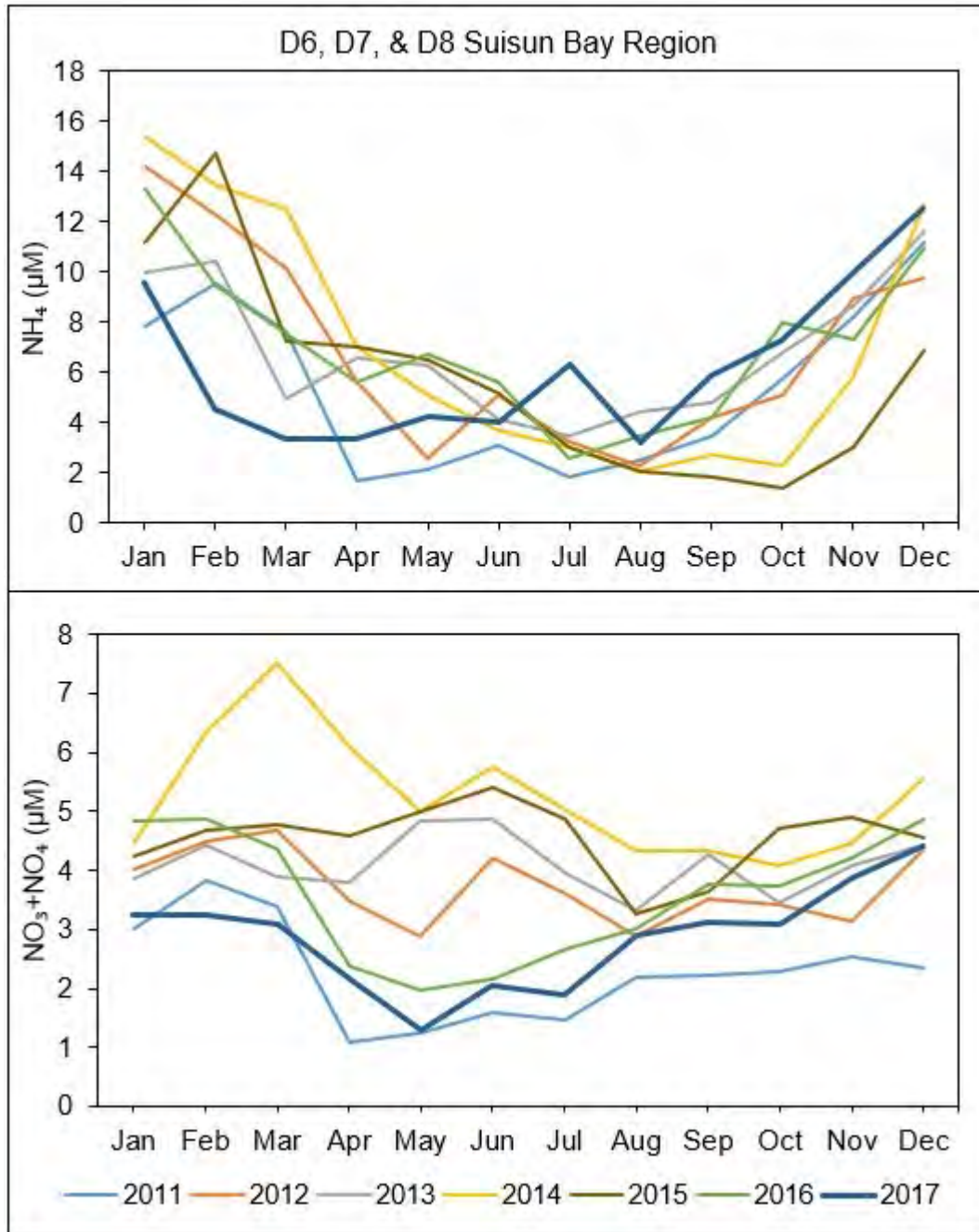


Figure 39. Suisun Bay region monthly mean ammonium (NH_4) and nitrate + nitrite ($\text{NO}_3 + \text{NO}_2$) concentrations for 2011 - 2017.

The Suisun Bay region had lower NH_4 concentration throughout the spring months of February and March of 2017 compared to other years, but concentrations were higher throughout the remaining summer and fall months of the year (Figure 39). NH_4 concentration in 2017 were

significantly higher (ANOVA, Tukey Test $p < 0.05$) than in the low outflow years of 2014 and 2015.

Mean NO_3+NO_2 concentration in 2017 followed a similar trend to the high outflow year of 2011, with summer and fall concentrations being significantly (ANOVA, Tukey Test $p < 0.05$) lower than 2012-2016 (Figure 39).

During the DWR North Delta Special Study (see Appendix 4 for details), the mean chlorophyll-*a* concentrations within the Yolo Bypass were similar for the managed flow pulse year of 2016 and 2017 (Figures 40A,B, and 41). However, there was a contrast between years in the Cache Slough Complex and Lower Sacramento River regions, with chlorophyll-*a* concentrations in the Cache Slough Complex being significantly higher (ANOVA, Tukey Test $p < 0.05$) during July and August 2016 compared to 2017 and the lower Sacramento River in August 2016 higher than in August 2017 (Figures 40A,B, and 41). The managed flow pulse in 2016 (July 14th – Aug 1st) resulted in the transport of high chlorophyll concentrations downstream from the upper Yolo Bypass through the Cache Slough Complex and into the Lower Sacramento River at Rio Vista (Figure 41), assuming a travel time of several weeks.

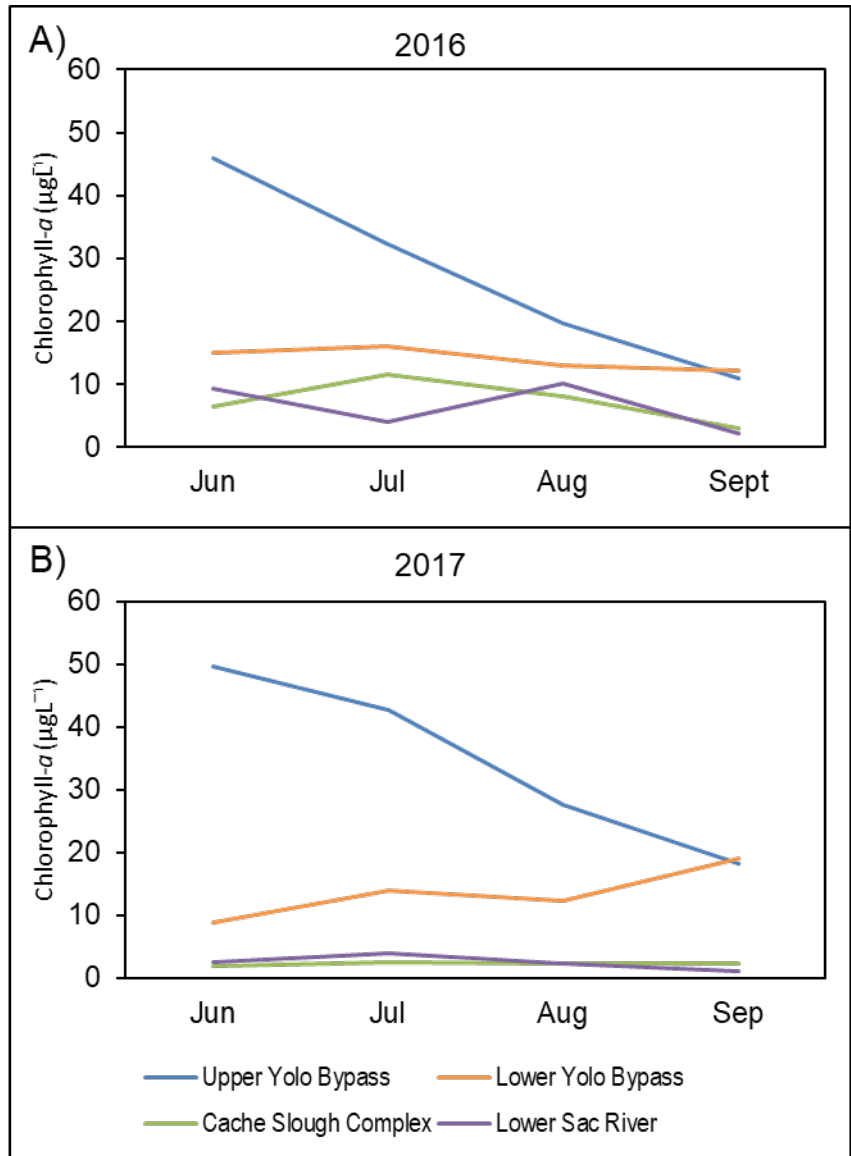


Figure 40. California Department of Water Resources North Delta Special Study region monthly mean chlorophyll-a ($\mu\text{g L}^{-1}$) for A) 2016 and B) 2017.

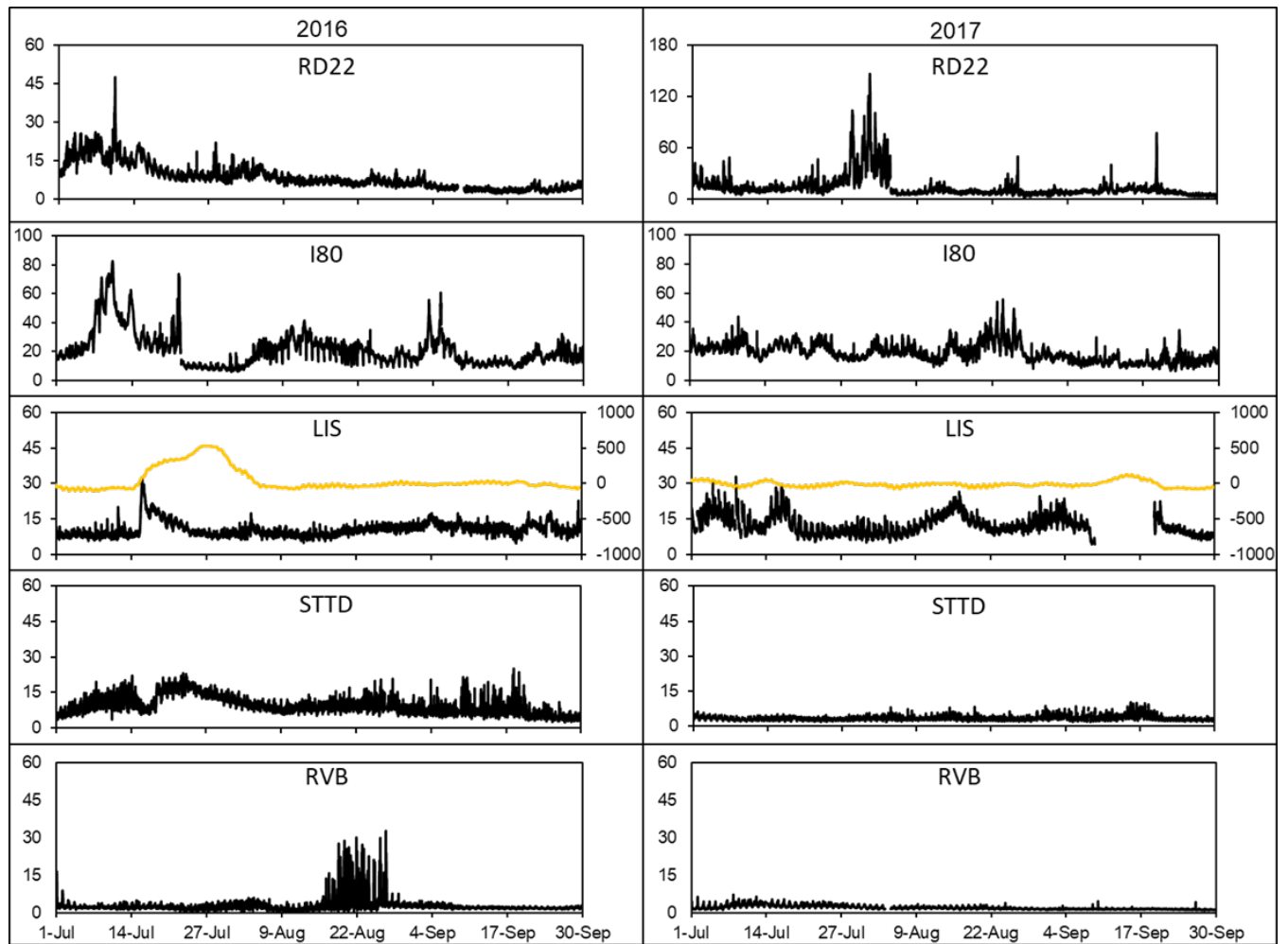


Figure 41. California Department of Water Resources North Delta Special Study 2016 and 2017 continuous total chlorophyll fluorescence $\mu\text{g L}^{-1}$ (black line and primary y axis) and daily average flow at site LIS (yellow line and secondary y-axis).

The phytoplankton total biovolume in 2016 and 2017 in the upper Yolo Bypass, much like chlorophyll-*a* concentration, was not significantly different (ANOSIM $p > 0.05$) in the month of July (Figure 42A). The lower Yolo Bypass and Cache Slough Complex had a significantly higher (ANOSIM $p < 0.05$) total phytoplankton biovolume in July 2016, primarily due to the large cell biovolume of the centric diatom *Aulacoseira* sp. (Figure 42B,C). In contrast to 2017, the elevated phytoplankton biovolume in 2016 persisted throughout the Cache Complex and downstream in the lower Sacramento River throughout the late summer months during and after the managed flow pulse in the Yolo Bypass

(Figure 42B,C). The 2016 mean phytoplankton biovolume in the lower Sacramento River at Rio Vista was 4-fold higher in July and 9-fold higher in August after the flow pulse compared to 2017 (Figure 42D). This difference in biovolume was almost entirely associated with the centric diatom *Aulacoseira* *sp.* in 2016 (see Appendix 4).

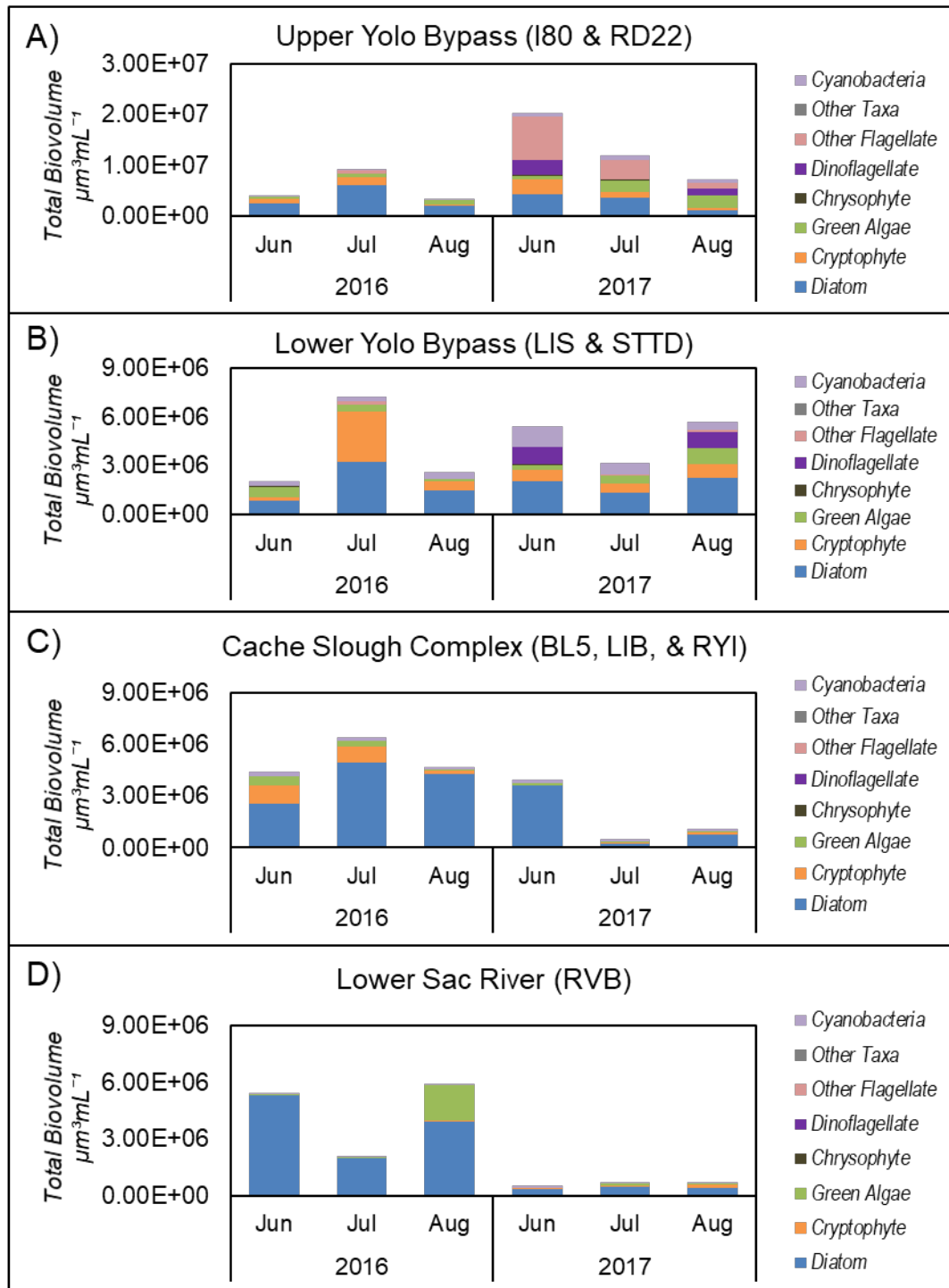


Figure 42. California Department of Water Resources North Delta Special Study region phytoplankton taxa total mean biovolume by taxa group. Regions: A) Upper Yolo Bypass, B) Lower Yolo Bypass, C) Cache Slough Complex, and D) Lower Sacramento River.

In fall 2017, additional pelagic food web monitoring transects for water quality, nutrients, chlorophyll-*a*, and primary productivity continued from lower Cache Slough at Ryer Island south into the LSZ near Port Chicago (Figure 43; see Appendix 4 for study description). This study was focused on providing additional downstream food web monitoring data related to the DSRS North Delta flow augmentation and to support IEP's evaluation of Delta Smelt habitat response to high Delta outflows in 2017. The mean chlorophyll-*a* concentrations were low in the fall months of September to November throughout the transect in 2017 (Figure 44B). This contrasted with the previous high outflow year of 2011, when a phytoplankton bloom occurred in the lower Sacramento River and fall chlorophyll-*a* concentrations exceeded $10 \mu\text{gL}^{-1}$ (Figures 33B and 44). In regard to physical conditions in the fall, Delta outflow (2011; $332 \text{ m}^3\text{sec}^{-1}$ and 2017; $373 \text{ m}^3\text{sec}^{-1}$) and location of X2 (2011; 74 km. and 2017; 74 km) were similar between years and did not appear to account for the difference in chlorophyll-*a* concentration. The mean water temperatures in September and October varied but were comparable for 2017 and 2011 among the lower Sacramento River, the Confluence and Middle Ground regions (Figure 43 and 45A). The fall light availability in all three regions was higher in 2017 than 2011 with mean Secchi depth ranging from 0.7-2.3m (Figure 45B).

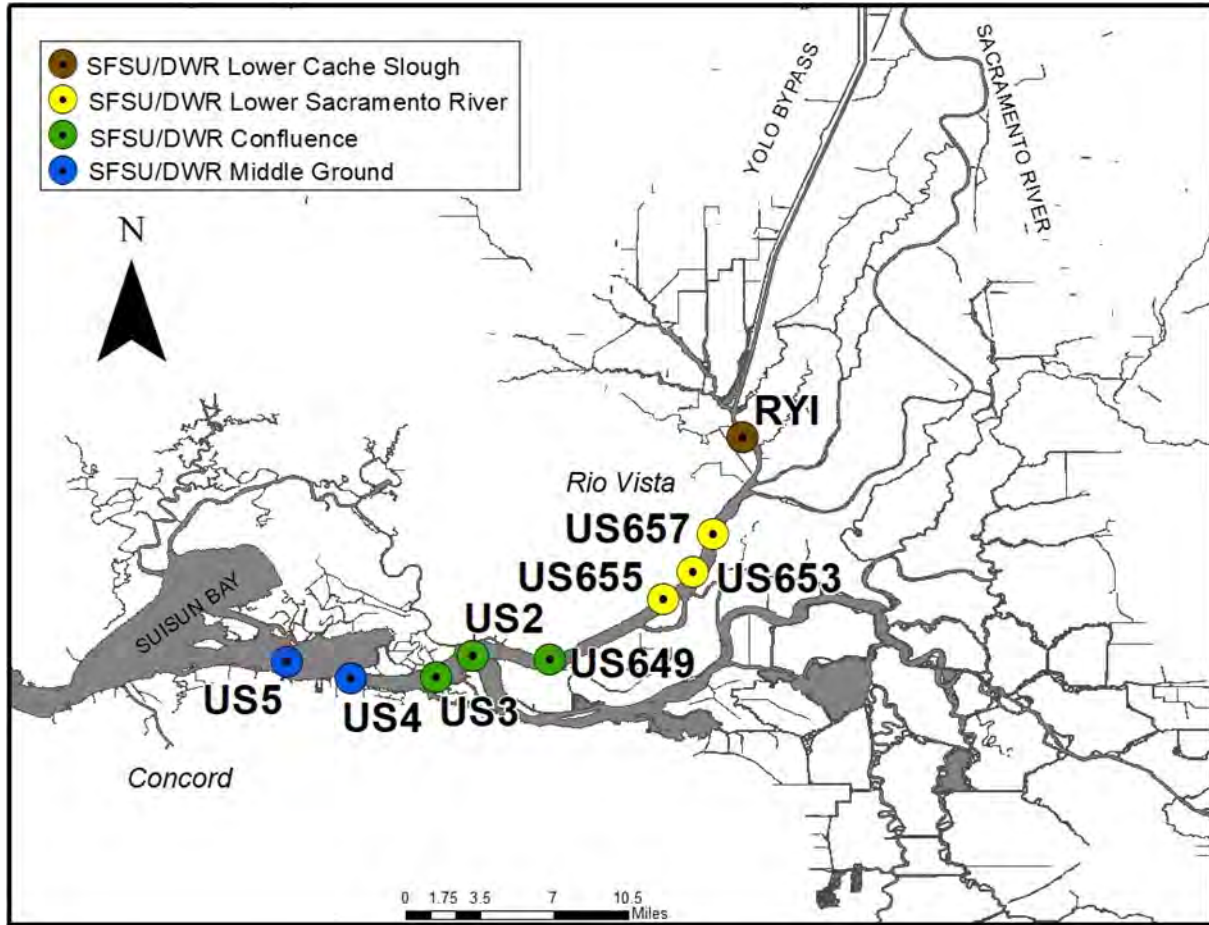


Figure 43. Region map for California Department of Water Resources and San Francisco State University and Low Salinity Zone Special Study water quality, nutrients, and chlorophyll-*a* sampling transects.

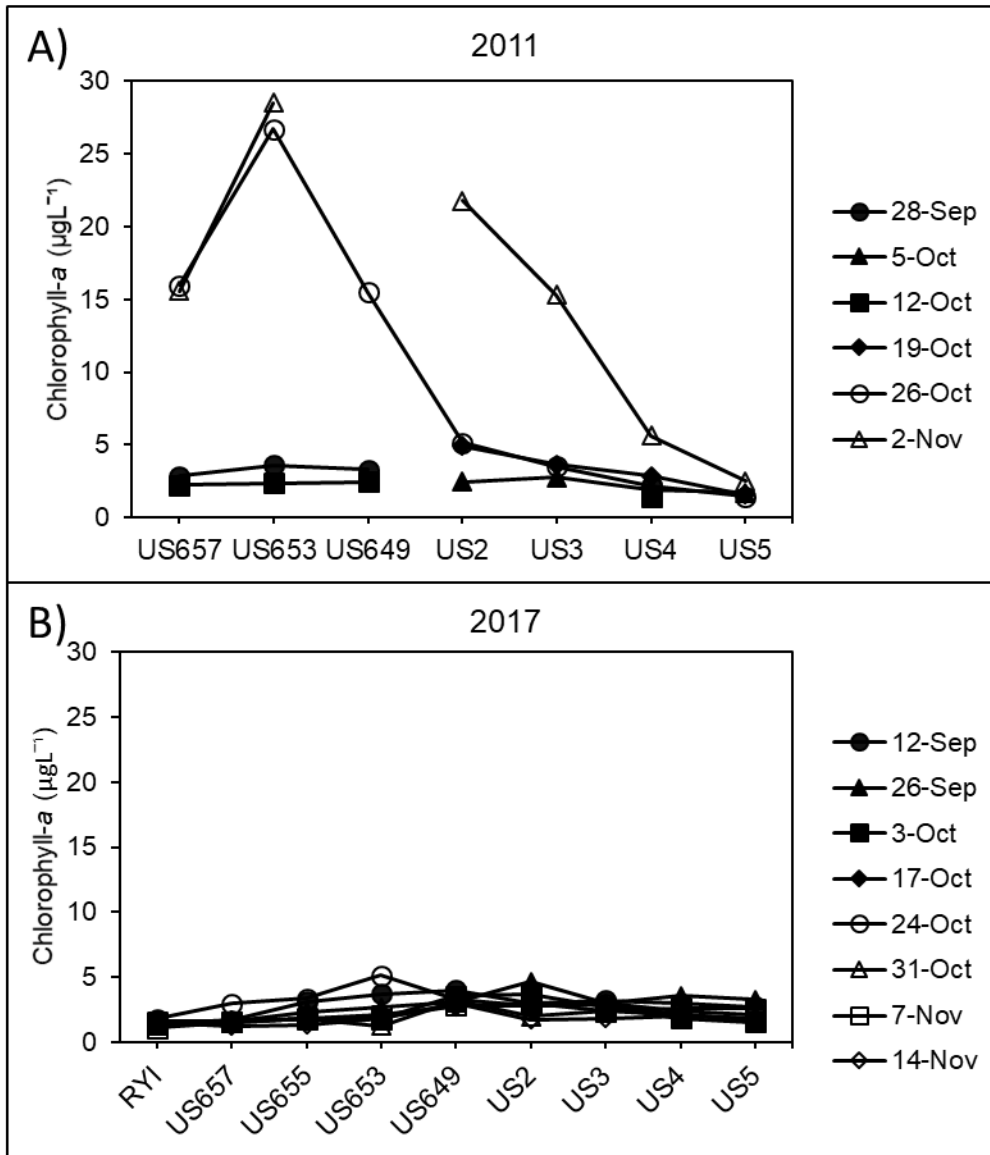


Figure 44. California Department of Water Resources and San Francisco State University Fall Low Salinity Zone Special Study chlorophyll-a concentration in A) 2011 and B) 2017.

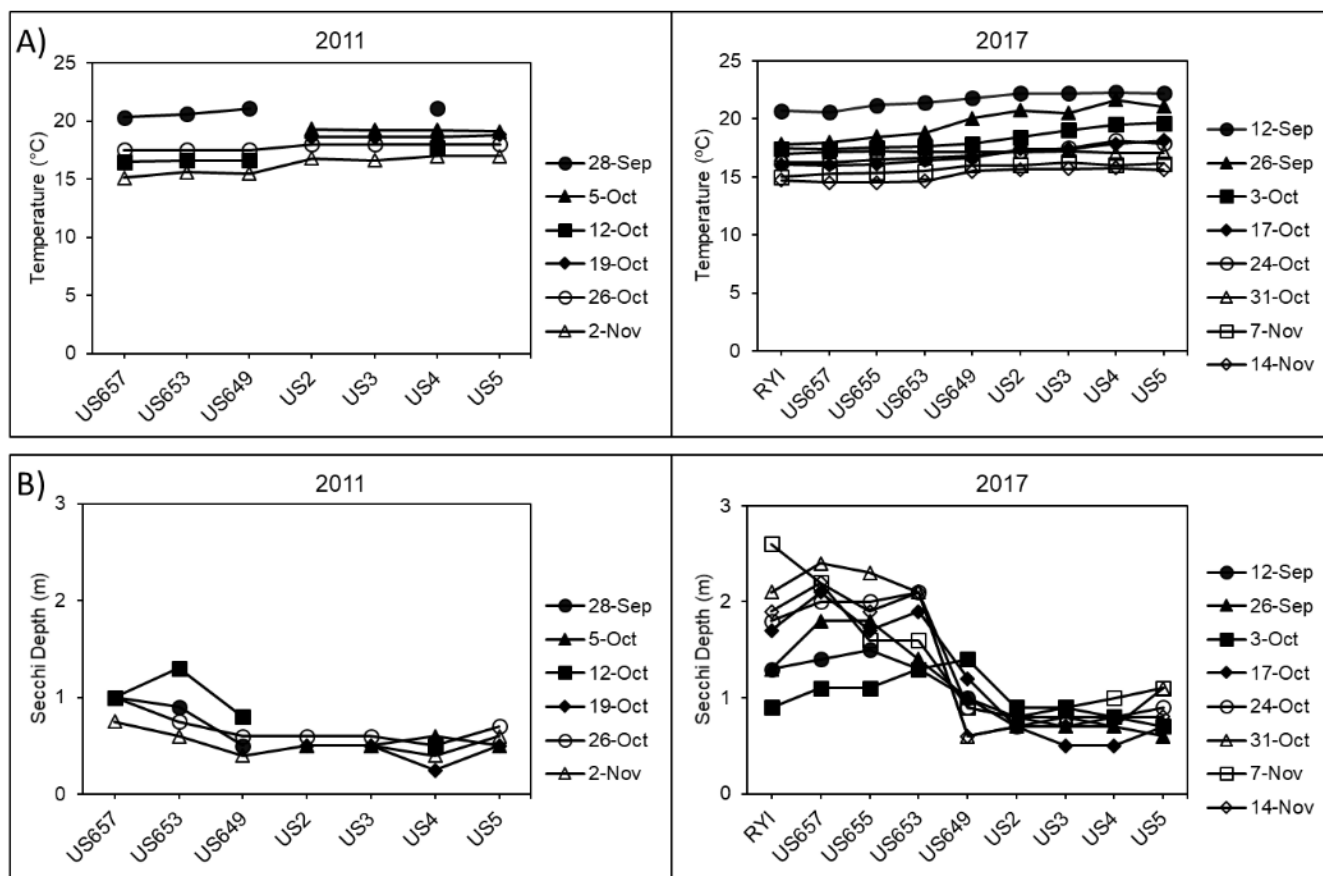


Figure 45. California Department of Water Resources and San Francisco State University Low Salinity Zone Special Study 2011 and 2017 A) water temperature (°C) and B) Secchi depth (m).

The mean NO₃ + NO₂ concentrations in 2017 were similar to those in 2011 throughout the LSZ, with levels in September and October ranging between 11.9-16.9 μM-N in the Lower Sacramento River, 17.1-19.4 μM-N in the Confluence, and 19.1-21.0 μM-N in Middle Ground (Figure 46A). In contrast, the NH₄ concentrations were 2-3 fold higher throughout the regions in 2017, Figure 46B) compared with 2011.

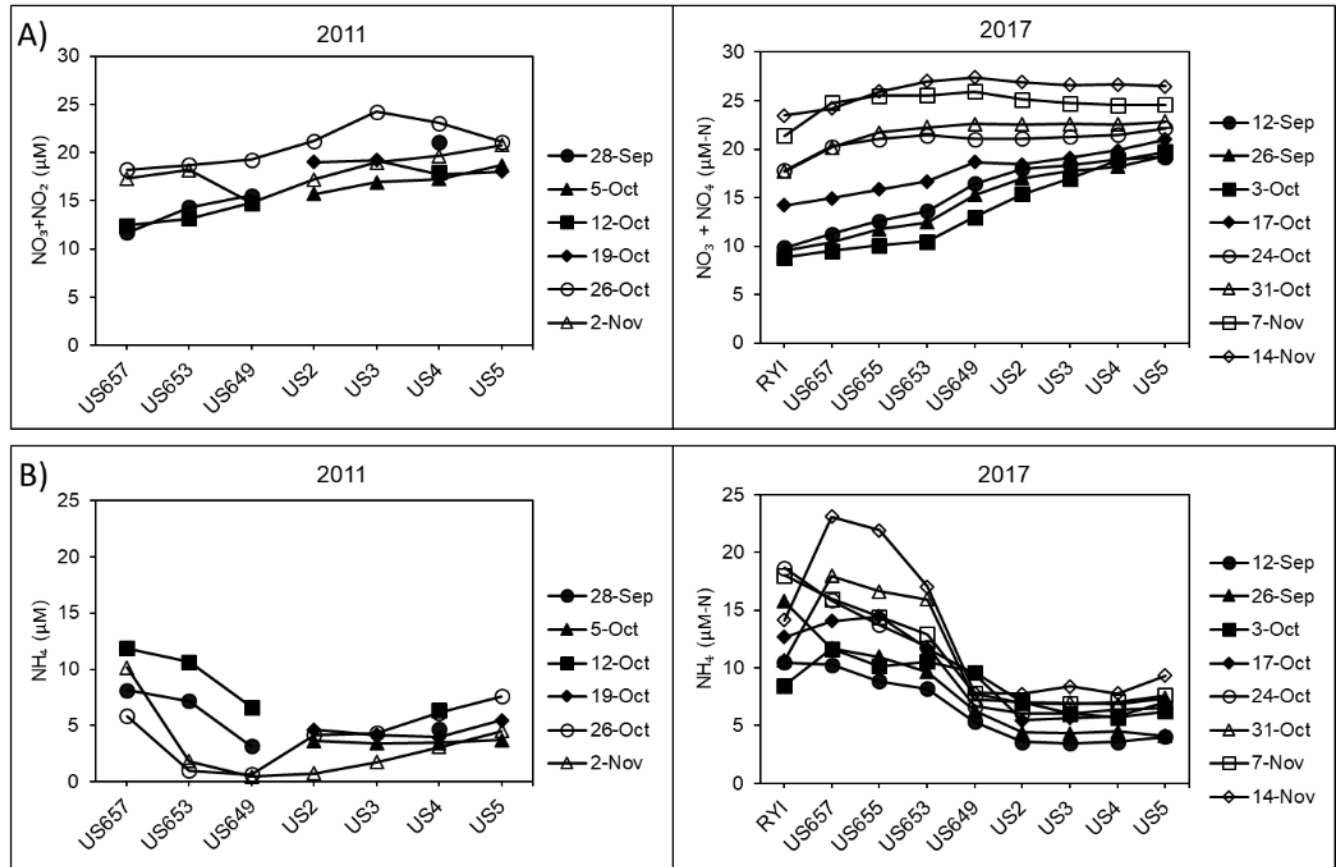


Figure 46. California Department of Water Resources and San Francisco State University Low Salinity Zone Special Study 2011 and 2017 A) $\text{NO}_3 + \text{NO}_2$ (μM) and B) NH_4 (μM).

Our prediction of higher phytoplankton biomass in fall of the high flow year 2017 compared to low flow years was not correct. Chlorophyll-*a* concentration was relatively high in fall 2017 the fall of 2017 was not statistically different from any other year, wet or dry. Patterns of phytoplankton biomass in the lower Sacramento and San Joaquin regions were variable. A large fall phytoplankton bloom like the one observed in 2011 was absent but there was a bloom in July 2017. The phytoplankton biomass in the lower Sacramento and San Joaquin Rivers in the fall of 2017 was only marginally higher than previous post-POD years (2003-2016). This contrasted from the last high outflow year of 2011 in which a fall phytoplankton bloom (chlorophyll-*a* $>10 \mu\text{g}\text{L}^{-1}$) occurred in the lower Sacramento and San Joaquin Rivers (Figures 33B and 44A). There was, however, a significant phytoplankton bloom in the summer of

2017 in the lower Sacramento and San Joaquin Rivers (Figures 33C, 34, 36A,B) composed of the same dominant centric diatom *Aulacoseira sp.* as observed in fall 2011. The Suisun Bay region had elevated phytoplankton biomass throughout the spring, summer, and fall of 2017 (Figures 33A,B,C) compared to other post-POD years, but there was not a consistent or strong pattern between high or low outflow water years. Our expectation that the higher phytoplankton biomass in fall 2017 would be composed of diatoms was incorrect. Much of the difference between 2017 and other years was explained by a higher biovolume of cyanobacteria, green algae, and cryptophytes (see Appendix 4).

The 2016 augmented flows in the Yolo Bypass as a restoration action showed promise in benefiting the downstream food web. The phytoplankton biomass in the lower Sacramento River in 2016 increased in response to the restoration action, likely due to the high phytoplankton biomass present within the Cache Slough Complex prior to the augmented outflow. The Yolo Bypass and Cache Slough Complex may be a critical seeding mechanism for summer and fall phytoplankton blooms within the lower Sacramento River.

The light, outflow, mean X2, and water temperature were all favorable for phytoplankton production in fall 2017 as we expected. There was some evidence through the LSZ transects that temperatures were slightly elevated in the fall of 2017 as compared to 2011 (also see Dynamic Physical Habitat section). This could be a key explanatory variable for the prevalence of cyanobacteria compared to diatoms. The NH_4 and NO_3+NO_2 concentrations were high in fall 2017 for all regions. Further, NH_4 levels were at concentrations that inhibit nitrate uptake by diatoms (Dugdale et al. 2007; Wilkerson et al. 2006) and could have been a factor in the absence of a fall bloom in 2017. Studies on nutrient loading have suggested that high flow years may increase the mobilization and loading of nutrients especially in intensive agricultural areas like the Sacramento-San Joaquin Valley (Garrett 2012, Murphy et al. 2014, Van Metre et al. 2016, Munn et al. 2018). In addition, the relatively longer period of drought prior to 2017 (2012-2016) compared to 2011 (2008-2010) may have contributed to differences in ammonia concentrations between the two years. A study by Van Metre et al. (2016)

found that intensively dry periods may increase loading of nutrients in the subsequent year compared less severe dry periods. The drought of 2012-2016 was one of the driest on record.

Harmful algal blooms

Harmful algal blooms (HABs) occur worldwide in fresh and brackish waters and are often composed of dinoflagellate and cyanobacteria species (Carey et al. 2012). Harmful algal blooms have increased in recent decades coincident with the increase in water temperature associated with climate change and the increase in nutrient concentration associated with eutrophication (O'Neil et al. 2012). In the Delta and Suisun Bay regions, total cyanobacteria abundance has increased over time (Lehman 1996, 2000, 2004, Glibert 2010, Lehman et al. 2013). The increase in cyanobacteria coincided with a decrease in diatoms, thought to be a high-quality food source for zooplankton at the base of the upper SFE food web (Lehman 1996, 2000, 2004, Glibert 2010, Lehman et al. 2017).

Cyanobacteria harmful algal blooms became a concern in SFE beginning in 1999, when surface blooms of *Microcystis* began in the Delta (Lehman et al. 2005). *Microcystis* blooms now occur yearly in the Delta during the summer and fall, particularly between July and September. *Microcystis* blooms increase in magnitude with high water temperature, low streamflow and brackish water conditions associated with drought (Lehman et al. 2008, 2017, 2018, Kurobe et al. 2018). Other cyanobacteria have also become abundant in SFE in recent years, including the potentially toxic HAB species *Aphanizomenon*, which was the dominant HAB in the Delta during the relatively cool water temperature conditions in 2011 (Lehman et al. 2013, Kurobe et al. 2013). During drought years, potentially toxic species of *Microcystis*, *Aphanizomenon*, and *Dolichospermum* can occur during the summer (Lehman et al. 2017, 2018). However, the frequent presence of the toxin microcystin, which is predominantly produced by *Microcystis*, suggests *Microcystis* is the most toxic HAB (Lehman et al. 2017).

Microcystis is a threat to the SFE aquatic food web because it can contain hepatotoxic microcystins that promote liver tumors and cancer in humans and wildlife (Zegura et al. 2011 International Agency for Research on Cancer 2006; Zanchett and Oliveira-Filho, 2013). *Microcystis* colonies also contain lipopolysaccharide endotoxins, which inhibit ion transport in fish gills, as well as, fish embryo development (Codd 2000). More recently *Microcystis* has been found to contain the

neurotoxin aminoB – methylamino-L-alanine (BMAA), a parkinsonism-dementia complex (Downing et al. 2011). Because these substances can be transported long distances across an estuary they have been implicated in the loss of health and survival of aquatic species from freshwater to marine habitats (Ibelings and Havens 2008, Miller et al. 2010). The potential ecological harm associated with *Microcystis* blooms is greater than for most freshwater HABs, because the ability of *Microcystis* to tolerate salinity allows it to expand into brackish and marine water environments during drought years (Tonk et al. 2007, Harke et al. 2016, Kurobe et al. 2018).

A suite of research studies has demonstrated the potential harm of *Microcystis* blooms to the aquatic food web in SFE. Laboratory bioassays suggested that at ambient concentrations, total and dissolved microcystins could have affected the health and survival of zooplankton, fish embryos, and juvenile and adult fish species in SFE (Ger et al. 2009, 2010, Deng et al. 2010, Acuña et al. 2012 a,b, Kurobe et al. 2018). Further, juvenile Striped Bass, Mississippi Silversides, and Threadfin Shad caught in the wild within the Delta and Suisun Bay demonstrated liver tissue lesions consistent with hepatotoxin exposure (Lehman et al. 2010, S. Acuña et al., in press). The presence of *Microcystis* was also associated with a decrease in diatom and green algal phytoplankton species biovolume in the Delta (Lehman et al. 2010).

Our prediction is that the high flows occurring in 2017 that maintained X2 in Suisun Bay would be associated with low *Microcystis* abundance in the Delta and Suisun Bay compared to drier years when X2 is located near the confluence. Reduced transport of potentially toxic HABs into the western Delta and Suisun Bay would benefit Delta Smelt growth and survival due to the reduction in direct impacts to the fish and planktonic organisms in its diet. Detailed methods and additional results regarding HABs in the upper SFE are available in Appendix 5.

Microcystis abundance is ranked on a qualitative visual scale of abundance at the water surface (range: 1, no *Microcystis*, to 5, very high concentration of contiguous colonies forming mats and scum) (see Morris and Civiello 2013 for details of the index). This ranking was applied at a subset of the EMP monitoring stations used in this analysis (Figure 47).

The surface *Microcystis* bloom index was lower for June through December in 2017 compared to 2007 through 2016 throughout the Delta and Suisun Bay, except for September. September of 2017 was characterized by elevated *Microcystis* index values in the Central Delta and Lower San Joaquin

River (LSJR) regions (Figures 47 and 48). There was also a slight increase in the *Microcystis* index seaward in the Lower Sacramento River (LSAC) and landward in East Delta (ED) during September or October of 2017. The next to lowest *Microcystis* index often occurred for many regions in 2011, another high outflow year. Importantly, there was no indication that the peak chlorophyll-*a* concentration in July (Figure 36) was due to *Microcystis*, a month when *Microcystis* is often abundant.

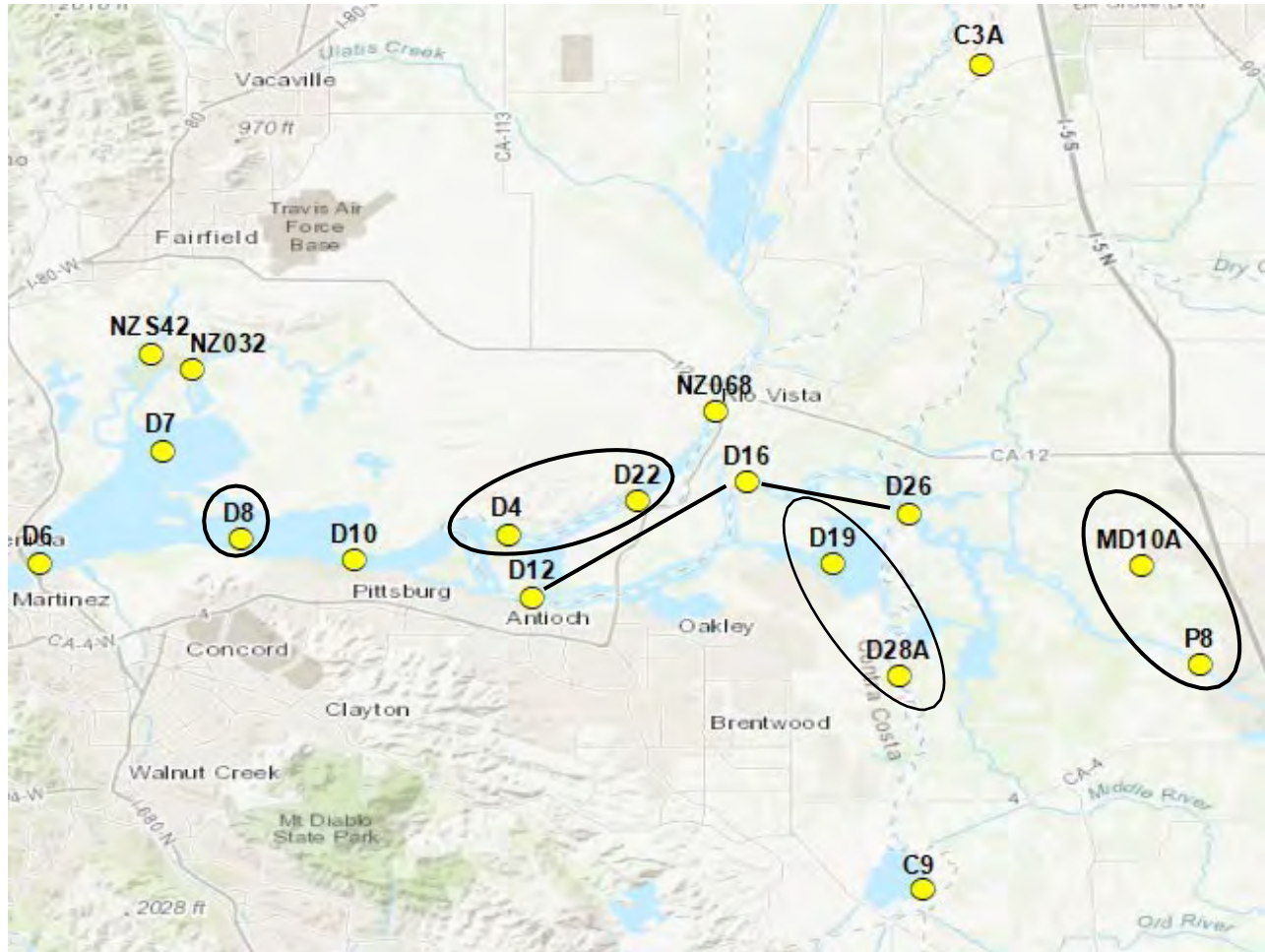


Figure 47. Map of Environmental Monitoring Program stations utilized in this analysis. Groups appear in ovals or are connected by lines. Groups are Suisun Bay (SBAY), lower Sacramento River (LSAC), lower San Joaquin River (LSJR), central Delta (CD), and eastern Delta (ED).

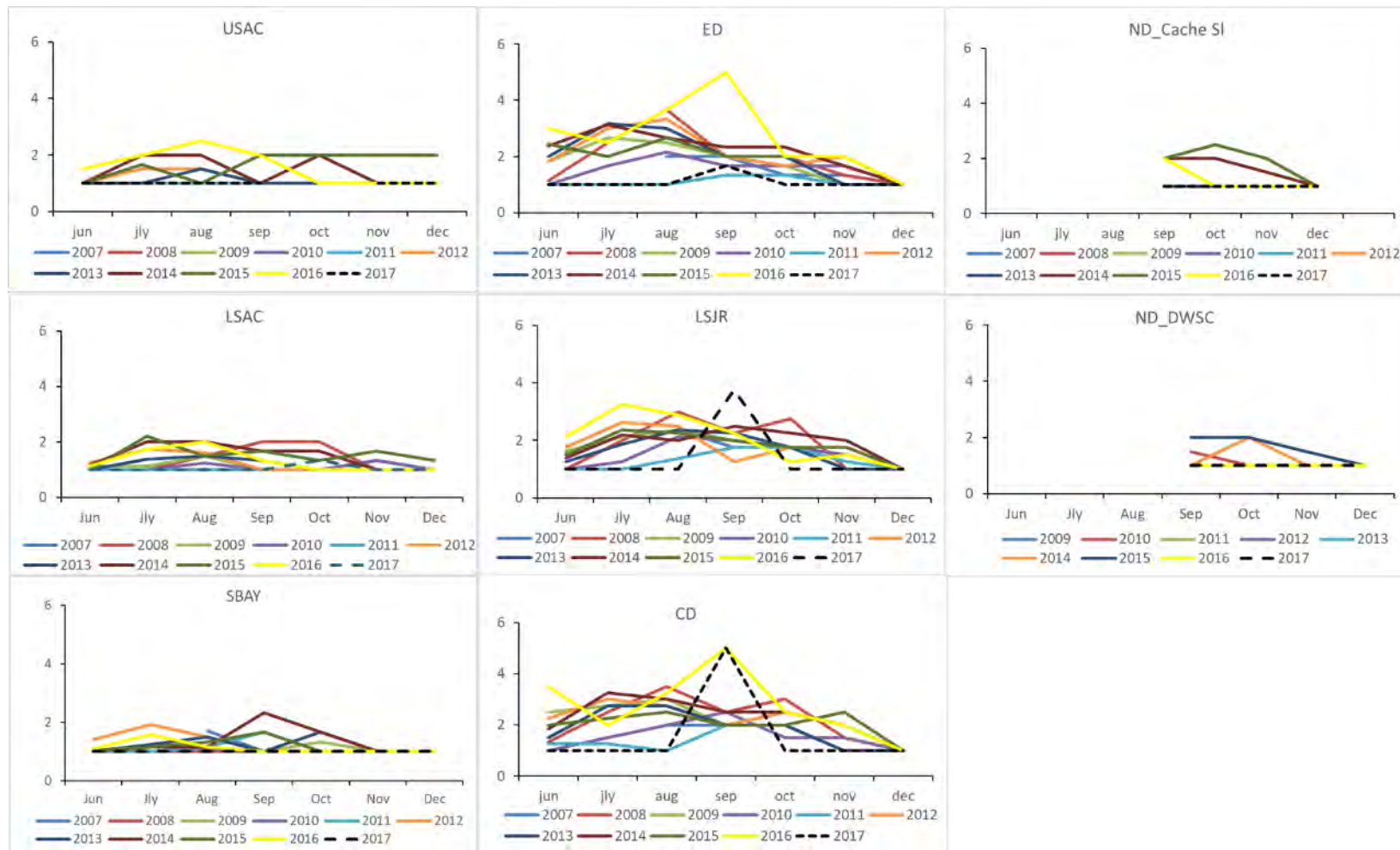


Figure 48. Mean surface *Microcystis* bloom visual index values collected during the Summer Townet and Fall Midwater Trawl surveys for June through December in regions throughout the Delta and Suisun Bay between 2007 and 2017. Index values range from 1 to 5; 1 indicates no *Microcystis* present. Regions include Upper Sacramento River (USAC), lower Sacramento River (LSAC), Suisun Bay (SBAY), Central Delta (CD), East Delta (ED), North Delta at Cache Slough (ND Cache SL) and North Delta at the Deep-Water Shipping Channel (ND_DWSC).

Quantitative identification and enumeration by microscope of surface *Microcystis* samples supported the presence of more *Microcystis* in the surface layer in September and October (ANOSIM, $p < 0.05$) than in other months in 2017 (Figure 49a). Most of the surface *Microcystis* colonies appeared to occur in September in the CD (station D19 and D28A) and LSJR (station D16) (see Figure 47 for station groupings). However, colonies also occurred in the LSAC (D4) and Suisun Bay (SBAY) (D8; Figure 49b). Because of high variability, surface *Microcystis* biovolume was not significantly greater in the CD and LSJR stations D16, D19 and D28A than other stations.

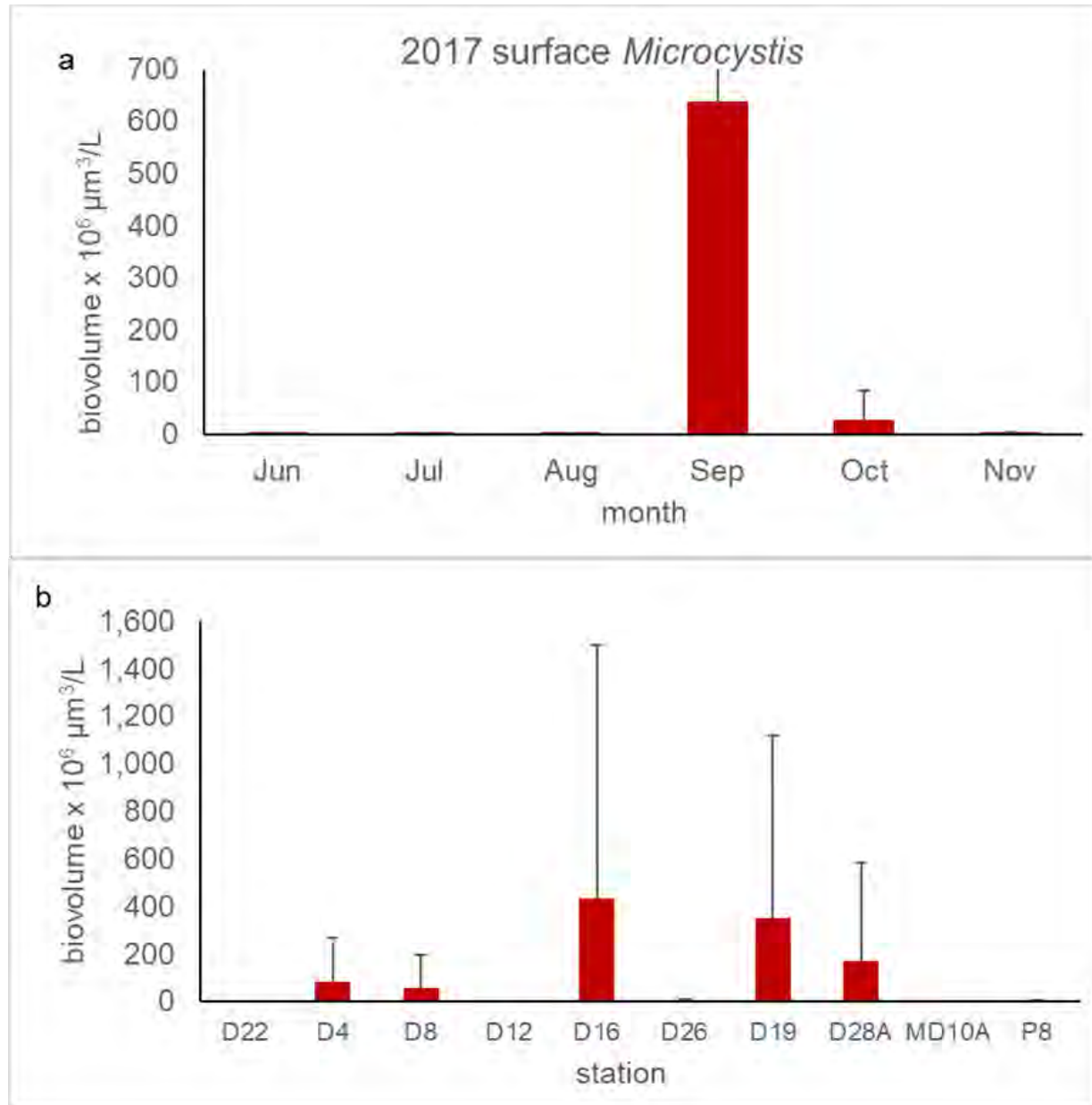


Figure 49. Mean biovolume and median absolute deviation of surface *Microcystis* colonies greater than 0.75 μm in diameter sampled with a surface net tow between June and November 2017 by month (a) and by station (b).

Microcystis was also more abundant in the subsurface water during September compared with other months (ANOSIM, $p < 0.05$) of 2017 (Figure 50a). Among stations, subsurface *Microcystis* was more abundant in the Delta than stations seaward in SBAY and LSAC (ANOSIM, $p < 0.05$) (Figure 50b). The abundance of toxic subsurface *Microcystis* cells was also greater in the central regions of the Delta, where stations D16, D26 and D28A had more toxic *Microcystis* cells than other stations

(ANOSIM, $p < 0.05$). Toxic *Microcystis* cells were less abundant in October and November compared to September (ANOSIM, $p < 0.05$), which suggested microcystin toxin concentration was greatest during the peak of the bloom in September.

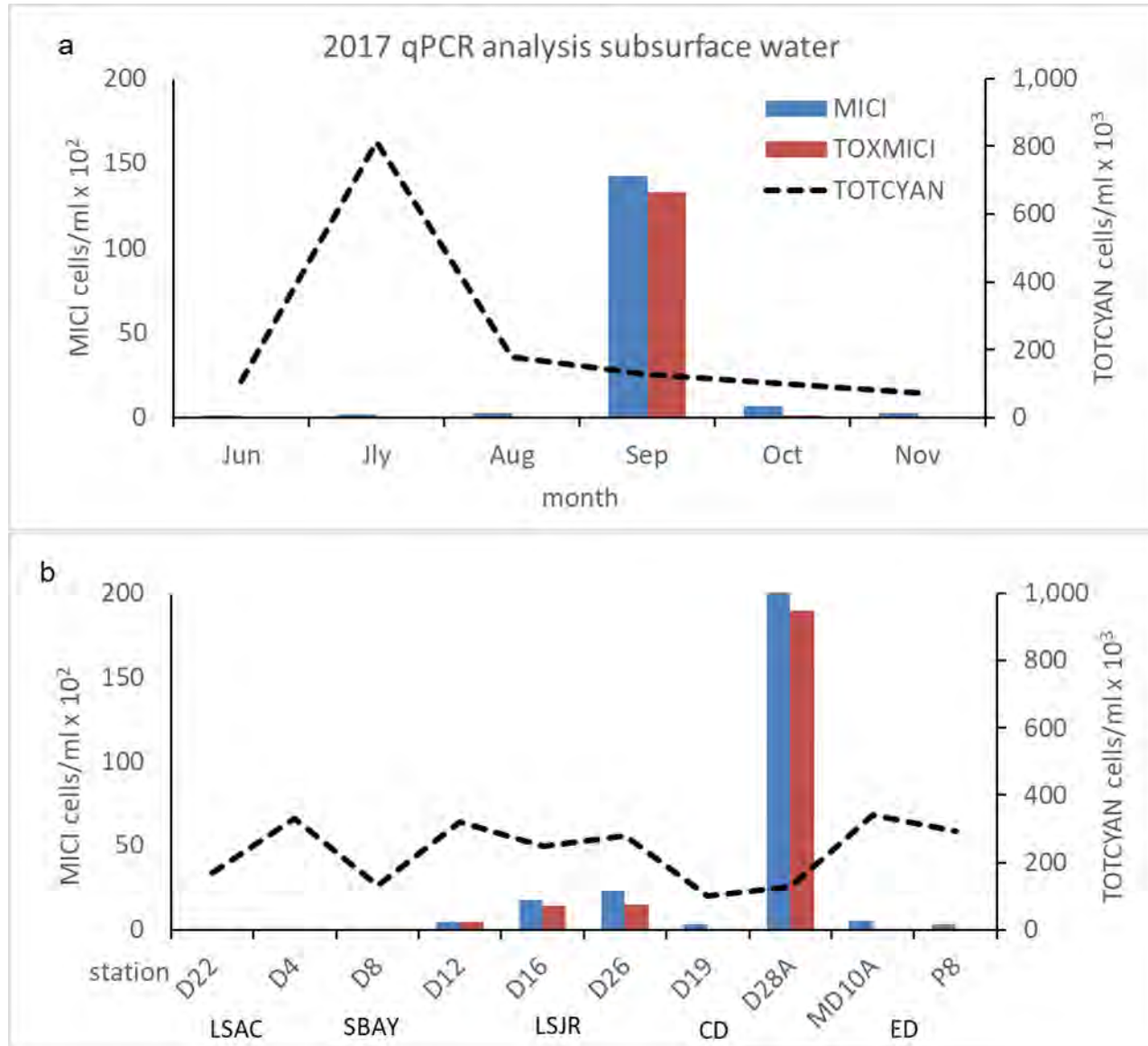


Figure 50. Mean abundance of total *Microcystis* cells (MICI), toxic *Microcystis* cells (TOXMICI), and total cyanobacteria (including *Microcystis*, TOTCYAN) in all size fractions within subsurface samples at 0.3 m depth determined by qPCR in 2017 by (a) month and by (b) station. Note differences in Y axis units.

The abundance of subsurface *Microcystis* and toxic *Microcystis* cells was relatively low in 2017 compared with the abundance of total cyanobacteria (Figure 50). Total cyanobacteria abundance exceeded *Microcystis* abundance by a factor of 8, even during the peak of the *Microcystis* bloom in

September (Figure 51a). Total cyanobacteria abundance was also highest in July 2017 in association with peak chlorophyll-*a* concentration (ANOSIM, $p < 0.05$; Figure 36), although the elevated chlorophyll-*a* is predominantly associated with diatom abundance (Figure 36). Greater total cyanobacteria abundance occurred in the eastern Delta at station P8, compared with stations D4 and D26 seaward (ANOSIM, $p < 0.05$). Overall, *Microcystis* did not contribute more than 20% of the total cyanobacteria abundance (Figure 51b).

Subsurface *Microcystis* abundance was lower in 2017 compared with the dry years 2014, 2015, and 2016 (Kruskal-Wallis, $p < 0.05$), even at the peak of the bloom in September 2017 (Figure 51a). Over time, *Microcystis* was more abundant (Kruskal-Wallis, $p < 0.05$) in the central Delta and LSJR (stations D28A, SJ, MI, D19 and D16) than the LSAC and SBAY (stations D4, D8 and D22; Figure 51b). Subsurface *Microcystis* abundance was also inversely correlated with total cyanobacteria abundance ($r = -0.49$; $p < 0.01$).

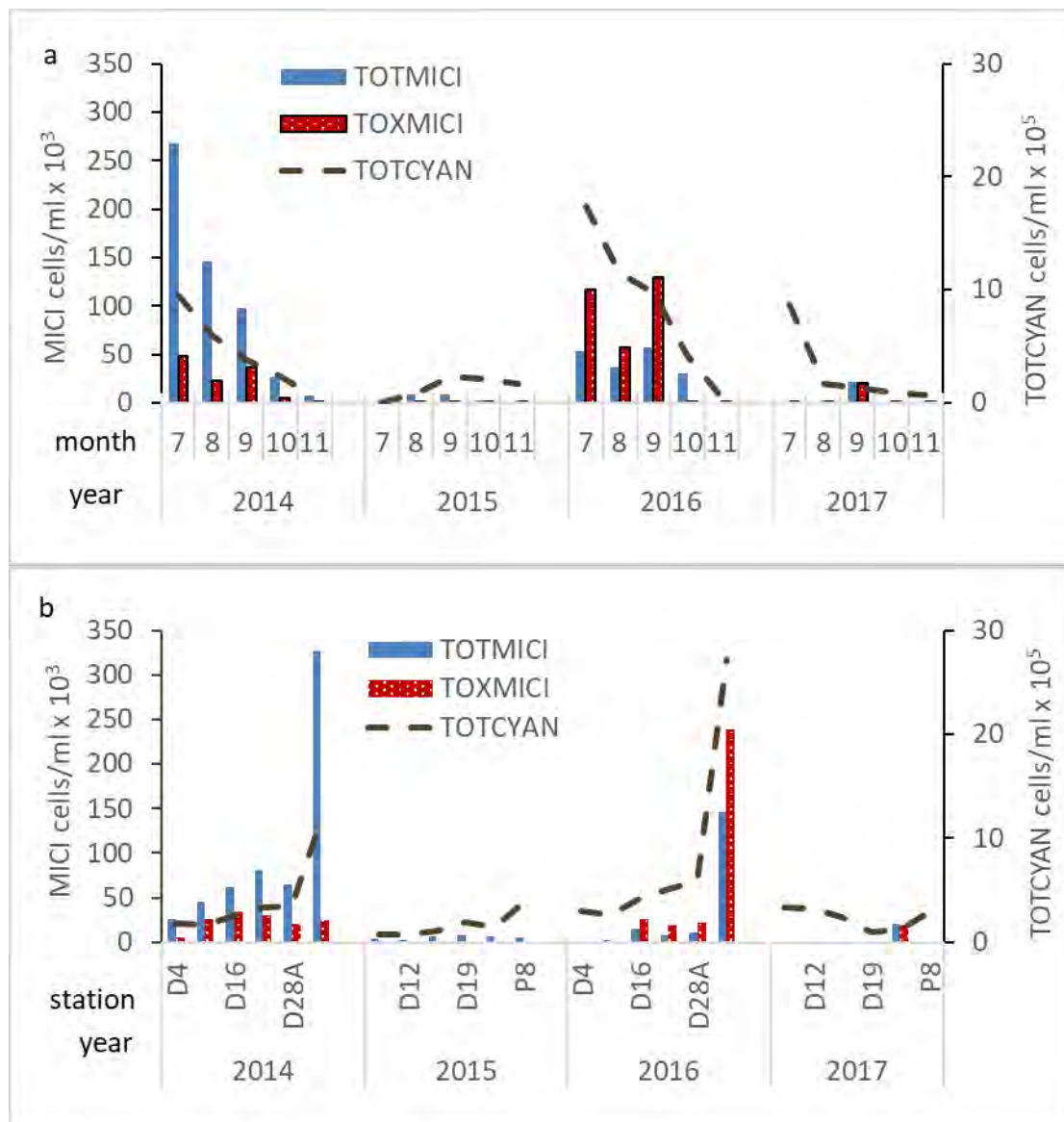


Figure 51. Comparison of the abundance of total *Microcystis* cells (TOTMICI), toxic *Microcystis* cells (TOXMICI), and total cyanobacteria cells (including *Microcystis*, TOTCYAN) in all size fractions within subsurface samples at 0.3 m depth determined by qPCR for (a) summer and fall months and (b) by station between 2014 and 2017. Note differences in Y axes units. Regions were LSAC (D4), LSJR (D12, D16), CD (D19, D28A) and ED (P8).

For all samples collected between 2014 and 2017, surface *Microcystis* biovolume and subsurface *Microcystis* abundance were both positively correlated with water temperature, pH, and X2 and negatively correlated with Delta outflow (OUT) and ammonium concentration for all samples collected between 2014 and 2017 (Table 5). Among years, *Microcystis* biovolume or abundance was consistently correlated with water temperature (positive), X2 (positive), and outflow (negative) (Table 6).

Within 2017, surface *Microcystis* biovolume was positively correlated with outflow and silicate (Table 7). Subsurface *Microcystis* abundance was positively correlated with water temperature, total and dissolved organic carbon, and dissolved organic nitrogen concentration and negatively correlated with turbidity (NTU), total suspended solids, and ammonium concentration (Table 7). Correlations also suggested that the presence of potentially toxic *Microcystis* cells increased with the surface biovolume or subsurface abundance of the bloom (Table 7). In contrast, total cyanobacteria abundance did not vary with *Microcystis* abundance.

Table 5. Spearman correlation coefficients computed between environmental variables and surface *Microcystis* biovolume and subsurface *Microcystis* abundance for six common stations sampled between 2014 and 2017 at biweekly to monthly intervals during July through November. Values greater than 0.30 are significant at the 0.05 level or higher.

Variable	Surface <i>Microcystis</i> biovolume ($\mu\text{m}^3/\text{L}$)	Subsurface <i>Microcystis</i> abundance (cells/ml)
Water temperature	0.40	0.38
Dissolved oxygen	-0.27	-0.23
Specific conductance	0.26	0.24
Turbidity	0.03	-0.29
pH	0.42	0.39
Ammonium	-0.43	-0.46
Nitrate	-0.23	-0.17
Chloride	0.25	0.04
Dissolved organic carbon	0.16	0.45
Total organic carbon	0.18	0.44
Dissolved organic nitrogen	0.25	0.28
Soluble reactive phosphorus	0.07	-0.19
Total phosphorus	0.25	0.24
Silicate	0.04	0.03
Volatile suspended solids	0.07	-0.19
Total dissolved solids	0.31	0.08
Total suspended solids	-0.02	-0.31
Outflow	-0.42	-0.42
X2	0.57	0.58

Table 6. Spearman correlation coefficients computed for surface *Microcystis* biovolume and subsurface *Microcystis* abundance with water temperature, X2, and outflow measured at six stations during the summer and fall for 2014 through 2017 and all years combined. Values in bold type are significant at the 0.05 level or higher.

	Year				All years
	2014	2015	2016	2017	
Surface <i>Microcystis</i> biovolume ($\mu\text{m}^3/\text{L}$)					
Water temperature	0.78	0.46	0.78	0.19	0.40
Outflow	-0.60	-0.21	-0.15	0.76	-0.42
X2	0.11	0.73	-0.30	-0.20	0.56
Subsurface <i>Microcystis</i> abundance (cells/ml)					
Water temperature	0.80	0.69	0.65	0.01	0.38
Outflow	-0.70	0.22	-0.10	0.22	-0.42
X2	0.35	0.77	-0.20	0.06	0.58

Table 7. Spearman correlation coefficients computed for 10 stations sampled monthly at 1m depth between July and November of 2017. Correlation coefficients greater than 0.3 were significant at the 0.05 level or higher. N=50.

Variable	Surface <i>Microcystis</i> biovolume ($\mu\text{m}^3/\text{L}$)	Subsurface <i>Microcystis</i> abundance (cells/ml)
Toxic <i>Microcystis</i> abundance	0.35	0.50
Total cyanobacteria abundance	-0.24	0.09
Water temperature	0.05	0.35
Dissolved oxygen	-0.13	-0.23
Specific conductance	0.05	-0.21
Turbidity	-0.12	-0.32
pH	-0.08	-0.09
Ammonium	0.08	-0.41
Nitrate	0.08	-0.10
Chloride	0.03	-0.19
Calcium	0.15	-0.14
Dissolved organic carbon	-0.14	0.43
Total organic carbon	-0.11	0.37
Dissolved organic nitrogen	0.05	0.32
Soluble reactive phosphorus	0.27	-0.04
Total phosphorus	0.12	-0.08
Silicate	0.42	-0.01
Volatile suspended solids	-0.17	-0.20
Total dissolved solids	0.06	-0.23
Total suspended solids	-0.14	-0.31
Outflow	0.61	0.17
X2	-0.15	-0.14

Overall, we consider our prediction that there would be a relatively small *Microcystis* bloom in the wet year of 2017 to be upheld (Tables 6 and 7); however, the response of *Microcystis* to outflow and X2 were not consistent from year to year (Table 6). Previous research comparing wet and dry years confirmed the lower abundance of *Microcystis* cells during wet years compared with dry years (Lehman et al. 2013, 2017). Low *Microcystis* abundance in 2017 was associated with average daily streamflow in the San Joaquin River between July and September of $149 \text{ m}^3 \text{ s}^{-1}$, which was well above the $28 - 35 \text{ m}^3 \text{ s}^{-1}$ measured during the small *Microcystis* bloom in the wet year 2004 (Lehman et al. 2008), and the median streamflow in the San Joaquin River of $9.6 \text{ m}^3 \text{ s}^{-1}$ during the largest *Microcystis* bloom in the severe drought year 2014 (Lehman et al. 2017). The streamflow in 2017 was also well above the suggested upper threshold for *Microcystis* blooms of $13-15 \text{ m}^3 \text{ s}^{-1}$ measured for the Swan River Estuary, Australia (Robson and Hamilton 2003). Recent research confirmed the positive correlation between high X2 or low outflow with the magnitude of the *Microcystis* surface and subsurface bloom (Lehman et al. 2018). *Microcystis* blooms commonly develop as a result of low streamflow in many rivers or tidal estuaries, including the Swan and Murray River, Australia, Nakong River, South Korea, Guadiana River Estuary, Spain and Portugal, and the Chesapeake and Neuse Rivers, United States (Robson and Hamilton 2003, Bowling et al. 2016, Ha et al. 1999, Lung and Paerl 1988, Sellner et al. 1988, Rocha et al. 2002).

However, streamflow was not the only variable associated with the *Microcystis* bloom in 2017 (Table 7). Water temperature, pH, organic carbon, and ammonia were also correlated with the *Microcystis* bloom. Among these, water temperature has been consistently identified as a key controlling factor, particularly for the subsurface colonies. Water temperature in combination with X2

accounted for most of the variation in *Microcystis* subsurface abundance or surface biovolume for the severe drought years 2014 and 2015 (Lehman et al. 2018), as well as 2014 through 2017 (Tables 6 and 7). *Microcystis* abundance increases once water temperature increases above 19°C in SFE (Lehman et al. 2008). Different timing of the increase in water temperature during the spring and decrease in water temperature during the fall controls the duration of the *Microcystis* bloom each year (Lehman et al. 2017). Although streamflow was high in the summer of 2017, the *Microcystis* bloom still occurred because water temperature was warm enough for bloom development, suggesting that high streamflow alone was not sufficient to eliminate the *Microcystis* bloom (Lehman et al. in press). Water temperature and streamflow combined with nutrient concentrations were also found to be major factors controlling *Microcystis* blooms worldwide, including the Swan, Murray, and Edward Rivers in Australia (Robson and Hamilton 2003, Bowling et al. 2016).

Zooplankton

Zooplankton are small aquatic animals that are a necessary part of fish diets in the SFE. Most larval and juvenile fish eat zooplankton while some smaller fish, such as Delta Smelt and Longfin Smelt, rely on zooplankton for food throughout their entire lives. The decline of several fishes in the SFE, including the Delta Smelt, has been linked to changes in the zooplankton community composition and abundance (Sommer et al. 2007, Winder and Jassby 2011). These changes were caused by introduced species, including the clam *Potamocorbula* and several new zooplankton species.

Potamocorbula, introduced in the late 1980s, eats both phytoplankton and zooplankton and has reduced food availability for fish in the LSZ (Winder and Jassby 2011, Orsi and Mecum 1996, Kimmerer 2006, Greene et al. 2011, also see Clam section), an important habitat for Delta Smelt. *Potamocorbula* reduces zooplankton abundance by consuming their shared food resources,

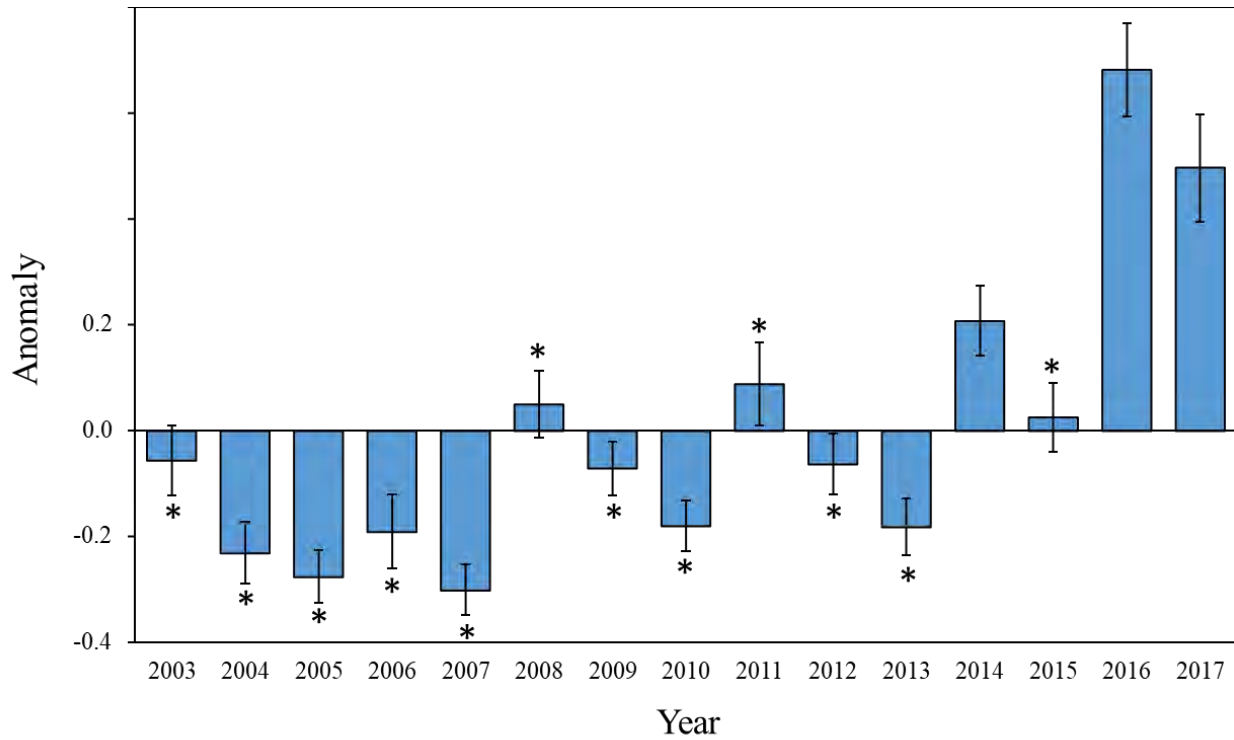
phytoplankton and microzooplankton. *Potamocorbula* also reduces zooplankton abundance by consuming copepod nauplii (early life stages of copepods) at a rate sufficient to explain the long-term decline of zooplankton in the low salinity zone (Kimmerer and Lougee 2015, Kimmerer et al. 1994, Kayfetz and Kimmerer 2017, Kimmerer et al. 2018).

When monitoring of zooplankton began in the upper SFE in the 1970s, the most abundant zooplankton were the native mysid *Neomysis mercedis* and the calanoid copepod *Eurytemora affinis* (Winder and Jassby 2011). Throughout the 1970s, 80s, and 90s many other copepods and mysids were introduced accidentally, which changed the zooplankton community composition (Winder and Jassby 2011).

Historically, abundance of some zooplankton species in the SFE such as *N. mercedis* and *E. affinis* was positively correlated with outflow (Jassby et al. 1995, Kimmerer 2002). We predicted that higher outflow in 2017, resulting in fall X2 located in the Suisun region, would result in higher zooplankton abundance than drier post-POD years when X2 is located near the confluence (from 2003 through 2016). To test this prediction, relative abundance of zooplankton at each sampling location was assessed by month and year to see which months and years abundance was higher or lower than the average. These are called anomalies. An average of these station anomalies was calculated for each month and year to see if overall zooplankton abundance was higher in 2017 compared to other years, and if so in which months high values were observed compared to other post-POD years. For the anomaly analysis, a year was considered the previous December through November to keep the months that comprised each season of the seasonal analysis (Appendix 6) together in the same year. The zooplankton groups chosen for analysis included the calanoid copepods that eat phytoplankton (“herbivorous calanoid copepods” and included *E. affinis*, *Pseudodiaptomus forbesi*, and *Sinocalanus*

doerrii) and mysids because these groups are important in the diet of Delta Smelt (Slater and Baxter 2014, Diet section). A description of the methods used, statistical results, and a summary by season and region can be found in the appendix (Appendix 6).

We found that in 2017, the abundance of herbivorous calanoid copepods was significantly higher than the other post-POD years, except 2014 and 2016 (Figure 52A). Abundance in 2016 was not significantly higher than 2017 but was significantly higher than every other post-POD year (Appendix 6). Interestingly, the largest abundances observed in 2016 occurred early in the year from January to April, with the preceding December 2015 also high (Figure 52B). The high abundances observed in 2017 occurred later in the year from May through November (Figure 52B). Like 2017, both 2006 and 2011 were wet years and higher monthly values in those years were also observed during the summer and fall (Figure 52B). This suggests that the observed high values in the summer and fall of 2006, 2011, and 2017 may have been due to higher freshwater outflow (Appendix 6). The magnitude of the increases seen in 2016 and 2017 compared to other years suggests that other mechanisms, such as increased water temperature, may also be important in determining abundance.



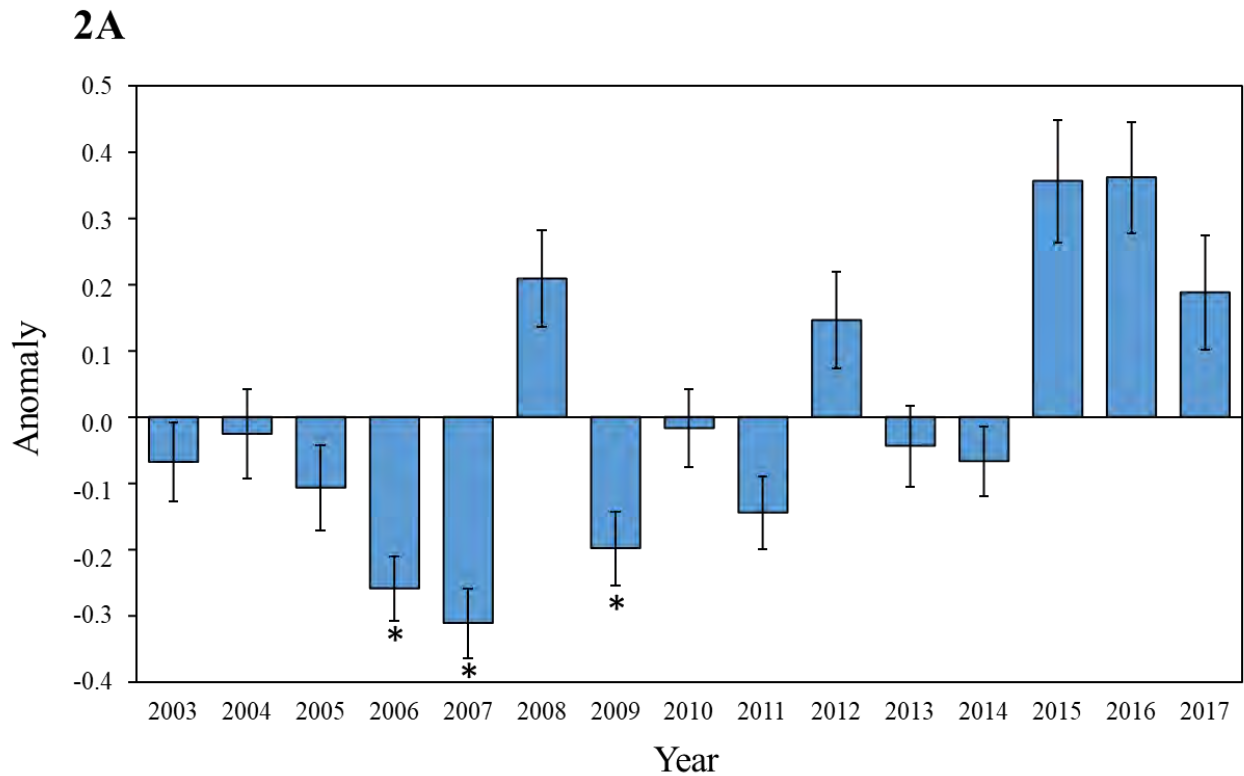
1B

Month	2003	2004	2005	2006	2007	2008	2009	2010	2011	2012	2013	2014	2015	2016	2017
Previous Dec	0.264	0.040	-0.156	-0.399	-0.670	0.163	0.095	-0.323	-0.295	-0.302	-0.091	0.136	0.297	1.354	-0.076
Jan	0.232	-0.529	0.235	-0.072	-0.453	0.289	-0.080	-0.208	-0.320	-0.344	-0.657	0.611	-0.193	1.445	0.009
Feb	-0.086	-0.362	-0.619	0.017	0.082	0.409	0.469	-0.274	-0.346	-0.084	-0.477	0.993	-0.264	0.697	-0.229
Mar	-0.201	0.202	-0.086	-0.463	-0.453	0.474	0.213	-0.478	-0.644	0.034	0.832	-0.095	-0.051	1.022	-0.333
Apr	-0.031	-0.180	-0.232	-0.492	-0.165	0.778	-0.126	-0.364	-0.415	-0.431	0.164	-0.051	0.354	1.467	-0.320
May	-0.575	0.353	-0.441	-0.243	-0.302	0.205	-0.139	0.053	-0.097	0.355	-0.039	0.136	0.635	-0.408	0.443
Jun	-0.182	-0.619	-0.456	0.356	0.147	-0.275	-0.097	-0.335	-0.258	0.101	-0.262	0.028	-0.147	0.712	1.222
Jul	0.106	-0.386	0.061	0.151	-0.228	-0.385	-0.433	-0.074	1.059	-0.343	-0.184	-0.345	-0.495	0.363	1.224
Aug	0.638	-0.246	-0.361	0.215	-0.751	-0.521	-0.041	0.539	0.690	-0.104	-0.328	-0.159	0.161	0.167	0.491
Sep	0.159	-0.464	-0.230	0.117	-0.573	-0.377	-0.361	-0.343	0.933	0.028	-0.596	0.310	-0.061	0.670	0.862
Oct	-0.422	-0.307	-0.553	-0.870	-0.275	0.246	-0.185	-0.186	1.014	0.170	-0.611	0.440	0.049	0.205	1.328
Nov	-0.576	-0.273	-0.471	-0.604	0.028	-0.405	-0.164	-0.163	-0.257	0.168	0.071	0.486	0.345	0.483	1.343

Figure 52. Herbivorous calanoid copepod anomalies 2003 through 2017: A) Annual average of monthly anomalies, asterisk indicates years that were significantly lower than 2017, and B) monthly anomalies by year.

In contrast to copepods, mysid abundance in 2017 was not higher than the other post-POD years (Figure 53A). In 2017, mysid abundance was less than it was in 2015 and 2016 and was only significantly higher than it was in 2006, 2007, and 2009 (Figure 53A). In 2017, high abundances of mysids were seen in summer and fall, but low abundances were observed from January through March

relative to other post-POD years (Figure 53B).



2B

Month	2003	2004	2005	2006	2007	2008	2009	2010	2011	2012	2013	2014	2015	2016	2017
Previous Dec	0.415	-0.290	-0.471	-0.447	-0.784	0.649	0.068	0.233	-0.024	0.303	-0.084	-0.015	0.094	-0.190	0.552
Jan	-0.209	-0.470	-0.293	-0.520	-0.338	0.116	-0.079	0.775	-0.065	0.370	-0.181	0.009	0.260	0.656	-0.117
Feb	-0.199	-0.241	-0.184	-0.430	-0.305	0.131	-0.107	-0.154	0.322	0.967	0.510	0.444	-0.209	-0.236	-0.376
Mar	0.044	-0.181	-0.148	-0.331	-0.300	0.914	-0.223	-0.237	-0.281	0.166	-0.005	0.020	0.658	-0.076	-0.057
Apr	-0.069	0.066	0.051	-0.116	-0.410	0.398	-0.269	-0.244	-0.298	0.096	0.297	-0.374	0.799	0.062	0.006
May	-0.280	0.110	-0.315	-0.273	-0.435	0.603	-0.429	-0.058	-0.277	-0.200	-0.157	-0.180	1.516	0.107	0.231
Jun	0.158	0.277	-0.500	-0.112	0.032	0.545	-0.501	-0.050	-0.404	0.457	0.010	-0.390	-0.313	1.115	-0.232
Jul	-0.167	0.250	-0.294	0.021	0.175	0.216	-0.368	0.119	0.080	-0.036	-0.540	-0.241	0.065	0.254	0.510
Aug	-0.222	-0.124	0.622	0.052	-0.199	-0.476	-0.470	0.022	-0.462	-0.190	-0.381	0.070	1.113	0.682	0.338
Sep	0.179	0.441	0.304	-0.078	-0.449	-0.389	-0.487	-0.434	-0.310	0.006	-0.100	-0.080	0.109	0.740	0.568
Oct	-0.199	0.037	0.129	-0.260	-0.327	-0.447	0.231	-0.149	-0.097	-0.445	0.130	0.003	-0.088	0.938	0.553
Nov	-0.267	-0.180	-0.182	-0.616	-0.332	0.244	0.256	-0.027	0.081	0.257	-0.023	-0.067	0.271	0.290	0.278

Figure 53. Mysid anomalies 2003 through 2017: A) annual average anomalies, asterisk indicates years that were significantly lower than 2017 ($P < 0.05$), and B) monthly anomalies by year.

In 2017, zooplankton abundance was lower earlier in the year, when freshwater outflow was the highest, and higher during summer and fall relative to most of the other post-POD years (Figures 52B and 53B). The increase in herbivorous calanoid copepods was mainly due to an increase in the

subtropical species *Pseudodiaptomus forbesi* (Appendix 6). *P. forbesi* increased due to a variety of factors which likely included: warm water temperatures in 2017, an increase in subsidies from upstream areas where densities are typically higher (Kimmerer et al. 2018, 2019), and decreased clam predation due to lower grazing rates in 2017 (see Clam section and Appendix 6). Although mysid abundance was also high in the summer and fall of 2017 relative to other post-POD years (Figure 53B), overall the 2017 mean wasn't significantly higher than most of the other post-POD years (Figure 53A).

As described above, the highest abundances in zooplankton in 2017 were observed in summer and fall (Figures 52B and 53B). However, high abundances were not necessarily equally distributed across months and regions. Winter densities of herbivorous calanoid copepods in San Pablo Bay in 2017 were significantly higher than every other post-POD year except 2011 (Table 8). During summer and fall 2017, densities of herbivorous calanoid copepods in the lower San Joaquin River were significantly higher than every other post-POD year (Table 8, Figure 54). During fall in the lower Sacramento River densities of herbivorous calanoid copepods were also significantly higher than every other post-POD year (Table 8, Figure 54). In Suisun Bay during summer 2011, densities of herbivorous calanoid copepods were significantly higher than every other post-POD year except 2006 and 2017, which were the only other high outflow years during this period (Table 8, Figure 54). However, in 2017 in Suisun Bay during summer, densities of herbivorous calanoid copepods were only significantly higher than only about half of the other post-POD years (Table 8) because of the high variability among samples in 2017 (Figure 54). During the high outflow years of 2006, 2011, and 2017, densities of herbivorous calanoid copepods in Suisun Bay were higher than every other post-POD year except 2003, 2005, and 2010 (Table 8, Figure 55). The only statistically significant increase in mysids in 2017 was in Suisun Marsh in the fall where densities were significantly higher than every other post-POD

year (Table 8). Increases in mysids were also observed during summer 2017 in Suisun Marsh and Suisun Bay, but these increases were not statistically significantly higher than other years because of high variability between samples (Figure 55). Increases in mysids were also observed during summer 2017 in Suisun Marsh and Suisun Bay, but these increases were not statistically significantly higher than other years because of high variability within years, particularly 2003, 2016, and 2017 (Figure 55).

Table 8. Summary of statistically significant comparisons of wet years (2006, 2011, 2017) against other years by region and season for herbivorous calanoid copepods and mysids.

Year	Region	Season	Year significantly higher ($P < 0.050$) than:	Zooplankton Group
2017	San Pablo Bay	Winter	all years from 2003-2016, except 2015	Herbivorous Calanoid Copepods
2011	Suisun Bay	Summer	2003-2016, except 2006 and 2017	Herbivorous Calanoid Copepods
2017	Suisun Bay	Summer	2004, 2005, 2007, 2008, 2013, 2014, 2016	Herbivorous Calanoid Copepods
2017	Suisun Bay	Fall	2003-2016, except 2011	Herbivorous Calanoid Copepods
2017	Lower Sacramento River	Fall	all years from 2003-2016	Herbivorous Calanoid Copepods
2017	Lower San Joaquin River	Summer	all years from 2003-2016	Herbivorous Calanoid Copepods
2017	Lower San Joaquin River	Fall	all years from 2003-2016	Herbivorous Calanoid Copepods
2017 2011 2006	Suisun Marsh	Summer	2004, 2007-2009, 2012-2015	Herbivorous Calanoid Copepods
2017	Suisun Marsh	Fall	all years from 2003-2015	Mysids

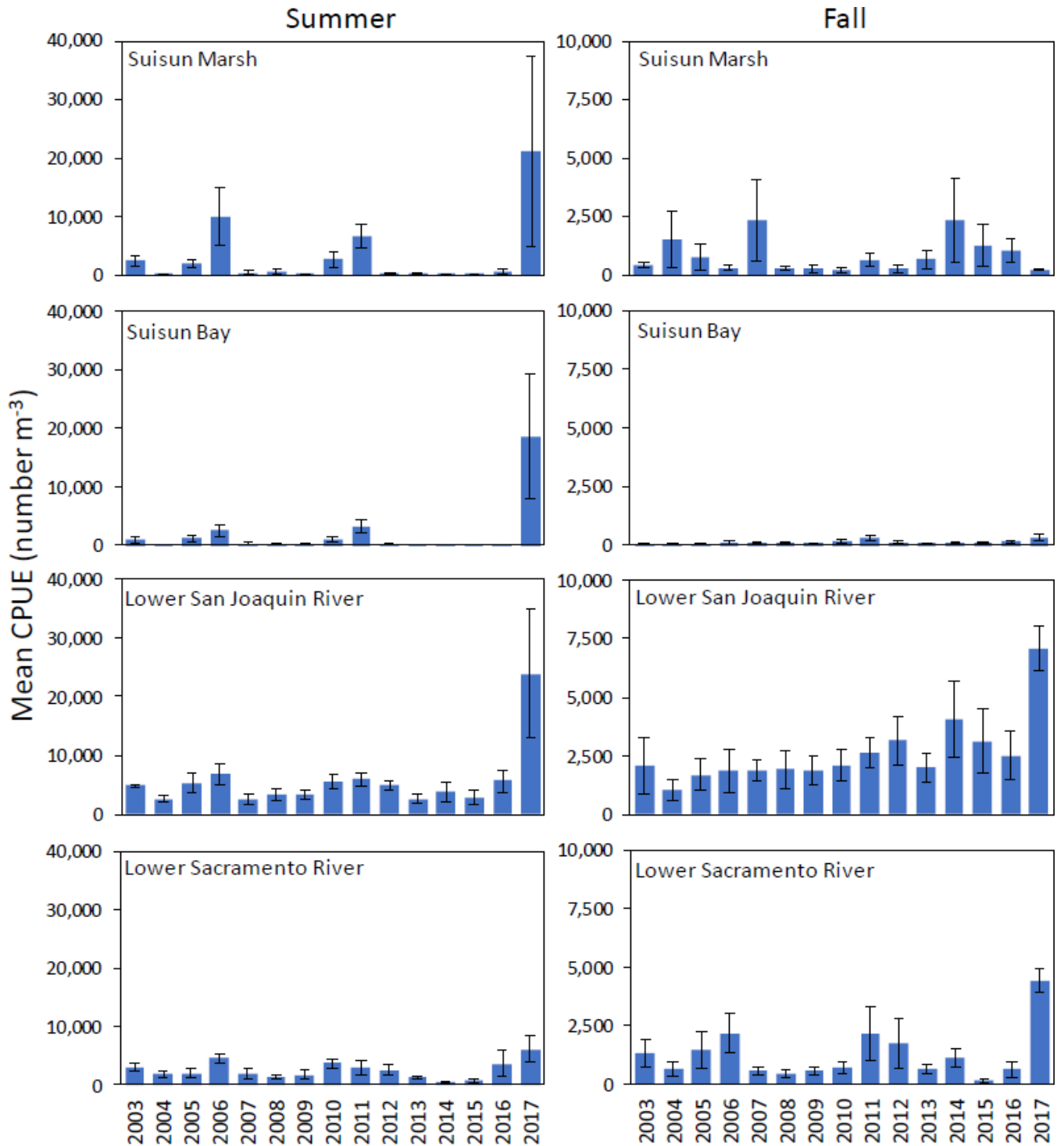


Figure 54. Herbivorous calanoid copepod (*Eurytemora*, *Pseudodiaptomus*, and *Sinocalanus* adults and juveniles) mean catch per unit effort (CPUE±SE) from 2003 through 2017 for summer (June through August) and fall (September through November) from Suisun Marsh, Suisun Bay, Lower San Joaquin River, and Lower Sacramento River. Note different y-axis scale between summer and fall.

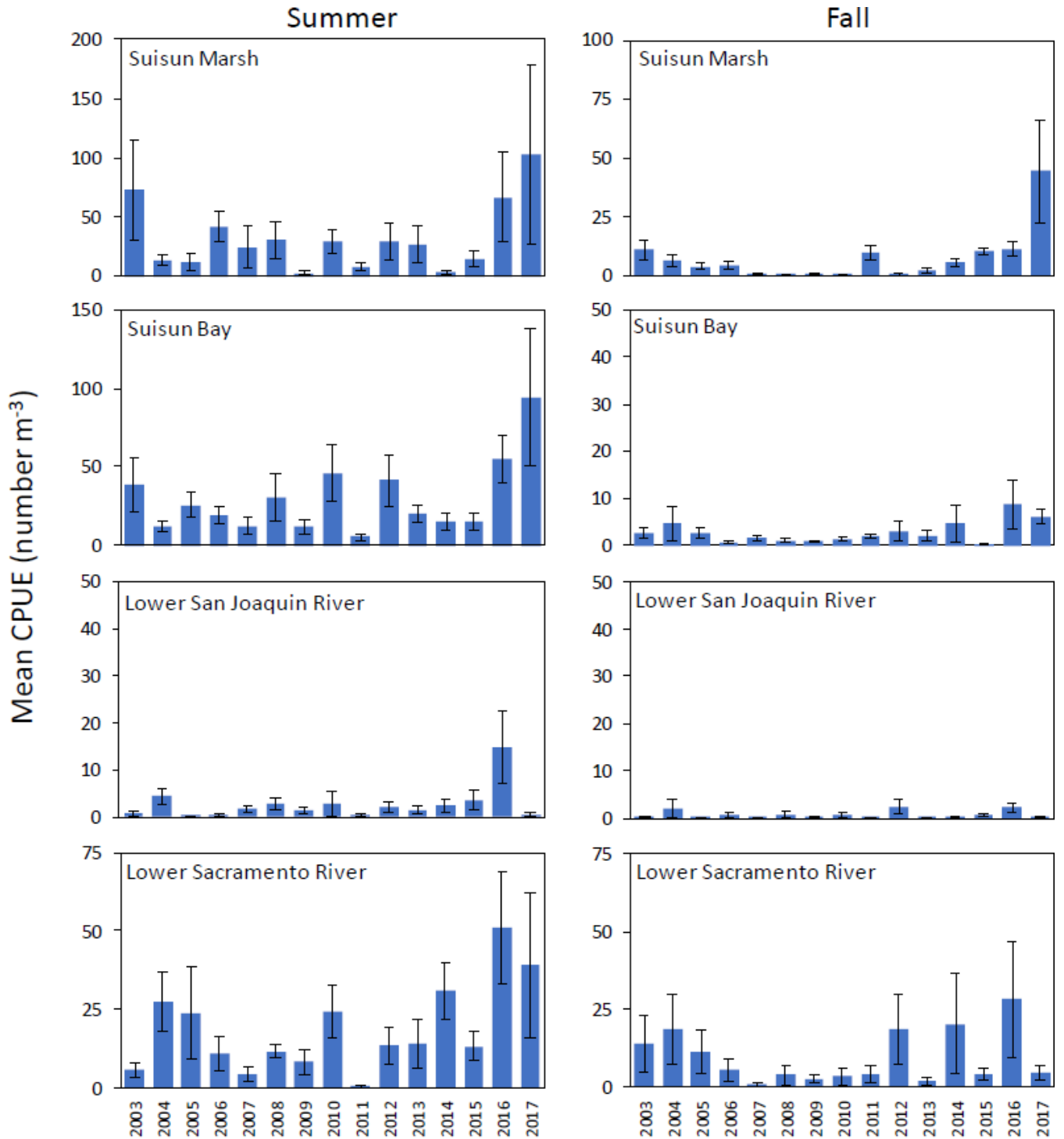


Figure 55. Mysid mean catch per unit effort (CPUE±SE) from 2003 through 2017 for summer (June through August) and fall (September through November) from Suisun Marsh, Suisun Bay, Lower San Joaquin River, and Lower Sacramento River. Note different y-axis scales between regions and seasons.

Although zooplankton abundance did not increase in every region and season of 2017, in the areas of the estuary where the low salinity zone resides, high abundances of herbivorous calanoid copepods were observed that support the prediction that in summer and fall an X2 location closer to Suisun Bay increases zooplankton abundance and thereby food availability for Delta Smelt (Appendix 6). However, not all wet years had high abundances of zooplankton in comparison to 2017 or other water year types. This suggests that other factors such as downstream transport of zooplankton and water temperature may also be important. Overall, the prediction that wet years when X2 is located in the Suisun region during the fall will have higher zooplankton abundances than dry years was not fully supported.

Recent results from the directed Outflow Project were generally consistent with our results for zooplankton but provided more detailed information for some topics (Schultz et al. 2019). In particular they sampled a wider geographic area, including the Cache Slough Complex and the SRDWSC. These areas tended to have high abundance of zooplankton in the summer and fall (Schultz et al. 2019), although by late summer 2017 water temperatures in these areas were too high for Delta Smelt. However, their dataset (from STN, FMWT and EDSM) did not cover all months or as many years. They also detected a slight increasing trend as X2 moved landward using data from 2010-2017, a trend opposite to our prediction. In 2017, they did observe an increase in zooplankton for Suisun Bay and Marsh when compared to non-wet years but did not detect any increase in zooplankton in these areas during the fall X2 action. However, since zooplankton abundance generally decreases seasonally from summer to fall, this result was not unexpected. The Schultz et al. (2019) analysis was innovative because it included the effects of water quality factors on zooplankton abundance, and results from additional years will likely improve our understanding of zooplankton ecology. Results from their work

also highlights the need to include the North Delta in long-term monitoring of zooplankton and other variables. It also highlights the importance of looking at multiple habitat factors simultaneously, because although some of these freshwater regions may have more abundant food resources than the LSZ, other factors such as high water temperatures or low turbidity may make these areas uninhabitable by Delta Smelt seasonally.

Clam Biomass, Grazing Rate and Recruitment

The 1987 invasion of the estuary by the “overbite” clam *Potamocorbula amurensis* (Nichols et al. 1990) caused a severe change in the food web (Brown et al. 2016a). Native to estuaries of mainland East Asia, *Potamocorbula* thrives in brackish water and tolerates variable salinity (Paganini et al. 2010). Following the *Potamocorbula* invasion, phytoplankton biomass decreased ~5-fold in Suisun Bay and the western Delta (Alpine and Cloern 1992), the size distribution of phytoplankton shifted toward smaller cells (Kimmerer and Thompson 2014), and production by diatoms nearly ceased in this region (Kimmerer 2005). The abundance of brackish-water rotifers and *E. affinis* and other copepods declined, apparently due to predation by and competition with *Potamocorbula* (Kimmerer et al. 1994, Kimmerer and Lougee 2015).

The freshwater clam *Corbicula fluminea*, introduced well before environmental monitoring began, likely had effects on the food web in the freshwater Delta given its substantial grazing impact on phytoplankton in the Delta and elsewhere (Cohen et al. 1984, Lopez et al. 2006, Lucas and Thompson 2012). *Corbicula* has been present in the estuary since at least 1945 (Hanna 1966). It appears to be food limited in the system (Prokopovich 1969, Foe and Knight 1985). Its population density is patchy throughout the Delta, with food availability, physiological tolerances, dispersal capabilities, and predator densities all hypothesized to influence distribution and abundance (Lopez et al. 2006).

The changes in lower trophic levels associated with the *Potamocorbula* invasion were followed by shifts in diets, distributions, and abundance of many fish species; for example, Striped Bass, Northern Anchovy (Kimmerer 2006), Splittail *Pogonichthys macrolepidotus*, and three other species in

Suisun Marsh (Feyrer et al. 2003). Abundance of Striped Bass and Longfin Smelt declined soon after the *Potamocorbula* invasion (Kimmerer et al. 2009, Thomson et al. 2010, Mac Nally et al. 2010).

Bivalve biomass distribution and magnitude are dependent on the ability of larvae to settle and of the recruits and adults to survive and grow at a location. Thus, adult distribution and population biomass of *Potamocorbula* and *Corbicula* varies with larval distribution, post-larval survival and growth rate, and the continued presence of previous years adults at a location. *Corbicula* live 5 years and *Potamocorbula* live 2 years and thus *Corbicula*'s impact on the biomass in downstream locations in dry and wet years reflects the freshwater distribution in the previous years. The brackish water clam *Potamocorbula* has a grazing rate of about four times that of the freshwater clam *Corbicula* so an equal biomass of the two species can graze significantly different volumes of water.

Our prediction was that *Potamocorbula* distribution and biomass (and therefore grazing rate) would decline when X2 was in the Suisun region in the fall and to be largest when X2 was upstream near the confluence. *Corbicula* distribution, relative to X2, was expected to be opposite that of *Potamocorbula*. Thus, in a wet year we expected (1) less brackish water habitat in Suisun Bay resulting in less *Potamocorbula* and total bivalve biomass and grazing pressure; and (2) *Corbicula* would settle in Suisun Bay in spring and have some influence on phytoplankton loss in fall.

Bivalve monitoring data (wdl.water.ca.gov/bdma/grts/) provides the distribution of these two bivalve species from 2006 to 2017 (see Appendix 7 for details of methods and extended discussion of results). We will use these data to examine the bivalve distribution and biomass in the wet years of 2017 and 2011 and to compare those data to that of two dry years, 2009 and 2014. These two dry years were chosen to control for previous wet conditions that can have important effects on the age structure of bivalve populations. The years 2009 and 2014 are each 3 years after the previous wet year, so will likely minimize the effect of intervening years on age structure of the population (2006 and 2011, respectively). In general, *Potamocorbula* biomass increases in the seaward direction and is strongly seasonal with lower biomass in the spring than in the fall. *Corbicula* biomass is usually higher in spring than fall and its biomass decreases in the seaward direction. The two-bivalve species commonly co-occur in Suisun Marsh and Honker Bay and overlap within the X2 region.

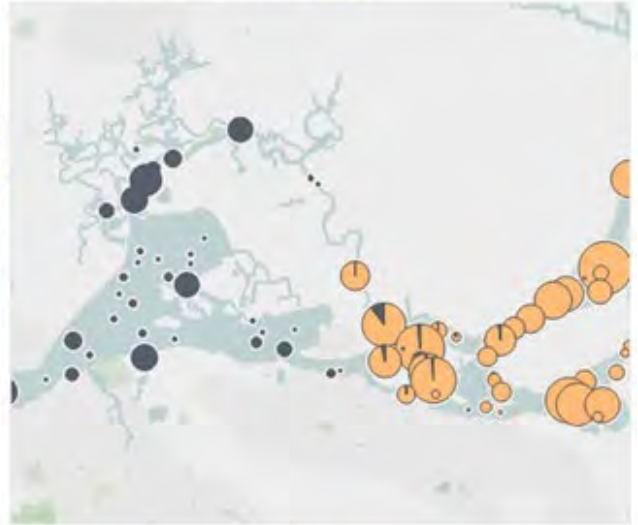
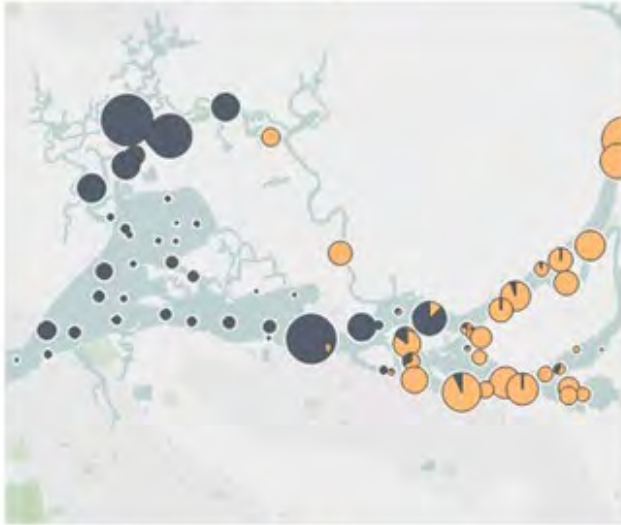
The high freshwater flows of 2011 and 2017 resulted in bivalve distributions reflecting the location of X2 in spring, downstream of Suisun Bay, and in fall, downstream of the confluence for most

of fall (mid-July through October). Our predictions would lead us to believe that (1) *Potamocorbula* biomass and grazing rate would be low in spring, (2) total bivalve biomass (i.e., both species) and grazing rate would increase in fall in the LSZ but would be less than we would see in dry years, and (3) *Corbicula* would be present downstream of the confluence in spring and fall.

Comparing bivalve biomass in wet years (2011, 2017) and dry years (2009, 2014) shows the potential impact of bivalve grazing on the pelagic food availability in extreme water years (Figures 56a,b). *Potamocorbula* responded as we would expect with high freshwater flow: lower biomass in the LSZ in spring in the wet years than in the dry years (Figure 56a). Suisun Bay *Potamocorbula* increased in biomass between May and October of all four years (Figure 56b). These increases in clam biomass suggest that food resources for the bivalves were relatively abundant in the LSZ during this period for both wet and dry years; the source of this production is unclear. *Corbicula* populations had less pronounced differences in biomass between spring and fall and between wet and dry in all years than was seen with *Potamocorbula*. *Corbicula's* distribution extended beyond the confluence in all years. *Corbicula's* downstream presence in dry years was due to large individuals surviving from earlier wet years (2006 bivalves present in 2009 and 2011 bivalves still present in 2014).

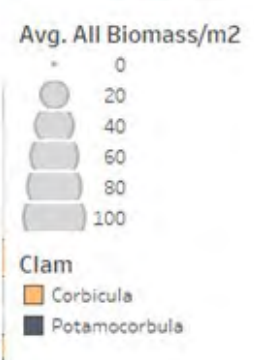
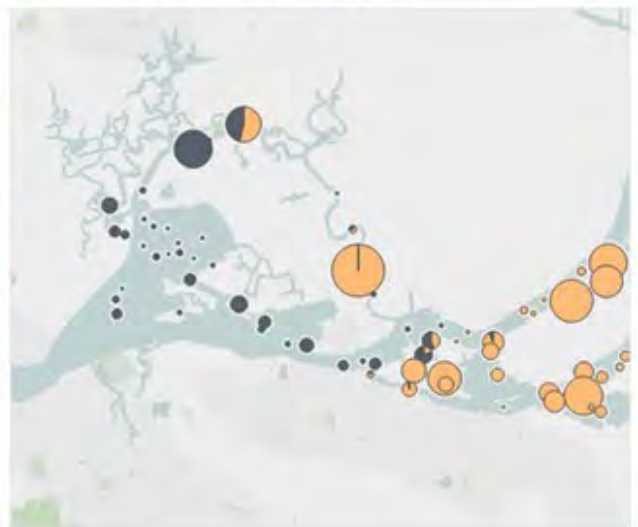
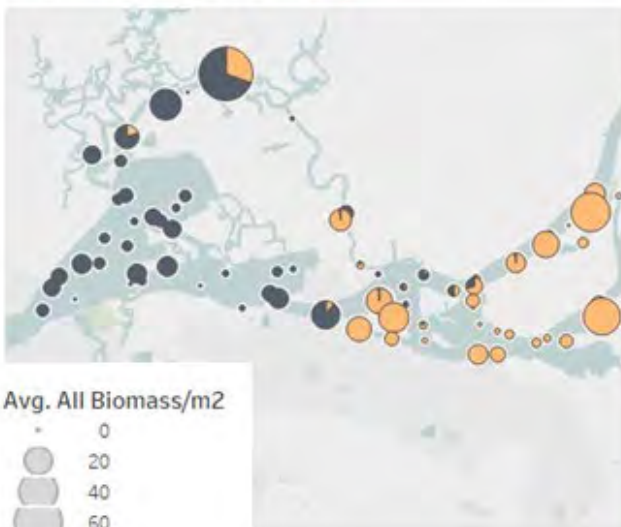
A) Biomass May 2009 - **Dry**

Biomass May 2011 - **Wet**



Biomass May 2014 - **Dry**

Biomass May 2017 - **Wet**



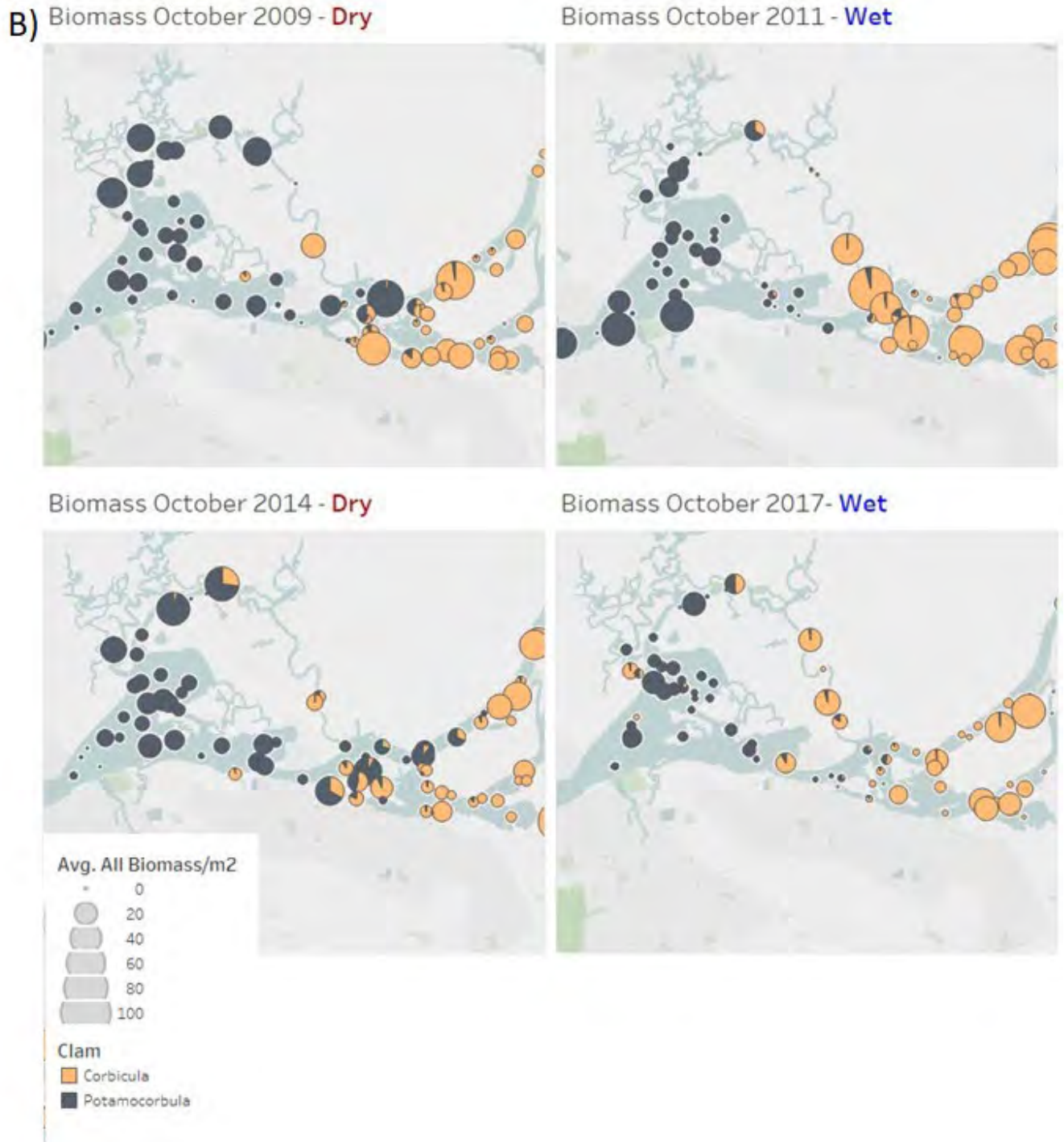
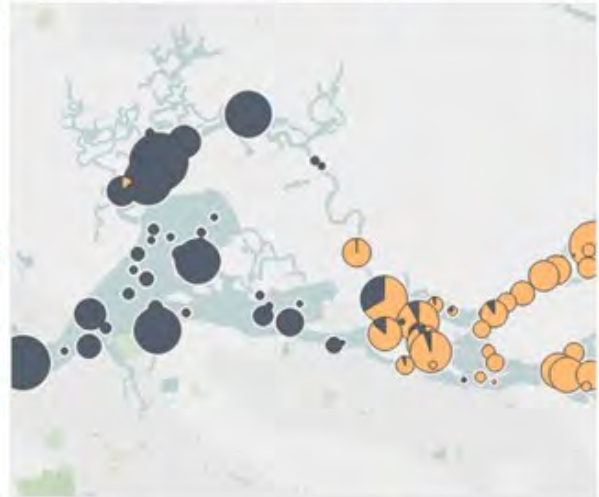
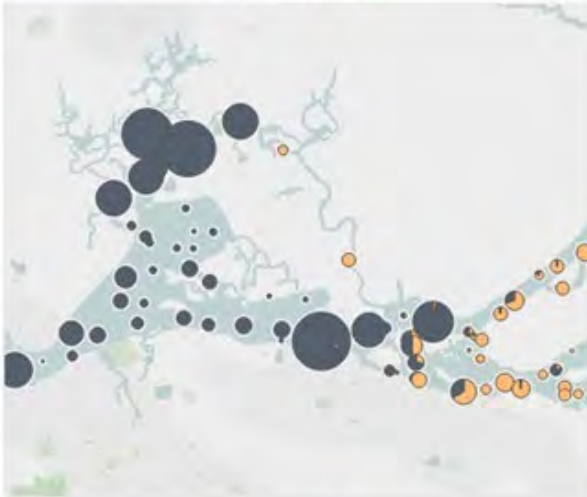


Figure 56. Ash-free-dry mass of *Potamocorbula* and *Corbicula* in the upper San Francisco Estuary during a) May of dry (2009, 2014) and wet (2011, 2017) years, and b) October of dry (2009, 2014) and wet (2011, 2017) years.

Grazing rate distributions of both species were unique in 2017 (Figure 57). *Potamocorbula* grazing rate was lower in spring than fall in all years. Fall *Potamocorbula* grazing rate was lower and more spatially homogenous in 2017 than in 2011 and was much lower than seen in the dry years (Figure 57b). The effect of bivalve grazing was likely to be much greater in the fall of 2011 and in the dry years than in the fall of 2017. There are periods and locations where clam grazing could control phytoplankton growth rate in 2011: *Potamocorbula* grazing was capable of limiting phytoplankton growth rate in fall in Suisun Bay and western Montezuma Slough and *Corbicula* had potentially been controlling grazing rates on local phytoplankton growth rate in the confluence and eastern Montezuma Slough. In fall of the dry years (Figure 57b) grazing rates of both species were high in the LSZ and were likely able to control phytoplankton growth rate within the LSZ. Bivalve grazing in fall 2017 was the lowest observed for *Potamocorbula* and *Corbicula* during the period examined. The low grazing rates occurred in spring and fall 2017 and were not likely to have limited phytoplankton growth rate in the LSZ.

A) Grazing Rate May 2009 - **Dry**

Grazing Rate May 2011 - **Wet**



Grazing Rate May 2014 - **Dry**

Grazing Rate May 2017 - **Wet**

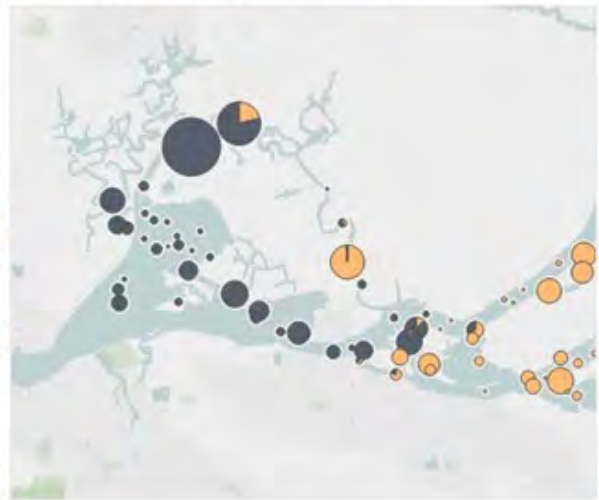
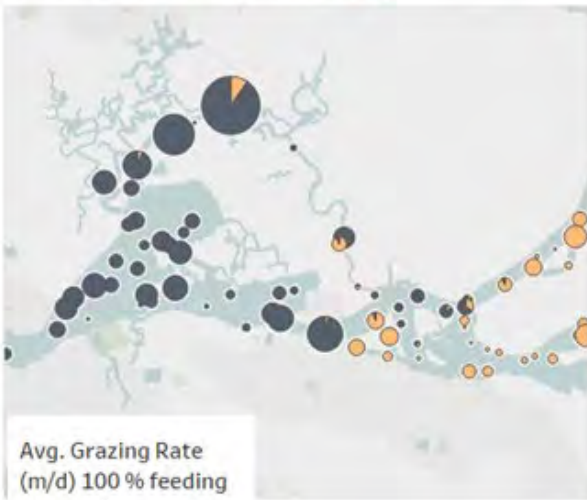




Figure 57. Grazing rate of *Potamocorbula* and *Corbicula* in the upper San Francisco Estuary during a) May of dry (2009, 2014) and wet (2011, 2017) years, and b) October of dry (2009, 2014) and wet (2011, 2017) years.

As we predicted, the total bivalve biomass and grazing pressure in spring and fall were greatly reduced with the increased freshwater flow in 2017 relative to previous dry years. The reduced brackish water habitat in Suisun Bay reduced *Potamocorbula*'s presence and grazing rate in spring and fall. *Corbicula* settled in upper Suisun Bay with the increased freshwater in spring, but the population

biomass grew slowly and had less effect on the fall grazing rate in Suisun Bay than was predicted. In comparison to bivalve grazing in 2011, 2017 bivalve population biomass and grazing rates were much smaller than in 2011. Freshwater flow was higher and X2 was farther downstream in 2017, possibly indicating a threshold of freshwater exposure time was exceeded for *Potamocorbula* juveniles.

Aquatic Vegetation

Invasive aquatic vegetation increased in coverage during the recent drought (2012-2016), with coverage of submerged aquatic vegetation (SAV) increasing by 50% between 2008 and 2014, while floating aquatic vegetation (FAV) increased almost exponentially over the same time period (The State of the Estuary Partnership 2015). While both the SAV and FAV communities in the Delta are composed of multiple native and non-native species, non-native Brazilian Waterweed (*Egeria densa*) dominates the SAV and non-native Water Hyacinth (*Eichhornia crassipes*) and Water Primrose (*Ludwigia* spp.) are the dominant species of FAV (Santos et al. 2009, Boyer and Sutula 2015, Khanna et al. 2018). Aquatic plants, and the dominant species in the Delta system specifically, have substantial potential for altering the local aquatic ecosystem, including effects on water quality (Boyer and Sutula 2015, Wilcock et al. 1999, Greenfield et al. 2007, Yarrow et al. 2009), the food web (Vanderstukken et al. 2011, Toft et al. 2003), and the fish community (Brown and Michniuk 2007, Nobriga and Feyrer 2007, Conrad et al. 2016). For Delta Smelt specifically, invasive aquatic vegetation may eliminate available habitat simply by occupying open water areas and may also contribute to a general deterioration of habitat by facilitating increased water clarity over the entire system (Hestir et al. 2016).

High flows, such as in 2017, are likely to have a stronger effect on FAV rather than SAV, simply because rooted (i.e., non-floating) forms of vegetation are less likely to be washed away. For this reason our prediction is that total coverage of Water Hyacinth, a truly floating plant that does not root to the sediment, would be reduced by high flows in 2017 associated with X2 location in the Suisun region during the fall.

Water Primrose, also an FAV species because its foliage resides above the water surface, is rooted like most species of SAV. Therefore, while Water Hyacinth may literally be swept away by high flows, Water Primrose and SAV are less likely to be affected in the same way. While high water velocities indeed may limit SAV distribution (Durand et al. 2016), the areas where SAV is already

located are typically lower-velocity, nearshore areas, which may be less affected than the center of channels by the high flows of 2017. In fact, any reduction in Water Hyacinth may be favorable for Water Primrose and SAV, because it may open up new habitat. Successful chemical control of Water Hyacinth was a likely factor in the expansion of Water Primrose from 2004 - 2016, particularly in the Central Delta (Santos et al. 2009, Khanna et al. 2018). In summary, because of the multiple factors affecting SAV and FAV coverage, it was not reasonable to make directional predictions about the effect of 2017 high flows on combined aquatic vegetation coverage.

Distribution and abundance of aquatic vegetation in the Delta is influenced by more than flow and water velocity. Other abiotic factors also influence growth and spread, including water temperature, salinity, nutrient concentrations, water clarity specifically for SAV and the substrate for all rooted plants (Boyer and Sutula 2015). Aquatic vegetation control efforts are also likely to influence distribution and abundance. The California State Parks and Recreation Division of Boating and Waterways (DBW) operates a major control program for SAV and FAV in the Delta, primarily using chemical treatment as a control method. The SAV control program began in 2001 and in 2017 was permitted to treat up to 5,000 acres of SAV between March 1 and November 30. The FAV control program began much earlier in 1983 and has focused on Water Hyacinth and more recently South American Spongeplant (*Limnobiium laevigatum*). Although Water Primrose has been reported in the Delta since 1949 (Light et al. 2005), chemical treatment did not begin until 2016. The FAV control program has treated up to 4,500 acres in a year.

High-resolution maps of Delta aquatic vegetation coverage were created for falls of 2014 – 2017 and compared for Water Hyacinth, Water Primrose, and SAV (see Appendix 8 for detailed methods and additional results). Hyperspectral imagery (collected by the National Aeronautic and Space Administration Jet Propulsion Laboratory) was classified to coverage of FAV and SAV. FAV is classified according to the plant genera, but it is not currently possible to classify SAV by species or genera, so maps provide basic coverage information for SAV. Field data of aquatic species were collected each year within a month of imagery collection to train and validate imagery classification.

To evaluate the prediction, aquatic vegetation maps for each year were divided into three regions (Liberty Island, West Delta, and East Delta) that were consistently surveyed through the 2014 – 2017 time series (Figure 58). Total acreage of Water Hyacinth, Water Primrose, and SAV were

calculated from the coverage maps developed for each year. As the imagery was only collected once per year, there are no averages or calculation of other summary statistics applied to the coverage data; instead, the sum of acreage for each aquatic vegetation class is shown for each year and region. To evaluate the coverage information in the context of abiotic and control measures that might influence the results, we summarize flow, turbidity, water temperature, salinity, nutrients, and chemical control efforts for each year. Delta outflow from DAYFLOW was summarized for the months of April – October for each year, as this is the general season for aquatic vegetation growth and conditions during this time would influence coverage observed in the aerial surveys conducted in the fall. Water quality data from the EMP were summarized for the East and West Delta regions on a monthly basis, April – October of each year. The EMP does not sample in the Liberty Island region.

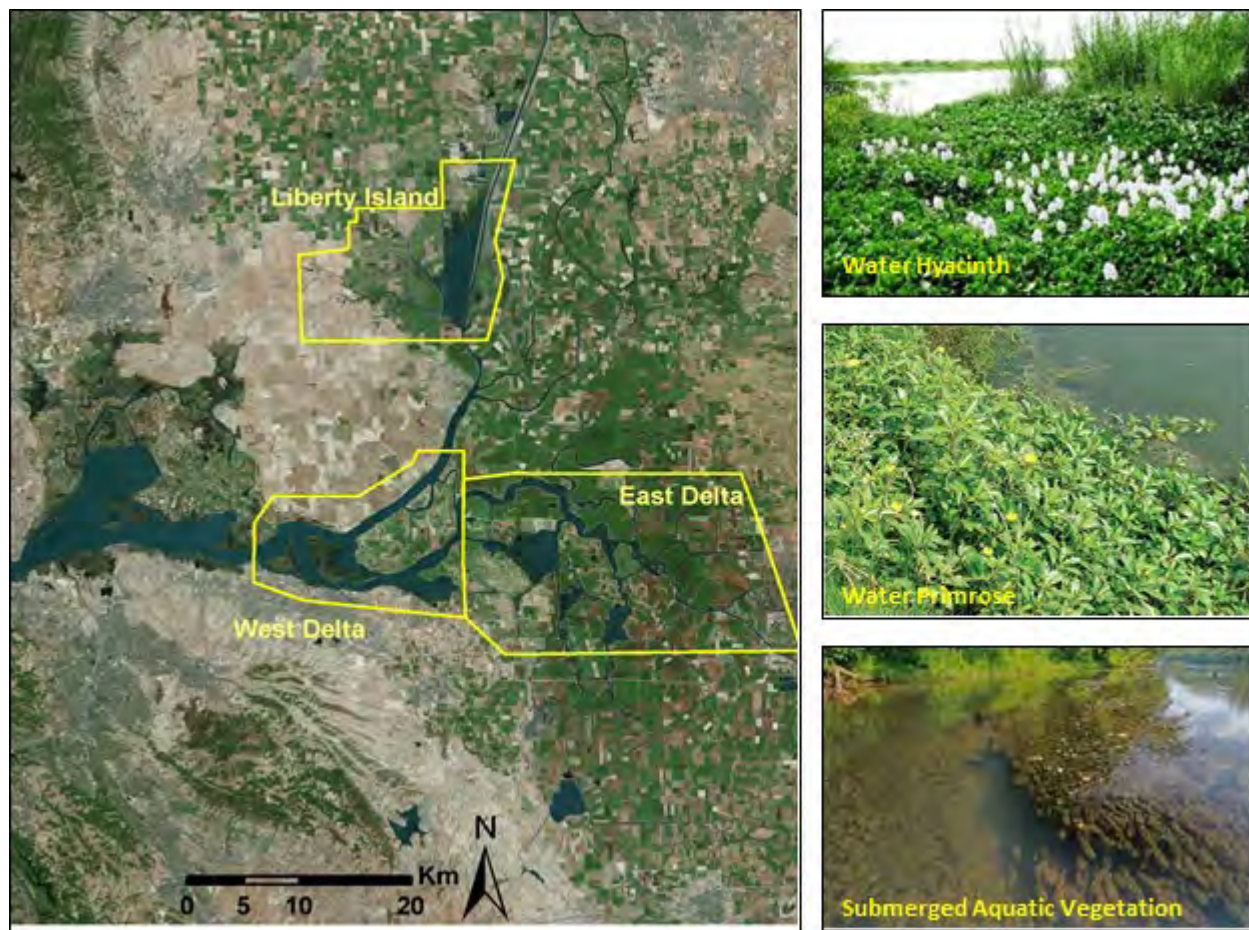


Figure 58. Delineation of Delta regions for comparison of aquatic vegetation coverage, 2014 – 2017 (left). Coverage was estimated for the fall period of each year for Water Hyacinth, Water Primrose, and submerged aquatic vegetation (right).

Across all regions surveyed, predictions regarding FAV and SAV coverage in 2017 compared to previous, drier years (2014 – 2016) were confirmed. Water Hyacinth was generally reduced in cover with major reductions in the East Delta. Changes in Water Hyacinth in Liberty Island and the West Delta were more variable from year to year, but overall coverage was small compared to the East Delta. Coverage of Water Primrose increased and SAV coverage increased slightly or stayed the same (Figures 59 and 60); however, the importance of the high flows in 2017 relative to other factors was not clear.

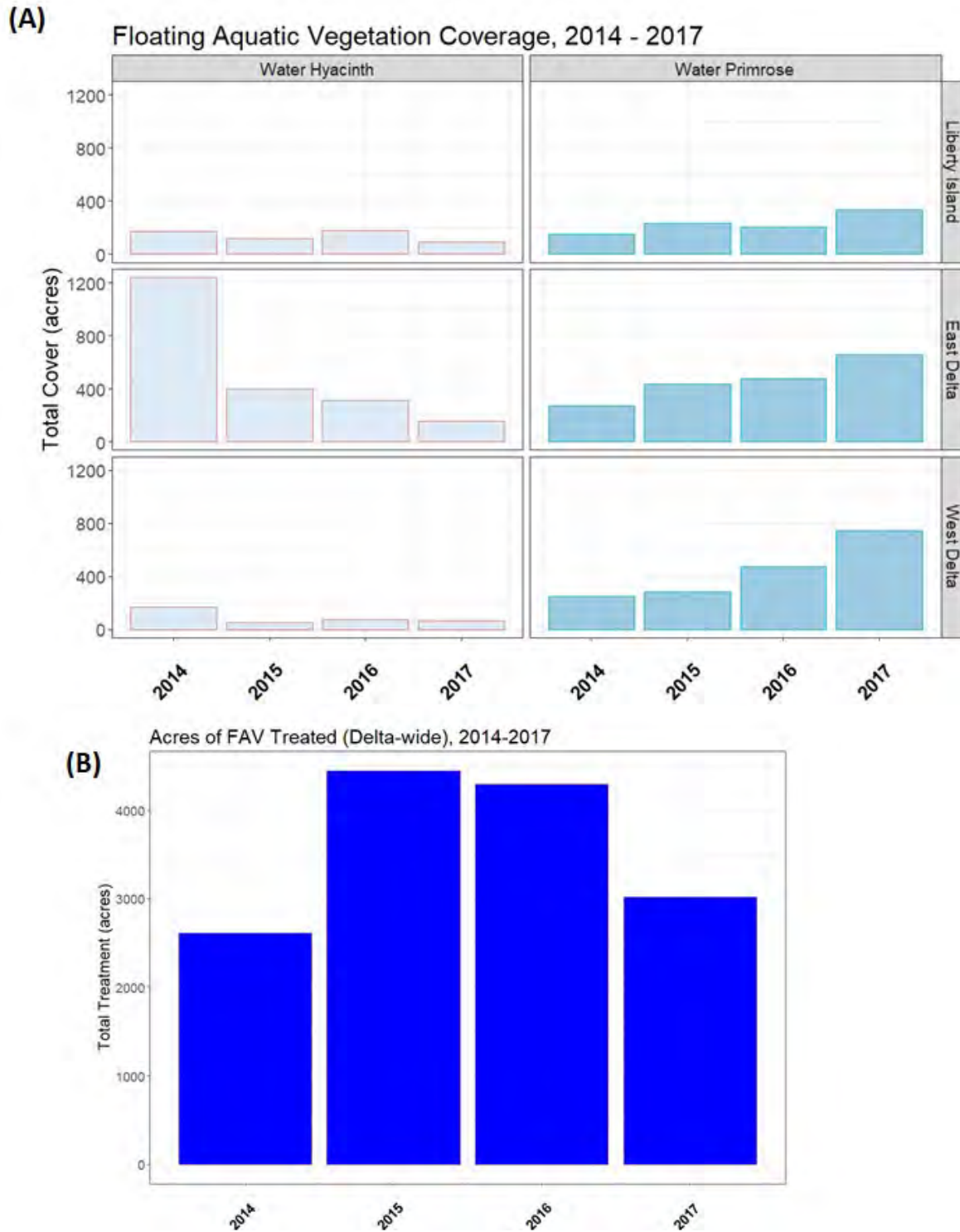
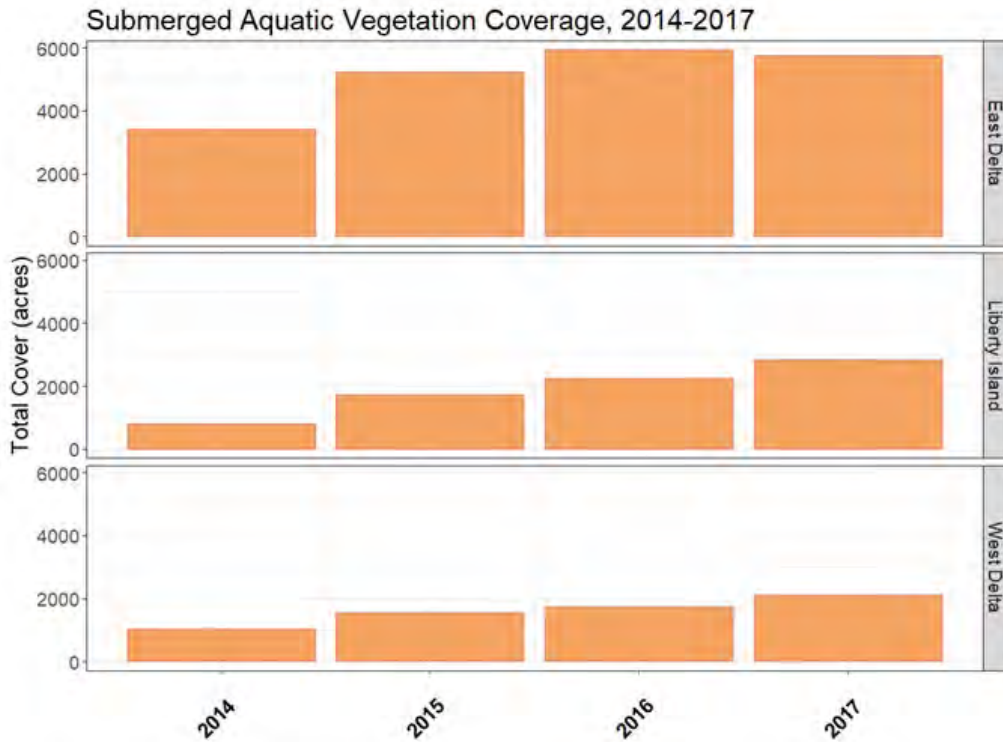


Figure 59. (A) Estimated coverage of Water Hyacinth and Water Primrose, from Center for Spatial Technologies and Remote Sensing (CSTARS) classification of hyperspectral imagery collected in the fall of each year. Coverage is estimated for regions consistently sampled across the time series. (B) Total acres treated (across

entire Delta) for floating aquatic vegetation (FAV) by California Department of Boating and Waterways, 2014 – 2017. Treatment of Water Primrose began in 2016, but treatment acreage by FAV species or region is not.

(A)



(B)

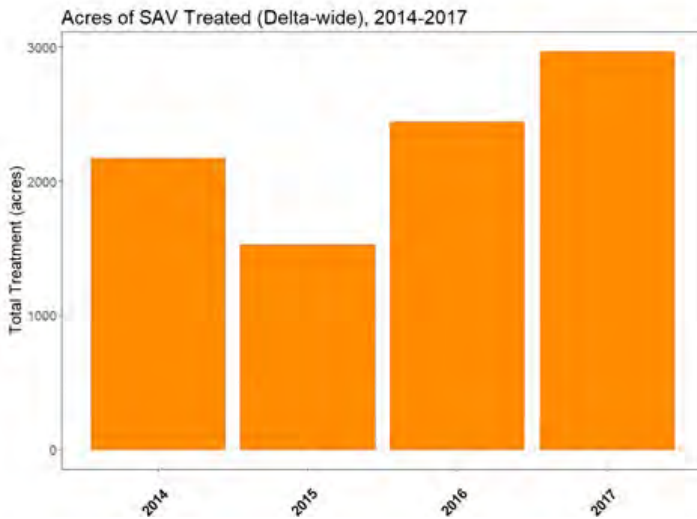


Figure 60. (A) Estimated coverage of submerged aquatic vegetation, from CSTARs classification of hyperspectral imagery collected in the fall of each year. Coverage is estimated for regions consistently sampled across the time series. (B) Total acres of SAV treated (across entire Delta) by California Department of Boating and Waterways, 2014 – 2017.

Examination of the full 2014 – 2017 time series for aquatic vegetation coverage and other environmental data shows that it is not possible to attribute the observed changes in coverage to increased outflow in 2017. For all vegetation types, there were progressive changes in coverage over the 2014 – 2017 time series for at least some regions. For example, incremental increases in SAV coverage were evident each year in Liberty Island and the West Delta, with stable coverage between 2016 and 2017 (Figure 60). In the West Delta and particularly in the East Delta, there was a marked reduction in Water Hyacinth coverage between 2014 and 2015 with coverage decreasing or stabilizing between 2015 and 2017 (Figure 59). These trends correspond to increased treatment of Water Hyacinth in 2015. Thus, while outflow during the growing season in 2017 was much higher than any of the previously surveyed years, larger reductions in Water Hyacinth occurred during the drought period, before the high flows in 2017.

In contrast to Water Hyacinth, Water Primrose saw expansions in each Delta region surveyed. Again, this was a progressive expansion, with incremental positive change over each year, 2014–2017. It is notable that FAV treatment did not include Water Primrose until 2016, and the acreage of Water Hyacinth treated reached record high levels for the DBW program in 2015 and 2016 (Figure AV 2). While this information suggests that Water Primrose expanded for lack of chemical treatment and had access to new habitat with effective treatment of Water Hyacinth, this may not be the case. Recent analyses have suggested that during the previous decade, Water Primrose expanded into areas of open water or where Water Hyacinth was reduced. In recent years (2014 – 2016), Water Primrose has displaced emergent marsh, and, in general, areas newly occupied by Water Primrose were not previously inhabited by Water Hyacinth (Khanna et al. 2018). In the West Delta, where the coverage of Water Primrose tripled between 2014 and 2017, it is notable that during the drought period, salinity (as measured by conductivity) was variable among the years, with the highest values occurring in 2014 and 2015. Water Primrose is generally more salinity-tolerant than Water Hyacinth (Grillas et al. 1992, Penfound and Earle 1948). Higher salinity in the West Delta during the drought (Figure 61) may have been more tolerable to Water Primrose than to Water Hyacinth.

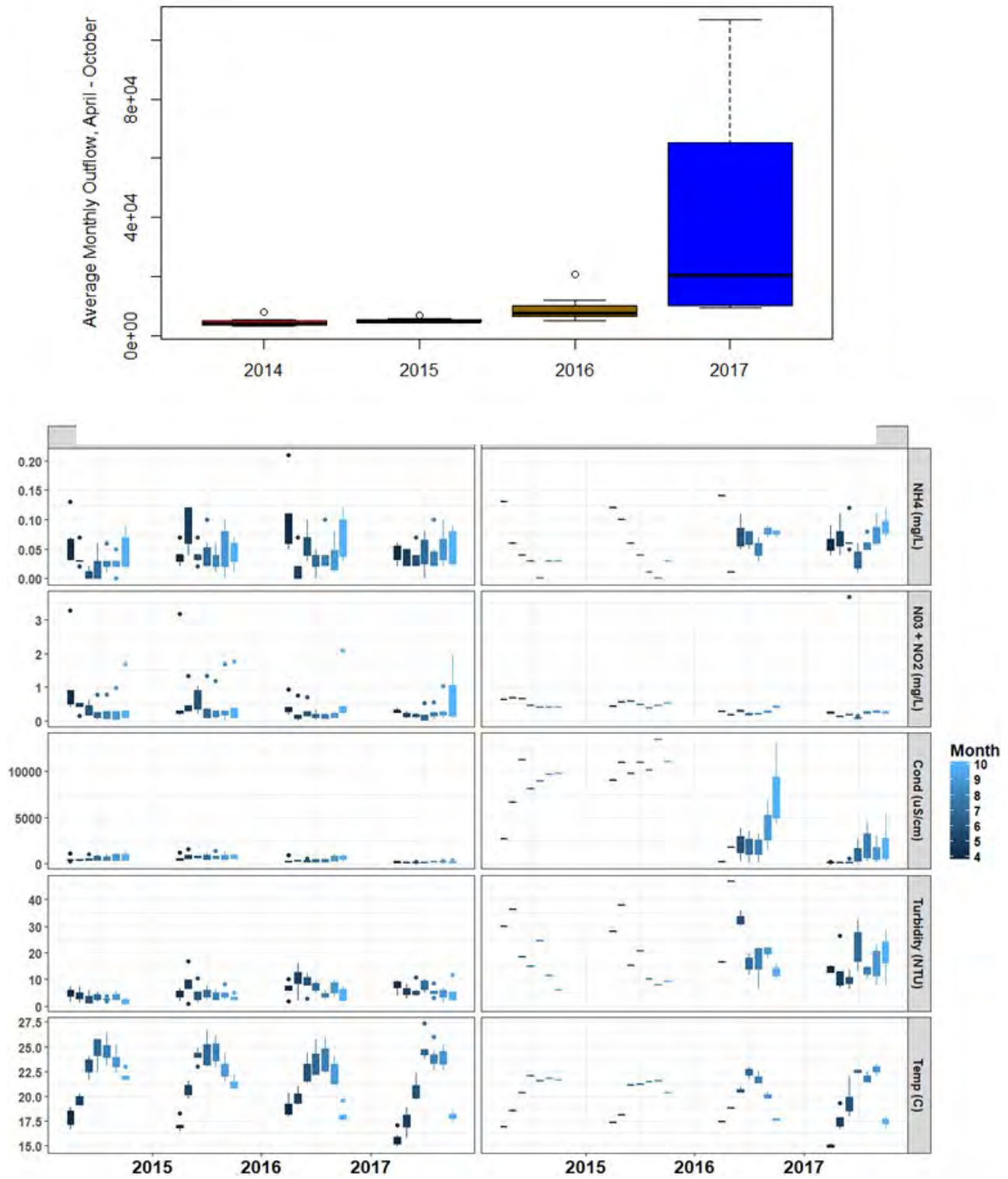


Figure 61. Average monthly outflow, April 2014– October 2017. (B) Boxplots of dissolved ammonium, nitrate + nitrite, conductivity, turbidity, and water temperature for each month, April 2014 – October 2017. Data are from

the Environmental Monitoring Program discrete station data. Regions are delineated as in Figure 58 (West Delta, n = 4; East Delta, n = 6).

Like Water Primrose, SAV showed a progressive increase from 2014 – 2017, with coverage more than tripling in the Liberty Island region and doubling in the West Delta (Figure 60). These increases occurred incrementally across all the years, and thus are unlikely to be a result of water conditions in any single year. Notably, chemical control efforts generally increased from 2014 – 2017. Water quality conditions in 2017 in the West Delta were more turbid in the late summer than in previous years, which should also not be favorable for SAV growth; however, water temperatures stayed warm in this region longer than in previous years (> 20°C into September, Figure 61), which would be favorable for SAV. The increased SAV coverage over this period may, also like Water Primrose, be in part due to the reduction of Water Hyacinth, which shades SAV and reduces its habitat (Khanna et al. 2012). Effective Water Hyacinth treatment, or other disturbance of Water Hyacinth map and subsequent colonization by SAV, has already been proposed as a succession pathway for Delta FAV (Khanna et al. 2012).

Fish Assemblage

Understanding the biological drivers that influence the population dynamics of Delta Smelt is key for the effective management of the species. The decline in food web productivity within the SFE due to the introduction of the invasive clam *Potamocorbula* in 1987 has been implicated as one of the main drivers of declines in pelagic fishes (Brown et al. 2016a). In addition, there was a roughly simultaneous decline in 4 species of pelagic fishes, including Delta Smelt, in the early 2000s that has been referred to as the POD (Sommer et al. 2007, Baxter et al. 2010, Thomson et al. 2010, Brown et al. 2014). Lack of food is one of several factors hypothesized to be responsible for the POD. Because higher freshwater flow into the SFE has been linked to an increase of phytoplankton biomass to some extent (Lehman 2000) and higher abundance of some zooplankton species (albeit prior to the POD) (Jassby et al. 1995, Kimmerer 2002), it has been hypothesized that wet years would lead to higher food web productivity in many regions within the SFE (Brown et al. 2014). One would expect that an increase in food production would then lead to an increase in biomass of planktivorous fish species such as the Delta Smelt. However, because the Delta Smelt population is at such low levels, the current biomass of the population cannot be estimated accurately. Therefore, we evaluated the biomass of

common pelagic fishes in the SFE to determine if the biomass of pelagic fishes is responsive to Delta outflow. Our prediction is that the wet year of 2017 resulting in X2 located in the Suisun region during the fall will be associated with an increased biomass of pelagic fishes, which includes Delta Smelt.

To evaluate our prediction that fish biomass is greater in wet years and that fish assemblage would be more similar across wet years, we compiled the available fish catch data from the 20-mm Survey (June and July; hereafter, summer 20-mm Survey), STN, FMWT, and Delta Juvenile Fish Monitoring Program (DJFMP) Beach Seine Survey (see Appendix 9 for details of methodology). Our goal was to gauge the overall post-POD pelagic fish assemblage's response to wet years (summer 20-mm Survey, STN, and FMWT). We also evaluated the response of littoral species, particularly Mississippi silverside (*Menidia audens*) (DJFMP).

The three most recent wet years (2006, 2011, and 2017) generally had high estuarine and freshwater pelagic fish biomass in at least one of the three surveys conducted from summer through fall: summer 20-mm Survey, STN, and FMWT (Figure 62-64). The year 2003 also had high abundance, even though water year 2003 was only classified as above normal; however, there were several unique aspects to 2003 that are important. For example, this was the last year of high abundance of Threadfin Shad before the POD began for that species (see Appendix 9 for further details). In 2003, catfish were unusually abundant in the STN (Figure 63) and American Shad were unusually dominant in the FMWT (Figure 64) for unknown reasons.

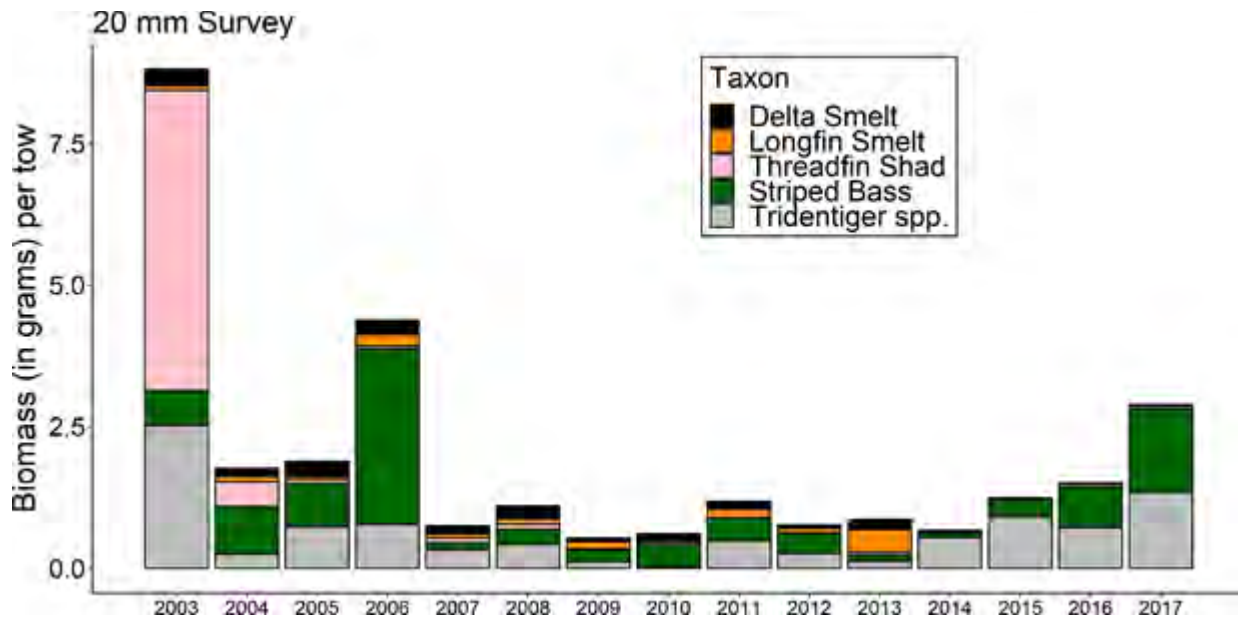


Figure 62. Annual mean biomass per tow for the 20-mm Survey in the summer (survey 7 to 9) with marine fish species removed. *Tridentiger* species in the San Francisco Estuary include both Shimofuri (*Tridentiger bifasciatus*) and Shokihaze (*Tridentiger barbatus*) gobies (see Appendix 9 if interested in excluded species).

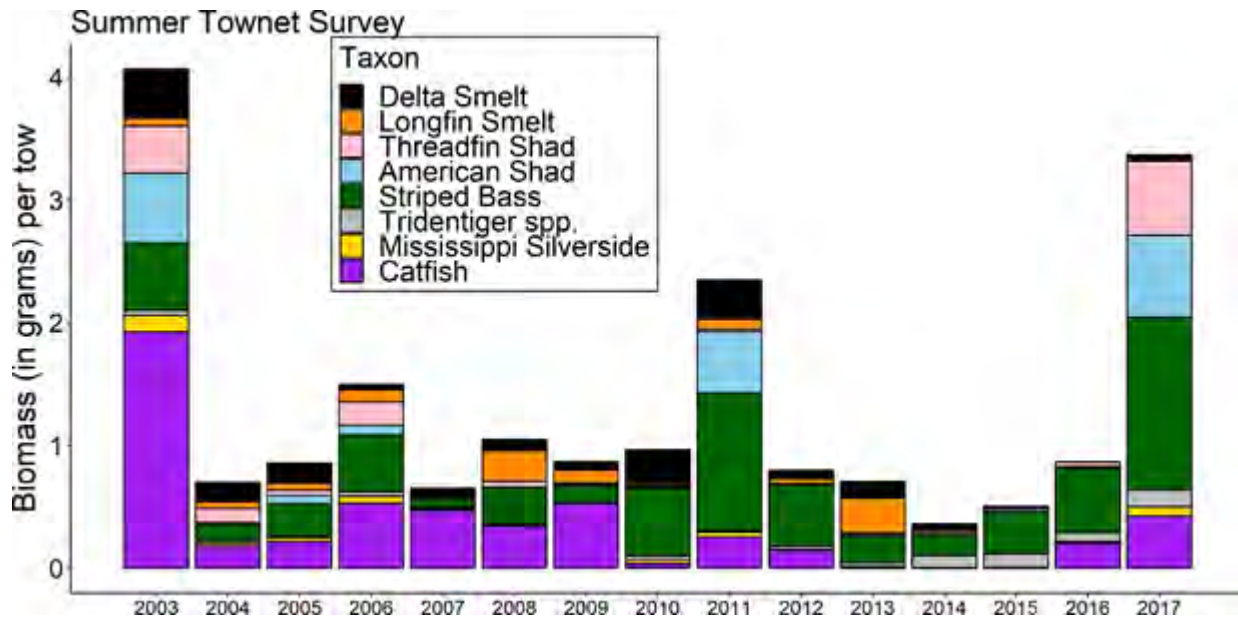


Figure 63. Annual mean biomass per tow for the Summer Townet with marine fish species excluded. *Tridentiger* species in the San Francisco Estuary include both Shimofuri (*Tridentiger bifasciatus*) and Shokihaze (*Tridentiger barbatus*) gobies (see Appendix 9 if interested in excluded species).

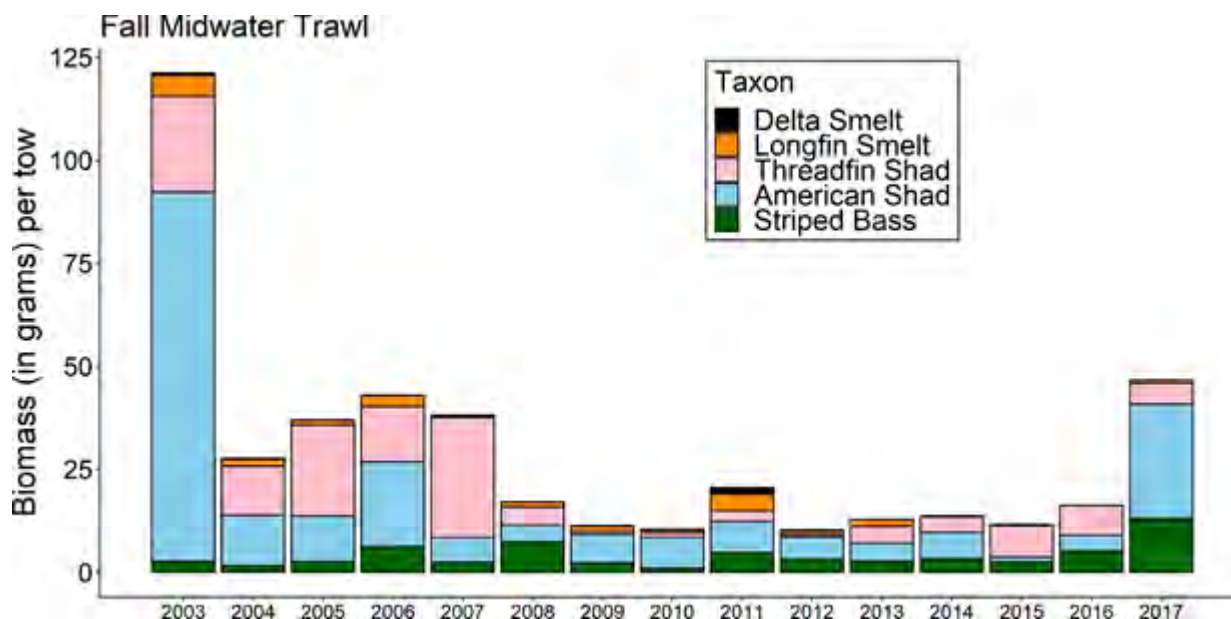


Figure 64. Annual average biomass per tow for the Fall Midwater Trawl with marine fish species excluded (see Appendix 9 if interested in excluded species).

The effects of wet years on the overall pelagic fish assemblage was also noticeable in our community analyses, where 2006 was identified as a highly similar year to 2017 (Appendix 9). However, except for the STN, 2011 was not particularly high compared to 2006 and 2017 (Figures 62-64). It seems possible that water temperatures may play a part. Except for the smelts, most of the species captured are non-native and are better adapted to warmer water temperatures.

The littoral fish biomass has increased substantially in the past decade (Mahardja et al. 2017, Appendix 9) and continued to be dominated by non-native fish species and remained at a relatively high level in 2017 (Figure 65). Of particular interest is the high biomass of Mississippi Silverside in 2017 and 2006 compared to 2011. Multiple studies indicated that survival of Delta Smelt from egg to larvae may be adversely affected by predation and competition with the invasive Mississippi Silverside (*Menidia audens*) (Bennett 2005, Schreier et al. 2016, Hamilton and Murphy 2018). Using methods developed by Mahardja et al. (2016), we calculated annual cohort strength of Mississippi Silverside (Figure 66) (see Appendix 10). Model results indicate that various combinations of spring Secchi depth, summer inflow, summer exports, spring exports, and spring water temperatures could plausibly explain Mississippi Silverside abundance (Table 9). Note that none of these important variables would be influenced by a fall flow action. Also, caution is warranted because the DJFMP seining program only

samples a portion of the silversides range in the SFE and does not include some key geographic areas of Delta Smelt abundance, such as the SRDWSC.

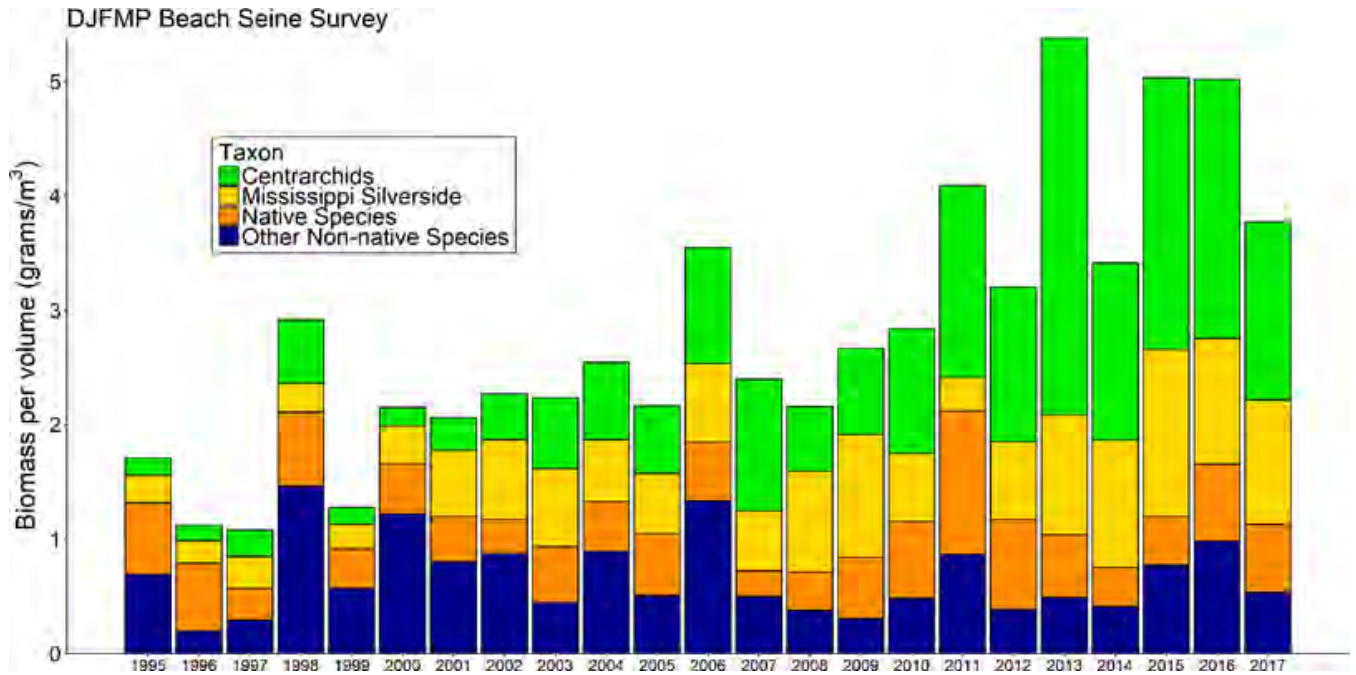


Figure 65. Annual mean biomass per volume for the Delta littoral fish assemblage based on Delta Juvenile Fishes Monitoring Program beach seine survey.

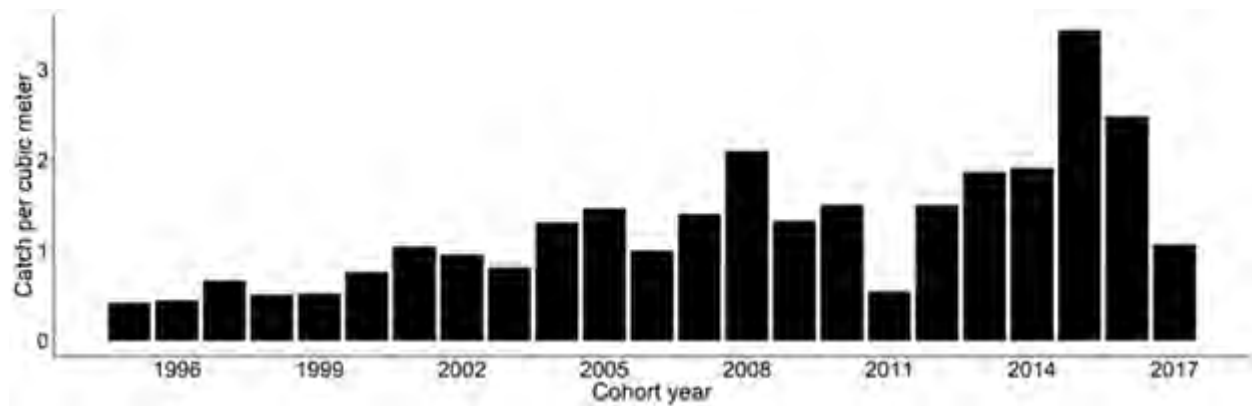


Figure 66. Mean catch per cubic meter (m³) at the 22 index beach seine stations sampled by the Delta Juvenile Fish Monitoring Program for each Mississippi Silverside cohort year (spanning from June of birth year to May of the following year). Mississippi Silverside catch is lower in 2017 relative to the recent drought years (2012-2016).

Table 9. Summary of model coefficients and fit for all models <2 Δ AICc away from the best ranked model.

*p<0.05; **p<0.01, ***p<0.001

Model	Spring Secchi depth	Summer Delta inflow	Spring Delta export	Summer Delta export	Spring temperature	Intercept	AICc	Δ AICc	w_i	Adjusted R^2
1	0.28**	-0.34**	-0.28**	-	-	1.26	31.9	0.00	0.099	0.71
2	0.31**	-0.19	-	-0.32**	-	1.26	32.6	0.66	0.071	0.70
3	0.34**	-	-	-0.42***	-	1.26	32.9	0.95	0.061	0.67
4	0.30**	-	-	-0.37***	0.15	1.26	33.4	1.49	0.047	0.69
5	-	-	-	-0.34***	0.20*	1.26	33.5	1.61	0.044	0.59

Although the prediction that high flows leading to fall X2 position in the Suisun region would lead to higher biomass of planktivorous fishes was upheld, the more general expectation for wet years in general was less well supported. Wet years generally led to higher biomass and produced similar fish assemblages but 2006 and 2011 gave more mixed results than 2017 (Appendix 9); thus, the scarcity of wet years in the San Francisco Estuary since the POD prevented us from making a firm conclusion. Mississippi Silversides were also more abundant in 2017 than in 2011, which may be a factor in the low numbers of Delta Smelt observed; however, more comprehensive sampling of Mississippi Silverside is needed before firm conclusions are possible. What was evident, however, was that Delta Smelt make up a small portion of the overall pelagic fish biomass in the post-POD era and especially so in the past few years.

Delta Smelt responses

Growth Rate

[This section is a summary of results from Hobbs et al. (2019c), a chapter in the Directed Outflow Project Technical Report (Schultz 2019). Hobbs et al. (2019c) represents the most recent analysis of growth rates and developing a separate analysis for this report was deemed repetitive and unnecessary. However, conclusions appearing at the end of this section are focused on questions specific to this report and do not necessarily match with Hobbs et al. (2019c) or Schultz (2019). The

text of this section has been edited from the original to meet the needs of this report. See Hobbs et al. (2019c) for additional detail.]

Growth in the early life of fishes is considered a critical vital rate, with rapid growth resulting in increased survival probability due to greater ability to avoid predation and capture prey (Cushing 1990, Hjort 1914). Subtle differences in growth and subsequent mortality in the larval stage can lead to large differences in recruitment and year-class strength (Anderson 1988, Houde 1989a, Leggett and Deblois 1994); thus, understanding the biotic factors that affect growth in the early life is critical for managing fisheries. Abiotic factors can also lead to significant variability in early life growth and recruitment. Water temperature has a direct effect on metabolic rates in poikilotherm fishes, where growth rates are generally higher in warmer temperature (Houde 1989b); however, when species are found at temperatures near their thermal limits, growth rates can be reduced significantly (Neuheimer et al. 2011, Neuheimer 2019, Wenger et al. 2016).

Otoliths have long been used to determine growth rates in fishes. Otoliths are small bone-like structures found in the inner ear of fishes and are formed by secretion of calcium carbonate and proteins into the endolymph of the inner ear creating layers of light and dark bands that can be observed in thin sections under light microscopy. These layers have been validated to infer daily age in Delta Smelt (Hobbs et al. 2007). The measurement of the width of otolith increments allows for reconstruction of daily growth chronologies, analogous to tree-ring based dendrochronology, assuming increment width is a good proxy for fish growth. Otolith size for cultured Delta Smelt has been shown to be a good proxy for fish size and growth (Hobbs et al. 2007), thus Hobbs et al. (2019a) used daily otolith increment widths as the primary variable for examining effects of environmental conditions on Delta Smelt growth.

To gain a better understanding of how freshwater flow management influences Delta Smelt growth, Hobbs et al. (2019c) used otolith age and increment widths as a proxy for fish growth in their study. Hobbs et al. (2019c) primary research objective was to determine if Delta Smelt occupying Suisun Bay grew faster when fall flows were managed to maintain the LSZ within Suisun Bay and Suisun Marsh. The years 2011 and 2017 were classified as wet years resulting in implementation of the Fall X2 Action, and the LSZ was located within the Suisun Bay/Marsh region in September and October. However, in 2011 the vast majority of Delta Smelt collected by monitoring surveys were from Suisun

Bay, while in 2017 fish in low numbers were collected in Suisun Bay and the Lower Sacramento River, precluding a comprehensive comparison of growth rates by area. Since Delta Smelt are a pelagic mobile species, and a portion of the population has been observed to migrate towards freshwater in the fall, Hobbs et al. (2019c) could not be certain fish collected in the Lower Sacramento River represented a distinct group of fish from those collected in Suisun Bay. Therefore, Hobbs et al. (2019c) could not directly address their primary objective. Instead they addressed growth response at an inter-annual scale and daily scale in response to habitat attributes that represent fall habitat conditions.

First, for the inter-annual scale, they included fish collected from 2012-2016, a period of drought and much reduced overlap of the LSZ with Suisun Bay to compare inter-annual growth variability to address the question: Did Delta Smelt grow faster in wetter years, when the LSZ occurred in the Suisun Bay/Marsh Region in the fall, compared to dry years? This approach relaxes the assumption that measured growth was attributable to the region and associated habitat attributes where a fish was captured. In this approach, Hobbs et al. (2019c) also addressed the growth response of Delta Smelt to drought conditions.

Second, the previous analysis did not provide a model for predicting Delta Smelts growth response to flows or abiotic habitat attributes that respond to flow management. Therefore, they used recent otolith growth and the abiotic water quality attributes, salinity, temperature and turbidity, the primary habitat variables thought to determine Delta Smelt habitat quality, to address the question: How do the abiotic habitat attributes salinity, temperature and turbidity influence Delta Smelt growth?

We use the results of Hobbs et al. (2019c) to address the prediction in this report that having the LSZ in Suisun Bay (as determined by X2) will result in faster growth compared to positioning the LSZ near the confluence.

The methods utilized by Hobbs et al. (2019c) are complex and detailed (see Hobbs et al. 2019c and references therein). In brief, otoliths were collected from Delta Smelt collected by various agencies from 2011 to 2017. Two growth metrics were used in analyses. The first was somatic growth rate, where somatic growth rate is the difference in length between length at capture and length at hatching divided by the age of the fish in days, providing a growth rate of individuals for the year. The second approaches used marginal otolith incremental growth over the 14 days prior to fish capture by determining the mean width of the most recent 14 otolith rings. This approach was employed to test

hypotheses regarding growth responses to capture regions, survey month, years and abiotic habitat attributes. Generalized additive models (GAMs) were used to model growth response to both intrinsic (age) and extrinsic abiotic habitat attributes measured at capture (salinity, water temperature [°C], and Secchi depth [cm]), which were assumed to be a reasonable proxy for the abiotic conditions experienced by each fish prior to capture. To facilitate regional comparisons of growth, sample stations from the California Department of Fish and Wildlife's long-term monitoring surveys were assigned to the regions defined by the U.S. Fish and Wildlife Services Enhanced Delta Smelt Monitoring Program. First, the ontogenetic effect of age/life stage was accounted for in the model because daily growth in fish is strongly driven by age; fish grow slowly post-hatch while living off of yolk provisions, then grow rapidly once fish forage on live prey and then growth slows as fish reach maturity because energy is diverted to gonad production (Morrongiello and Thresher 2015). Previous otolith growth studies have demonstrated the strong ontogenetic (age) effect that occurs in Delta Smelt (Hobbs unpublished report). In the fall, Delta Smelt can vary as much as 3-months in age leading to individual differences in maturation state. Second, the model accounts for abiotic habitat metrics (salinity, temperature, and turbidity), factors that vary with freshwater flows. Finally, the model compares capture region (Fig. 1), month, and year as categorical variables in GAMs to examine growth response to spatial and temporal variability that is independent of ontogeny and abiotic habitat attributes.

Hobbs et al. (2019c) analyzed a total of 1,445 Delta Smelt collected from 2011 to 2017. Somatic growth rates of Delta Smelt appeared to vary by year, with 2011 and 2015 exhibiting higher median growth. Growth in 2016 was also high, but the sample size was small and the data had a bimodal distribution suggesting that conclusions about this year are suspect. Growth was generally low during the drought (except 2015) and remained relatively low during the 2017 wet year (Figure 67). Growth rates also varied by survey month, being higher during the summer months than fall months and were higher in September and October of 2011 compared to other years (Figure 68A). Because of small samples sizes in some regions, months, and years, Hobbs et al. (2019a) could not make direct comparisons within years between regions, even when aggregating Suisun Bay and Marsh into a single region, except for 2017 (Figure 68B). In 2017 there appeared to be no difference in somatic growth rates between Suisun Bay/Marsh and the Lower Sacramento River.

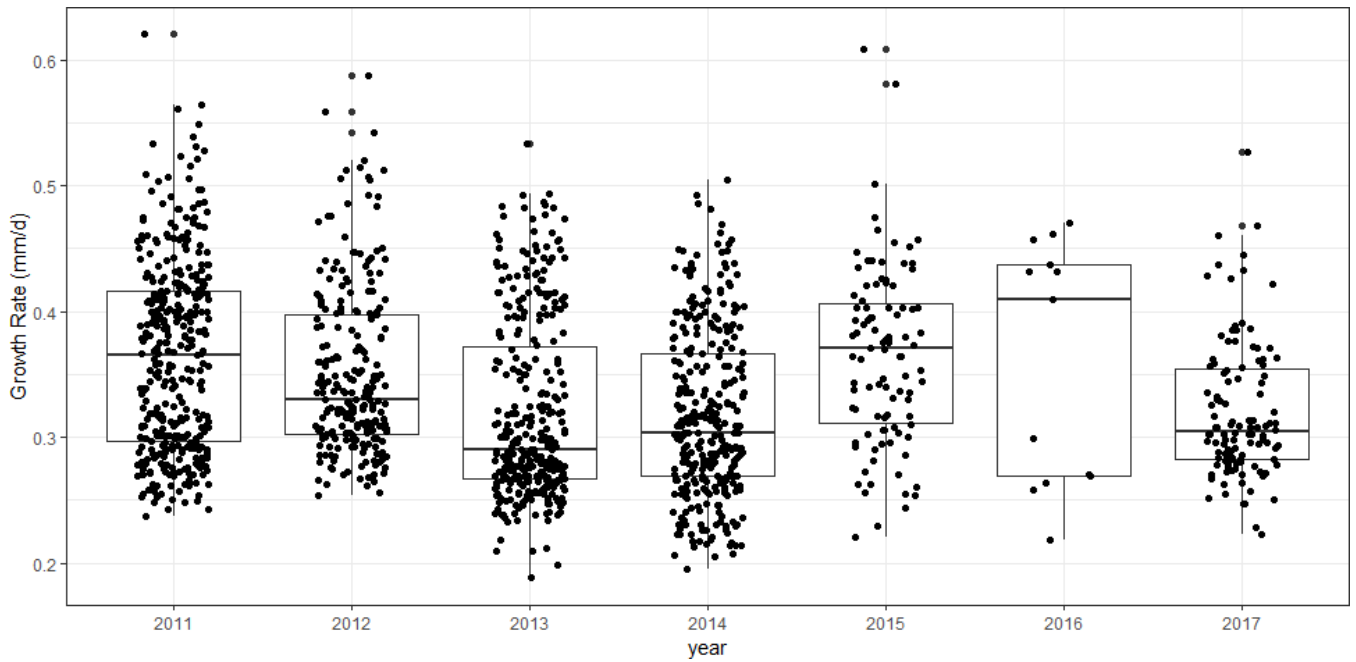


Figure 67. Somatic growth rates of Delta Smelt collected from surveys conducted from 2011 to 2017. Data represent fish collected throughout the estuary from a variety of surveys from May through December (modified from Hobbs et al. 2019c).

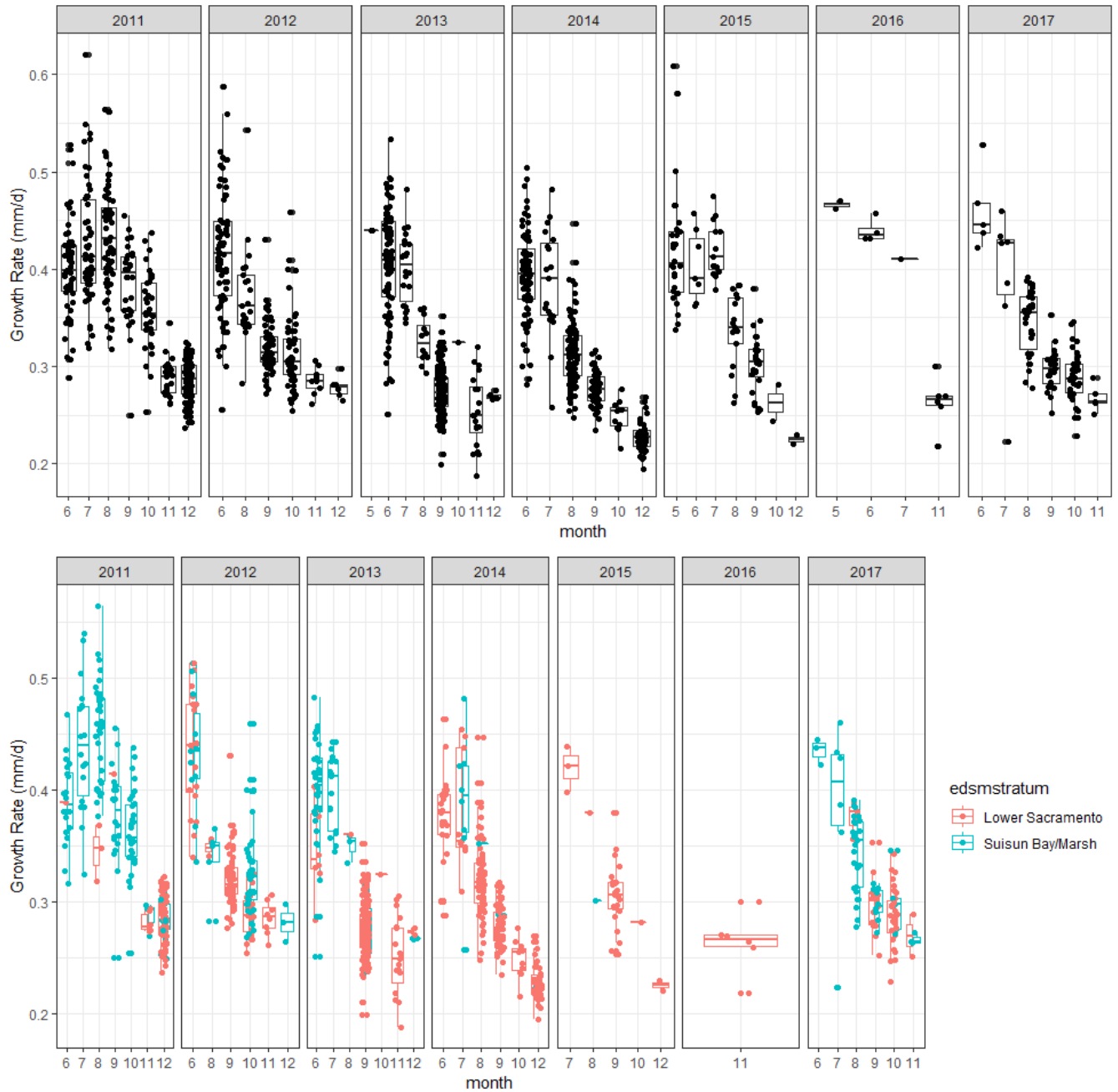


Figure 68. Boxplots of somatic growth rates of Delta Smelt by month collected from surveys conducted from 2011 to 2017. Data represent fish collected throughout the estuary from a variety of surveys from May through December (modified from Hobbs et al. 2019c).

For the recent “marginal growth” (14-days prior to capture) analyses, as expected, recent otolith growth was strongly driven by ontogeny (age), where young fish <125-days old grew faster than older fish (Figure 69); therefore, subsequent analyses were corrected for age effects. All models

testing the categorical variables of region, month, and year that included region as a factor were generally weaker than models with year and month factors. The year effect was the strongest of the categorical models. Year explained 32% of model deviance and had an $R^2 = 0.26$ and was the only term that had a significant p-value. Age-corrected marginal growth over the last 14-days was high in 2011, 2012, and 2014 compared to 2013, 2015, 2016 (Figure 70). Growth during the wet year of 2017 was generally low for the study period but exhibited greater variation than the later years of the drought, likely due to the larger sample size acquired by the EDSM. Median growth for the North Delta, specifically the Cache Slough/Liberty Island and Sacramento River Deepwater Shipping channel was elevated relative to the other regions (Figure 70), but these differences were not statistically significant (Hobbs et al. 2019c).

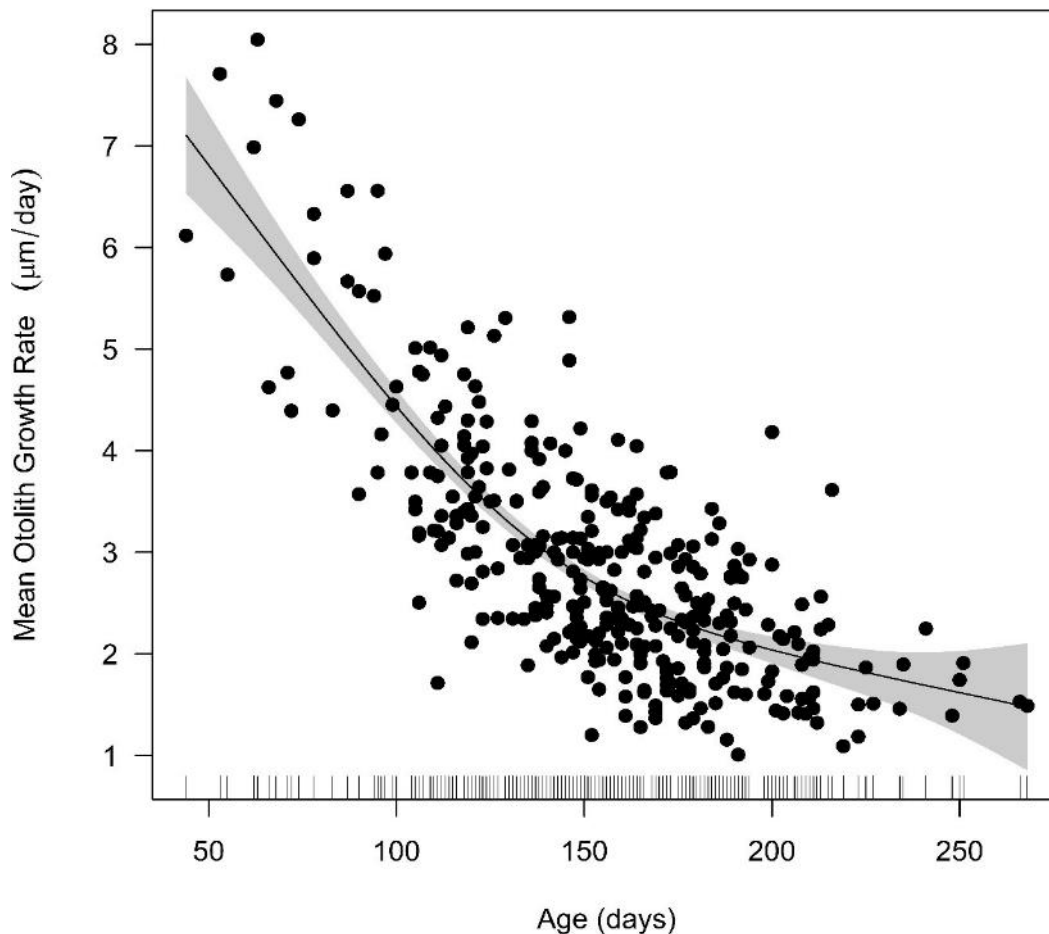


Figure 69. Intrinsic effect of age (days post-hatch) on marginal otolith growth (zero-centered 14-day mean otolith growth rate in microns/d) rate from 2011-2017 (modified from Hobbs et al. 2019c).

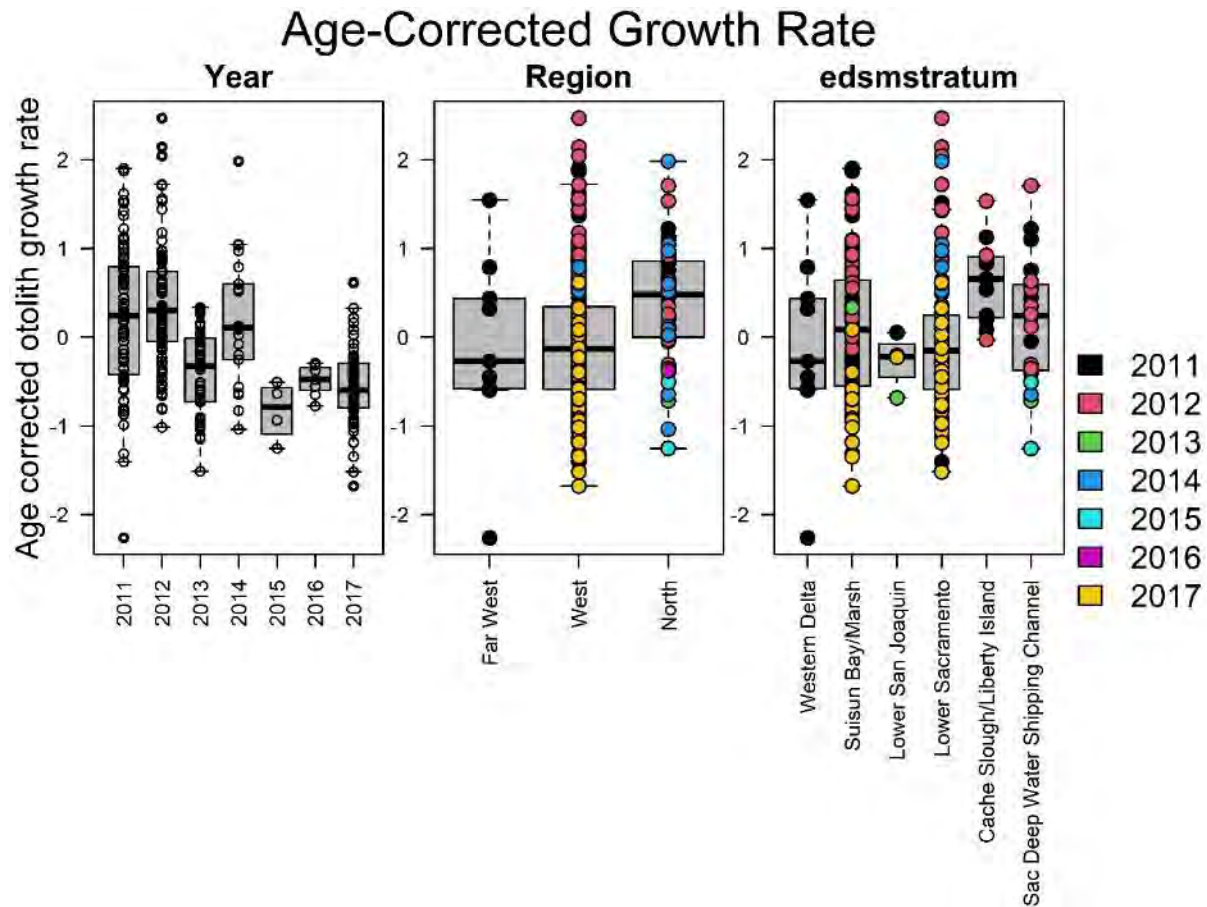


Figure 70. Age corrected marginal otolith growth rate (zero-centered 14-day mean otolith growth rate in microns/d corrected for age post-hatch) by year, EDSM region and EDSM strata for 2011-2017 (modified from Hobbs et al. 2019c).

Models for extrinsic abiotic habitat attributes (water temperature, salinity, and Secchi depth), after accounting for age effects, explained 66% to 72% percent of model deviance, with R^2 ranging from 0.63–0.77. The model including the three abiotic habitat attributes and their interactions had the highest model deviance explained but was also the most complex model. The interaction term explained only about 5% more deviance than the model including only water temperature and salinity. In all the models, the effect of temperature was the strongest driver of marginal otolith growth and in general, trends for all three variables varied little among model structures. Growth declined with increasing water temperature and salinity and was slightly reduced when fish were caught in areas with Secchi depths less than 0.2 m (Figure 71).

TEMP*SAL*SECCHI_rrm_k=6

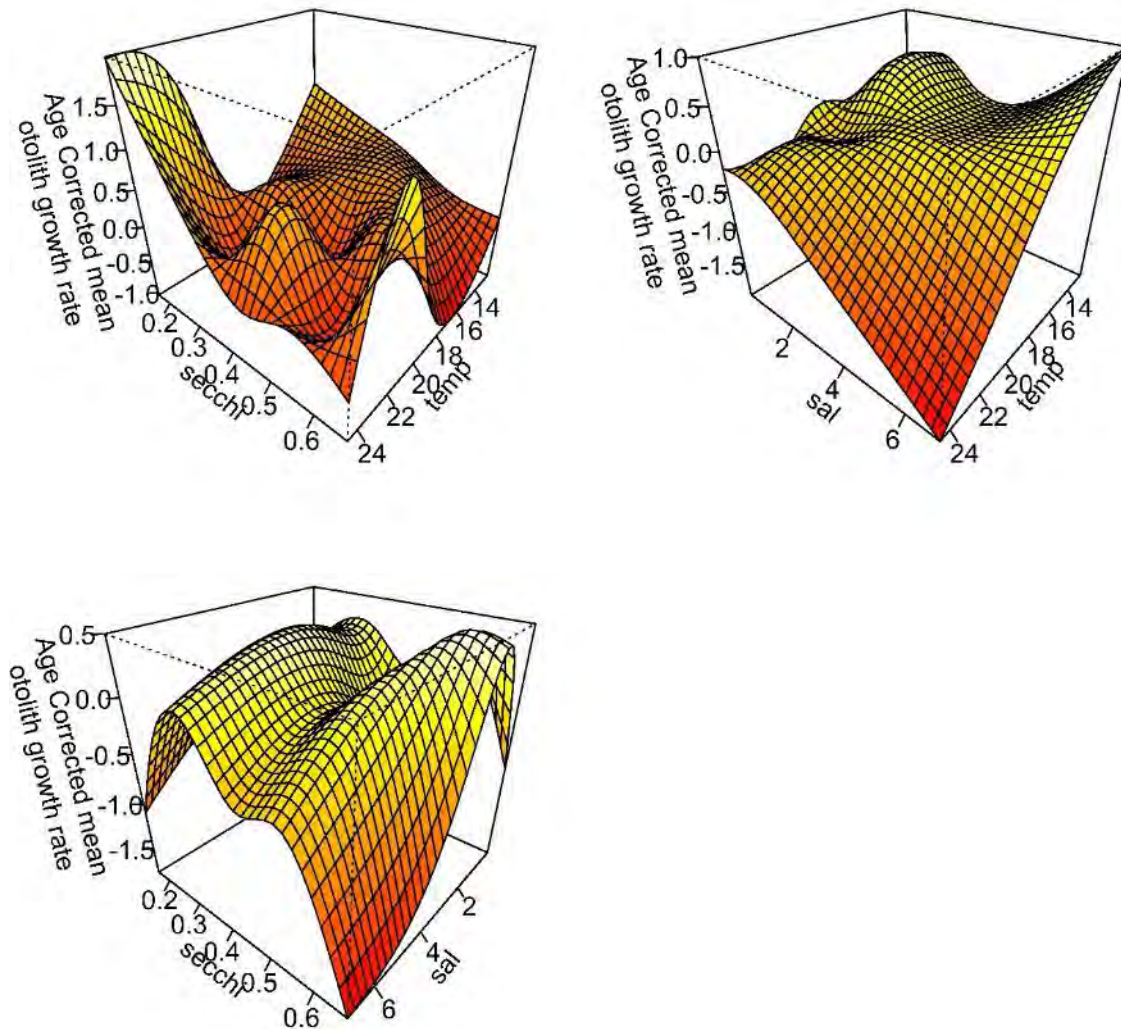


Figure 71. Three-dimensional plots for associations of water temperature (temp), salinity (sal) and Secchi depth (secchi) at capture with 14-day age-corrected zero-centered marginal otolith growth rate (modified from Hobbs et al. 2019c).

After accounting for both the ontogenetic effect and abiotic effect on growth, inter-annual differences in growth were reduced (Figure 72) relative to the models with only the ontogenetic effect (Figure 70). This result led Hobbs et al. (2019a) to suggest that the abiotic water quality attributes were the principal drivers of Delta Smelt growth and that regional differences would likely be driven by the differences among regions in abiotic attributes encountered by fish.

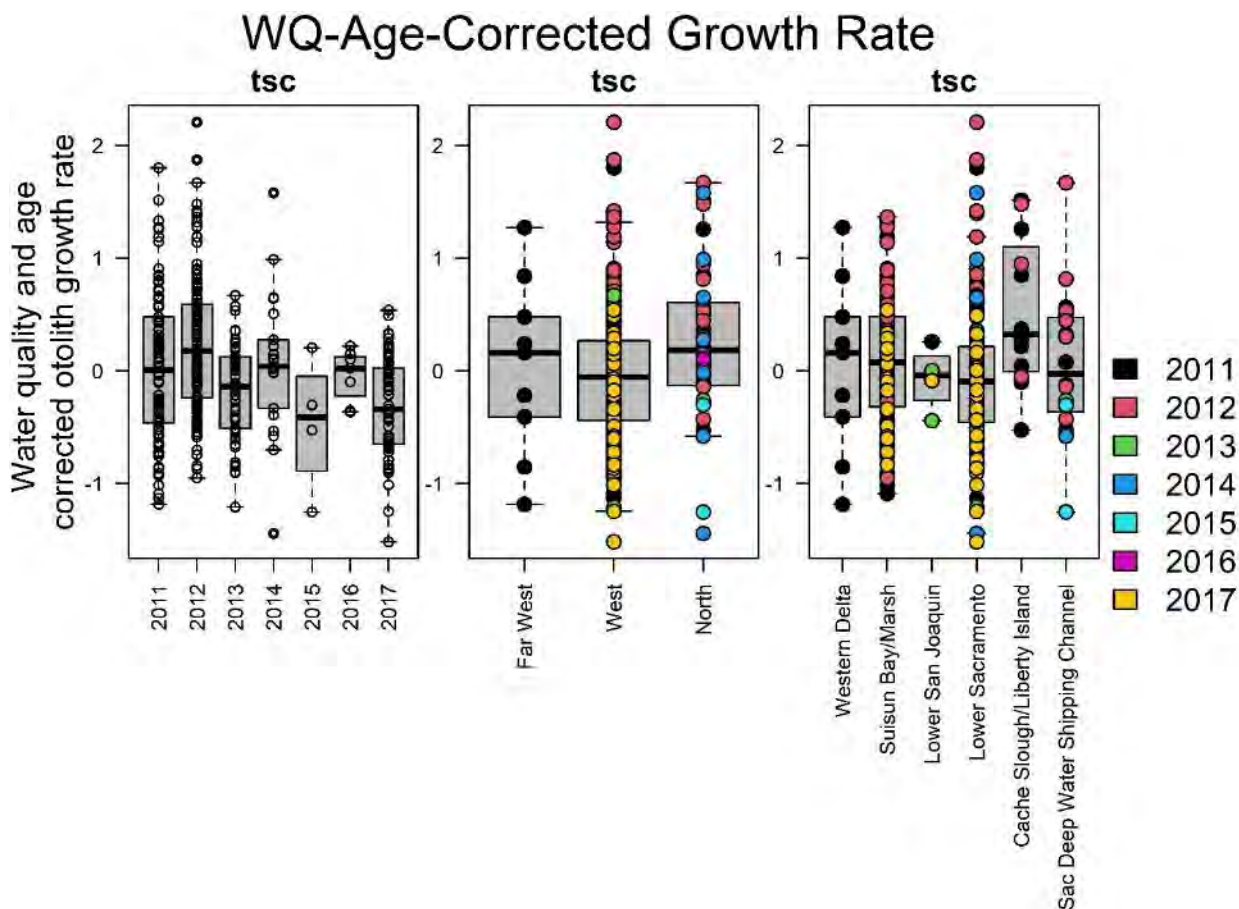


Figure 72. Age and water quality (WQ) corrected marginal otolith growth rate (14-day age and water-corrected zero-centered marginal otolith growth rate) by year, EDSM region and EDSM strata for 2011-2017 (modified from Hobbs et al. 2019c).

Conclusion

The prediction in this report that Delta Smelt would grow better in 2017, when the LSZ was positioned in Suisun Bay during the fall compared to when it was positioned near the confluence as in drought years, was not supported. Further, growth in 2017 was lower than observed in 2011. Hobbs et al. (2019a) attributed this difference to differences in summer water temperature between these two wet years. Based on their data analysis (Hobbs et al. 2019c), they noted that summer daily mean water temperatures were 1-2°C higher in 2017 compared to 2011 and was likely an important driver of growth differences between these two wet years (Figure 73). Small increases in water temperature can have large effects on growth in young fishes such as Delta Smelt. Moreover, several studies have

indicated Delta Smelt are particularly sensitive to warm water (Jeffries et al. 2016; Komoroske et al. 2015; Komoroske et al. 2014).

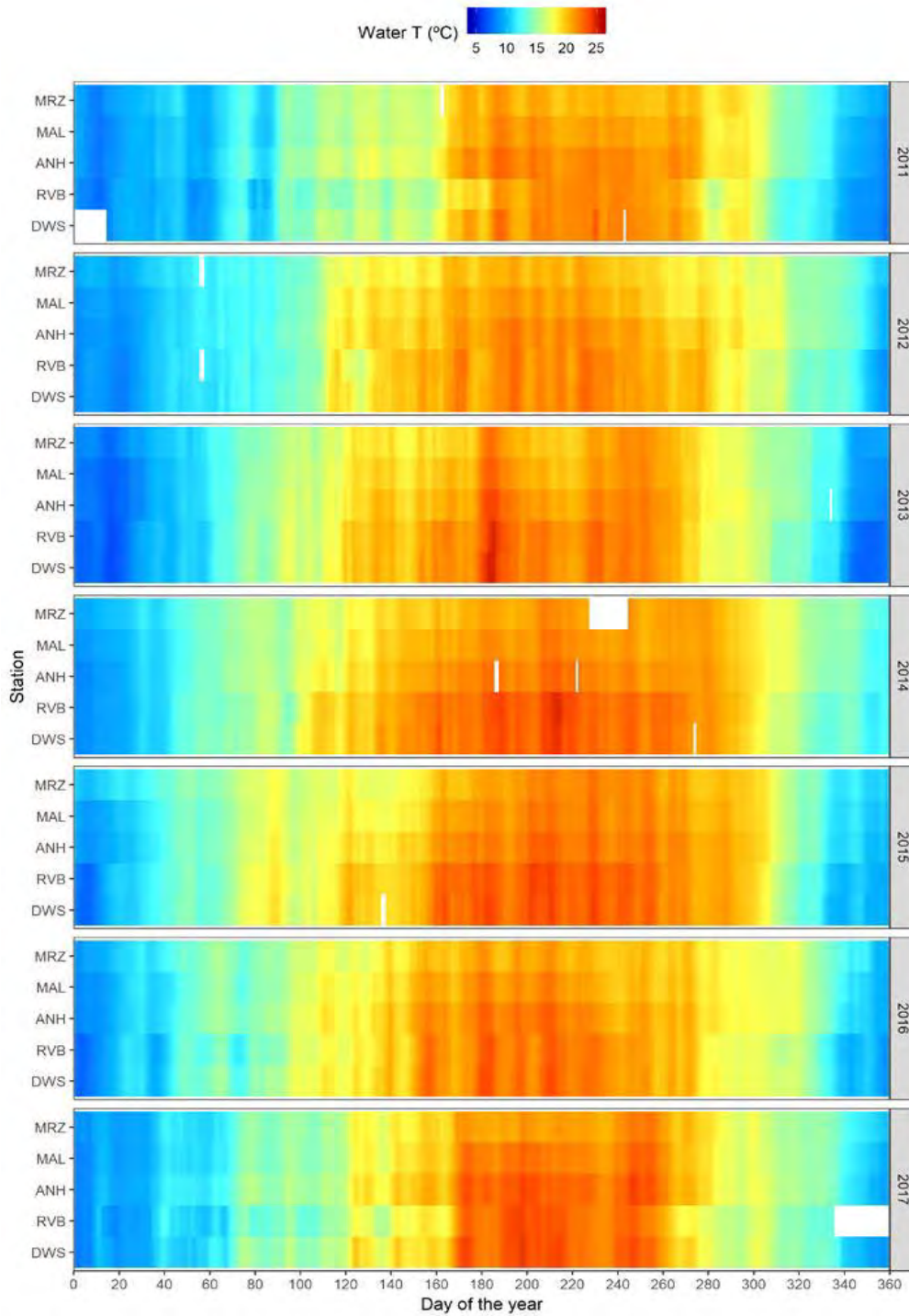


Figure 73. Heatmap of daily mean water temperature from five continuous water quality sondes, 2011-2017. Sites are arranged vertically, the upstream-most site at the bottom and downstream-most site at the top of each graph. North Delta (DWS-bottom) to far western Suisun Bay (MRZ-top) (modified from Hobbs et al. 2019c).

Station names are Deepwater Ship Channel (DWS), Rio Vista (RVB), Antioch (ANH), Mallard (MAL), and Martinez (MRZ), operated by California Department of Water Resources.

We agree with Hobbs et al. (2019c) that their results suggest that temperature is an important abiotic factor that could be limiting recruitment success for Delta Smelt. As reviewed earlier, laboratory studies examining the biochemical and molecular response to thermal stress show that the species expresses a suite of sub-lethal biochemical responses at temperatures 4-6°C below their critical thermal maximum, which would correspond to acute exposures ranging from 22-23°C (Komoroske et al. 2015, Komoroske et al. 2014). During the drought, water temperatures throughout the estuary were frequently near this threshold and at times higher (Figure 73). The growth model would indicate that much of the estuary was marginally suitable for growing Delta Smelt in the summer and early fall months in 2017. Poor growth likely results in higher mortality and could further explain the extremely low abundance during the drought. Poor growth in the sub-adult stage fish may also contribute to overall lower egg production by producing smaller fish at maturity, delaying maturity, or limiting the capacity of fish to produce multiple batches of eggs within a season (Damon et al. 2016). The drought also had a significant impact on the maturation window, a theorized period of time when temperatures are suitable for growth and fish are capable of investing energy into gonad maturation (Brown et al. 2016b). During the peak of the drought in 2014 and 2015, the maturation window was approximately one month shorter, precluding the potential production of multiple batch-spawns in those years (Hobbs et al. 2019b).

Growth was generally higher for fish caught in freshwater to salinity of approximately 4, after which growth declined. Komoroske et al. (2016) discovered that while Delta Smelt are capable of living in a wide range of salinity (0.4 to 32) during 2-week trials, fish reared at 32 experienced reduced condition factor while fish experiencing salinity greater than 6 (12 and 18) treatments exhibited significantly different transcriptomic responses (gene activation), which included a suite of genes associated with metabolism, suggesting prolonged exposure to salinity greater than 6 could be energetically detrimental. The trend with salinity might also be indicative of poor feeding conditions in higher salinity habitats. Several studies have documented lower herbivorous zooplankton prey density and biomass in more brackish areas than freshwater (Hammock et al. 2015, Kimmerer et al. 2018). However, despite differences in zooplankton density, feeding success was higher for Delta Smelt occupying the LSZ (see Slater et al. 2019). Turbidity is thought to be an important habitat attribute,

providing refuge from predators while also being important for detecting prey for larval Delta Smelt (Hasenbein et al. 2013). The combination of higher turbidity and available herbivorous zooplankton prey in the LSZ likely explains the trend in feeding success.

Life History Diversity

[This section is a summary of results from Hobbs et al. (2019b), a chapter in the Directed Outflow Project Technical Report (Schultz 2019). Hobbs et al. (2019b) represents the most recent analysis of Delta Smelt life history characteristics, and developing a separate analysis for this report was deemed repetitive and unnecessary. However, conclusions appearing at the end of this section are focused on questions specific to this report and do not necessarily match with Hobbs et al. (2019b) or Schultz (2019). The text of this section has been edited from the original to meet the needs of this report. See Hobbs et al. (2019b) for additional detail.]

Similar to the IEP MAST (IEP-MAST 2015) for this report, we predict that life history diversity of Delta Smelt will be improved when the LSZ occurs within Suisun Bay (Table 3) during the fall. In this report we utilize recent work by Hobbs et al. (2019b) to assess this prediction using a variety of life history characteristics.

In earlier work, Delta Smelt have been described as semi-anadromous, spawning in tidal freshwater regions of the Delta in spring and rearing in the LSZ from juvenile to sub-adult life stages in the summer-fall months before migrating back to freshwater in the late-fall and winter (Bennett 2005, Moyle et al. 2016, Moyle et al. 1992). This life history type suggests Delta Smelt are obligate to the LSZ and recruitment success is likely dictated by habitat conditions therein. However, Delta Smelt have also been found in the tidal freshwaters of the North Delta year-round in recent monitoring surveys (Sommer and Mejia 2013, Sommer et al. 2011), and studies using otolith strontium isotope ratios have discovered both freshwater and brackish water year-round residents in addition to the semi-anadromous life history. The discovery of a freshwater resident life history suggests Delta Smelt use of the LSZ is facultative, and conditions outside the LSZ maybe also be important for recruitment (Bush 2017, Hobbs et al. 2019a). This may seemingly contradict the concept underlying the fall X2 management; however, we note that when fall X2 is located westward, more freshwater habitat is a created, thus the underlying mechanism(s) may apply to the LSZ and freshwater habitats in the Delta.

Maintaining such diversity in these life history phenotypes (semi-anadromy, freshwater, and brackish residency) is thought to promote population resilience by spreading the risk of catastrophic mortality across the estuarine landscape.

Delta Smelt can also spread the risk of mortality across time. Delta Smelt are predominately an annual species with a relatively protracted reproductive period (February-July) often lasting 4-6 months (Bennett 2005). Bennett (2005) demonstrated that hatching success in culture is largely driven by temperature where optimal hatch success occurs between 15°C and 20°C and referred to this period of time the “Hatching Window” and suggested the duration of the Hatching Window may be an important driver of recruitment success (Bennett 2005). Females can produce multiple clutches of eggs, allowing individuals the opportunity to spawn multiple times within the Hatch Window and thereby increase life history diversity (Damon et al. 2016; Kurobe et al. 2016).

Warm temperature in the fall has been hypothesized to delay maturation in Delta Smelt reducing the fish’s ability to produce eggs and ultimately limit recruitment success (Brown et al. 2016 a, b, IEP-MAST 2015). Several studies have documented acute lethal temperature and thermal stress thresholds for juvenile and adult Delta Smelt, establishing their thermal sensitivity to temperatures generally above 24°C (Brown et al. 2016 a, b, Jeffries et al. 2016, Jeffries et al. 2018, Komoroske et al. 2015). However, Delta Smelt experience high mortality when cultured for extended periods of time at or above 20°C (Tien Chieh-Hung personal communication), and otolith growth studies (Hobbs et al. 2019c) suggest Delta Smelt grow poorly when inhabiting habitats above 20°C; thus, thermal stress may be limiting growth and survival in summer and reducing the time which Delta Smelt have to mature. Hobbs et al. (2019b) defined the “Maturation Window” as the duration of time (days) between water temperature decreasing below 20°C in the fall and water temperature increasing about 12°C in the spring (Figure 74). The 12°C cutoff for the Maturation Window was based on the mean temperature when first yolk-sac (~4-5 mm) Delta Smelt were encountered during larval surveys (CDFW 20-mm Survey). Summer temperatures are also likely to influence the life history of Delta Smelt. Summer temperatures can approach sub-lethal stress levels causing fish to seek thermal refuge. Temperatures in freshwater habitats are typically warmer than in Suisun Bay in the summer and fall, thus Delta Smelt dispersal from freshwater natal habitats to the LSZ may be cued when temperatures exceed 20°C. They also define a “Hatching Window,” based on the duration of time (days) between the end of the

maturation window at 12°C and water temperature increasing above 20°C in the spring, assuming poor survival for fish hatching into habitats above 20°C (Figure 74). Summer temperatures are also likely to influence the life history of Delta Smelt. Summer temperatures can approach sub-lethal stress inducing levels, causing fish to seek thermal refuge. Temperatures in freshwater habitats are typically warmer than in Suisun Bay in the summer and fall, thus Delta Smelt dispersal from freshwater natal habitats to the LSZ may be cued when temperatures exceed 20°C.

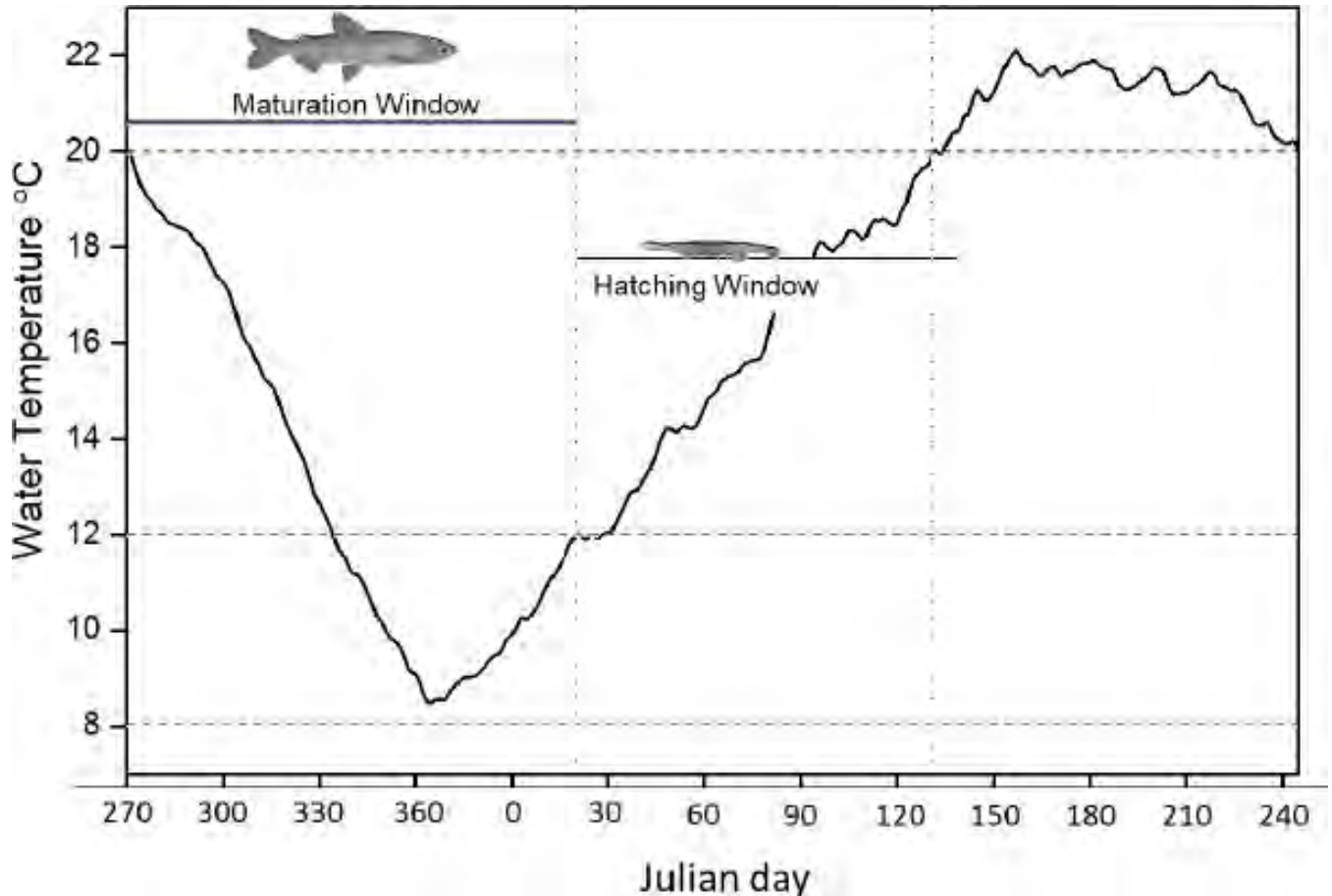


Figure 74. Conceptual model describing the relationship between water temperature, timing and duration of the maturation window and hatching window for Delta Smelt. The maturation window, modified from Brown et al. (2016) begins in the fall when daily estuary wide temperatures drop below 20°C and ends when hatching begins in the spring at 12°C. The hatching window ends in the late-spring when temperatures exceed 20°C (modified from Hobbs et al. 2019b).

Hobbs et al. (2019b) used otolith microstructure and microchemistry to quantify key life history attributes (hatch dates, natal origins, dispersal dates, and life history phenotypes) for Delta Smelt collected from 2011 to 2017. This time period included a wet-cool year (2011) and a wet-warm year

(2017) bracketing a period of extreme drought (2012-2016) and allowed them to explore how environmental variability influences Delta Smelt life history attributes. How fall flow management will influence Delta Smelt life history diversity is an ongoing area of research. Managing X2 to be westward in wet and above normal years can result in cooler conditions within the LSZ, which may influence fish condition and maturation. Hobbs et al. (2019b) tested a series of predictions for how Delta Smelt life history attributes would respond to droughts and high flow years when fall X2 was managed. First, they predicted that the duration of maturation window and hatching window will have a positive effect on the duration of hatching, which increases life history diversity. In addition to duration metrics they predicted the 'timing', or thermal phenology of the maturation and hatch windows (dates when temps surpass 12 and 20°C), will correspond with hatch phenology. Next, they predicted the Julian date when spring temperatures exceed 20°C in the estuary will correspond with dispersal phenology (from freshwater natal habitats to the LSZ). Lastly, they predicted weather conditions during the fall-winter and spring months of high flow years (with associated flow management actions) will have longer maturation windows and hatch windows due to the associated cooler air temperatures and water temperatures, and these patterns will result in overall greater life history diversity in wet years. This last prediction is similar to the prediction tested for this report. The prediction of this report is that the life history characteristics defined by Hobbs et al. (2019b) will improve when high flows position the LSZ in the Suisun region rather than in the confluence region as in drier years.

Delta Smelt used by Hobbs et al. (2019c) are the same fish utilized in Hobbs et al. (2019b). Detailed methods are available in (Hobbs et al. 2019b). Briefly, the salinity histories of fish were determined by analyzing otolith strontium isotope ratios ($^{87}\text{Sr}/^{86}\text{Sr}$) via laser ablation. These data make it possible to determine the ages at which fish move to areas with different salinities. They used water temperature recorded at 15-min intervals from five stations (Antioch-ANH, Deepwater Ship Channel-DWS, Mallard-MAL, Martinez-MRZ, Rio Vista-RVB) monitored by the California Department of Water Resources (DWR) and archived on the California Data Exchange Center (<https://cdec.water.ca.gov/>) to calculate the mean daily temperature in the Delta Smelt's primary habitat. Freshwater flows through the estuary (Delta Outflow) were obtained from the DAYFLOW model (available at, <https://water.ca.gov/Programs/Environmental-Services/Compliance-Monitoring->

And-Assessment/Dayflow-Data), which provides daily net Delta Outflows in cubic feet per second (cfs). Hobbs et al. (2019b) analyzed otoliths from 1,445 Delta Smelt in their study

Delta Smelt collected during the study exhibited a prolonged period of hatching lasting on average about three months, beginning approximately 2-3 weeks following the last peak in Delta outflow in 2011, 2016, and 2017 (Figure 75). Hatch distributions were relatively continuous during the spring but did appear to exhibit some brief episodic modality. Hatching phenology shifted to earlier in the year during the drought years and occurred on average 13-days earlier per year from 2011 to 2015 (Figure 75). Unfortunately, very few fish (N=13) were collected in 2016, precluding a reliable assessment of hatch distributions in that year; however, in 2017, the mean date was approximately two weeks later than the 2013-2015 time period (Table 10). The hatching phenology tracked the Julian date when temperatures surpassed 12°C (Table 11), which occurred earlier during the drought years, and later during the wet years. However, from 2014-2016 hatching began 9-25 days after temperatures exceeded 12°C (Figure 75). Warm summer conditions also persisted later during the drought, shortening the maturation windows in 2015 and 2016 by approximately 1 month (Table 11) corresponding with delayed hatching in those years (Figure 76).

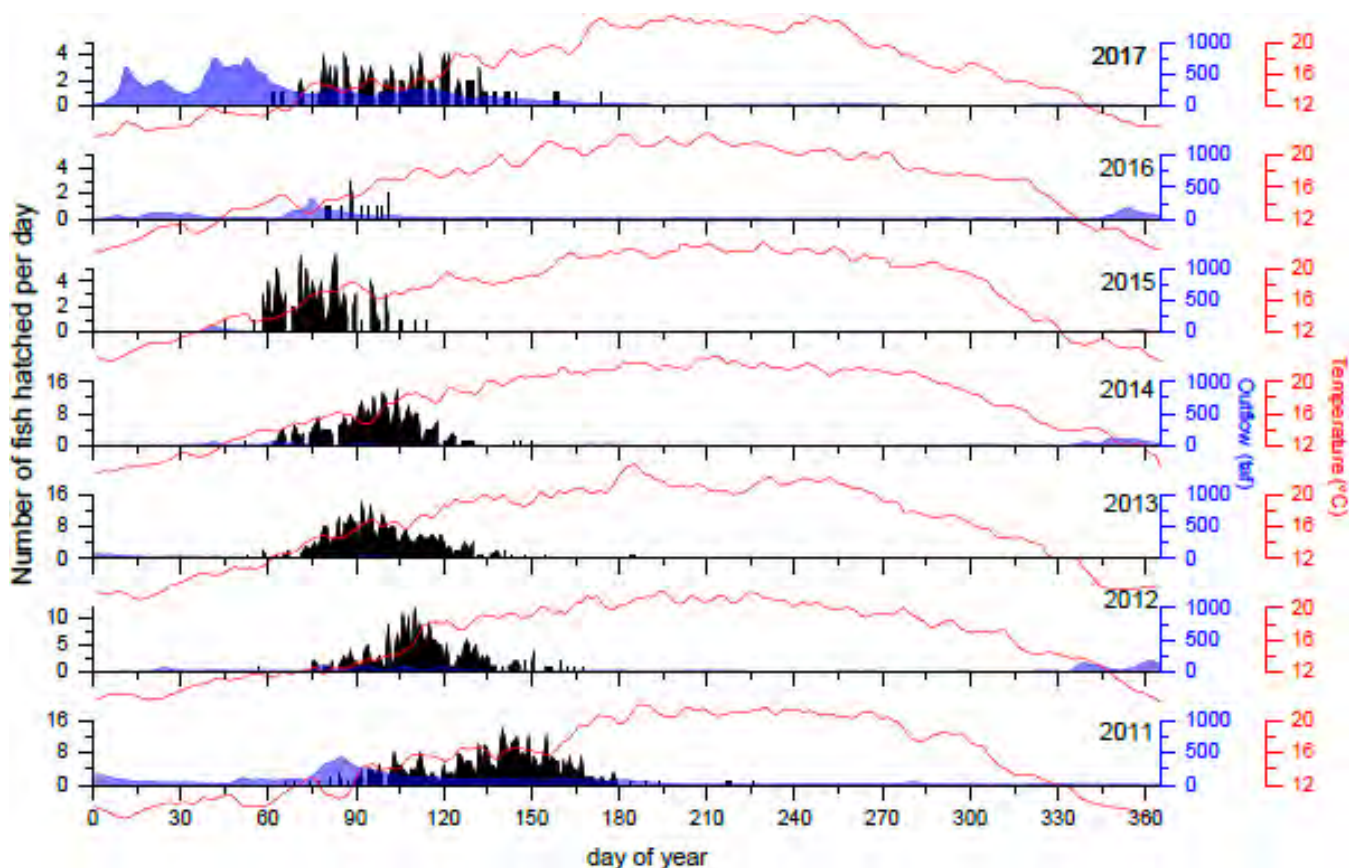


Figure 75. Julian hatch-date distributions (black vertical bars) for Delta Smelt from 2011-2017. Filled blue polygons represent Delta outflow, red lines depict daily mean water temperatures at the 5-index stations (modified from Hobbs et al. 2019b). Note the temperature is scaled from 12 to 20°C to emphasize the period of suitable maturing and hatching.

Table 10. Summary of Delta Smelt hatching from 2011-2017. Hatch range was calculated both as the interquartile range (IQR) and as the percentile range (95%-5%) (modified from Hobbs et al. 2019b).

Year	Beginning of hatch		Mean hatch		End of hatch		Hatch IQR	Hatch percentile
	Julian date	Date	Julian date	Date	Julian date	Date	(days)	(days)
2011	74	15-Mar	137	17-May	195	14-Jul	29	78
2012	50	19-Feb	109	18-Apr	160	9-Jun	22	63
2013	59	28-Feb	99	9-Apr	158	7-Jun	25	55
2014	54	23-Feb	97	6-Apr	145	25-May	21	53
2015	44	13 Fed	78	18-Mar	116	26-Apr	19	44
2016	79	20-Mar	91	31-Mar	102	12-Apr	14	21
2017	60	1-Mar	108	18-Apr	168	17-Jun	33	71

Table 11. Summary of thermal phenology from 2011-2017 (modified from Hobbs et al. 2019b).

Year	Julian date of water temperature exceeding 12°C	Julian date of water temperature exceeding 20°C	Hatch window (days)	Maturation window (days)
2011	71	172	101	160
2012	65	153	88	156
2013	62	134	72	150
2014	44	135	91	142
2015	35	156	121	112
2016	44	139	95	118
2017	69	168	99	161

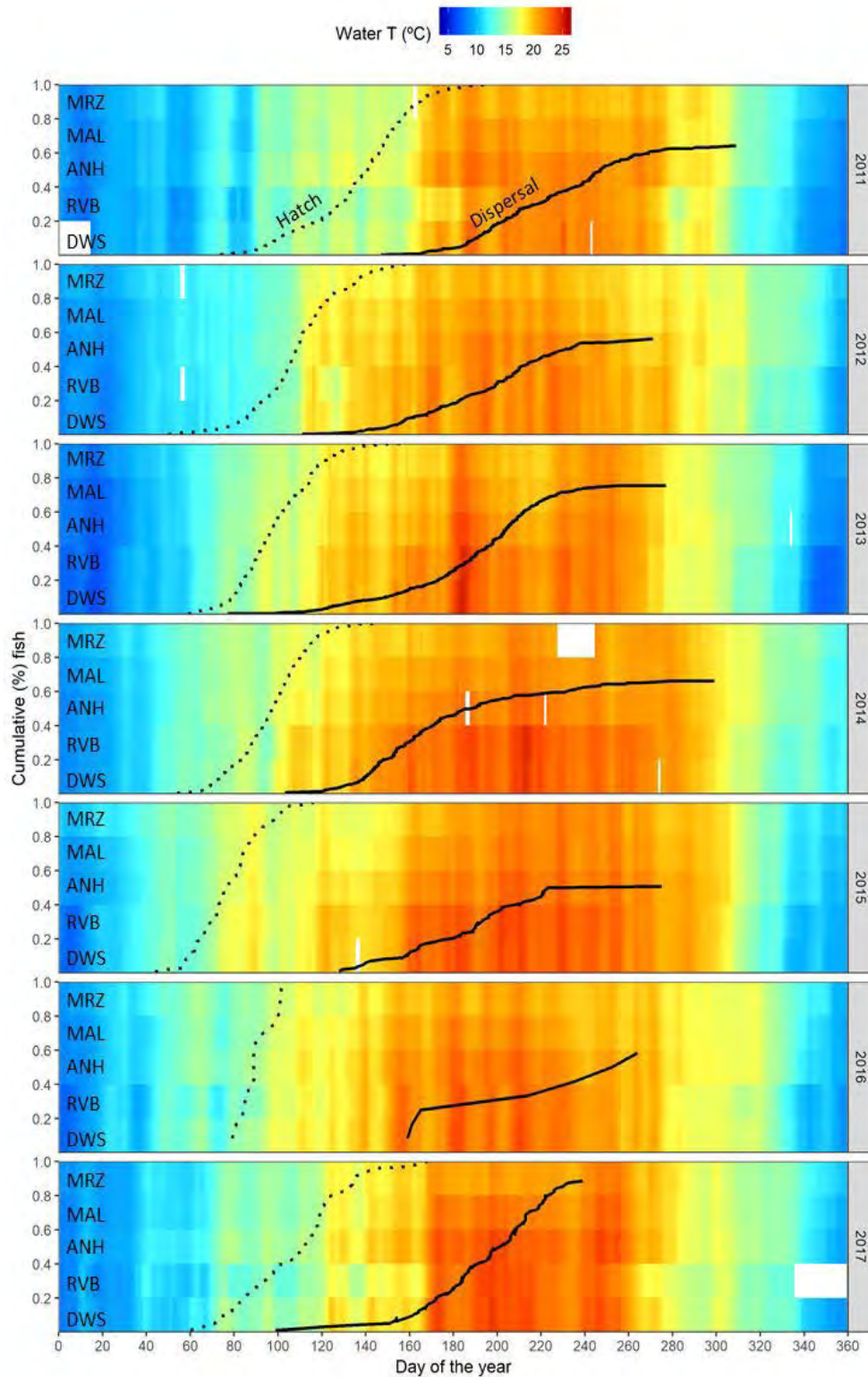


Figure 76. Cumulative distribution of -Date (dotted line) and dispersal date (solid line) for Delta Smelt from 2011 to 2017. The heatmap represents daily mean water temperature from the five sonde stations arranged vertically from the North Delta (DWS-bottom) to far western Suisun Bay (MRZ-top) (modified from Hobbs et al. 2019b).

Station names are Deepwater Ship Channel (DWS), Rio Vista (RVB), Antioch (ANH), Mallard (MAL), and Martinez (MRZ).

Temperature also appeared to be associated with the timing of Delta Smelt dispersal from freshwater to the LSZ (Figure 76). As with hatching, dispersal began earlier during the drought years, beginning approximately when temperatures exceeded 20°C. Delta Smelt exhibited relatively broad distributions for dispersal dates, ages, and lengths (Figure 77). The mean Julian date of dispersal ranged from day 171 in 2014 to 221 in 2011 (Table 12) and occurred earlier during the drought (Figure 77A). The mean age at dispersal (i.e., residence time in freshwater) varied from 71 days in 2014 to 116 days in 2016, the next longest freshwater residence time being 103 days in 2015 (Table 12). The mean lengths at dispersal ranged from 29 mm in 2014 to 44 mm in 2016, the next largest mean occurring in 2015 (42 mm).

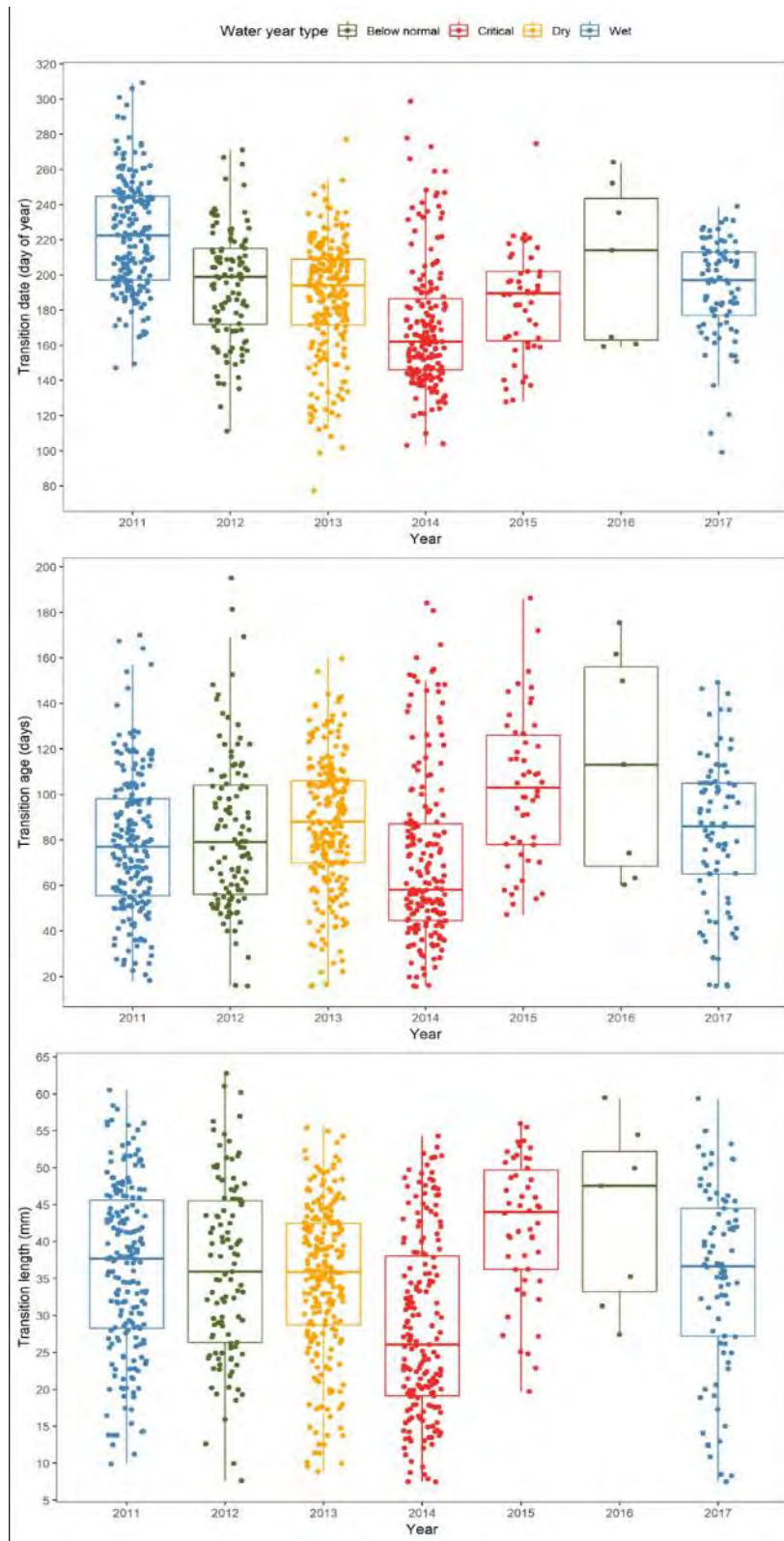


Figure 77. Boxplots of Julian date (A), age (B) and length (C) when Delta Smelt dispersed from freshwater to the LSZ from 2011-2017 (modified from Hobbs et al. 2019b).

Table 12. Summary of dispersal phenology from 2011-2017 (modified from Hobbs et al. 2019b).

Year	Mean dispersal date		Mean age at dispersal (days)	Mean length at dispersal (mm)
	Julian	Calendar		
2011	222	11-Aug	78	36
2012	195	14-Jul	83	36
2013	188	7-Jul	87	35
2014	171	20-Jun	71	28
2015	184	4-Jul	103	42
2016	207	27-Jul	114	44
2017	193	12-Jul	83	35

The Maturation Window had a strong positive effect on the hatch-date duration (Figure 78A), while surprisingly, there was no clear trend with the duration of the hatch window (Figure 78B). The Julian date when hatching began was positively correlated with the Julian date when temperatures exceeded 12°C (Figure 78C). The Julian date when hatching ended was positively correlated with the Julian date when temperatures exceeded 20°C (Figure 78D). Interestingly, the onset of hatching was also positively correlated with the Maturation Window duration (Figure 78E), suggesting more complex interactions during the reproductive period may be influencing hatch phenology. The onset of dispersal corresponded positively with the Julian date water temperatures exceeded 20°C (Figure 78F). The years of high outflow (2011, 2017) corresponded with longer maturation windows and hatch windows, in part due to temperatures exceeding 12°C and 20°C, respectively, later in those years.

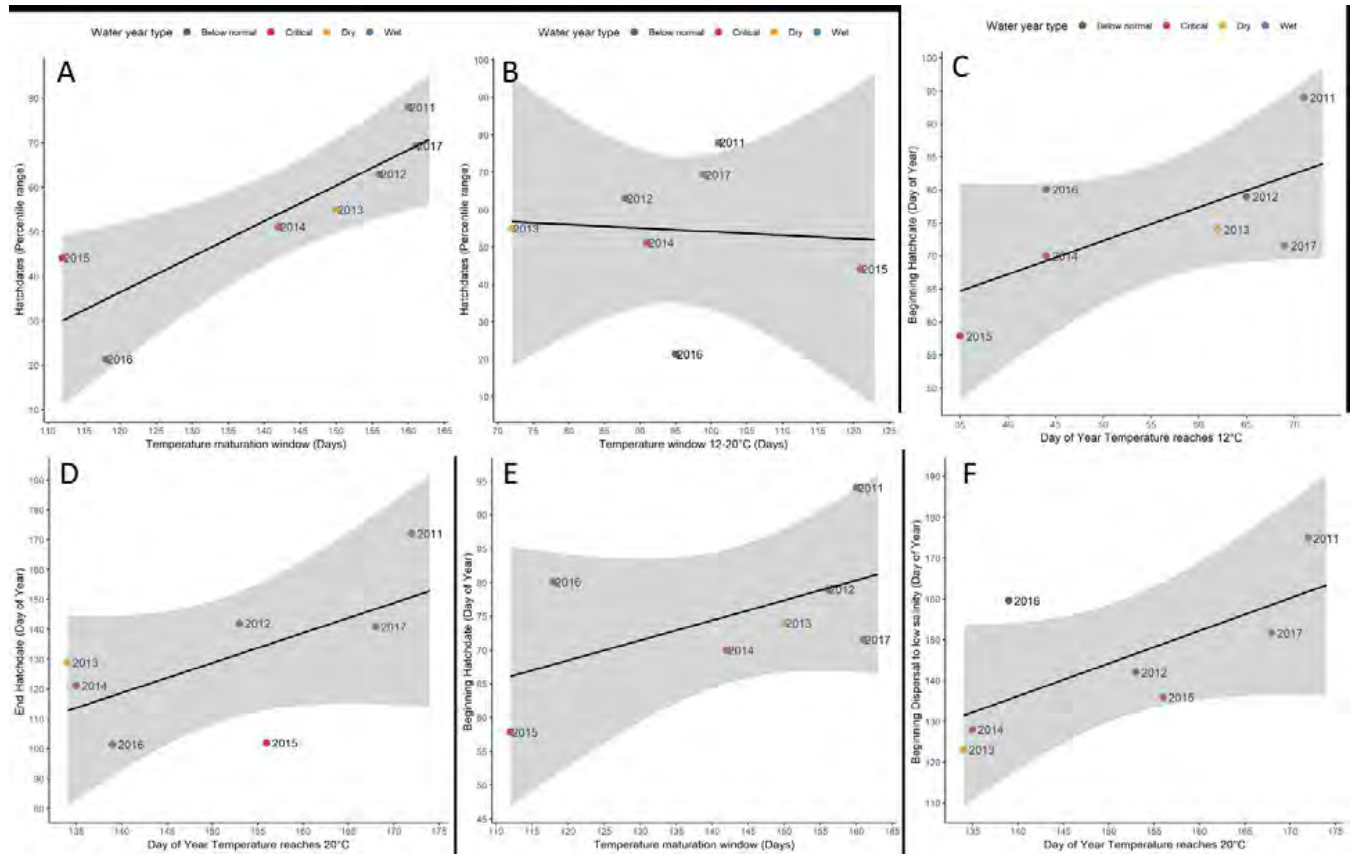


Figure 78. Trends in hatch-date duration and phenology: A) effect of the maturation window on hatch-date durations, B) effect of hatch window on hatch duration, C) effect of Julian day 12°C on beginning of hatch, D) effect of Julian day 20°C on end of hatch, E) effect of the maturation window on beginning of hatch, F) effect of Julian day 20°C on beginning of dispersal to the LSZ (modified from Hobbs et al. 2019b).

The vast majority of fish in all survey years had freshwater natal origins (Figure 79). The distributions in most years appeared to be continuous; however, in 2017 there appeared to be several modes of natal origin. A few fish hatched in habitats with very low salinity (0.5 to 1) or LSZ (1-6), except in 2015 and 2016. There did not appear to be a strong difference between Julian hatch-dates for fish with different natal origins, although hatching did appear to begin slightly earlier in freshwater habitats (Figure 80).

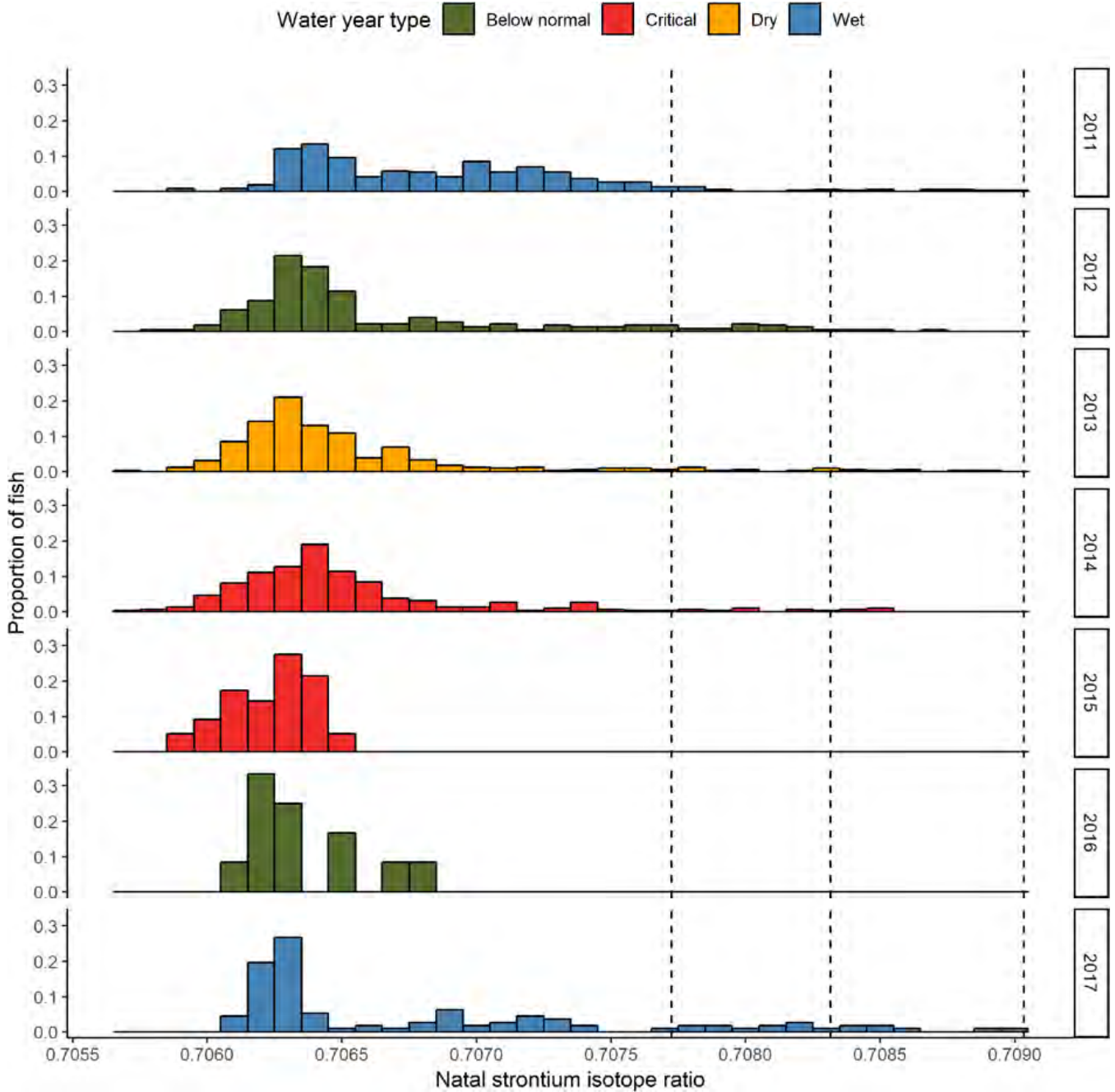


Figure 79. Natal origins (strontium isotope ratios) for Delta Smelt from 2011-2017. Vertical dotted lines depict the isotope ratio corresponding to thresholds between fresh (salinity <0.5), salinity 0.5 to 1 and salinity 1-6, occurring from left to right (modified from Hobbs et al. 2019b).

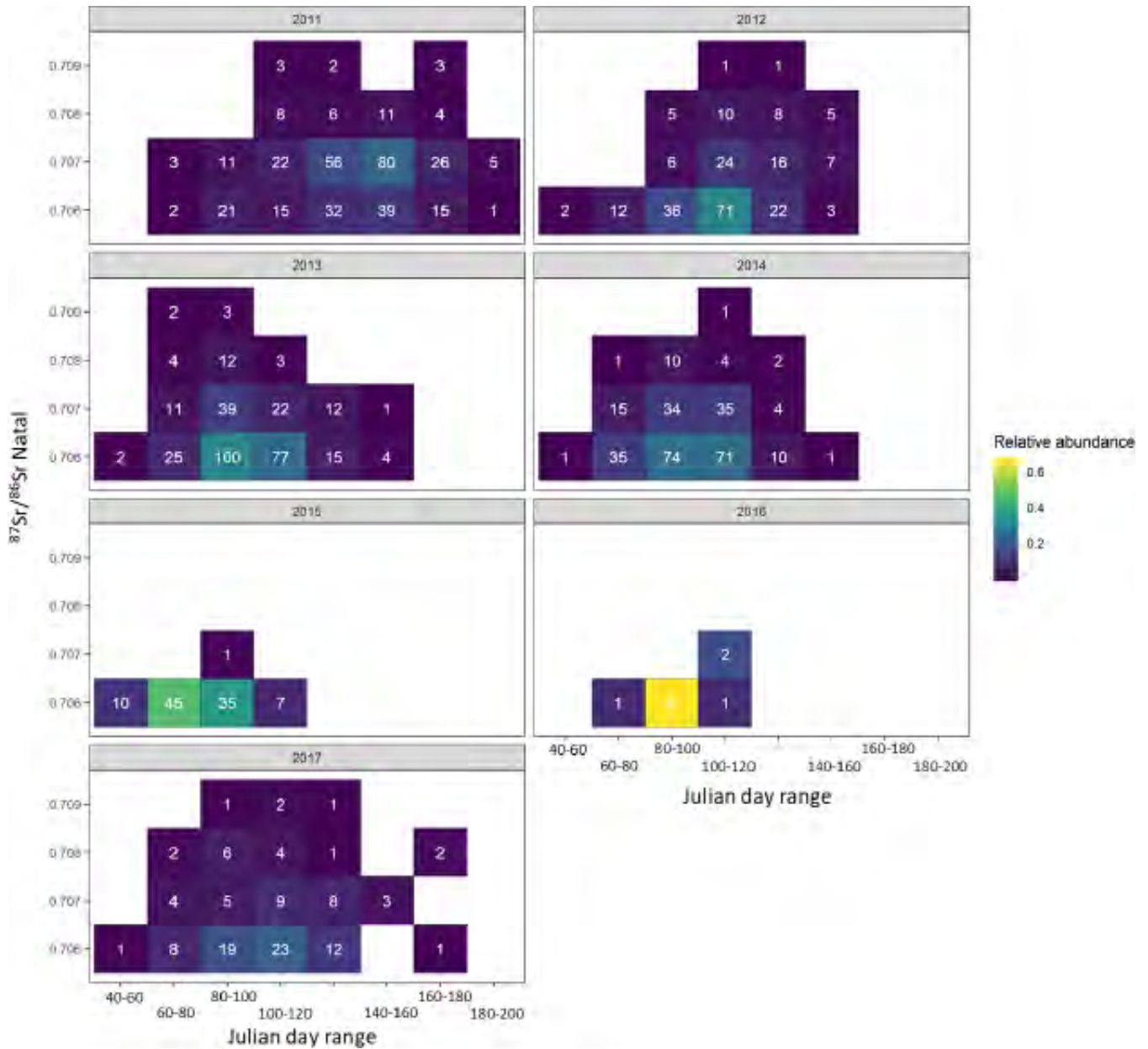


Figure 80. Heatmap of Julian hatch date and natal origins ($^{87}\text{Sr}/^{86}\text{Sr}$). Low values of $^{87}\text{Sr}/^{86}\text{Sr}$ indicate fresher water. The colors and numbers inside boxes depict the number of fish with the corresponding combination of Julian hatch date and natal $^{87}\text{Sr}/^{86}\text{Sr}$ (modified from Hobbs et al. 2019b).

The semi-anadromous phenotype was the dominant life history for adult Delta Smelt collected during the CDFW Spring Kodiak Trawl Survey from 2011 to 2017 (Figure 81). Water year type did not appear to have a strong effect on the life history phenotype composition. The freshwater resident life history type contributed 48% in the wet year of 2011 but was less than 20% in 2017. All drought years except 2015 had proportionally more freshwater residents than 2017, but all dry years were lower

than the wet year of 2011; thus, water year type did not have a strong effect on the life history phenotype composition (Figure LHC 8). In each year, brackish resident fish were found but consistently contributed the fewest individuals to the adult population (Figure 81).

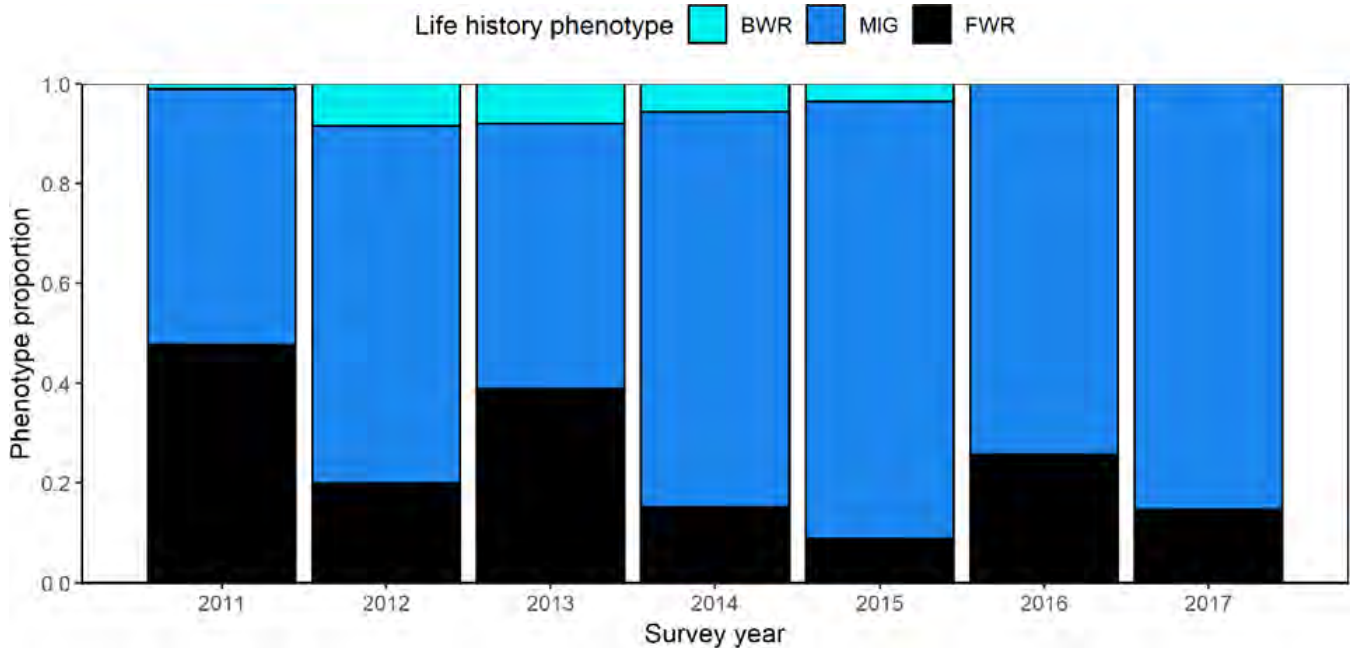


Figure 81. The proportion of different life history phenotypes contributing to adult abundance in the California Department of Fish and Wildlife's Spring Kodiak Trawl Survey, which samples maturing adults from January-May (modified from Hobbs et al. 2019b). BWR = brackish water phenotype; MIG = semi-anadromous phenotype; FWR = freshwater phenotype.

Conclusion

The data of Hobbs et al. (2019b) did not provide clear support for the prediction of this study that life history diversity is higher when the LSZ is located in Suisun Bay during the fall compared to when the LSZ is located near the confluence. In addition, water year type did not appear to be an influence on the relative success of freshwater residents, brackish water residents, and the more common semi-anadromous phenotypes.

However, Hobbs et al. (2019b) provided substantial data that water temperature at various times of the year and spring outflow can have important effects on various life history characteristics that collectively contribute to life history diversity. In relation to fall, warm water temperatures $>20^{\circ}\text{C}$ that extend into the fall can shorten the Maturation Window, which can subsequently affect the initiation and duration of the spawning period. This can have substantial effects on the number of eggs

produced by the population. To the extent that flow can be used to manage water temperatures, fall flows may be important. Summer water temperatures $>20^{\circ}\text{C}$ appeared to be an important cue for dispersal of juvenile Delta Smelt from Delta freshwater habitats into the LSZ. The interaction of summer with flow actions to influence the duration of rearing in the LSZ is a new avenue of research that may need to be addressed in future efforts.

Delta Smelt have a complex life history (Bush 2017). Hobbs et al. (2019b) found that the proportion of freshwater residents contributing to the adult population varied but did not appear to correspond with variability in freshwater outflow at the annual timescale. For example, freshwater residents comprised a substantial proportion of the population (48%) in 2011, a wet year, and 2013, a dry year (39%). Thus, another factor may be important in driving the relative recruitment of freshwater resident and semi-anadromous individuals. Summer water temperature is a likely factor that limits recruitment of freshwater resident Delta Smelt. During the summer months, the freshwater portion of the Delta often reaches or exceeds levels that cause physiological stress (see Dynamic Abiotic Habitat section, Jeffries et al. 2016, Jeffries et al. 2018, Komoroske et al. 2014), yet a portion of the population remains in freshwater year-round and in some years the freshwater resident contingent can be a significant fraction of the spawning fish. Hobbs et al. (2019b) suggested that this phenomenon raises several questions regarding the biology and ecology of the species. For example, are freshwater resident Delta Smelt more ‘tolerant’ of warm water or do freshwater residents find thermal refuge in freshwater that is currently not sampled by monitoring surveys? Regardless of how Delta Smelt live in the Delta during the summer-fall, the fact that in some years a large number of adults are freshwater residents suggests that current management of critical habitat and flow actions to maintain fall habitat may need to be expanded to include freshwater habitats, particularly in the North Delta. Hobbs et al. (2019b) noted that while the North Delta food web action may provide a food subsidy to the freshwater resident fish, if these increased flows to the North Delta are warm, this could have a detrimental effect, thus they urge caution in executing such actions.

Health Metrics

[This section is a summary of results from Teh et al. (2019), a chapter in the Directed Outflow Project Technical Report (Schultz 2019). Teh et al. (2019) represents the most recent analysis of Delta Smelt

health metrics and developing a separate analysis for this report was deemed repetitive and unnecessary. However, conclusions appearing at the end of this section are focused on questions specific to this report and do not necessarily match with Teh et al. (2019) or Schultz (2019). The text of this section has been edited from the original to meet the needs of this report. See Teh et al. (2019) for additional detail.]

Teh et al. (2019) examined the severity and incidence of lesions (i.e., tissue abnormalities; see below and Teh et al. (2019) for lesions types) in the liver and gill of Delta Smelt and level of glycogen depletion in the liver from 2011 through 2017 in the Sacramento-San Joaquin Delta and San Francisco Estuary (n=1053). This period encompassed a wet and cool period (2011), a period of drought (2012-2016), and a wet, warm period (2017). Liver and gill are the two most widely used organs in fish histopathology studies (Mallatt 1985, Hinton et al. 1992, Myers et al. 1998, Poleksic and Mitrovic-Tutundzic 1994, ICES 1997), and the condition of these organs was evaluated to assess the response in health of Delta Smelt to changes in environmental conditions. These organs are sensitive to a variety of environmental stressors, which, in turn, are indicators of population/community effects such as survival, growth and reproduction (Adams et al. 1992, Teh et al. 1997). In fish, the liver performs metabolic and detoxification functions, stores glycogen for short-term energy, and is the site of choriogenin and vitellogenin protein production for egg chorion and yolk, respectively. Therefore, impairment of liver function has negative consequences for growth, survival, and reproductive success of fish. Gills are gas exchange and osmotic regulation organs and as such are in constant, direct contact with water. Gills respond more rapidly than the liver to stressors and therefore represent an important and sensitive target to assess water quality and contaminant exposure.

Previous work by Hammock et al. (2015) demonstrated that juvenile Delta Smelt collected from certain geographic regions exhibited significantly depressed nutritional indices and elevated levels of histopathological lesions, suggesting that the species is, at a minimum, regionally stressed by contaminants and food limitation. Specifically, Delta Smelt collected from Suisun Bay were under relatively higher nutritional stress during summer, Delta Smelt collected from Cache Slough showed the most severe level of liver damage, while individuals from Suisun Marsh were in relatively good condition overall (Hammock et al. 2015). Teh et al. (2019) extends this health analysis, both from 2 to 7 years and across all life-stages and examines whether variations in fish health and nutritional status

maintained their regional specificity. Using identical field and laboratory methodology across the 7-year study, they asked whether there are differences in histopathological condition (liver lesions, gill lesions, and liver glycogen levels) associated with region, year class, salinity, and freshwater outflow, a factor that is of interest to water managers. Teh et al. (2019) used a model-fitting and comparison procedure to identify important predictors of liver and gill condition.

The prediction for this report is that histopathological condition will be better in wet years like 2011 and 2017 compared to the intervening drier years (2012-2016). Although contaminant loading would likely increase under wet conditions as more of the pollutants are mobilized and transported into the water, as earlier described for nutrients (see Phytoplankton section and Garrett 2012, Murphy et al. 2014, Van Metre et al. 2016, Munn et al. 2018), extraordinarily high flows may deplete the contaminant sources much like sediment loading under a wet year; thus, contaminant exposure concentrations could be low. In addition, other environmental conditions such as salinity and prey densities may improve under wet conditions. Detailed methods and additional results are available in Teh et al. (2019). Results are presented in terms of year classes (e.g., 2015/16) such that the first year indicates the year a fish was hatched and reared and the second year indicates the year the fish matured.

The majority of Delta Smelt examined (65.6%) had at least one lesion suggesting that the majority of the Delta Smelt were exposed to an environmental stressor. The three most common lesions were gill ionocyte hyperplasia, liver lipidosis, and gill aneurysm, lesions which may be symptomatic of contaminant exposure. Model comparison was used to identify and quantify the drivers of the spatial and temporal patterns observed in gill and liver lesion scores (see Teh et al. 2019 for detail). Liver and gill lesion scores were a summation of the severity scores of each lesion, except glycogen depletion because it responds both to contaminants and foraging success. Thus, higher scores indicate worse liver or gill condition. Fork length was an important variable in all of the best models. Both liver (Figure 82) and gill (Figure 83) lesion score increased with fork length, either indicating that Delta Smelt accumulate lesions throughout their lives, or that larger individuals were more tolerant of liver and gill damage (or both). In either case, the results suggest contaminant exposure and toxicity is common in the population. The response to fork length was stronger for liver than gill lesion score (see Teh et al. 2019).

Liver lesion score showed significant regional differences (Figure 82 HIST 1), while salinity was a better predictor of gill lesions than region, with increasing salinity decreasing gill lesion score (Fig. HIST 2). Regionally, Delta Smelt collected from the confluence region and Suisun Marsh had the lowest liver lesion score, while Delta Smelt collected from Cache Slough and Suisun Bay had the highest lesion scores (Figure 82A). The SRDWSC was intermediate. Although lesions were found in all regions, the results suggest that contaminant exposure may be lower or environmental conditions less stressful for Delta Smelt in Suisun Marsh and the confluence region.

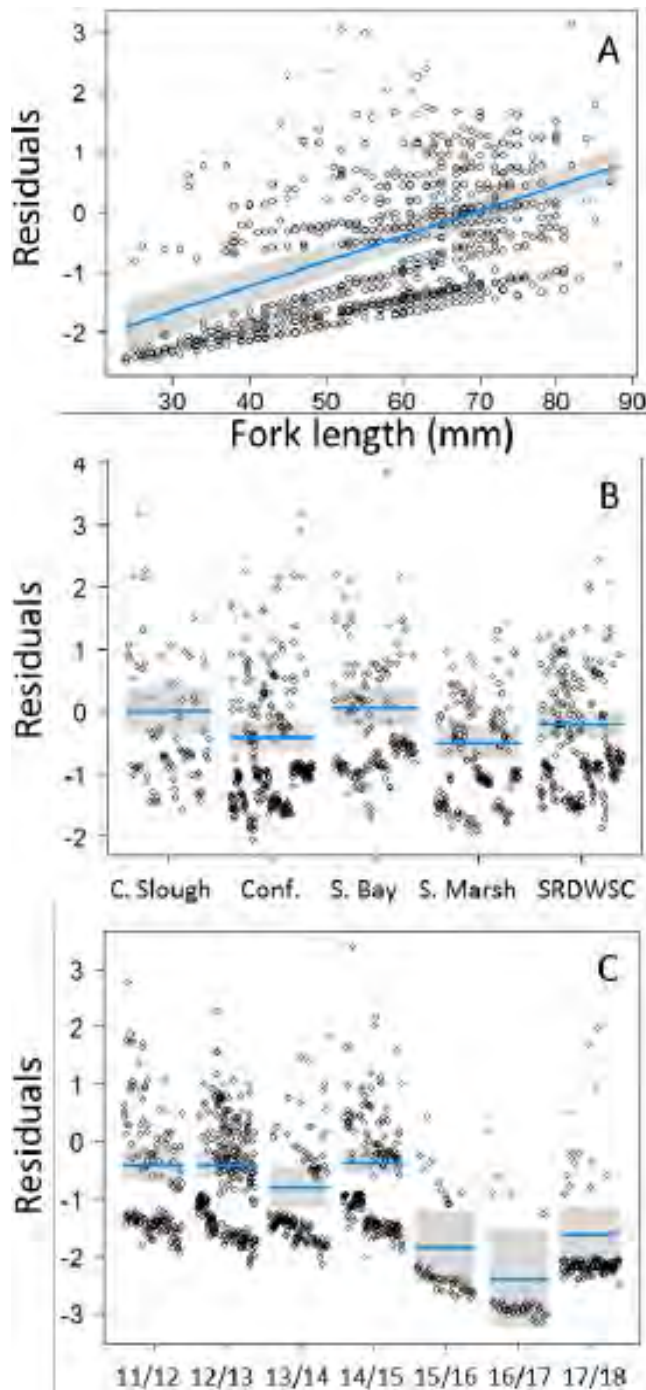


Figure 82. Partial residuals (lesion scores) from the selected liver lesion model by A) region Cache Slough Complex (C. Slough), confluence region (Conf), Suisun Bay (S. Bay), Suisun Marsh (S. Marsh), and Sacramento River Deepwater Shipchannel (SRDWSC) and B) year class 2011/2012 (1112), 2012/2013 (1213), 2013/2014 (1314), 2014/2015 (1415), 2015/2016 (1516), 2016/2017 (1617), and 2017/2018 (1718). The gray bands show the 95% confidence interval. Note that lower lesion scores are associated with healthier individuals (modified from Teh et al. 2019).

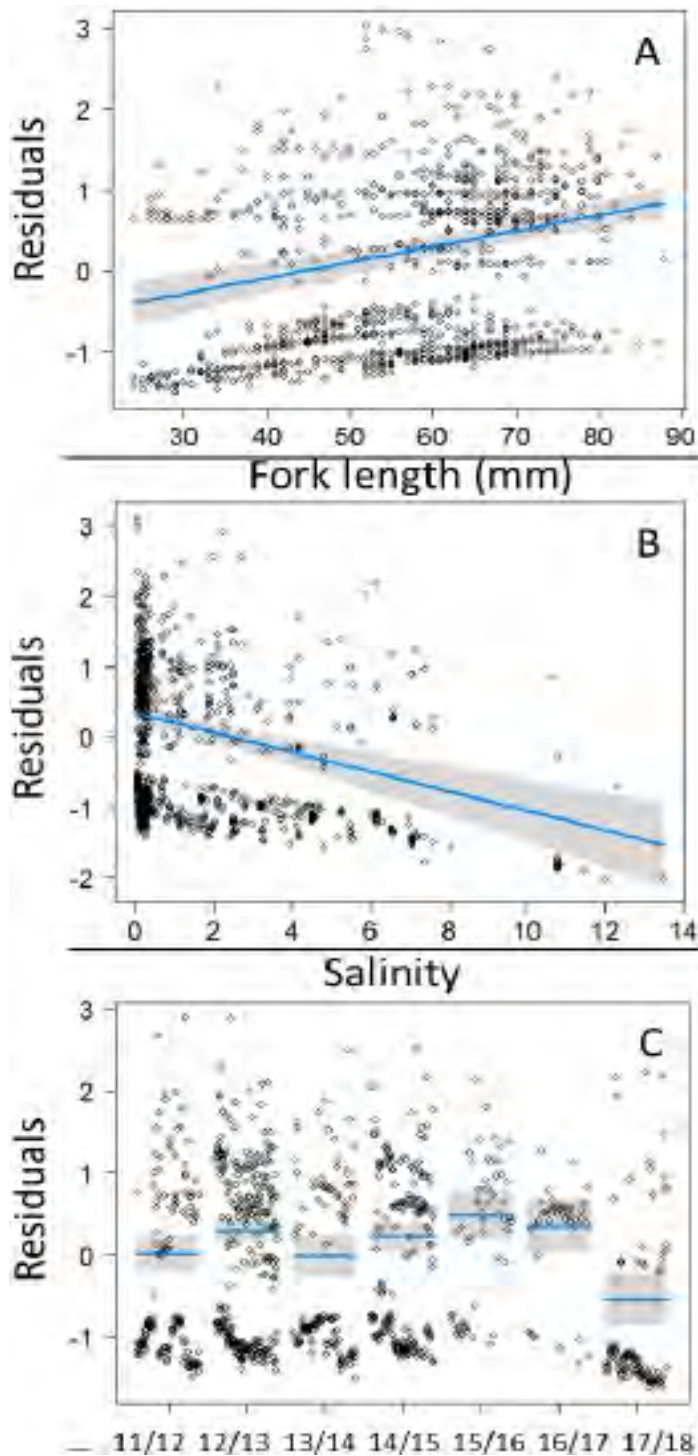


Figure 83. The partial residuals for the top-ranked gill lesion score model by A) fork length, B) salinity, and C) year class 2011/2012 (1112), 2012/2013 (1213), 2013/2014 (1314), 2014/2015 (1415), 2015/2016 (1516), 2016/2017 (1617), and 2017/2018 (1718). The gray bands show the 95% confidence interval (modified from Teh et al. 2019).

Liver and gill lesion score also varied significantly with year class. For liver lesion score, relatively unhealthy fish persisted in the population regardless of water year type until the 2014/15 year class. The mean liver lesion score improved substantially for the 2015/16 and 2016/17 year classes (Figure 82). Mean liver lesions in the 2017/18 year class were somewhat intermediate compared to other years. The 2011/12 year class was more similar to the earlier drought years of the 2012/13 to 2014/15 year classes that coincided with the drought than the wet year class of 2017/18. The later drought year classes of 2015/16 and 2016/17 were more similar to the 2017/18 year class. The highest gill lesion scores occurred in the 2015/16 year class, and the lowest occurred in the 2017/18 year class (Figure 83). The 2011/12 year class was more similar to the drought years than to the wet year of 2017/18 suggesting that water year type did not impact gill lesion score.

Glycogen depletion was observed in 85.2% of individuals, and 66.6% of individuals exhibited moderate or severe glycogen depletion. Liver glycogen depletion was related to fork length, X2, and region (Figure 84). Glycogen depletion increased with increasing fork length, was lowest in Suisun Marsh, and decreased with increasing X2 (i.e., Delta Smelt exhibited livers that were richer in glycogen under drier conditions) (Figure 84).

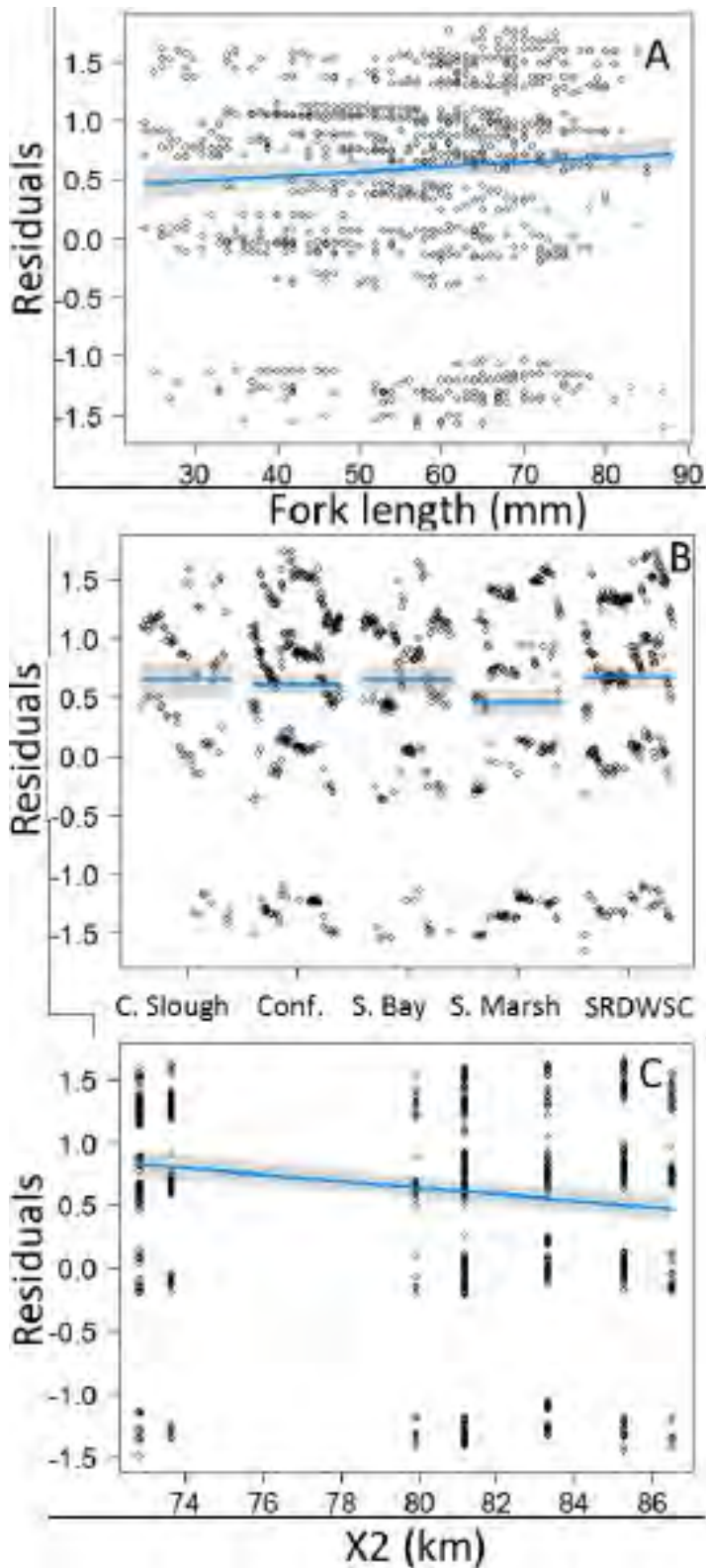


Figure 84. The partial residuals (liver glycogen scores) for the top-ranked liver glycogen score model by fork length (A), region (B), and X2 (C). The gray bands show the 95% confidence interval (modified from Teh et al. 2019).

Conclusion

The prediction of healthier Delta Smelt (low lesions and low liver glycogen depletion) during wet conditions of 2017 was not supported for liver lesions compared to the previous drier years of 2015 and 2016 (Figure 82). The Delta Smelt from the 2017/18 year class exhibited an elevation in the severity of lesions scores compared to Delta Smelt from the 2016/17 year class, but compared to 2011 (a wet, cool year) and 2012-2014 (below normal and dry years), there was a lower lesion score. Although reduced contaminant loading during a dry period may explain why 2015/16 and 2016/17 year classes exhibited low prevalence of lesions, it cannot explain why it was not the case for previous dry years of 2012/13, 2013/14, and 2014/15.

The improvement in liver condition during the drought occurred both because individuals with unhealthy livers were less prevalent than during previous years and because individuals with livers in the best condition exhibited improved liver condition compared to previous years (Figure 82). Teh et al. (2019) proposed two nonexclusive interpretations: 1) decreased prevalence of liver lesions indicates either reduced contaminant exposure under drier conditions or 2) drier conditions reduce the ability of Delta Smelt to tolerate liver damage. Generally, dry versus wet year comparisons suggest that more contaminant loading is likely during wetter periods (Garrett 2012, Murphy et al. 2014, Van Metre et al. 2016, Munn et al. 2018), but Teh et al. (2019) suggested that extreme dry periods like in 2015 and 2016 may result in fish that exhibit low lesions scores due to the cumulative stress of the dry period and other stressors. The absence of individuals with the highest liver lesion scores during the latter years of the drought suggests that the least healthy individuals were not able to persist under the stressful conditions (e.g., high temperatures, scarce prey, high salinities) and were therefore not sampled. For the healthiest individuals, liver health may have improved due to improved water quality due to reduced runoff (e.g., Sansalone and Buchberger 1997). Whatever the causes, improving liver health was not a positive sign for the population as the severity of the drought increased, since the population reached historical lows even as liver health improved.

Reduced mobilization of contaminants under drought conditions could explain the reduced prevalence of lesions from 2012-2016. However, the evaluation of the year classes did not find a strong relationship with water year type. The drier years of 2012-2014 did not result in reduced lesions in the respective year classes (2012/13-2014/15) compared to the 2011/12 year class, while the 2016

was a wetter year than the prior three and would have resulted in increased mobilization of contaminants comparatively yet the 2016/17 year class also had reduced prevalence of liver lesions. Our interpretation is that multiple stressors became important in determining the health of Delta Smelt during the drought (e.g., such as increasing temperatures). Individuals either exhibited fewer lesions due to reduced contaminant loading or fish with lesions could not tolerate the increasing stress from other factors and died, making the population appear healthier on average. Water temperature was higher during the later years of the drought, nearing the limits of Delta Smelt physiology as was noted in the earlier section on water temperature (see Dynamic Abiotic Habitat). Delta Smelt exhibiting moderate and higher lesion prevalence and severity may not have survived the harsh drought conditions, leaving only the healthier individuals. More studies would need to be conducted to evaluate the hypothesis that unhealthy fish, as determined by health metrics, are less tolerant of other environmental stressors.

Some level of liver glycogen depletion was observed in 85.2% of individuals, and 66.6% of individuals exhibited moderate or severe glycogen depletion. This suggests that most of the Delta Smelt may be experiencing nutritional stress. The loss of hepatic glycogen can occur as a direct toxic effect of contaminants (Schwaiger et al. 1997, Teh et al. 1997), or because of reduced health condition caused by nutritional or physicochemical stress. In addition to having fish with the lowest liver lesion score, fish collected from Suisun Marsh showed the most glycogen rich livers (Teh et al. 2019), suggesting that Delta Smelt in Suisun Marsh generally have reduced toxicity risk and improved nutritional status.

The spatial distribution of liver damage described by Hammock et al. (2015) persisted in the far larger study by Teh et al. (2019), which included 809 more individuals and five more year classes. Similar to Hammock et al. (2015), the fish with the most damaged livers occurred in Cache Slough and Suisun Bay, while the healthiest fish occurred in Suisun Marsh. In addition to having fish with the lowest liver lesion score, fish collected from Suisun Marsh showed the most glycogen rich livers. Thus, Suisun Marsh continues to appear to be good habitat, as Delta Smelt exhibit relatively low liver lesion scores and rich liver glycogen.

Regional differences suggest that Suisun Marsh may provide better habitat as indicated by lower liver lesion scores. However, assuming the interpretation that stressful conditions during the

drought removed unhealthy fish from the population, another interpretation of the regional differences is possible (Teh et al. 2019). It is hypothesized that fish exhibiting healthy condition from regions such as Suisun Marsh may be an indication of stressful environmental conditions. The question of whether unhealthy fish are a good sign for a region or year class, because it shows that an unhealthy fish can persist in the relatively better environment, or if they are a bad sign, because the unhealthy environment resulted in unhealthy fish, cannot be resolved with the available data. Teh et al. (2019) concluded that lesion severity and prevalence require a more thorough evaluation of interactions with other factors to draw more definitive conclusions. Regardless of the interpretation, the prevalence of liver lesions suggests that contaminant impacts are harming Delta Smelt at all life stages over multiple years throughout their life cycle, with multiple instances of lesions that likely reduce survival.

In summary, the prediction of this study of improved health status in response to wet conditions in 2017 following the dry years was not supported. Consistent with Hammock et al. (2015), Suisun Marsh continues to appear to be favorable habitat when available to Delta Smelt (i.e., not too saline), as fish show relatively low liver lesion scores and rich liver glycogen, combined with relatively full stomachs (Hammock et al. 2015). The livers of fish in Cache Slough and Suisun Bay had higher lesion scores, suggesting contaminant exposure, while patterns in gill condition suggest there may have been increased contaminant exposure in fresher water. Surprisingly, liver condition improved as a historic drought progressed in California, possibly because the least healthy fish have lower tolerance to other environmental stresses so could not survive the harsh conditions, or because of decreased loading of contaminants during low flow conditions. We cannot distinguish between these interpretations with available data. Given the difficulties of interpreting histopathology of Delta Smelt, multiple variables should therefore be considered, including the population dynamics of the species, additional complementary indicator species if possible, and the ambient and antecedent environmental conditions.

Feeding Success

[This section is a summary of results from Slater et al. (2019), a chapter in the Directed Outflow Project Technical Report (Schultz 2019). Slater et al. (2019) represents the most recent analysis of Delta Smelt

diet, and developing a separate analysis for this report was deemed repetitive and unnecessary. However, conclusions appearing at the end of this section are focused on questions specific to this report and do not necessarily match with Slater et al. (2019) or Schultz (2019). The text of this section has been edited from the original to meet the needs of this report. See Slater et al. (2019) for additional detail.]

Delta Smelt is primarily a zooplanktivore that consumes a broad array of prey items that increase in size as the fish matures (Moyle et al. 1992, Lott 1998, Nobriga 2002, Feyrer et al. 2003, Mager et al. 2004, Slater and Baxter 2014, Hammock et al. 2019). Nobriga (2002) found that the smallest Delta Smelt larvae consumed mostly copepod nauplii and copepodites, with larger larvae (~20 mm) switching to mostly adult copepods, primarily *Eurytemora affinis* and *Pseudodiaptomus forbesi*, and cyclopoid copepods. Slater and Baxter (2014) showed selection for *E. affinis* and *P. forbesi* extending well into the juvenile life stage during summer. During the summer *P. forbesi* adults became the major food item with *Limnoithona* spp. (a small, introduced cyclopoid copepod) also consumed. The smaller *Limnoithona* spp. was generally avoided but was consumed when at extremely high densities and other prey were limited. Selectivity analyses for April through July showed that Delta Smelt often showed positive selection for both *E. affinis* and *P. forbesi*. Types of prey consumed is also a function of regional differences in availability (IEP-MAST 2015, Hammock et al. 2017). Laboratory feeding experiments show similar patterns with Delta Smelt larvae transitioning to larger copepod prey as fish mature, with selection for larger calanoid copepods *E. affinis* and *P. forbesi* over smaller zooplankton life stages and species (e.g., *Limnoithona* spp.) (Sullivan et al. 2016). Adult Delta Smelt consume larger zooplankton prey including mysids and larval fish (IEP-MAST 2015, Hammock et al. 2017).

The pelagic food web, on which Delta Smelt depends, has undergone radical changes over the last ~50 years (Brown et al. 2016 a, b). Slater and Baxter (2014) summarized the substantial changes in the prey of Delta Smelt from the 1970s through the 1990s as a result of numerous species introductions.

Most notable changes in the upper San Francisco Estuary and the Sacramento-San Joaquin Delta occurred in the late 1980s with new zooplankton species, notably copepods, and the reduction in primary and secondary production following invasion of the bivalve *Potamocorbula amurensis* (see Clam Section). The decline of the Delta Smelt population has been attributed in part to changes in the food web (Bennett and Moyle 1996, Moyle 2002, Sommer et al. 2007, Mac Nally et al. 2010, IEP-MAST 2015, Moyle et al. 2016). It has been hypothesized that Delta Smelt are food limited during the spring through fall periods (Bennett and Moyle 1996, Bennett 2005).

Our prediction for this report is that during wet years when fall X2 is located in the Suisun Region, availability of food will increase resulting in greater feeding success by Delta Smelt. Slater et al. (2019) analyzed diet information from 1,962 Delta Smelt collected from 2011-2017 including several life stages to expand the knowledge base and evaluate this prediction (Table INTRO 3). Specifically, Slater et al. (2019) assessed results for diet composition by number and weight and gut fullness. Monthly sample collections were grouped into three bins (June-July, August-November, and December-May) to allow comparisons among life stages (young juvenile, older juvenile and adult) and between field surveys. Gut fullness was compared across years, regions, and salinity groups (salinity groups: <0.5 [freshwater], 0.5-6.0 [low salinity zone], >6.0) using Kruskal-Wallis tests. A Conover-Iman post-hoc test was applied to test for significance differences among the pairwise comparisons when the Kruskal-Wallis test was significant. Slater et al. (2019) used least squares linear regression to assess the relationship between gut fullness and condition factor. Multivariate analyses were conducted to examine patterns in zooplankton consumption by Delta Smelt from stomach content data among years, salinity groups, and seasons using PRIMER 7. Fish with empty stomachs (N = 66) were not included in the multivariate analyses. A square-root transformation was applied to mean diet by percent number, and mean diet by percent weight data, and Bray-Curtis similarity matrices (abundance) were produced. One-

way Analysis of Similarity (ANOSIM) to test for statistical differences in diet between year, seasons, and salinity groups. An ANOSIM R value close to zero indicates no difference between groups, an R value close to 1 indicates strong differences between groups, and the maximum value of 1 is the greatest level of dissimilarity possible (Clarke and Warwick 2001, Sampson et al. 2009). Non-metric Multidimensional Scaling (NMDS) on the Bray-Curtis matrices was used to illustrate diet overlap. Similarity Percentage (SIMPER procedure) was used to determine which prey categories contributed to the differences in diets. See Slater et al. (2019) for detailed methods and additional results.

Cyclopoid and calanoid copepods were the numerically dominant prey items in the guts of Delta Smelt during most years, salinity ranges and seasons (Tables 13-15), with cladocerans dominant in the December-May period in freshwater. In terms of prey mass in the diet of Delta Smelt, cyclopoid and calanoid copepods were dominant for young juveniles during the summer period. Diet by weight for juveniles was more variable as the fish matured with larger prey items such as mysids, amphipods and larval fishes important during several years and the latter being important during the spring period only (Tables 16-18). Similar to diet by number, diet by weight had a pattern of generally consistent prey use among years within seasons and variable among salinity regions, with increased contribution of larger prey (Tables 16-18). Cladocerans were important in freshwater in some years for adults but not older juveniles (Table 17 and 18).

Table 13. Diet by percent number of major prey categories in stomachs of Delta Smelt collected in salinity <0.5 for months June-August (J-A), September-November (S-N), and December-May (D-M) among years 2011-2017.

[Each year includes December from the preceding year (e.g., 2012 includes December 2011-May 2012). Number of stomachs with food present in parentheses. No samples (NS) occurred in some years and months reported as blank fields. Fields are shaded darker green with higher percentage values. * Identifies samples collected by USFWS in 2017]

Prey Category	J-A 2011 (42)	J-A 2012 (66)	J-A 2013 (38)	J-A 2014 (47)	J-A 2015 (15)	J-A 2016 (0)	J-A 2017 (2)	J-A 2017* (4)	S-N 2011 (59)	S-N 2012 (16)	S-N 2013 (2)	S-N 2014 (3)	S-N 2015 (1)	S-N 2016 (0)	S-N 2017 (0)	S-N 2017* (53)	D-M 2012 (286)	D-M 2013 (99)	D-M 2014 (81)	D-M 2015 (73)	D-M 2016 (26)	D-M 2017 (51)	
Calanoid copepods																							
<i>Eurytemora</i> spp.	0.0	0.0	0.0	0.0	0.1		0.7	0.0	0.0	0.0	0.0	0.0	0.0		0.0	4.1	3.6	3.7	1.0	14.2	2.3		
<i>Pseudodiaptomus</i> spp.	71.3	63.0	52.7	59.0	61.5		92.8	22.0	63.5	52.4	18.6	70.2	65.3		63.4	7.4	8.0	6.7	8.5	5.6	0.9		
<i>Sinocalanus doerrii</i>	1.7	10.6	5.4	5.9	5.8		0.0	4.1	5.0	8.1	3.5	3.6	2.0		0.0	43.4	26.7	36.2	1.3	54.5	10.8		
<i>Acartiella sinensis</i>	0.2	0.0	0.0	0.2	0.0		0.0	4.6	15.4	1.4	0.0	0.0	0.0		6.6	0.3	0.0	0.0	0.0	0.0	0.0		
<i>Tortanus</i> spp.	0.0	0.0	0.0	0.0	0.0		0.0	0.0	0.0	0.0	0.0	0.0	0.0		0.0	0.0	0.0	0.0	0.0	0.0	0.0		
Other calanoids	17.4	7.3	8.9	8.0	6.5		0.0	2.3	3.2	0.5	0.0	3.6	26.7		8.3	6.1	11.7	4.9	5.0	10.2	5.4		
Cyclopoid copepods																							
<i>Limnoithona</i> spp.	0.6	11.4	4.7	13.7	9.2		0.0	42.7	2.4	4.2	20.9	16.7	5.0		0.2	0.0	0.0	0.0	0.4	0.2	0.2		
<i>Acanthocyclops</i> spp.	0.0	0.0	0.0	0.0	0.0		0.0	0.0	0.0	0.0	0.0	0.0	0.0		0.0	2.5	5.8	5.0	3.3	2.0	1.2		
Other cyclopoids	1.0	1.2	0.1	1.4	4.6		0.7	6.9	1.2	3.2	17.4	2.4	0.0		1.1	10.5	11.9	24.7	35.1	5.5	6.3		
Other Copepods																							
Harpacticoids	1.1	0.1	7.1	0.4	0.1		0.0	10.1	1.2	4.6	29.1	0.0	0.0		1.4	1.8	0.2	0.2	0.9	0.6	0.0		
Copepod nauplii	2.9	0.3	15.9	2.6	0.3		0.0	2.8	1.5	1.6	8.1	0.0	0.0		0.2	0.0	0.0	0.0	0.2	0.1	0.0		
Cladocerans	0.8	2.5	0.9	6.0	6.4		4.6	2.8	1.0	0.0	0.0	2.4	0.0		0.9	13.2	28.9	14.6	41.9	6.1	68.3		
Mysids	0.0	0.2	0.1	0.1	0.0		1.3	0.9	1.9	20.6	0.0	0.0	0.0		0.1	0.1	0.1	0.0	0.0	0.0	0.0		
Amphipods																							
<i>Gammarus</i> spp.	0.0	0.0	0.0	0.0	0.0		0.0	0.0	0.0	0.5	0.0	0.0	0.0		13.4	0.3	0.2	0.7	0.2	0.4	0.6		
<i>Corophium</i> spp.	0.0	0.1	0.0	0.0	2.2		0.0	0.5	1.7	1.8	1.2	0.0	1.0		2.6	9.1	0.4	0.6	0.3	0.1	0.7		
Unidentified amphipods	0.0	0.0	0.0	0.0	0.0		0.0	0.0	0.0	0.0	0.0	0.0	0.0		0.4	0.1	0.0	0.1	0.0	0.0	0.1		
Cumaceans	0.0	0.0	0.0	0.0	0.0		0.0	0.0	0.2	0.0	0.0	1.2	0.0		0.0	0.2	0.0	0.4	0.1	0.0	0.4		
Fish	0.0	0.0	0.0	0.0	0.0		0.0	0.0	0.0	0.0	0.0	0.0	0.0		0.0	0.2	0.0	0.1	0.0	0.0	0.5		
Other	3.0	3.2	4.1	2.7	3.4		0.0	0.5	1.9	1.2	1.2	0.0	0.0		1.3	0.7	2.6	2.2	1.8	0.5	2.0		
Total	100	100	100	100	100		100	100	100	100	100	100	100		100	100	100	100	100	100	100	100	

Table 14. Diet by percent number of major prey categories in stomachs of Delta Smelt collected in salinity 0.5-6 for months June-August (J-A), September-November (S-N), and December-May (D-M) among years 2011-2017 (Table from Slater et al. 2019). [Each year includes December from the preceding year (e.g., 2012 includes December 2011-May 2012). Number of stomachs with food present in parentheses. No samples (NS) occurred in some years and months reported as blank fields. Fields are shaded darker green with higher percentage values. * Identifies samples collected by USFWS in 2017]

Prey Category	Diet by percent number (%N)																					
	J-A 2011 (24)	J-A 2012 (21)	J-A 2013 (32)	J-A 2014 (88)	J-A 2015 (0)	J-A 2016 (0)	J-A 2017 (10)	J-A 2017* (17)	S-N 2011 (61)	S-N 2012 (17)	S-N 2013 (6)	S-N 2014 (75)	S-N 2015 (4)	S-N 2016 (7)	S-N 2017 (1)	S-N 2017* (19)	D-M 2012 (177)	D-M 2013 (71)	D-M 2014 (83)	D-M 2015 (52)	D-M 2016 (8)	D-M 2017 (3)
Calanoid copepods																						
<i>Eurytemora</i> spp.	0.0	0.0	6.2	0.0			0.0	0.0	0.3	0.1	0.0	0.0	0.0	0.0	25.0	5.5	3.8	9.9	61.8	14.1	47.7	47.6
<i>Pseudodiaptomus</i> spp.	4.3	20.7	31.2	9.7			90.0	1.1	11.2	67.2	3.6	42.9	78.7	19.9	75.0	3.7	1.1	0.4	1.5	2.2	1.6	0.2
<i>Sinocalanus doerrii</i>	0.0	1.2	0.0	0.0			0.2	0.0	0.1	0.0	0.0	0.0	0.0	0.0	0.0	0.0	0.1	0.0	0.1	0.0	0.0	0.0
<i>Acartiella sinensis</i>	12.9	1.1	2.3	8.7			0.2	1.9	8.5	10.1	15.9	6.2	1.3	8.0	0.0	1.0	3.3	0.3	1.9	0.4	0.3	0.2
<i>Tortanus</i> spp.	1.2	0.2	0.2	0.0			0.3	0.0	0.2	0.3	0.0	0.0	0.0	0.2	0.0	0.0	0.0	0.1	0.0	0.0	0.0	0.0
Other calanoids	0.0	1.0	1.0	1.3			2.3	0.1	0.3	0.9	0.6	4.2	14.1	0.3	0.0	1.4	0.4	0.7	9.2	3.5	4.6	4.1
Cyclopoid copepods																						
<i>Limnoithona</i> spp.	76.8	73.7	52.0	65.8			5.6	90.2	4.5	8.1	69.9	38.9	4.0	64.4	0.0	51.6	1.4	0.2	0.6	3.7	12.0	0.2
<i>Acanthocyclops</i> spp.	0.0	0.0	1.0	0.0			0.0	0.0	3.8	0.0	0.0	0.0	0.0	0.0	0.0	4.5	19.7	19.4	5.2	16.7	7.4	10.9
Other cyclopoids	0.0	0.0	1.1	14.0			0.6	5.1	66.7	0.9	8.0	5.9	1.2	4.6	0.0	28.4	36.1	26.1	13.0	48.3	9.5	18.8
Other Copepods																						
Harpacticoids	3.2	0.1	0.2	0.1			0.1	0.7	0.3	0.4	0.4	0.2	0.0	1.1	0.0	0.7	1.1	0.9	0.2	0.2	0.5	0.0
Copepod nauplii	0.3	0.4	0.2	0.1			0.0	0.2	0.0	0.0	0.0	0.0	0.0	0.0	0.0	0.4	0.0	0.2	0.3	0.1	0.6	0.0
Cladocerans	0.1	0.0	0.3	0.1			0.1	0.0	2.5	0.0	0.0	0.0	0.3	0.3	0.0	1.4	27.0	38.2	1.2	8.6	9.6	14.2
Mysids	0.4	0.8	1.6	0.1			0.1	0.0	0.5	3.4	1.4	0.2	0.2	0.2	0.0	0.1	0.3	0.3	0.0	0.0	0.1	0.0
Amphipods																						
<i>Gammarus</i> spp.	0.0	0.1	0.0	0.0			0.0	0.0	0.0	0.4	0.0	0.0	0.0	0.3	0.0	0.0	0.1	0.3	0.1	0.0	0.3	0.0
<i>Corophium</i> spp.	0.3	0.1	0.2	0.0			0.4	0.2	0.8	7.4	0.0	0.1	0.2	0.5	0.0	0.1	3.5	0.4	0.2	0.1	2.6	0.2
Unidentified amphipods	0.1	0.0	0.0	0.0			0.0	0.0	0.0	0.1	0.0	0.0	0.0	0.0	0.0	0.0	0.0	0.1	0.0	0.0	0.1	0.0
Cumaceans	0.3	0.0	0.2	0.0			0.0	0.1	0.0	0.1	0.0	0.7	0.0	0.2	0.0	0.2	1.4	1.6	1.9	0.5	3.0	1.7
Fish	0.0	0.1	0.1	0.0			0.0	0.0	0.0	0.0	0.0	0.0	0.0	0.0	0.0	0.0	0.3	0.4	0.9	0.0	0.0	0.0
Other	0.3	0.5	1.7	0.1			0.2	0.4	0.3	0.5	0.1	0.7	0.0	0.0	0.0	0.9	0.2	0.5	1.7	1.5	0.1	2.1
Total	100	100	100	100			100	100	100	100	100	100	100	100	100	100	100	100	100	100	100	100

Table 15. Diet by percent number of major prey categories in stomachs of Delta Smelt collected in salinity >6 for months June-August (J-A), September-November (S-N), and December-May (D-M) among years 2011-2017 (Table from Slater et al. 2019). [Each year includes December from the preceding year (e.g., 2012 includes December 2011-May 2012). Number of stomachs with food present in parentheses. No samples (NS) occurred in some years and months reported as blank fields. Fields are shaded darker green with higher percentage values. * Identifies samples collected by USFWS in 2017].

Prey Category	Diet by percent number (%N)																					
	J-A 2011 (3)	J-A 2012 (0)	J-A 2013 (30)	J-A 2014 (5)	J-A 2015 (0)	J-A 2016 (0)	J-A 2017 (15)	J-A 2017* (0)	S-N 2011 (5)	S-N 2012 (1)	S-N 2013 (2)	S-N 2014 (1)	S-N 2015 (0)	S-N 2016 (0)	S-N 2017 (0)	S-N 2017* (2)	D-M 2012 (74)	D-M 2013 (0)	D-M 2014 (12)	D-M 2015 (0)	D-M 2016 (3)	D-M 2017 (3)
Calanoid copepods																						
<i>Eurytemora</i> spp.	0.0		0.0	0.0			0.0		0.0	0.0	0.0	0.0				0.0	2.0		42.6		85.5	78.2
<i>Pseudodiaptomus</i> spp.	3.7		0.8	0.0			0.1		6.3	0.0	4.3	0.0				0.0	0.3		0.1		0.0	0.0
<i>Sinocalanus doerrii</i>	0.0		0.0	0.0			0.0		0.1	0.0	0.0	0.0				0.0	0.1		0.0		0.0	0.0
<i>Acartiella sinensis</i>	18.5		0.4	0.0			0.1		21.6	0.0	6.4	0.0				0.1	2.4		2.2		0.0	0.0
<i>Tortanus</i> spp.	3.7		3.3	11.1			0.2		1.0	0.0	14.9	69.2				0.0	0.6		2.1		0.0	0.0
Other calanoids	0.0		0.1	0.0			0.0		0.0	0.0	0.0	11.5				0.0	0.9		2.3		2.7	8.2
Cyclopoid copepods																						
<i>Limnoithona</i> spp.	3.7		89.4	0.0			86.5		3.1	100.0	63.8	3.8				91.1	2.5		12.1		0.9	0.4
<i>Acanthocyclops</i> spp.	0.0		0.0	0.0			0.0		1.2	0.0	0.0	0.0				0.0	12.6		6.0		4.2	2.7
Other cyclopoids	0.0		4.4	5.6			12.2		26.3	0.0	0.0	0.0				8.6	55.2		21.1		1.8	8.0
Other Copepods																						
Harpacticoids	3.7		0.2	0.0			0.2		0.2	0.0	8.5	0.0				0.0	2.0		0.5		0.0	0.0
Copepod nauplii	0.0		0.2	0.0			0.3		0.0	0.0	0.0	0.0				0.1	0.1		0.5		0.3	0.1
Cladocerans	0.0		0.0	0.0			0.0		35.0	0.0	0.0	0.0				0.0	19.1		1.2		0.0	0.0
Mysids	7.4		0.1	0.0			0.0		0.0	0.0	2.1	3.8				0.0	0.2		0.0		0.0	0.0
Amphipods																						
<i>Gammarus</i> spp.	0.0		0.0	0.0			0.0		0.0	0.0	0.0	0.0				0.0	0.0		0.1		0.0	0.0
<i>Corophium</i> spp.	25.9		0.1	16.7			0.1		4.4	0.0	0.0	0.0				0.0	0.3		0.6		2.7	0.1
Unidentified amphipods	0.0		0.0	16.7			0.0		0.1	0.0	0.0	0.0				0.0	0.0		0.0		0.0	0.0
Cumaceans	33.3		0.2	5.6			0.0		0.7	0.0	0.0	3.8				0.0	1.3		2.5		1.8	0.1
Fish	0.0		0.1	0.0			0.0		0.0	0.0	0.0	0.0				0.0	0.2		0.0		0.0	0.0
Other	0.0		0.6	44.4			0.3		0.1	0.0	0.0	7.7				0.0	0.2		6.2		0.0	2.0
Total	100		100	100			100		100	100	100	100				100	100		100		100	100

Table 16. Diet by percent weight of major prey categories in stomachs of Delta Smelt collected in salinity <0.5 for months June-August (J-A), September-November (S-N), and December-May (D-M) among years 2011-2017 (Table from Slater et al. 2019). [Each year includes December from the preceding year (e.g., 2012 includes December 2011-May 2012). Number of stomachs with food present in parentheses. No samples (NS) occurred in some years and months reported as blank fields. Fields are shaded darker blue with higher percentage values. * Identifies samples collected by USFWS in 2017].

Prey Category	Diet by percent weight (%W)																						
	J-A 2011 (42)	J-A 2012 (66)	J-A 2013 (38)	J-A 2014 (47)	J-A 2015 (15)	J-A 2016 (0)	J-A 2017 (2)	J-A 2017* (4)	S-N 2011 (59)	S-N 2012 (16)	S-N 2013 (2)	S-N 2014 (3)	S-N 2015 (1)	S-N 2016 (0)	S-N 2017 (0)	S-N 2017* (53)	D-M 2012 (286)	D-M 2013 (99)	D-M 2014 (81)	D-M 2015 (73)	D-M 2016 (26)	D-M 2017 (51)	
Calanoid copepods																							
<i>Eurytemora</i> spp.	0.0	0.0	0.0	0.0	0.1		0.1	0.0	0.0	0.0	0.0	0.0	0.0			0.0	2.4	2.4	2.1	0.6	6.8	1.1	
<i>Pseudodiaptomus</i> spp.	69.2	71.5	65.0	56.1	64.0		65.6	32.9	43.7	2.8	8.7	43.0	81.6			1.3	6.1	7.8	6.2	10.0	4.0	0.6	
<i>Sinocalanus doerrii</i>	4.7	17.7	11.4	15.3	9.2		0.0	9.5	4.7	0.7	15.6	14.3	4.0			0.0	44.9	34.1	43.0	2.1	64.4	9.8	
<i>Acartiella sinensis</i>	0.8	0.0	0.0	0.6	0.0		0.0	12.1	15.9	0.1	0.0	0.0	0.0			0.3	0.3	0.0	0.0	0.0	0.0	0.0	
<i>Tortanus</i> spp.	0.0	0.0	0.0	0.0	0.0		0.0	0.0	0.0	0.0	0.0	0.0	0.0			0.0	0.0	0.1	0.0	0.0	0.0	0.0	
Other calanoids	17.2	3.8	7.0	6.9	4.6		0.0	2.0	1.1	0.0	0.0	6.8	13.2			0.1	4.2	9.3	3.6	5.9	8.5	3.7	
Cyclopoid copepods																							
<i>Limnoithona</i> spp.	0.1	1.6	0.6	2.8	1.3		0.0	8.2	0.2	0.0	7.1	5.3	0.8			0.0	0.0	0.0	0.0	0.0	0.0	0.0	
<i>Acanthocyclops</i> spp.	0.0	0.0	0.0	0.0	0.0		0.0	0.0	0.0	0.0	0.0	0.0	0.0			0.0	1.5	4.1	3.3	3.0	1.3	0.6	
Other cyclopoids	1.4	0.7	0.1	1.2	4.7		0.4	7.6	0.7	0.2	22.8	4.5	0.0			0.0	4.5	6.4	6.9	27.0	2.6	2.4	
Other Copepods																							
Harpacticoids	1.1	0.1	5.9	0.4	0.1		0.0	8.0	0.4	0.1	41.8	0.0	0.0			0.0	0.7	0.1	0.1	0.5	0.2	0.0	
Copepod nauplii	0.3	0.0	1.4	0.2	0.0		0.0	0.2	0.0	0.0	1.2	0.0	0.0			0.0	0.0	0.0	0.0	0.0	0.0	0.0	
Cladocerans	0.9	1.8	0.9	6.6	4.6		2.8	2.6	0.2	0.0	0.0	3.8	0.0			0.0	8.3	20.2	10.1	34.3	3.8	35.8	
Mysids	0.0	0.6	0.6	2.0	0.0		31.2	9.7	30.6	93.8	0.0	0.0	0.0			0.1	1.9	4.4	0.6	0.1	0.0	1.6	
Amphipods																							
<i>Gammarus</i> spp.	0.0	0.0	0.0	0.0	0.0		0.0	0.0	0.0	1.1	0.0	0.0	0.0			91.4	4.9	4.2	8.4	4.9	6.2	8.9	
<i>Corophium</i> spp.	0.0	0.1	0.0	0.0	1.6		0.0	6.8	0.8	0.8	0.9	0.0	0.5			5.5	9.0	3.9	3.0	1.9	1.1	7.5	
Unidentified amphipods	0.0	0.0	0.0	0.0	0.0		0.0	0.0	0.0	0.0	0.0	0.0	0.0			1.2	1.4	0.1	1.2	0.2	0.0	0.2	
Cumaceans	0.0	0.0	0.0	0.0	0.0		0.0	0.0	0.8	0.0	0.0	22.3	0.0			0.0	0.9	0.1	2.3	0.9	0.2	1.7	
Fish	0.0	0.0	0.0	0.0	0.0		0.0	0.0	0.0	0.0	0.0	0.0	0.0			0.0	7.8	1.2	3.8	0.0	0.0	20.3	
Other	4.2	2.0	7.0	7.9	9.9		0.0	0.4	0.9	0.2	1.8	0.0	0.0			0.1	1.3	1.7	5.5	8.3	0.8	5.7	
Total	100	100	100	100	100		100	100	100	100	100	100	100			100	100	100	100	100	100	100	

Table 17. Diet by percent weight of major prey categories in stomachs of Delta Smelt collected in salinity 0.5-6 for months June-August (J-A), September-November (S-N), and December-May (D-M) among years 2011-2017 (Table from Slater et al. 2019). [Each year includes December from the preceding year (e.g., 2012 includes December 2011-May 2012). Number of stomachs with food present in parentheses. No samples (NS) occurred in some years and months reported as blank fields. Fields are shaded darker blue with higher percentage values. * Identifies samples collected by USFWS in 2017].

Prey Category	Diet by percent weight (%W)																					
	J-A 2011 (24)	J-A 2012 (21)	J-A 2013 (32)	J-A 2014 (88)	J-A 2015 (0)	J-A 2016 (0)	J-A 2017 (10)	J-A 2017* (17)	S-N 2011 (61)	S-N 2012 (17)	S-N 2013 (6)	S-N 2014 (75)	S-N 2015 (4)	S-N 2016 (7)	S-N 2017 (1)	S-N 2017* (19)	D-M 2012 (177)	D-M 2013 (71)	D-M 2014 (83)	D-M 2015 (52)	D-M 2016 (8)	D-M 2017 (3)
Calanoid copepods																						
<i>Eurytemora</i> spp.	0.0	0.0	6.8	0.0			0.0	0.0	0.3	0.0	0.0	0.0	0.0	0.0	19.7	8.2	2.5	4.0	19.6	13.7	26.2	35.5
<i>Pseudodiaptomus</i> spp.	11.0	50.9	54.9	25.3			94.4	5.8	20.3	24.0	7.6	48.4	73.6	39.4	80.3	9.5	1.2	0.2	0.6	3.9	1.3	0.3
<i>Sinocalanus doerrii</i>	0.0	3.4	0.1	0.0			0.2	0.0	0.3	0.0	0.0	0.0	0.0	0.0	0.0	0.0	0.2	0.0	0.1	0.0	0.0	0.0
<i>Acartiella sinensis</i>	44.1	3.7	5.5	34.4			0.4	12.6	21.3	4.9	50.4	16.2	2.7	23.0	0.0	3.6	5.2	0.2	1.7	0.9	0.4	0.4
<i>Tortanus</i> spp.	11.2	2.4	1.8	0.0			1.5	0.0	1.3	0.4	0.0	0.0	0.0	1.4	0.0	0.3	0.1	0.2	0.1	0.0	0.0	0.0
Other calanoids	0.0	1.4	0.8	1.5			1.2	0.2	0.2	0.2	0.7	3.6	8.6	0.3	0.0	1.2	0.4	0.4	2.0	4.3	2.2	1.8
Cyclopoid copepods																						
<i>Limnoithona</i> spp.	19.4	16.8	9.4	19.3			0.7	48.0	0.8	0.3	14.9	7.6	0.6	13.6	0.0	16.3	0.2	0.0	0.0	0.7	1.1	0.0
<i>Acanthocyclops</i> spp.	0.0	0.0	1.3	0.0			0.0	0.0	4.9	0.0	0.0	0.0	0.0	0.0	0.0	9.8	16.0	8.1	2.5	22.1	4.6	12.9
Other cyclopoids	0.0	0.0	0.7	15.9			0.5	10.7	37.6	0.2	8.2	4.4	0.8	3.8	0.0	25.3	11.0	4.2	2.4	26.0	2.6	8.0
Other Copepods																						
Harpacticoids	3.4	0.1	0.2	0.1			0.0	1.5	0.2	0.1	0.4	0.2	0.0	1.0	0.0	0.9	0.5	0.2	0.1	0.1	0.2	0.0
Copepod nauplii	0.0	0.0	0.0	0.0			0.0	0.0	0.0	0.0	0.0	0.0	0.0	0.0	0.0	0.1	0.0	0.0	0.0	0.0	0.0	0.0
Cladocerans	0.1	0.0	0.2	0.1			0.0	0.0	4.2	0.0	0.0	0.0	0.3	0.4	0.0	3.8	25.9	18.9	0.7	10.4	7.0	21.6
Mysids	5.0	10.1	8.2	2.1			0.8	0.4	6.2	67.2	14.7	9.7	13.4	0.9	0.0	6.2	1.8	7.0	0.8	0.5	7.0	0.0
Amphipods																						
<i>Gammarus</i> spp.	0.0	0.3	0.0	0.1			0.0	0.0	1.3	0.4	1.0	0.9	0.0	6.6	0.0	0.8	2.2	4.3	0.6	0.9	5.6	0.0
<i>Corophium</i> spp.	0.6	0.1	1.9	0.1			0.2	16.1	0.4	1.8	1.3	0.3	0.0	7.6	0.0	9.2	5.0	1.9	1.0	1.6	24.9	0.1
Unidentified amphipods	0.0	0.0	0.0	0.0			0.0	0.0	0.0	0.0	0.0	0.0	0.0	0.0	0.0	0.0	0.2	0.1	0.2	0.0	1.3	0.0
Cumaceans	4.0	0.0	2.7	0.5			0.0	2.9	0.3	0.3	0.0	7.8	0.0	2.1	0.0	3.7	9.8	5.6	7.7	5.9	15.8	17.8
Fish	0.0	5.8	0.3	0.0			0.0	0.0	0.0	0.0	0.0	0.0	0.0	0.0	0.0	0.0	17.4	44.3	56.3	0.0	0.0	0.0
Other	1.1	5.1	5.2	0.5			0.2	1.6	0.5	0.3	0.8	0.9	0.0	0.0	0.0	1.2	0.5	0.3	3.5	8.8	0.0	1.6
Total	100	100	100	100			100	100	100	100	100	100	100	100	100	100	100	100	100	100	100	100

Table 18. Diet by percent weight of major prey categories in stomachs of Delta Smelt collected in salinity >6 for months June-August (J-A), September-November (S-N), and December-May (D-M) among years 2011-2017 (Table from Slater et al. 2019). [Each year includes December from the preceding year (e.g., 2012 includes December 2011-May 2012). Number of stomachs with food present in parentheses. No samples (NS) occurred in some years and months reported as blank fields. Fields are shaded darker blue with higher percentage values. * Identifies samples collected by USFWS in 2017].

Prey Category	Diet by percent weight (%W)																						
	J-A	J-A	J-A	J-A	J-A	J-A	J-A	J-A	S-N	S-N	S-N	S-N	S-N	S-N	S-N	S-N	S-N	D-M	D-M	D-M	D-M	D-M	D-M
	2011	2012	2013	2014	2015	2016	2017	2017*	2011	2012	2013	2014	2015	2016	2017	2017*	2012	2013	2014	2015	2016	2017	
	(3)	(0)	(30)	(5)	(0)	(0)	(15)	(0)	(5)	(1)	(2)	(1)	(0)	(0)	(0)	(2)	(74)	(0)	(12)	(0)	(3)	(3)	
Calanoid copepods																							
<i>Eurytemora</i> spp.	0.0		0.1	0.0			0.0		0.0	0.0	0.0	0.0				0.0	1.4		24.4		64.6	80.7	
<i>Pseudodiaptomus</i> spp.	1.2		2.1	0.0			0.3		7.1	0.0	3.6	0.0				0.0	0.4		0.1		0.0	0.1	
<i>Sinocalanus doerrii</i>	0.0		0.0	0.0			0.1		0.1	0.0	0.0	0.0				0.0	0.1		0.0		0.0	0.0	
<i>Acartiella sinensis</i>	8.2		1.5	0.0			0.7		31.7	0.0	6.3	0.0				1.5	4.2		4.3		0.0	0.0	
<i>Tortanus</i> spp.	4.8		28.0	3.0			0.7		4.5	0.0	37.8	30.6				0.0	2.6		12.0		0.0	0.0	
Other calanoids	0.0		0.1	0.0			0.1		0.0	0.0	0.0	2.0				0.0	0.9		1.4		1.4	5.1	
Cyclopoid copepods																							
<i>Limnoithona</i> spp.	0.1		25.6	0.0			59.1		0.4	100.0	4.7	0.0				72.0	0.3		1.7		0.1	0.1	
<i>Acanthocyclops</i> spp.	0.0		0.0	0.0			0.0		1.0	0.0	0.0	0.0				0.0	11.5		6.0		3.5	4.5	
Other cyclopoids	0.0		5.0	0.3			32.8		13.0	0.0	0.0	0.0				26.4	24.0		7.7		0.8	4.8	
Other Copepods																							
Harpacticoids	0.5		0.3	0.0			0.6		0.1	0.0	2.5	0.0				0.0	1.1		0.3		0.0	0.0	
Copepod nauplii	0.0		0.0	0.0			0.1		0.0	0.0	0.0	0.0				0.0	0.0		0.0		0.0	0.0	
Cladocerans	0.0		0.0	0.0			0.0		33.9	0.0	0.0	0.0				0.0	21.1		1.4		0.0	0.1	
Mysids	11.4		5.7	0.0			0.0		0.0	0.0	45.0	13.2				0.0	6.8		0.0		0.0	0.0	
Amphipods																							
<i>Gammarus</i> spp.	0.0		0.0	0.0			0.0		0.0	0.0	0.0	0.0				0.0	0.0		0.2		0.0	0.0	
<i>Corophium</i> spp.	9.3		0.7	6.6			4.6		2.7	0.0	0.0	0.0				0.0	1.2		11.4		16.4	0.4	
Unidentified amphipods	0.0		0.0	17.6			0.0		0.0	0.0	0.0	0.0				0.0	0.2		0.4		0.0	0.0	
Cumaceans	64.6		3.6	4.0			0.4		4.9	0.0	0.0	7.8				0.0	10.5		22.3		13.2	2.1	
Fish	0.0		11.4	0.0			0.0		0.0	0.0	0.0	0.0				0.0	13.5		0.0		0.0	0.0	
Other	0.0		15.9	68.5			0.6		0.6	0.0	0.0	46.5				0.0	0.2		6.4		0.0	2.2	
Total	100		100	100			100		100	100	100	100				100	100		100		100	100	

There was a significant difference in calculated stomach fullness (%) among years ($P < 0.003$; Figure 85). Fullness was significantly lower in 2013 compared to 2011, 2012, 2014, 2015, and 2017, but other pairwise combinations of years were not significantly different. There was a significant difference in stomach fullness among salinity regions ($P = 0.014$, Figure 85), with significant differences between <0.5 and $0.5-6$ salinity ($P = 0.009$) and also <0.5 and >6 salinity ($P = 0.0497$), but not between $0.5-6$ and >6 salinity ($P = 0.661$). These results indicate fullness was lower in freshwater compared to the low salinity zone and >6 . Seasonal fullness was significantly different among June-August, September-November, and December-May ($P = 0.0004$, Figure 85). There were significant differences between June-August and September-November ($P = 0.0004$) and significant differences between September-November and December-May ($P = 0.0002$) due to higher September-November fullness, but there was not a significant difference between June-August and December-May ($P = 0.761$). Thus, stomach fullness was higher in September-November compared to the other periods. Fullness (%) differed among hour of collection ($P < 0.0001$, Figure 85). Most of the 55 post hoc pairwise comparisons were significantly different, except between 4 PM and 6 AM or 7 AM or between 8 AM and 9 AM, 10 AM, 11 AM, or 1 PM and between 12 PM and 2 PM (Figure 85). Overall, fullness was lowest in the morning and late afternoon and tended to be high in late morning and early afternoon (Figure 85). The extreme high mean value at 3 PM was a small sample size ($n=17$) with the stomach contents all large prey of amphipods, mysids, cumaceans, and larval fish.

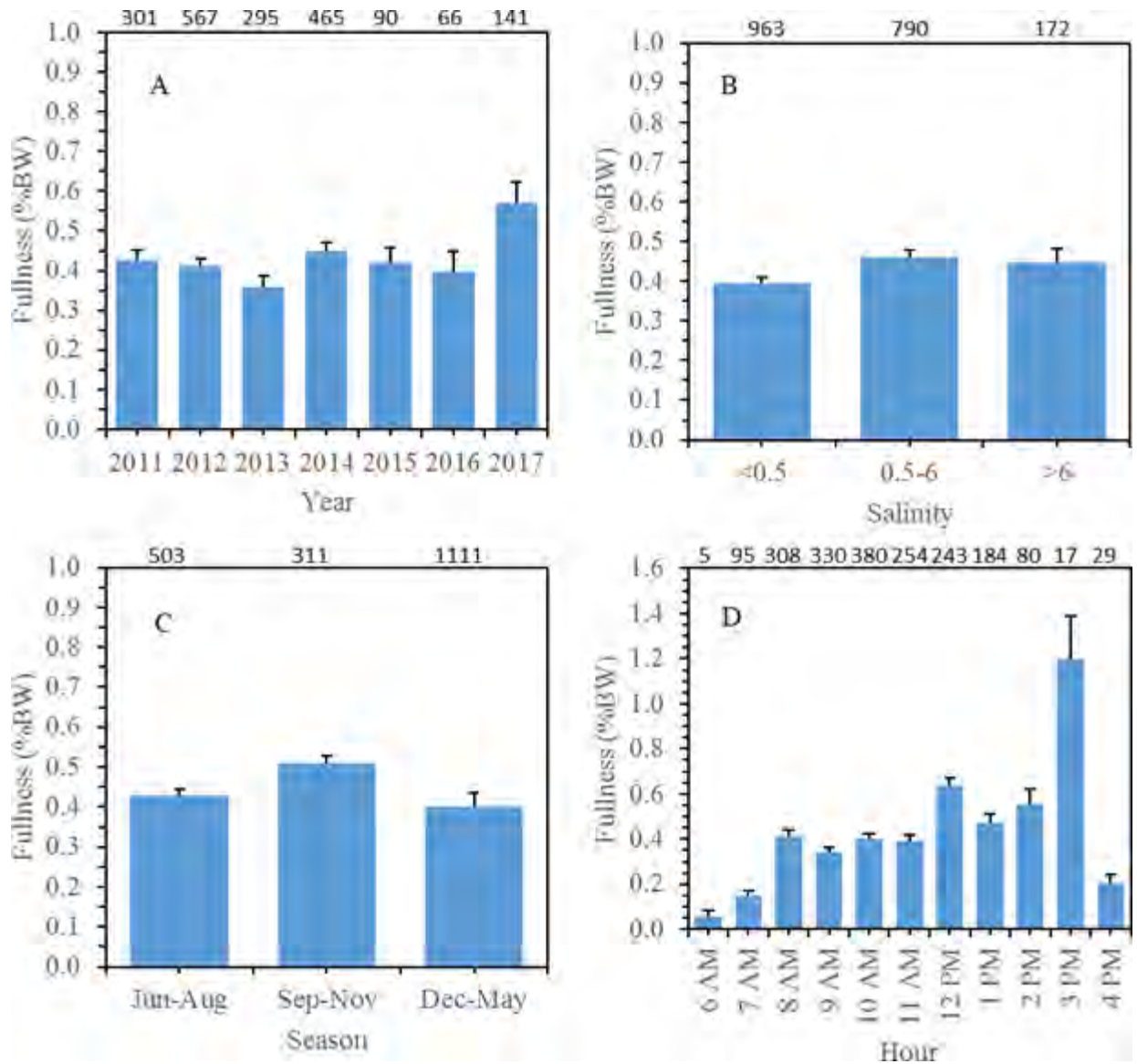


Figure 85. Mean (\pm SE) Delta Smelt gut fullness (% body weight, BW) by A) year, B) salinity, C) season, and D) hour of collection during 2011-2017 CDFW and 2017 USFWS Surveys. Sample size included above each bar.

There was no statistically significant relationship between stomach fullness and fish condition (Figure 86). Slater et al. (2019) calculated Fulton’s condition factor for each fish as: $K = (W / L^3) * 100,000$, where W is body weight (g) and L is fork length (mm). The lack of a relationship indicates that stomach fullness of a fish on the day of capture is not a reliable predictor of the general nutritional status of the fish as measured by Fulton’s condition factor.

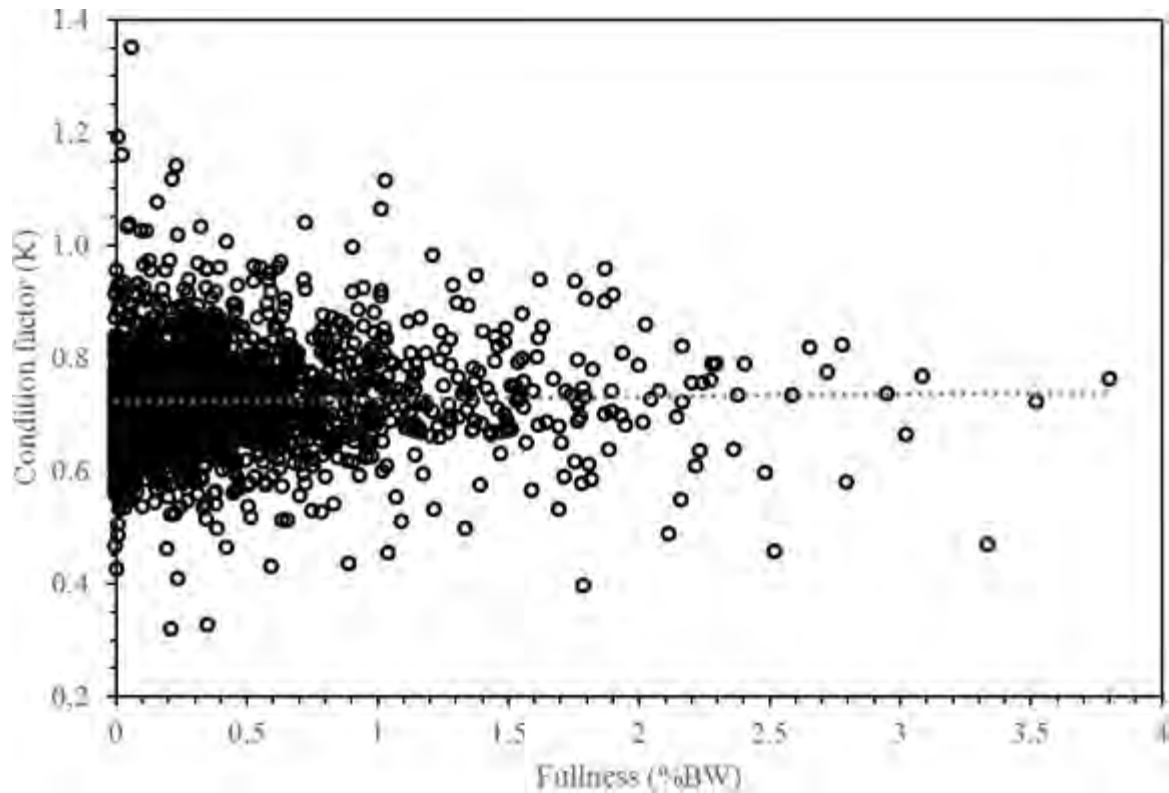


Figure 86. Condition factor plotted against gut fullness (% body weight, BW) for Delta Smelt (N = 1925). A linear regression (dotted line) was not statistically significant.

The multivariate analyses revealed patterns among seasons and salinity groups for diet by number and diet by weight. There were no statistically significant differences between years or collecting agency. One-way ANOSIM statistical global-test showed a significant difference in diet by percent number between groups of months (seasons) ($R = 0.357$, $P = 0.001$) and salinity ranges ($R = 0.332$, $P = 0.001$).

December-May percent by number diets were strongly dissimilar from June-August ($R = 0.623$) and September-November ($R = 0.546$), whereas diets were similar among June-August and September-November ($R = -0.035$). Results for percent by weight were similar. December-May diet by weight was strongly dissimilar from June-August ($R = 0.586$) and September-November ($R = 0.395$), whereas diets were similar among June-August and September-November ($R = -0.015$). This indicates that the December-May (adult) diet was distinctly different from the June-August (young juvenile) and September-November (juvenile) diet. This likely results from both a seasonal change in the zooplankton community in winter and the ability of larger fish to consume larger organisms.

For salinity ranges, results for percent number appeared to follow a gradient, with significant differences among all pairs with the greatest difference between salinity <0.5 and >6 ($R = 0.6$, $P = 0.001$), with decreasing difference between salinity <0.5 and 0.5-6 ($R = 0.281$, $P = 0.001$) and lastly salinity >6 and 0.5-6 ($R = 0.19$, $P = 0.008$). As for season, results were similar for percent weight. There was a significant difference between salinity ranges in diet by weight for all groups (<0.5 and 0.5-6 $R = 0.248$, 0.5-6 and > 6 $R = 0.271$, and <0.5 and >6 $R = 0.546$). These results show differences in diet depending on the location of a fish along the salinity gradient. This suggests that the prey field a fish encounters depends on the differing responses of prey species to salinity and other environmental factors.

The dissimilarity among salinity groups was due mostly to changing percentages of *P. forbesi* and *Limnoithona* spp. in the diet, with other prey (*S. doerrii*, other cyclopoids, cladocerans, *E. affinis*) contributing differently among salinity groups. The dissimilarity among seasons was similar in many ways, but the importance of *E. affinis* was high relative to other species for dissimilarity between December-May and the other seasons.

Conclusion

Overall, the data do not support our prediction that during wet years feeding success will increase, resulting in greater food consumption by Delta Smelt. Gut fullness was high in the wet year of 2017 but neither the wet year of 2011 nor 2017 had gut fullness statistically higher than most of the intervening drier years. The lack of a relationship between gut fullness and condition of a fish on the day of capture indicates that gut fullness is not a reliable predictor of the general nutritional status of the fish. Delta Smelt had relatively consistent and broad diets within seasons and salinities across years, but diets did vary significantly among salinities and seasons within years. These data suggest that the diet must be considered in the context of the dynamics of the prey populations and the ability of Delta Smelt to exploit them. Single metrics of Delta Smelt prey availability likely do not capture this complexity.

Delta Smelt Range and Distribution

Several previous analyses of the range and distribution of Delta Smelt have relied on determination of the centroid (median) of the population along the main axis of the estuary (Dege and

Brown 2004, Sommer and Meija 2013, Brown et al. 2014). We conducted similar analyses using data for the STN and FMWT for the post-POD period (2003-2017). We calculated median distance from the Golden Gate for fish captures at STN and FMWT index stations weighted by number of fish captured at each station and also determined mean X2 position (Figures 87 and 88). Sample sizes were small (<20) for the STN in 2015 and 2016 and for the FMWT in 10 of 15 years. Also, in 2015 and 2016, all the fish captured in the STN survey were caught at a single station. This type of centroid analysis has a number of shortcomings. Use of the index stations is a problem because the northern Delta is excluded as are other locations outside of the sampling frame. The current low levels of catch also make measures of central tendency highly suspect, because of low probability of detection.

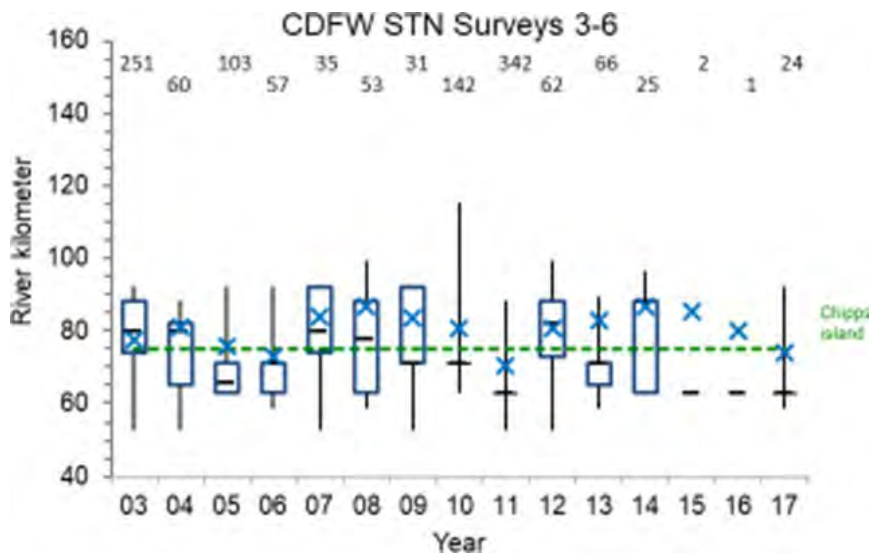


Figure 87. Delta Smelt distribution in river kilometers in the upper Estuary from Summer Townet Survey (STN) catch at index stations in July and August during 2003-2017. Line in bar is the median, upper bar is the 75% percentile and lower bar in the 25th percentile, upper and lower whiskers are the maximum and minimum, respectively. Blue "X" indicates average location of X2 during July and August and the green line indicates the location of Chipps Island. Numbers across top of figure is annual catch.

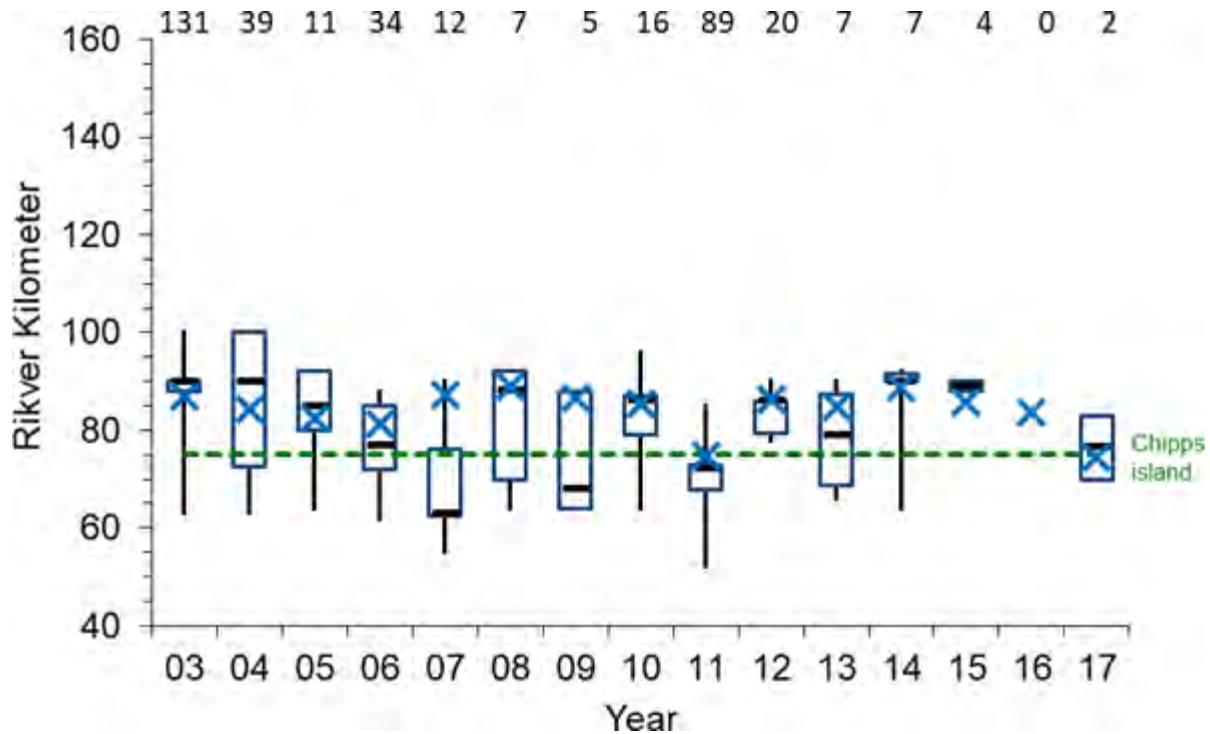


Figure 88. Delta Smelt distribution in river kilometers in the upper Estuary from Fall Midwater Trawl Survey (FMWT) catch at index stations in September and October during 2003-2017. Line in bar is the median, upper bar is the 75% percentile and lower bar in the 25th percentile, upper and lower whiskers are the maximum and minimum, respectively. Blue "X" indicates average location of X2 during September-October and the green line indicates the location of Chipps Island. Numbers across top of figure is catch.

Patterns of distribution were clearer when median position of fish was plotted against X2 position (Figures 89 and 90). After excluding 2015 and 2016, because fish were only collected at a single station and catches were extremely low, STN centroids showed a significant relationship to X2 position (DIST 3). When X2 was more seaward in wetter years, the center of the Delta Smelt distribution also moved seaward; however, the overall range of the population showed no clear pattern between wet and dry years (Figure 87).

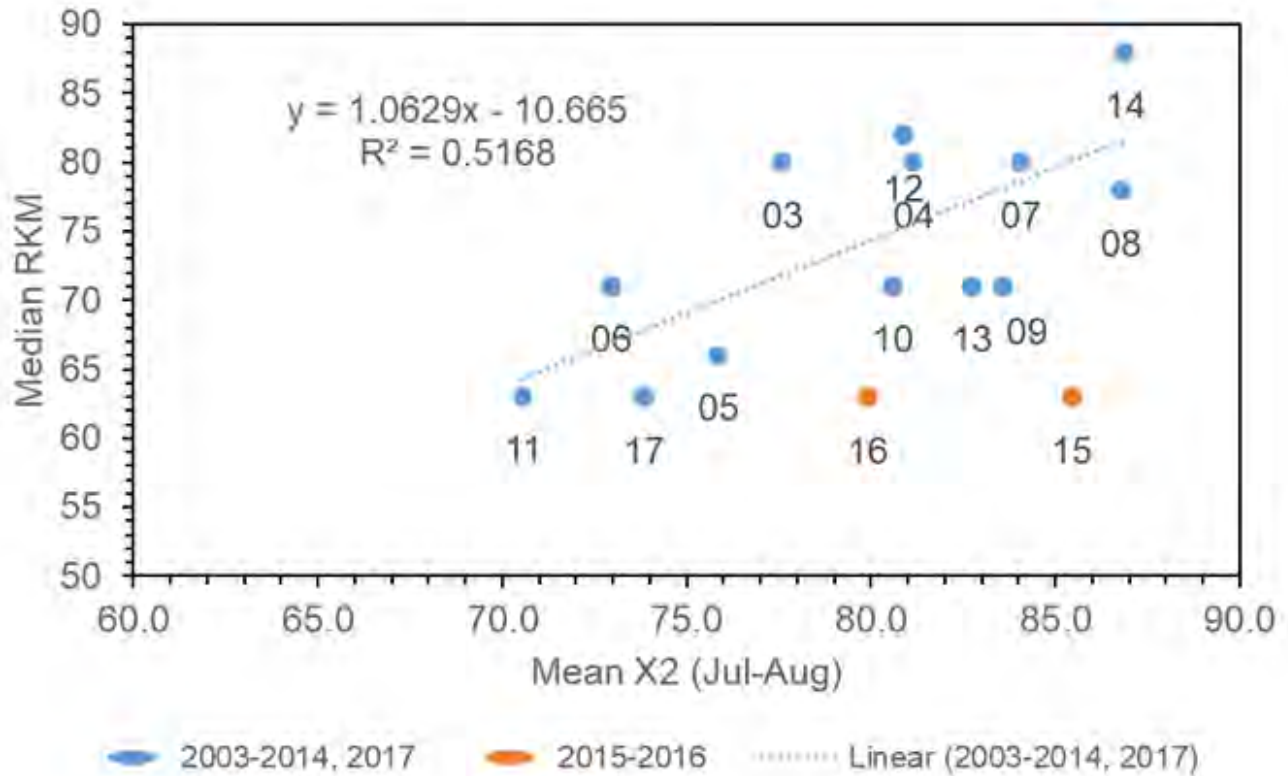


Figure 89. Scatterplot of median Delta Smelt distribution based on river kilometers in the upper Estuary from Summer Towner Survey (STN) CPUE at index stations and the average location of X2 during July and August. Points are labeled with year. Simple linear regression included years 2003-2014 and 2017. Years 2015 and 2016 were excluded from correlation as only 1 station was positive for catch in both years, which was Station 602 (at RKM 63) for both years.

FMWT centroids did not show a strong relationship to X2 (Figure 90) when all years were considered. The years 2007 and 2009 appeared to be outliers and excluding those years resulted in a significant relationship; however, there is no reasonable biological argument for excluding those years. As for the STN, the range of the population showed no clear pattern with water year type (Figure 88) and the small sample sizes make any conclusions questionable.

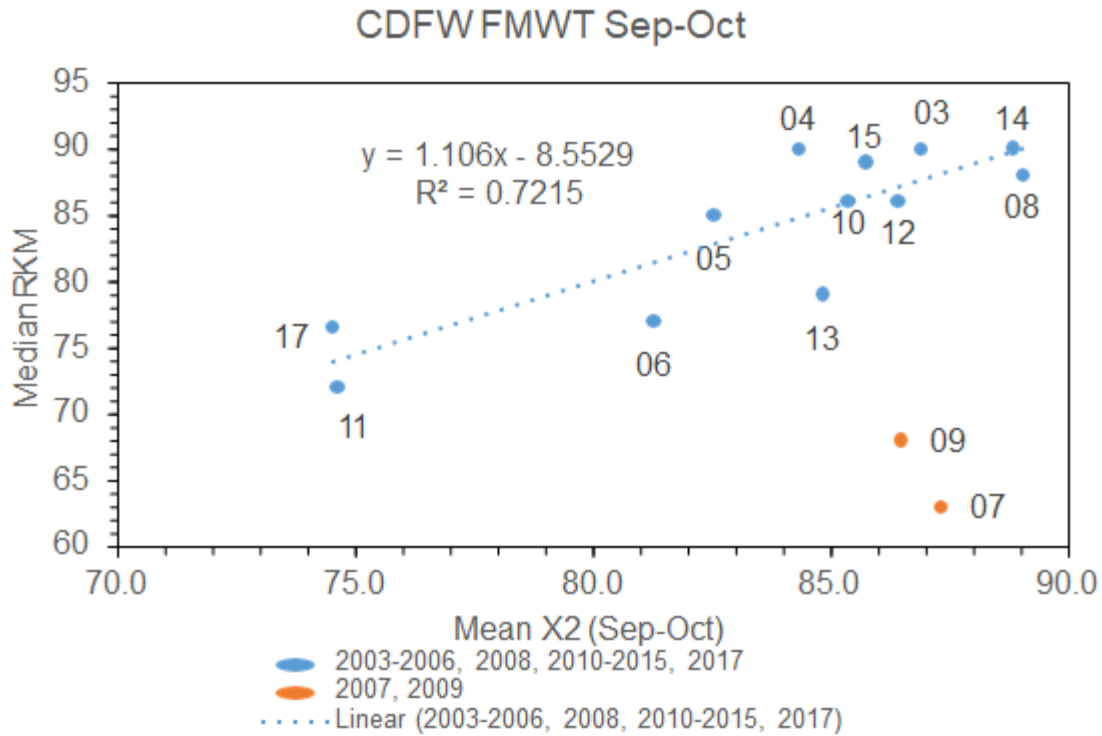


Figure 90. Scatterplot of median Delta Smelt distribution based on river kilometers in the upper Estuary from Fall Midwater Trawl Survey (FMWT) catch at index stations and the average location of X2 during September-October. Points are labeled with year. Simple linear correlation included years 2003-2006, 2008, 2010-2015 and 2017. Years 2007 and 2009 were excluded from correlation as outliers and no catch occurred in 2016 for this period.

The current conceptual models (Figures 8 and 9) suggest that in drier years the LSZ is located farther upstream and Delta Smelt habitat is constricted, thus we expect that Delta Smelt distribution will be broader in wet years like 2017 than in dry years. Current IEP fish monitoring programs (20-mm survey, STN, FMWT, and EDSM) sample the upper SFE and provided a fairly complete description of changes in annual Delta Smelt distribution. For example, it is typical for larval and juvenile fish (20-mm Survey) to be present in the Napa River in wet years like 2006, but fish are rarely collected there in dry years like 2013 (Figure DIST 5).

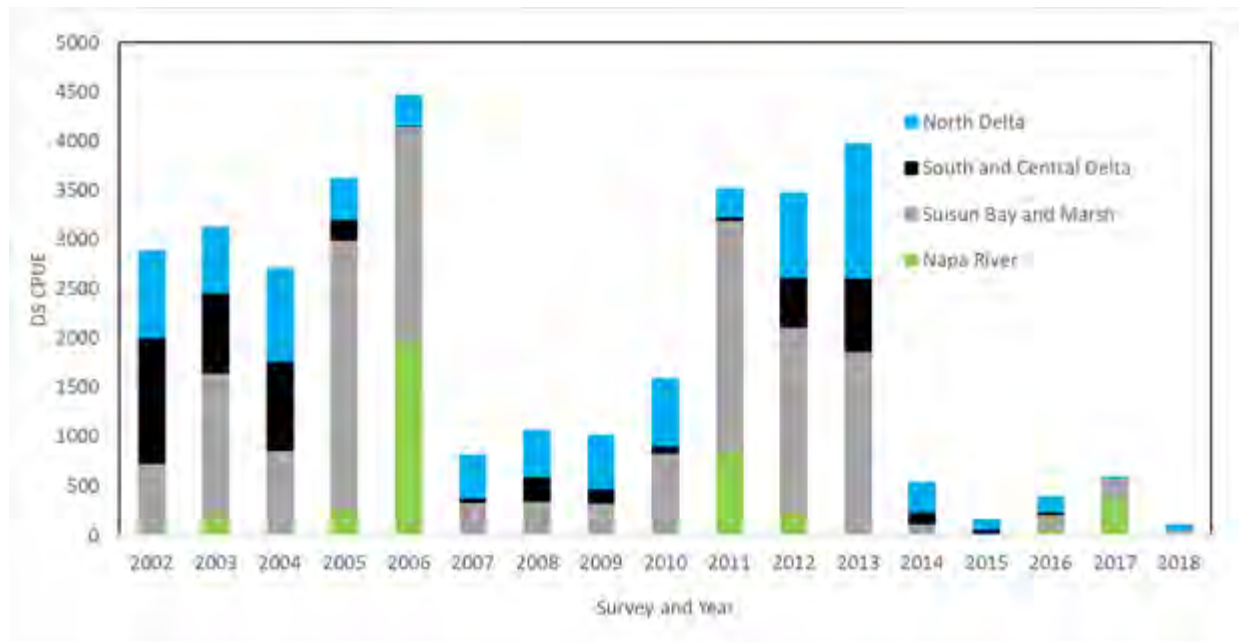


Figure 91. 20-mm Survey Delta Smelt catch per 10,000 m³ (CPUE) since 2002 (post-POD). CPUE summed by region includes only regularly sampled stations, although effort may be slightly inconsistent among years.

In 2017, post-larval Delta Smelt caught in the 20-mm Survey were widely distributed throughout the Estuary but were most heavily concentrated in the Napa River and North Delta (Sacramento Deep Water Ship Channel) from March through May. By June, catches of Delta Smelt in the 20-mm Survey decreased in the Napa River and increased in Suisun Bay and Marsh, such that Delta Smelt were only caught in Suisun Bay in July (Survey 9; DIST 6). The distribution shift out of the North Delta is understood to be a common young juvenile Delta Smelt movement from spawning habitat to rearing habitat (Sommer et al. 2011); however, there are often some Delta Smelt in the North Delta through the summer (Bush 2017). The absence of Delta Smelt in the North Delta is likely related to water temperature (see Dynamic Abiotic Habitat and Life History Diversity sections). It is likely that Delta Smelt moved out of the Napa River coinciding with the encroaching salinity.

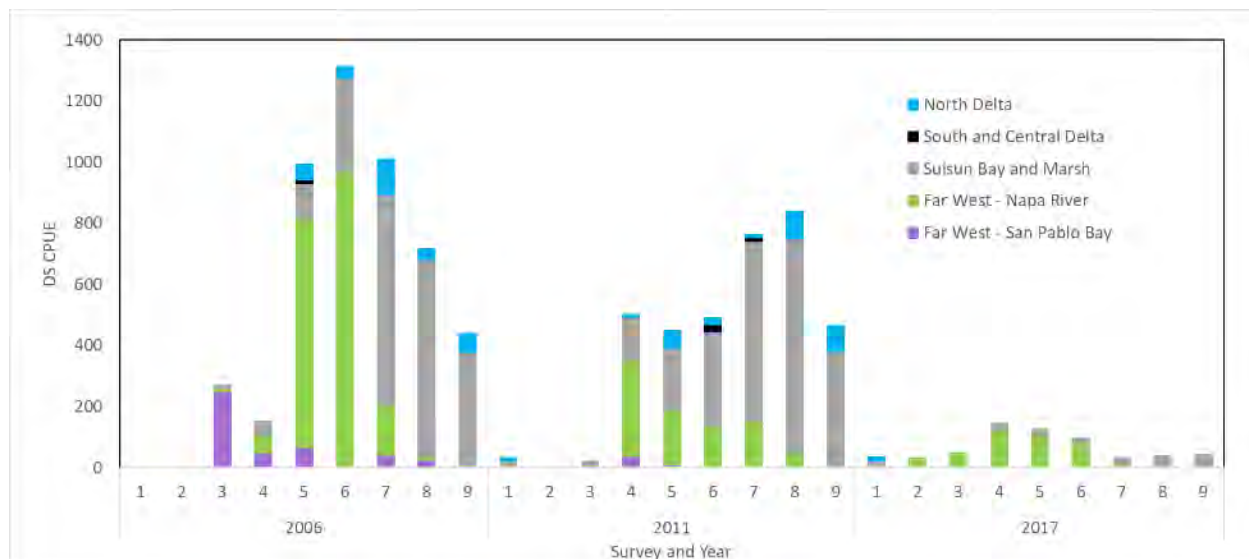


Figure 92. 20-mm Survey Delta Smelt catch per 10,000 m³ (CPUE) in 2006, 2011, and 2017 grouped by region across the upper San Francisco Estuary. CPUE is summed by region and includes regularly sampled index stations and five high-outflow stations (San Pablo Bay). Effort at high-outflow stations may be inconsistent among years.

The low salinity zone shifted upstream into Suisun Bay in early summer, making downstream habitats less suitable for Delta Smelt. Even though abundance was extremely low in both the summer and fall (Summer Townet Survey and Fall Midwater Trawl), Delta Smelt distribution was most heavily concentrated in Suisun Marsh during those months. Similarly, distribution also shifted upstream in the Enhanced Delta Smelt Monitoring program, indicating Delta Smelt moved with the increasing salinity. This shift in Delta Smelt distribution corresponding to the shift in the location of the low salinity zone is as predicted based on their life history (Brown et al. 2014; IEP-MAST 2015). A similar shift occurred in both 2006 and 2011 in the 20-mm Survey (Figure 91). However, it is difficult to compare 2006, 2011, and 2017 distributions because the numbers of Delta Smelt captured in the low salinity zone in 2017 were substantially lower than what was observed in 2011 or 2006 based on the CDFW Surveys. We also cannot compare EDSM distributions because the EDSM was not conducted prior to 2017.

Although the center of Delta Smelt distribution in the summer (Figure 89) seems to track the low salinity zone, Delta Smelt can also be found year-round in perennially freshwater areas such as the Cache Slough Complex (Bush 2017, Sommer et al. 2011, Merz et al. 2011). Delta Smelt presumably remain year-round in the Cache Slough Complex due to the region's complex bathymetry, relatively high turbidity, and low entrainment risk relative to the south Delta (Brown et al. 2014; Frantzich et al.

2018). However, the Cache Slough Complex exposes Delta Smelt to other risks. That area can experience high summer temperatures that have been found to cause lethal and non-lethal stress for Delta Smelt (Jeffries et al. 2016, Komoroske et al. 2014, Frantzich et al. 2018, Dynamic Abiotic Habitat section) and, in 2012 and 2013, Delta Smelt that were caught in that area showed the most severe signs of contaminant exposure (Hammock et al. 2015) as well as overall poor health (Figure 82; Health Metric section).

Despite some stressors, the Cache Slough Complex, and particularly the Sacramento Deep Water Ship Channel, was considered a refuge for Delta Smelt because the fish were consistently caught there in historical but sporadic surveys, especially in dry years when downstream habitat is less suitable (Wang 2007, Mahardja et al. 2019). To better understand their use of the region, routine spring sampling (20-mm Survey) commenced in 2008, and young-of-the-year catch occurs regularly there since the addition of those stations (Tempel 2017). Routine sampling during the summer and fall started later, but Delta Smelt were similarly present in those surveys. In 2011, the Cache Slough Complex was highly productive in the spring, producing a large year class that survived through the fall (Figure 93; 2006 data are limited due to additional stations not having been added yet, so we cannot investigate here). The lack of recruitment in this region in 2017 indicates that it became unsuitable for the species. This corresponds to high temperatures during late July and early August of 2017 (Abiotic Habitat section, Appendix 2).

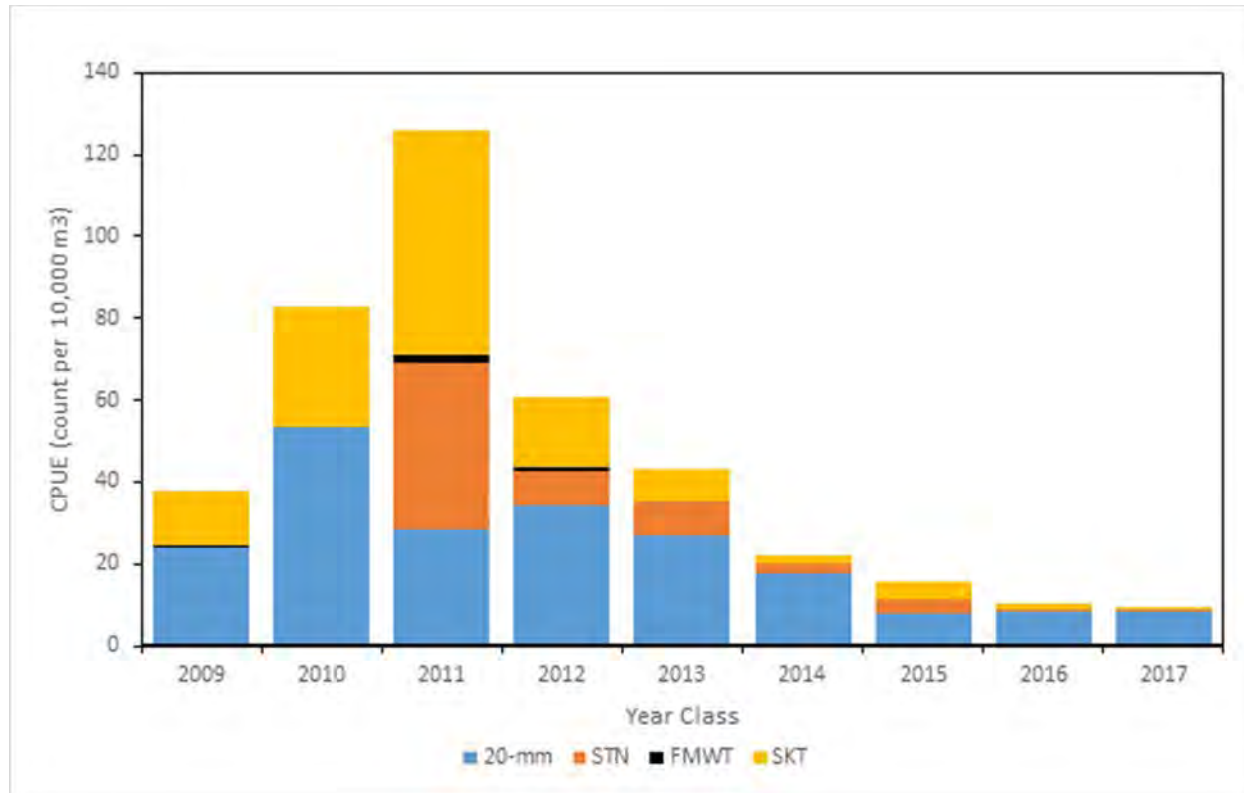


Figure 93. Mean CPUE of Delta Smelt by year class collected by CDFW 20-mm, Summer Towner (STN), Fall Midwater Trawl (FMWT) and Spring Kodiak Trawl during routine surveys at stations in the North Delta (711, 716, 719, and 723). These stations were not sampled by STN in 2008-2011 and FMWT in 2008.

Because of the sparse catches of Delta Smelt in the post-POD years, we consider the data insufficient to reach firm conclusions about the predictions concerning range and distribution of Delta Smelt, especially in the fall. There is some support for the idea that the center of the population is associated with the location of the low-salinity zone in the post-POD years (Figures DIST 1 and 3), but the data are weak in the fall. There is evidence that the northern Delta was poorer habitat in 2017 (Figure 92) compared to the previous wet year of 2011.

Survival and Population Growth

The growth and survival of the Delta Smelt population was evaluated in the context of conditions in 2017 relative to recent years. The FLOAT prediction was that survival in fall 2017 and other wet years would be higher with X2 being centered over Suisun Bay and Marsh compared to survival with X2 farther upstream near the confluence of the Sacramento and San Joaquin Rivers. The extreme flows that occurred in 2017 resulted in mean monthly X2 located downstream of the

confluence below or near Chipps Island (<76 km) through summer and fall with X2 shifting upstream of Chipps Island beginning in November.

To address the prediction, survival of the population was examined by life stage in the fall relative to a previous life stage or several life stages. The sub-sections that follow evaluate survival from spring to summer, summer to fall, and fall to winter, among seasons within 2017, and among years. In recent years the detections of so few Delta Smelt complicate and even prevent regional comparisons by most monitoring elements, so the focus was the population scale, as sampled by the long-term IEP monitoring surveys. An important clarifying point for the following analyses is the term “survival,” which in this report includes several measures including survival indices and population estimates from models. As in the Delta Smelt MAST Report (IEP-MAST 2015), a survival index is simply the ratio of a relative abundance index for a life stage divided by the relative abundance index of a previous life stage of the same year class. This approach has been used in a variety of previous analyses (Miller et al. 2012, IEP-MAST 2015), and while informative, the results should be interpreted cautiously because of potential variability in the individual index scores and the calculated ratios.

“Growth” in this section refers to growth of the population and not of the individual. Population growth is a function of both production of young and survivorship. For an annual fish like Delta Smelt, an increase in annual abundance could be the result of increased production of young and stable survivorship or a similar level of production of young and increased survivorship, or some dynamic shifting of both factors that can vary among years. Since a low number of adults can result in a low number of young produced, favorable environmental conditions might be necessary for both increased production and survival to occur at the same time, allowing the population to increase between successive year classes. The production of young has been examined by abundance indices as stock-recruitment relationships. A recruitment index is similar to the survival index, where annual abundance indices of Delta Smelt are used to examine the ratios of a year class relative to the preceding year class. The survival and recruitment indices were also examined by application of anomaly based approach to examine trends over time. Standardized anomalies from survival indices were calculated as: $(\text{value} - \text{mean}) / \text{SD}$, from the mean and SD (standard deviation) for each period considered.

Spring-to-summer survival index

The ratio of the STN index to 20-mm index (STN/20-mm) for Delta Smelt was used for the spring to summer survival index. The year 2017 was a low survival index for the period of record among the 21 years, but higher than 2012-2013 (Figure 94). The preceding years 2015-2016 were not included (NI) due to STN abundance indices of 0, which suggests low spring to summer survival. The mean (± 1 standard deviation) survival index for the period 1995-2014 and 2017 was 0.28 ± 0.18 . The 2017 survival index anomaly was the 9th most negative, part of a pattern of poor spring survival since 2012, with the exception of 2014 (Figure 95).

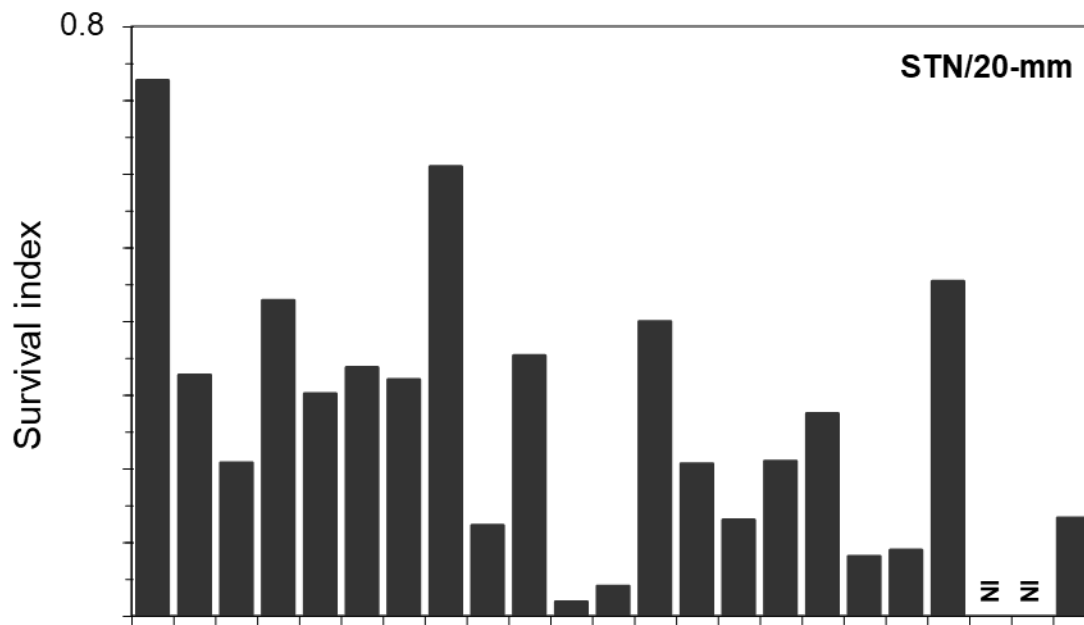


Figure 94. Spring to summer survival index (STN/20-mm) for Delta Smelt based on the ratio of the Summer Townet (STN) to 20-mm Survey (20-mm) relative abundance indices. The STN abundance indices were 0 in 2015 and 2016 and were not included in determination of the survival index.

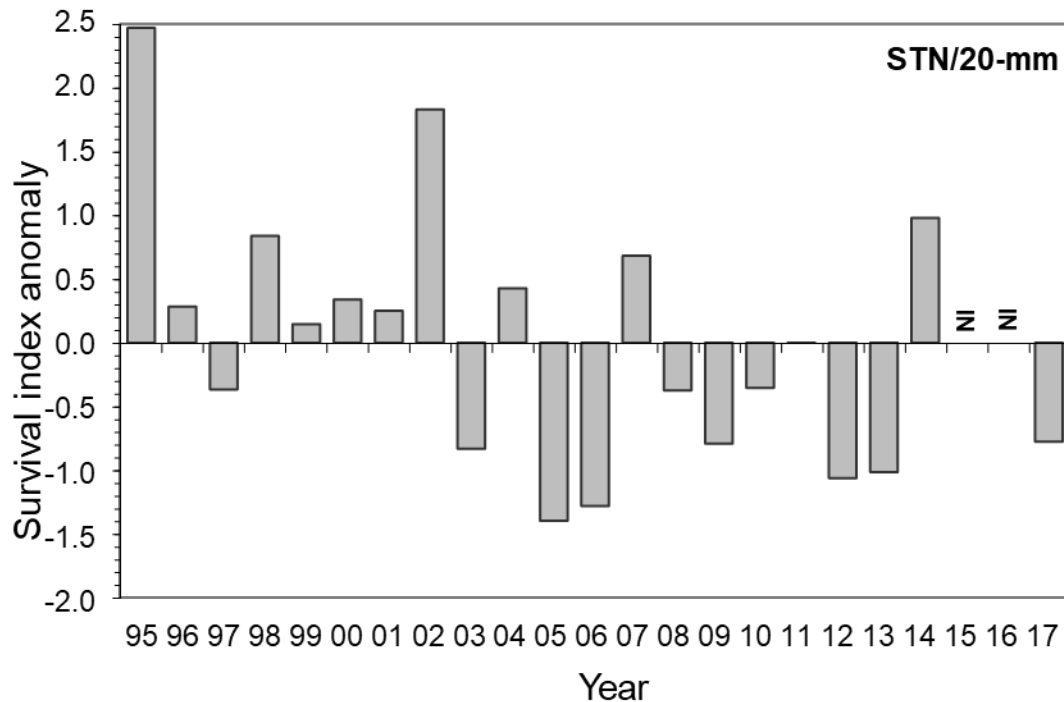


Figure 95. Anomalies of spring to summer survival indices (STN/20-mm) for Delta Smelt based on the ratio of the Summer Townet (STN) to 20-mm Survey (20-mm) relative abundance indices. The STN abundance indices were 0 in 2015 and 2016 and were not included in determination of the survival anomaly.

Summer-to-fall survival index

The ratio of the FMWT index to the STN index (FMWT/STN) for Delta Smelt was used for the summer to fall survival index. Years with missing FMWT (1974 and 1979) or STN surveys (1966-1968) and years with zero STN indices (2015, 2016) were excluded from these analyses. The year 2017 showed one of the lowest survival indices on record (Figure 96). The mean \pm SD survival index over the period 1969 to 2017 was 87.3 ± 73.0 . Compared to previous years, the 2017 survival index anomaly was the 5th most negative, with only 3 pre-POD years (1976, 1978, and 1994) having more negative anomalies (Figure 97).

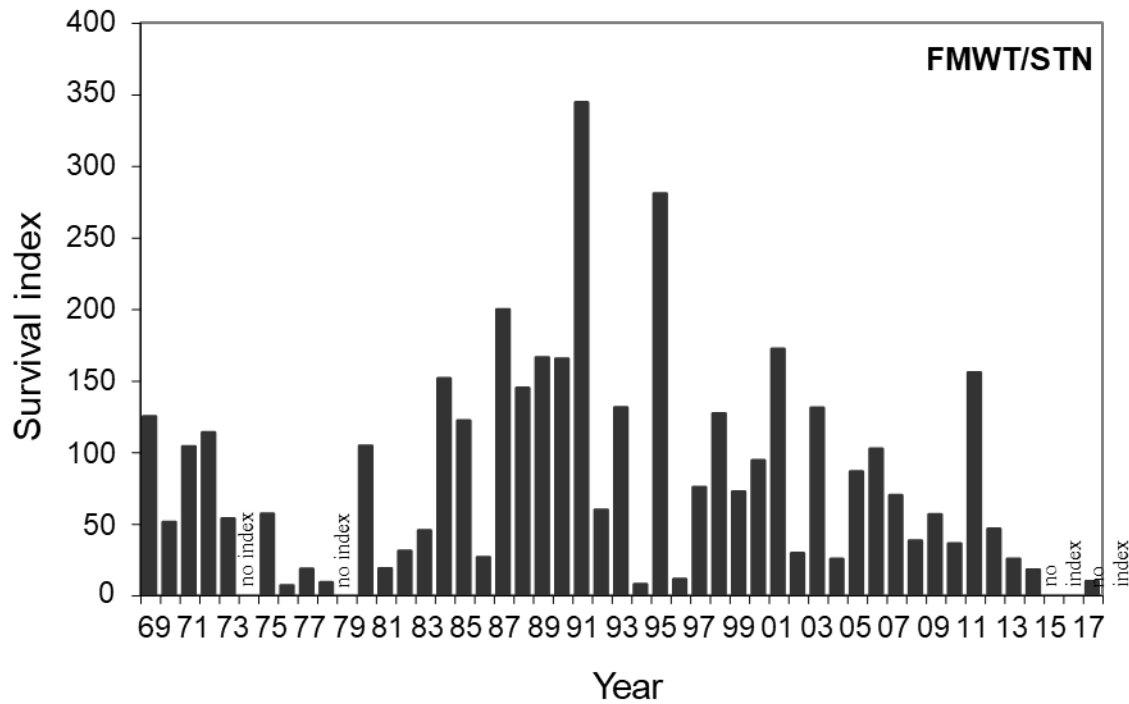


Figure 96. Summer to fall survival index (FMWT/STN) for Delta Smelt based on the ratio of the Fall Midwater Trawl (FMWT) to Summer Tonet (STN) relative abundance indices. The STN abundance indices were 0 in 2015 and 2016 and were not included in determination of the survival index.

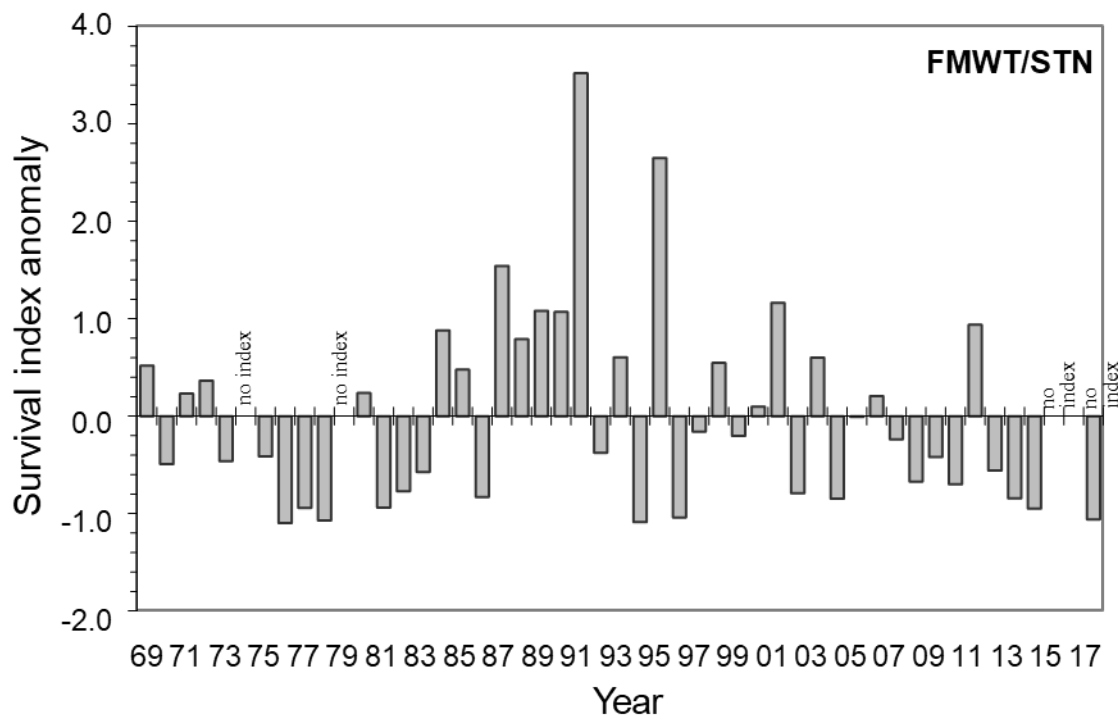


Figure 97. Anomalies of summer to fall survival index (FMWT/STN) for Delta Smelt based on the ratio of the Fall Midwater Trawl (FMWT) to Summer Towner (STN) relative abundance indices. The STN abundance indices were 0 in 2015 and 2016 and were not included in determination of the survival index.

Fall-to-winter survival index

The ratio of the Spring Kodiak Trawl (SKT) index to the FMWT index (SKT/FMWT) for Delta Smelt was used for the fall to winter survival index. This index indicates survival of subadults in the fall into the winter and early spring period of the adult life stages in the following year (i.e., FMWT from year x leads to SKT from year $x+1$). The SKT index is generated from the first 4 monthly surveys, which is usually January-April. A regression between FMWT and SKT relative abundance indices indicates a consistent survival rate of subadults to the adult life stage (Figure 98); however, the relationship is highly dependent on two years (2003 and 2011). The year 2017 was the sixth highest of 14 survival indices (Figure 99). The mean \pm SD survival index over the period 2004 to 2017 was 1.52 ± 1.02 . The 2017 anomaly was positive but was the smallest of positive anomalies in the post-POD period (Figure 100).

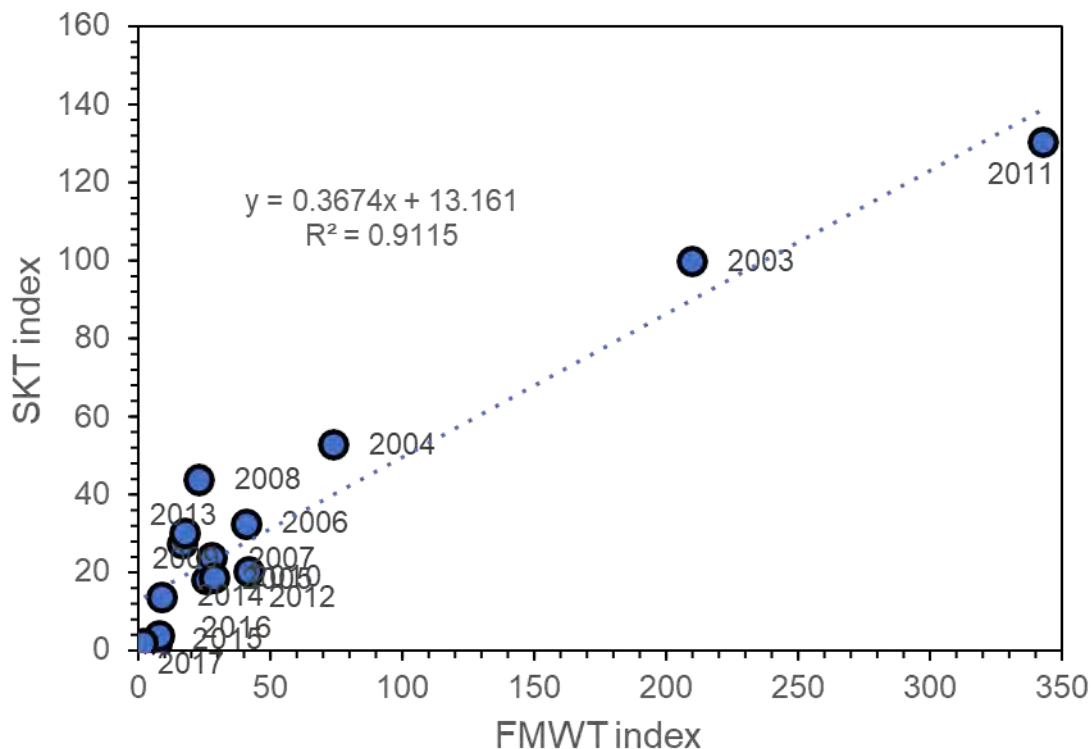


Figure 98. Least squares linear regression ($y = 0.3674x + 13.161$; $R^2 = 0.9115$) of the FMWT and SKT relative abundance indices for Delta Smelt year classes 2003-2017. The year labels correspond to year the fish was

born (FMWT; i.e., 2003 FMWT Index) and extends into the winter and spring of the following year when the adults spawn (SKT; i.e., 2004 SKT index).

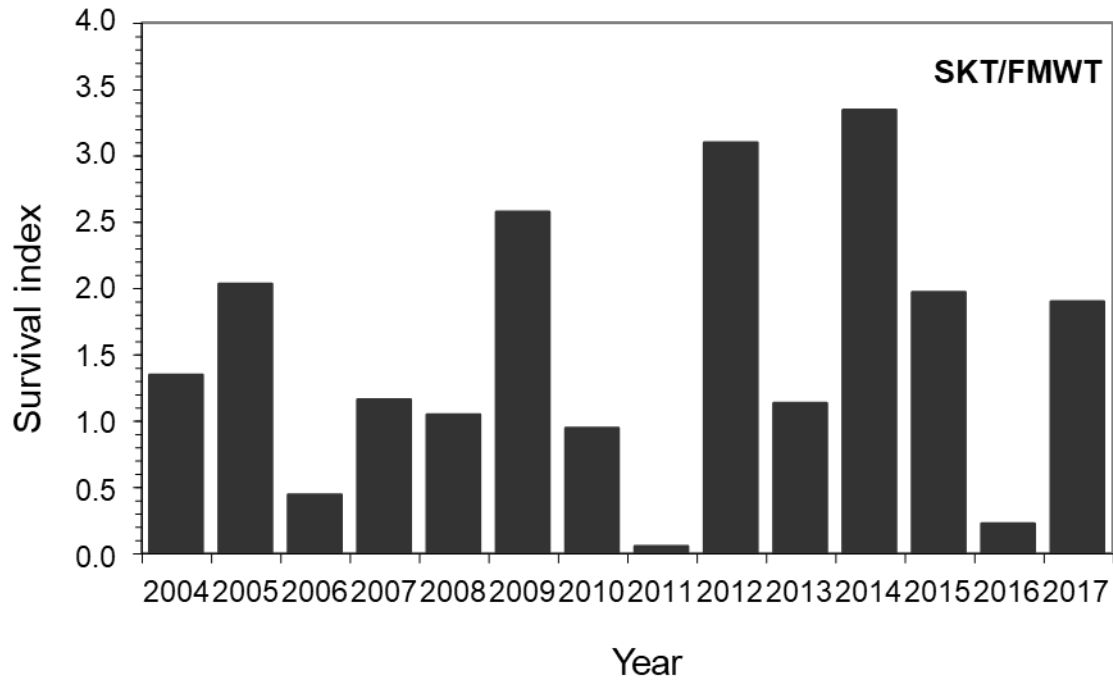


Figure 99. Fall to winter survival index (SKT/FMWT) for Delta Smelt based on the ratio of the Spring Kodiak Trawl (SKT) to Fall Midwater Trawl (FMWT) relative abundance indices. The year labels correspond to year the fish was born (FMWT) and extends into the winter and spring of the following year when the adults spawn (SKT).

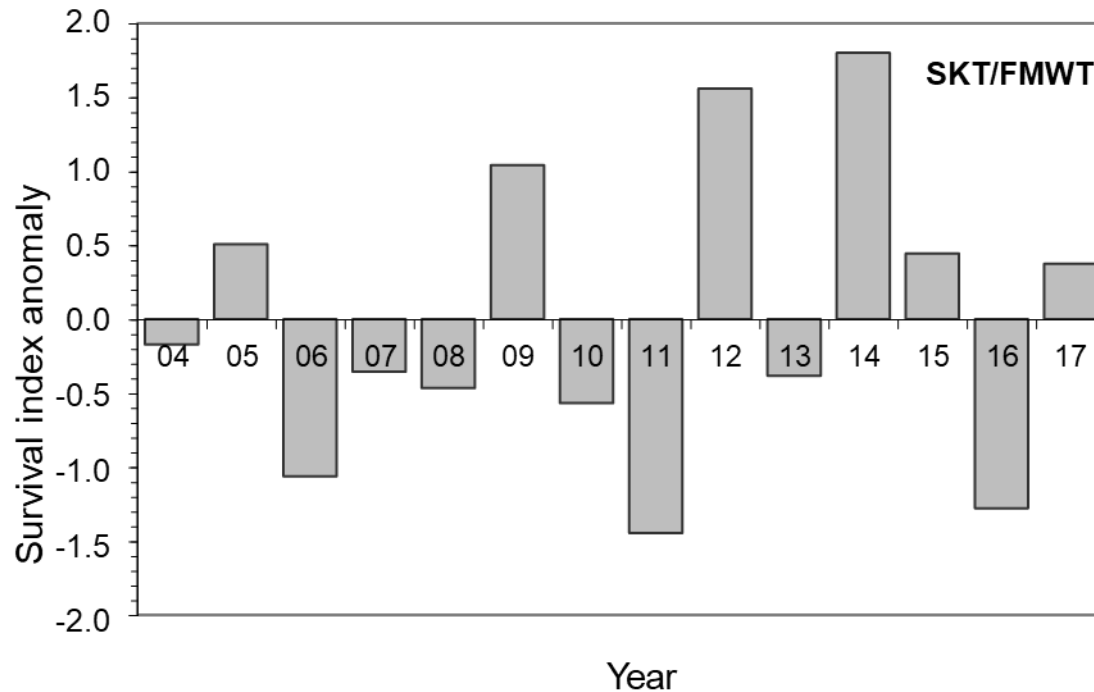


Figure 100. Anomalies of fall to winter survival index (SKT/FMWT) for Delta Smelt based on the ratio of the Spring Kodiak Trawl (SKT) to Fall Midwater Trawl (FMWT) relative abundance indices.

Overall, it is difficult to assess the effect of flow on Delta Smelt survival in the post-POD era because the 2 years with the lowest X2 values, 2011 and 2017, have very different summer to fall survival indices and fall abundance indices. These are the only 2 years with X2 less than 81 km during the fall. From a statistical perspective, it will be difficult to develop a reliable model until additional high flow years are observed. From a practical perspective, understanding differences in other factors besides flow in 2011 and 2017 is important as we wait for higher flow years to occur.

Potential effects of X2 on the Abundance and Survival of Delta Smelt

Potential associations between X2 and relative abundance of Delta Smelt in the fall (FMWT index) and between X2 and the summer to fall survival index (FMWT/STN) were evaluated with linear and non-linear models (see Appendix 11). Models examined included two parameters to account for linear or curvilinear responses in survival or abundance to changes in X2 while minimizing overfitting. Selected models for each data set minimized the Akaike's Information Criterion correction for finite sample size (AICc). Reasonable representation of the data by the model was based on assessment of the distribution of residuals (Wald-Wolfowitz runs test), and visual curve inspection.

There was no significant relationship between the summer to fall survival index and X2 for the period 1969-2017 (Figure 101). Only 2 years in the post-POD era (2011 and 2017) had X2 values less than 77 km, while there were 16 such points in the entire data record. Considering only data from 2002-2017 (no index in 2015 and 2016) there was also no relationship between summer to fall survival and X2; however, if 2017 is excluded, there is a reasonably strong relationship (Figure 102). It is interesting that 2006 fell very close to the regression line, even though it is another wet year with warm summer temperatures. This is not to say that 2017 represents unreliable data and should not be considered but that previous data would lead one to expect higher survival at low X2 values. The fact that 2017 is well outside the 95% prediction interval (light pink area) reinforces the idea that 2017 represents a set of conditions not previously occurring in the post-POD era.

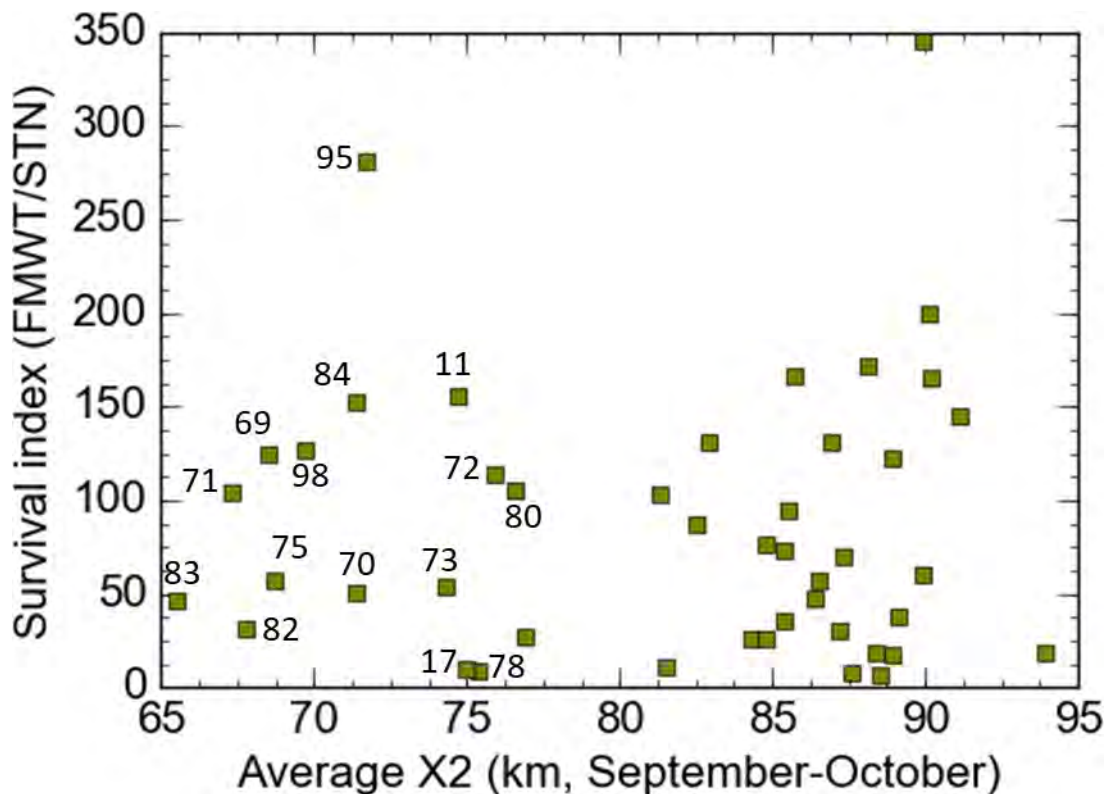


Figure 101. Summer to fall survival index (FMWT/STN) for Delta Smelt versus the average position of X2 during September-October during the period 1969-2017. No significant association was suggested from regression analysis. Indicated are years when average X2 in September-October was <77 km.

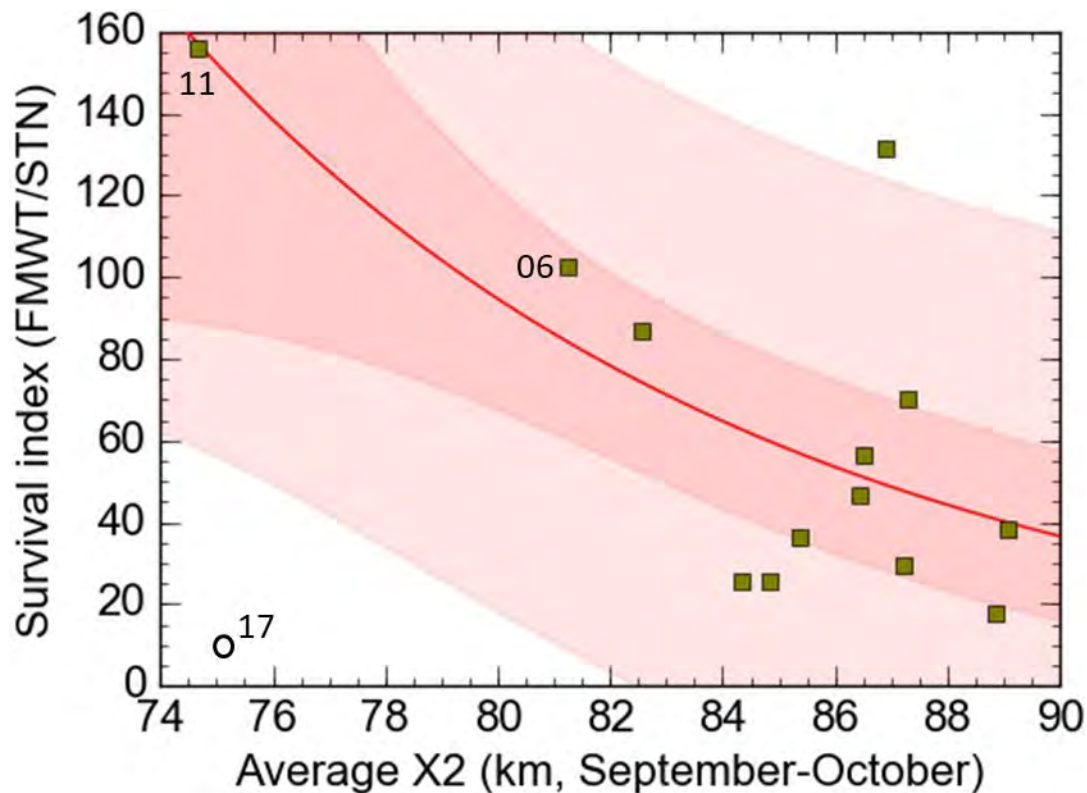


Figure 102. Summer to fall survival index for Delta Smelt (Y) versus the average position of X2 (X) during September-October for the period 2002-2014. Regression line for modified power model ($Y = 188638 [0.9094^X]$, $R^2 = 0.49$, $P < 0.01$; 11 df) excludes outlier year 2017 (white circle). Inclusion of year 2017 in the model resulted in a non-significant model. Dark pink indicates the 95% confidence interval for the line. The lighter pink indicates the 95% prediction interval for predictions of values for new observations.

The association between the FMWT index and the average X2 in September-October was statistically significant for the entire record of FMWT surveys examined 1967-2017 (Figure 103). For the period 2002-2017, the association between these variables was also statistically significant (Figure 104); however, the selected model had no obvious ecological interpretation and the shape of the curve is highly dependent on the relative X2 values of 2011 and 2017. As discussed above, 2017 appears to represent a new set of circumstances in the post-POD era that corresponds to low survival and abundance of fish at low average September-October X2, in contrast to 2011 (Figures SURVIVAL 9 and 11). Notably the highest FMWT index observed since the POD occurred in 2011, but that value was still below the predicted regression line for the period 1967-2017 (Figure SURVIVAL Figure 10), reflecting the generally depressed level of the population since the POD.

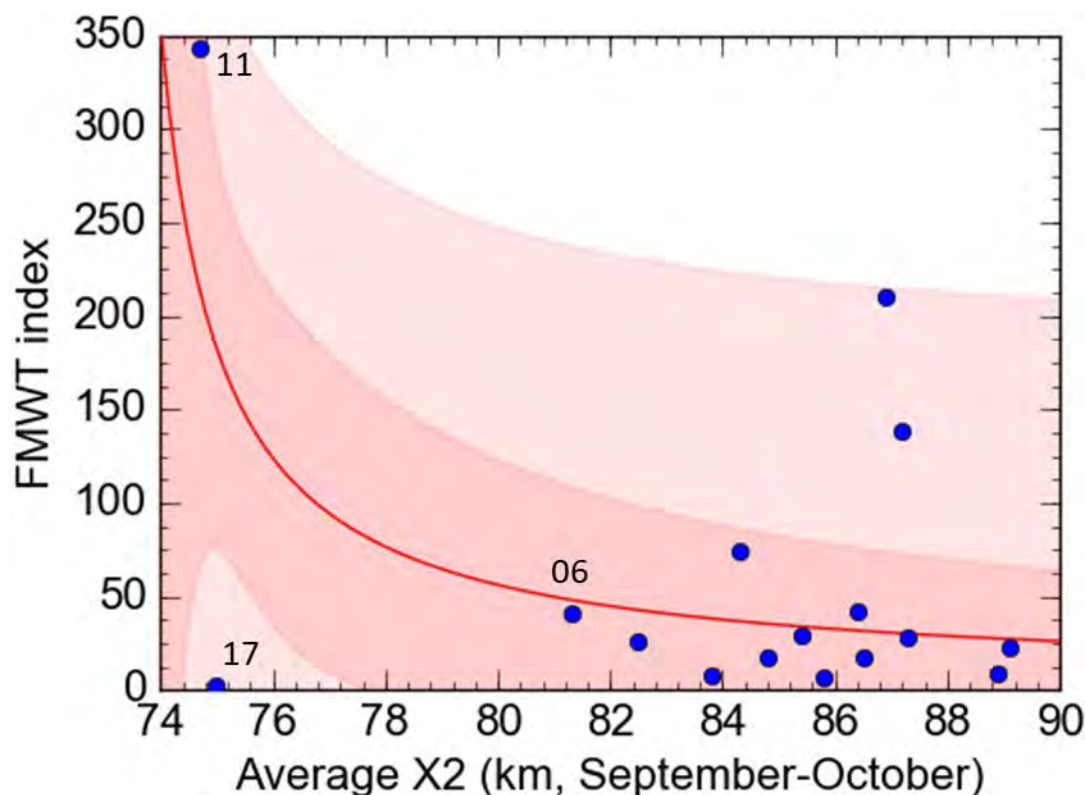


Figure 104. Relative abundance index for Delta Smelt during fall (Y) versus the average position of X2 during September-October for the period 2002-2017 (X). Regression line shows reciprocal model ($Y = X/(-14.77 + 0.2024 X, R^2 = 0.24, P = 0.05; 14 \text{ df})$). Dark pink indicates the 95% confidence interval for the line. The lighter pink indicates the 95% prediction interval for predictions of values for new observations.

Relative and actual abundance estimates for Delta Smelt from the EDSM survey

The relative abundance (catch per unit effort adjusted to 10,000 m³ sampled) of juvenile and subadult-adult Delta Smelt varied greatly among EDSM strata between December 2016 and December 2017 (Figure 105, Appendix 11). The strata with the highest relative abundance were Suisun Marsh, Liberty Island/Cache Slough, Sacramento Deep Water Shipping Channel (Figure 105). Intermediate relative abundance was observed in Suisun Bay and the lower Sacramento River, and low relative abundance strata included the lower San Joaquin River, the southern and western Delta. No Delta Smelt were observed in the eastern Delta and the upper Sacramento River (Figure 105). During December 2017 no Delta Smelt was detected in any of the strata, including strata occupied in December 2016 (Figure 105). Due to extremely low catches, absolute abundance (estimate of actual number of fish) of Delta Smelt could not be estimated for all the months in which this species was detected. However, the available monthly estimates of absolute abundance showed generally similar

patterns to relative abundance in those strata with high and intermediate relative abundances (Figure 106). Between April and July 2017, the relative abundance of larval-juvenile Delta Smelt was highest in Liberty Island/Cache Slough, intermediate in the western Delta and Suisun Bay, and zero in all but one of the remaining strata, with no Delta Smelt detections in any of the 10 strata during July 2017 (Figure 107).

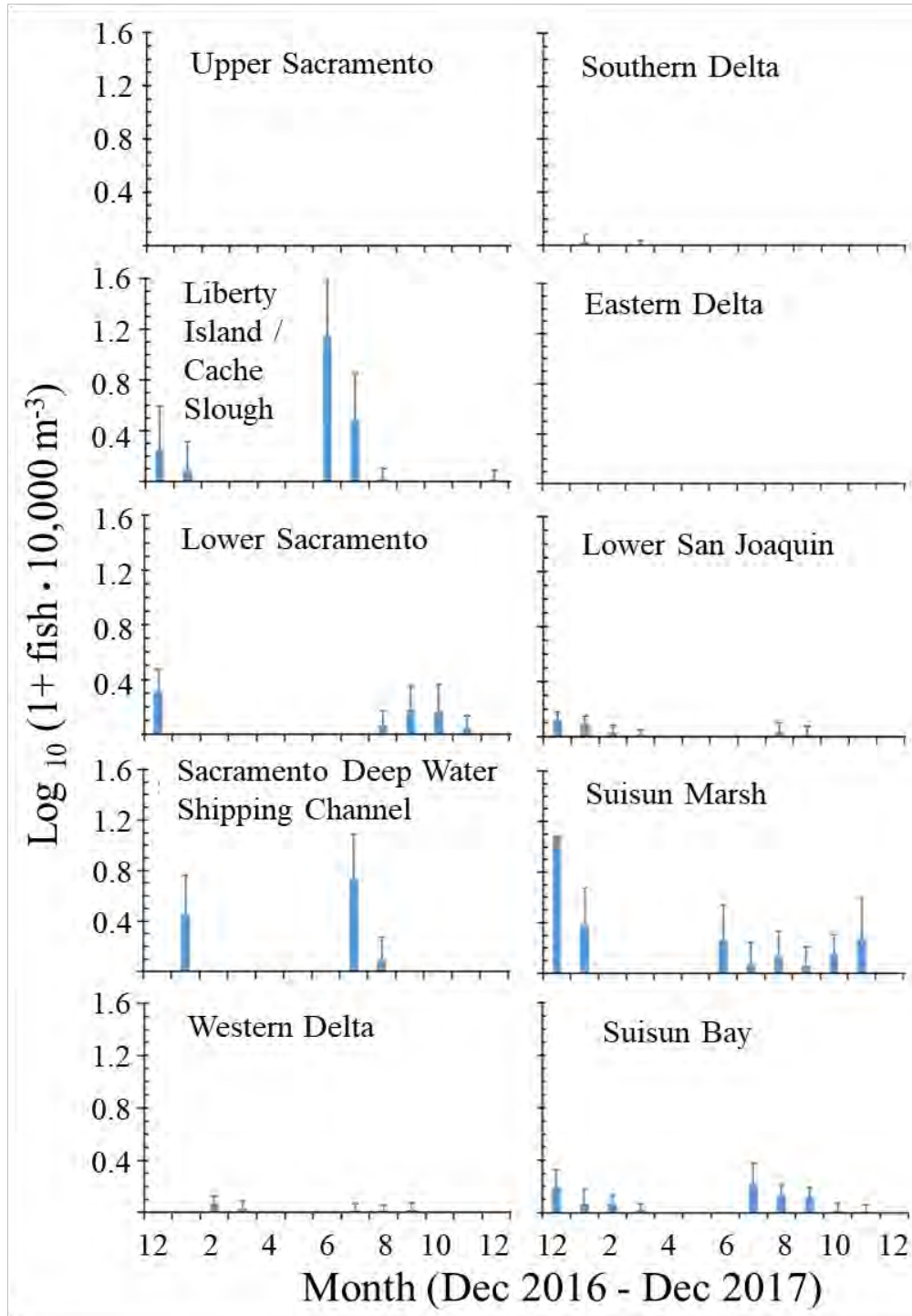


Figure 105. Catch per unit effort of juvenile, sub-adult, and adult Delta Smelt across 10 strata sampled by the Enhanced Delta Smelt Monitoring Kodiak trawl between December 2016 and December 2017. Data were log transformed because of high variability between months.

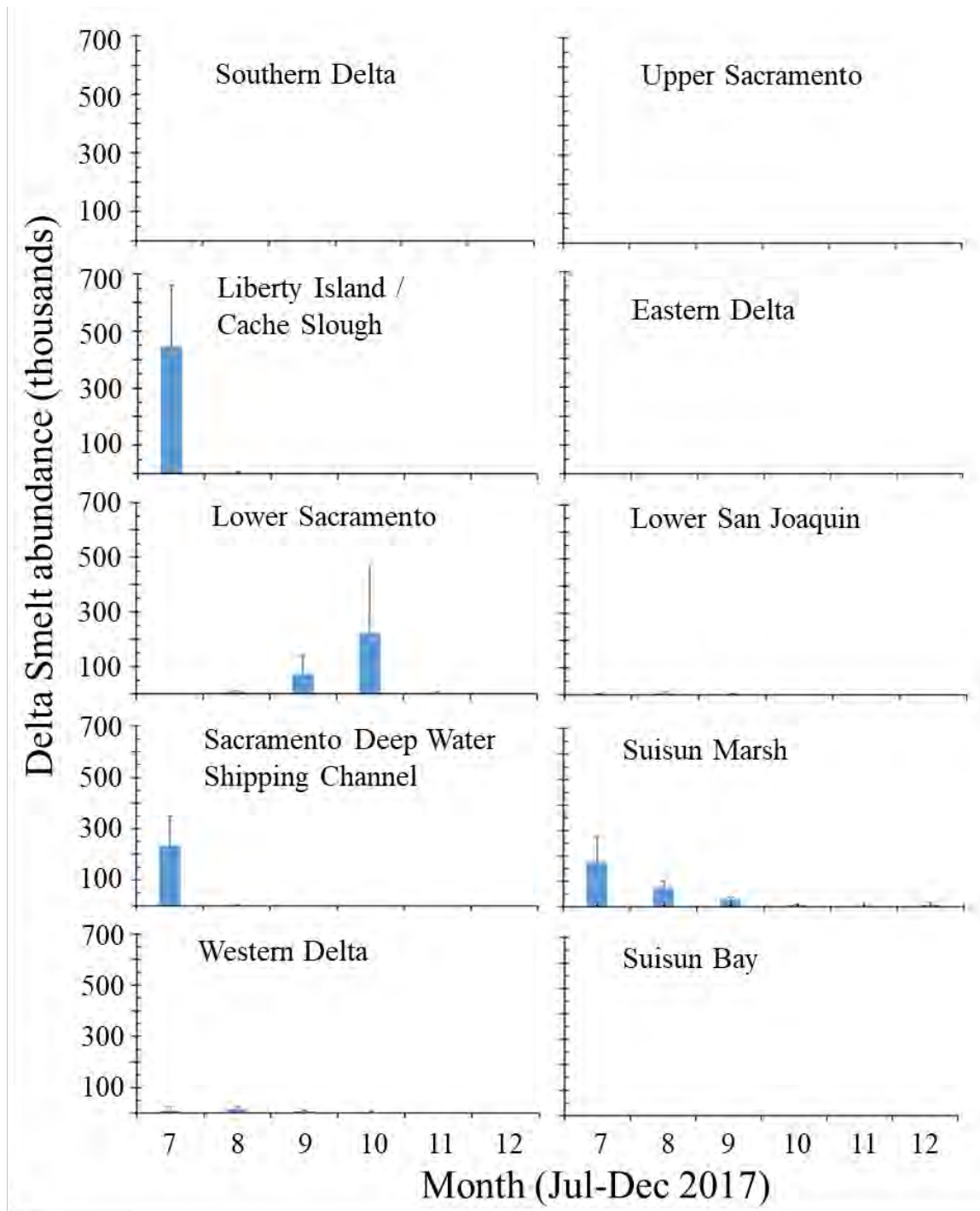


Figure 106. Estimated abundance (mean ± SE) of juvenile-subadult Delta Smelt between July and December 2017 across 10 Enhanced Delta Smelt Monitoring strata. Based on weekly Kodiak Trawl Enhanced Delta Smelt Monitoring estimates by Lara Mitchell, Lodi U.S. Fish and Wildlife Office.

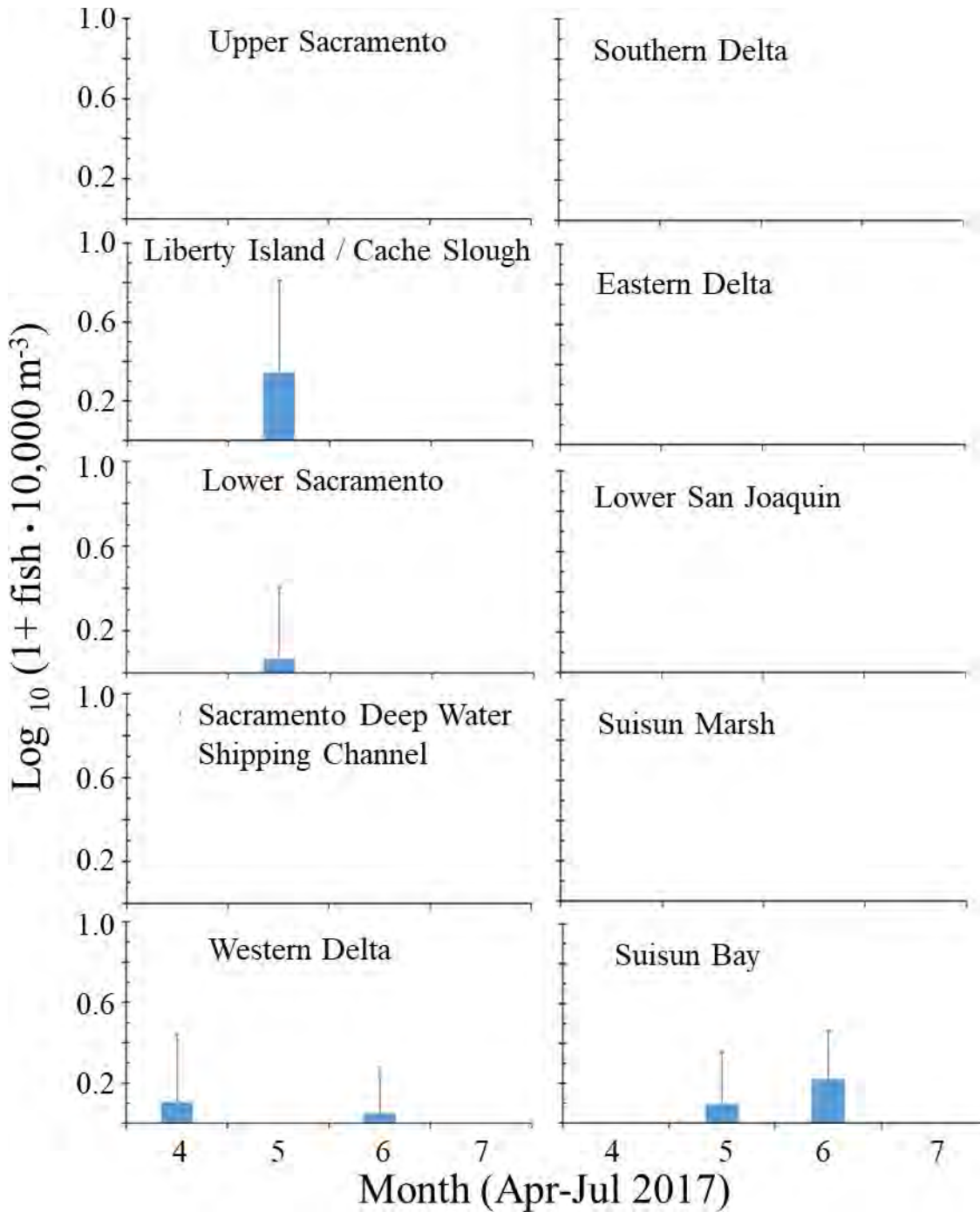


Figure 107. Catch per unit effort of larval-juvenile Delta Smelt across 10 strata sampled by the 20 mm Enhanced Delta Smelt Monitoring survey between April and July 2017. Data were log transformed because of high variability between months.

Production and Survival

Recruitment of each year class of Delta Smelt is a function of several factors including number and size of females and the duration of the spawning period, which influences the number of clutches per female. Bennett (2005) presented a life history model of young produced by a single female with a single clutch (Figure 108).

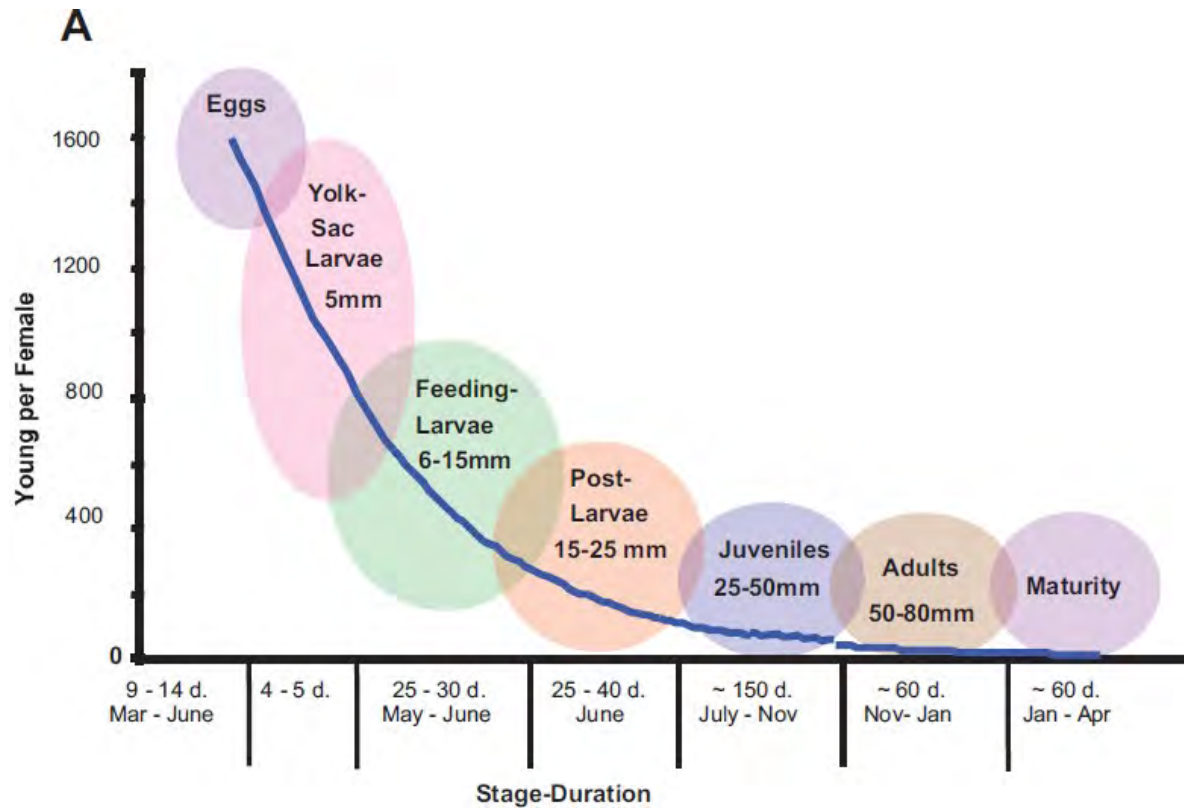


Figure 108. Delta Smelt conceptual life history model from Bennett (2005) as example of potential production of eggs from an individual female producing a single clutch of eggs followed by survival of hatched larvae over time.

Our current understanding of production is informed by work with fish in culture (FCCL, Lindberg et al. 2013) and wild fish (Damon et al. 2016), which shows that Delta Smelt females are capable of producing multiple clutches of eggs in a season, if conditions permit, with a recovery period between clutches (Damon et al. 2016). Knowing the number and mean length of adult Delta Smelt along with the duration of the spawning period to estimate the number of clutches possible allows calculation of the number of eggs in females, which can serve as a measure of the maximum reproductive potential of the population (Figure 109). The mean number of female Delta Smelt spawning events (clutches) per year was estimated based on difference in Julian days between

detections of first mature female by CDFW Spring Kodiak Trawl (SKT) and last newly hatched larvae (5-6 mm FL) by CDFW 20-mm Study, applying a 50-day refractory period between clutches for fish in culture. (M. Nagel UC Davis, personal communication, Damon et al. 2016; see Appendix 11 for details). The 50-day interval was used in the calculation to provide a more conservative estimate of production rather than the maximum possible production based on a 30-day period. Calculations of annual potential egg production by the population are highly correlated with the 20-mm Survey indices, our earliest measure of the abundance of Delta Smelt, suggesting that our calculation of reproductive potential is reasonable (Figure 110).

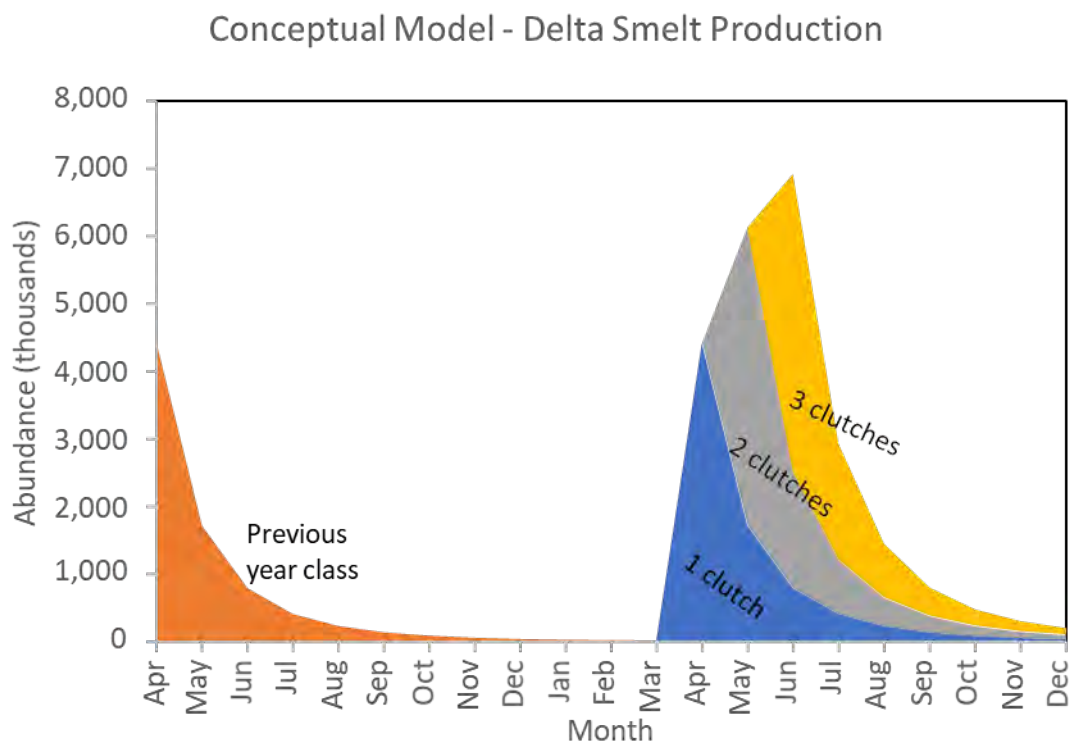


Figure 109. Conceptual model of variability in production of a new year class of Delta Smelt based on 1-3 clutches per female (note y-axis is log₁₀ scale). The abundance of fish per month is based on the non-linear model: $y = 1,173,533,700 x^{-3.983}$ ($R^2=0.56$) (see Appendix 12), where x is month, and y is abundance. The abundance of clutch 1 was added as clutch 2 and again as clutch 3, with a 1-month delay per clutch, assuming same production of eggs per clutch following a 30-day refractory period. The 30-day refractory period is the minimum refractory period estimated for wild fish (Damon et al. 2016).

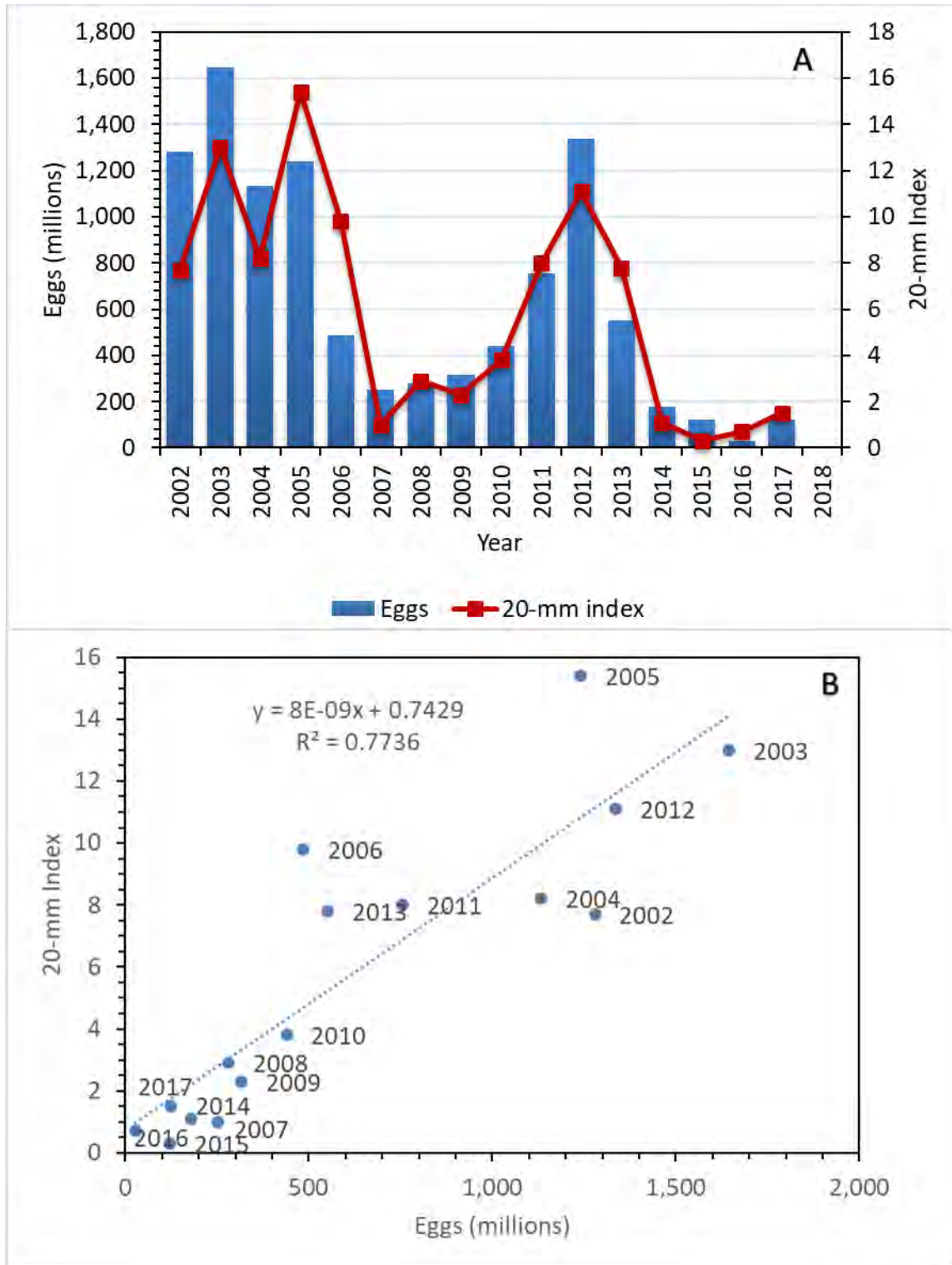


Figure 110. Relationship between potential population fecundity (number of eggs) from adult Delta Smelt population estimates and CDFW 20-mm Survey Delta Smelt annual indices of young for the period 2002-2017 with A) bar

chart of eggs and line for the 20-mm index by year and B) Least squares linear regression between 20 mm index and number of eggs.

With a measure of egg production and adult abundance at the end of each year, we can model survival in a more quantitative way. We estimated egg production as described above based on adult population estimates provided by USFWS (Appendix 11). Adult abundance was used to estimate number of females each February (assuming 1:1 ratio of males to females; this is the last month for which USFWS provided an estimate), then estimate potential egg production for the population from those females based on a length-fecundity relationship (Damon et al. 2016) and mean March length of 68.3 mm FL, resulting in an average of 1,730 eggs per female. Length in March was used since this is generally the first month during which significant reproduction occurs preceding peak spawning in April. Potential egg production includes a multiplier of 1, 2, or 3 clutches possible based on duration in days of the spawning period and refractory periods between clutches around 50 days. Survival from eggs to adults was then modeled using non-linear regression to fit a power function between potential egg production in February by females and the resulting adult abundance 12 months later (Figure 111).

$$\text{Abundance} = a \times \text{Months}^b,$$

where a is the calculated number of eggs at the beginning of the year, Months is the number of months since the eggs were spawned, and b is an exponent.

The joint baseline for all years with available data (2002-2017) provides a common baseline for comparison. For 2015 and 2016 adult abundance was clearly lower than the other years. The shape of the model curve for these two years was not notably different from the baseline curve but the curve was lower, reflecting lower abundance. In 2017, abundance remained low but the curve had a slightly steeper slope than the other two lines indicating decreased survival over the year compared to the other low abundance years modeled and the overall average; however, the difference is small and was not tested statistically because of small sample size. The estimated February abundance (Appendix 11) of adults in 2017 (47,786) was followed by very low recruitment of adults present in February 2018 (17,606), with a year-to-year ratio of 0.37. Of note, the conditions prior with the adult abundance from 2016 (16,159) to 2017 (47,786) was a high of 2.96 for the period 2003-2018, nearly tripling the abundance between adult year classes. Clearly, there may be differences in month-to-month or life stage-to-life stage survival occurring between egg production and adult spawning (Figures 94, 96, and

99). As this modeling approach is developed for other comparisons and incorporates population estimates for additional life stages, more quantitative inferences about survival rates will be possible.

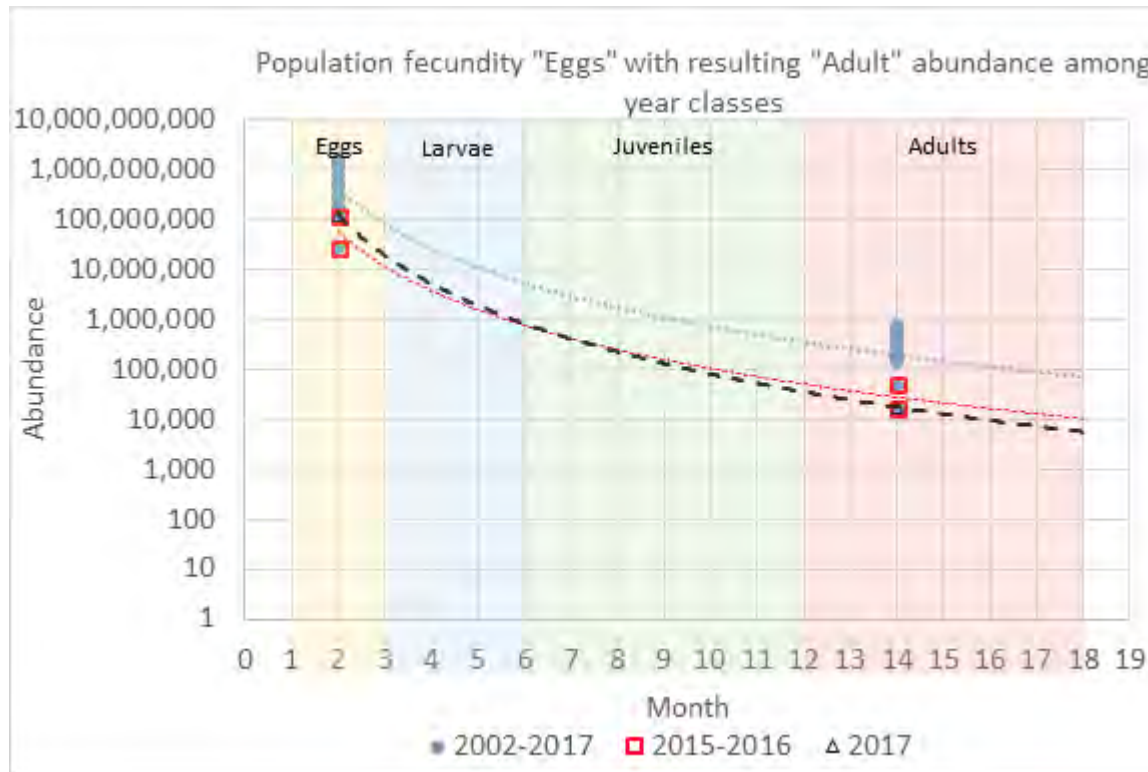


Figure 111. Non-linear regression (power function) relationship between potential population fecundity (number of eggs) and adult abundance estimates for Delta Smelt year classes 2002-2017 (blue line), 2015-2016 (red line), and 2017 (dashed line). Adult February estimates (month 14) from Appendix 11 produced by USFWS (courtesy Lara Mitchell). Note that the 2017 value for eggs (triangle) is in the same position as the upper 2015-2016 box and the 2017 value for adults is in the same position as the lower 2015-2016 box.

Winter-to-spring recruitment index

The ratio of the 20-mm abundance index of young Delta Smelt to the adults of the previous year class in the SKT abundance index (20-mm/SKT) provides a recruitment index for young Delta Smelt (Figure 112). In 2017, recruitment was low, very similar to the previous year and substantially lower than recent years 2014-2015.

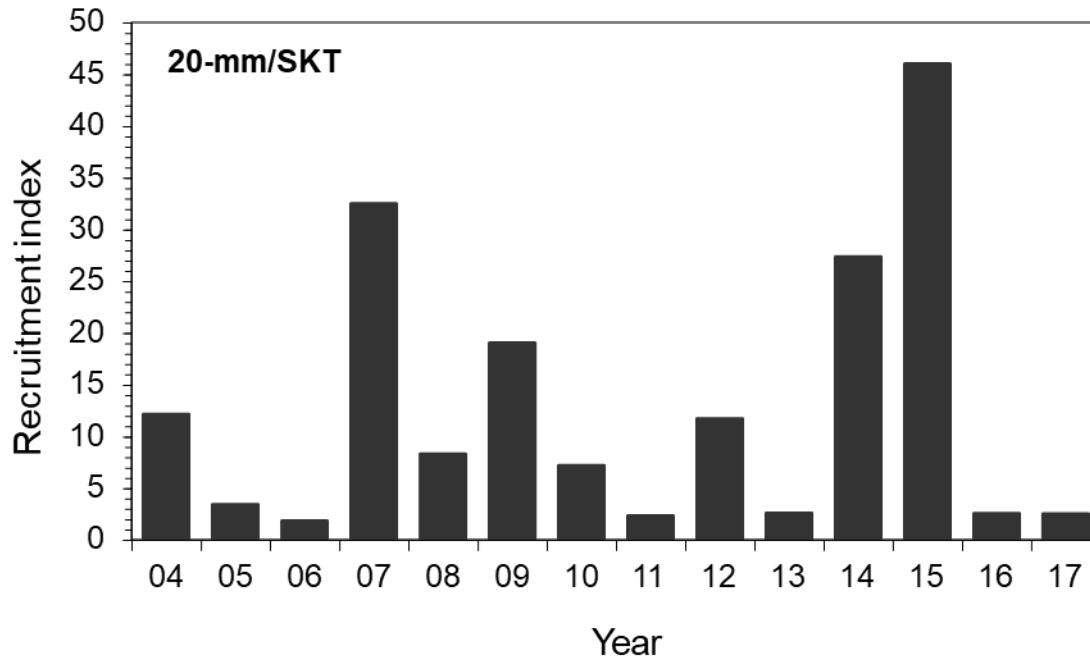


Figure 112. Spring recruitment index (20-mm/SKT) for larval and juvenile Delta Smelt based on the ratio of the 20-mm Survey (20-mm) and Spring Kodiak Trawl (SKT) relative abundance indices.

Fall-to-fall recruitment index

The ratio of the FMWT abundance index to the previous year FMWT abundance index ($FMWT/FMWT_{\text{previous year}}$) for subadult Delta Smelt was used for the fall recruitment index. Years 1974-1975 and 1979-1980 were not included in calculation of the index because a FMWT index was not available for 1974 and 1979. The fall recruitment index in 2017 was the seventh lowest value of the 46 years spanning 1968-2017 (Figure 113).

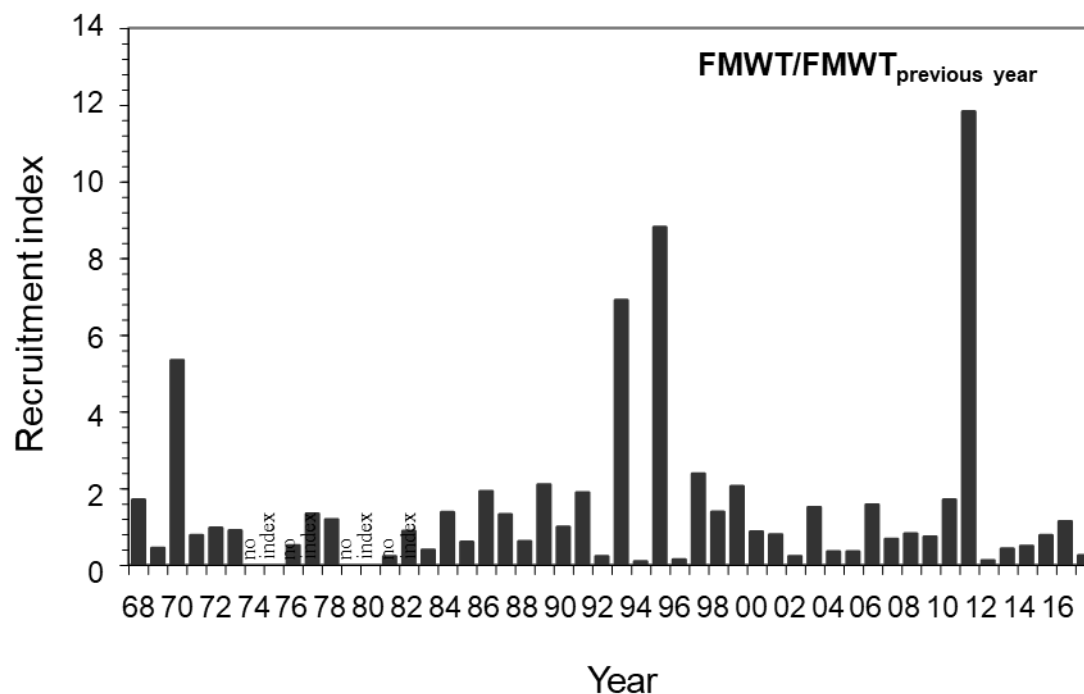


Figure 113. Fall recruitment index ($FMWT/FMWT_{previous\ year}$) for subadult Delta Smelt based on the ratio of the Fall Midwater Trawl (FMWT) relative abundance indices.

Summary

The prediction that survival in fall 2017 and other wet years would be higher with X2 being centered over Suisun Bay and Marsh compared to survival with X2 farther upstream near the confluence of the Sacramento and San Joaquin Rivers was not supported. The 2017 Delta Smelt year class began with poor recruitment in spring of 2017 with evidence of a short spawning window for adults and low production of young seen in 20-mm Survey catches, relative to years prior to 2014. The estimated survival of the 2017 year class among life stages was below average for spring to summer and summer to fall. Thus, low production and low survival led to low abundance of all life stages. The fall to winter period survival improved, yet the resulting adults were low in number.

Discussion

Of the 17 (including the 4 variable-specific predictions under Delta Smelt physical habitat) predictions made at the beginning of this report, 4 were supported by the data and 7 were not supported by the data (Table 19). Note that it is possible for one wet year, such as 2017, to meet the

prediction but the prediction is considered unsupported if the same response does not occur in the other wet years. There were 6 predictions with insufficient data to make a clear determination. For example, the turbidity prediction was true early in 2017 but not later in the fall and the Delta Smelt habitat index was only calculated for wet years (because other year types were not modeled for this report) so comparisons could not be made relative to other years. Because of these shortcomings of the data, we also could not make a definitive judgement about the response of Delta Smelt physical habitat. We also did not feel comfortable reaching conclusions regarding Delta Smelt range and distribution, primarily because catches have been so low in most years of the post-POD era that robust conclusions are not possible.

Table 19. Outcomes for predictions regarding the effects of high flows on Delta Smelt and Delta Smelt habitat.

Green means that data supported the prediction and red means the prediction was not supported. Gray indicates that data were insufficient to support a conclusion. No shading indicates there were no data to assess or that a prediction based on flow was not appropriate.

2017 FLOAT MAST Prediction Table		
Variable (September-October)	Fall X2 location	
	Sac-San Joaquin confluence	Suisun region
<i>Dynamic abiotic habitat components</i>		
Delta Smelt physical habitat	Lower	Higher
Low-salinity zone	Smaller area	Larger area
Turbidity	Lower	Higher
Delta Smelt habitat index (based on turbidity, salinity, and hydrodynamic complexity in the Suisun Region)	Lower	Higher
Water temperature	Higher	Lower
<i>Dynamic biotic habitat components</i>		
Phytoplankton - food availability for zooplankton	Lower	Higher
Harmful algal blooms	Increase	Decrease
Zooplankton - food availability for Delta Smelt	Lower	Higher
Clam biomass and grazing rate	Higher	Lower

Aquatic Vegetation (floating and submerged aquatic vegetation)	Increase in Water Hyacinth, unknown for other species	Decrease in Water Hyacinth, unknown for other species
Fish assemblage – biomass of pelagic fishes	Lower	Higher
<i>Delta Smelt responses</i>		
Growth rate	Lower	Higher
Life history diversity (freshwater vs. LSZ); timing of migration to brackish water	Lower	Higher
Health metrics (liver and gill condition)	Poor	Good
Feeding success (diet); prey composition	Poor	Good
Delta Smelt range/distribution	More constricted	Wider distribution
Delta Smelt survival in the fall months (can include survival to winter, spring, etc.)	Lower	Higher

Biological responses in the wild are typically uncertain because of the many interacting factors affecting any response. Thus, it is not surprising that the predictions for Delta Smelt responses were the least successful. Conceptual models of Delta Smelt biology include a variety of additional factors and interactions beyond flow that can be important in determining the success of each Delta Smelt life stage (Figures 9-13). Such other factors can be directly (e.g., position of salinity field), indirectly (e.g., transport of sediment for subsequent resuspension), or not (e.g., summer/fall air temperatures) related to Delta outflow. In addition, conditions in the previous year can have important effects on the subsequent year, through processes such as total egg production. For the post-POD era, an appropriate corollary to the expression “it takes a year to make a smelt” (IEP-MAST 2015), appears to be that “high Delta outflow alone is not sufficient for high production of Delta Smelt.” For the remainder of this Discussion we avoid detailed discussions of the specific predictions and focus more on findings that increase our understanding of Delta Smelt biology and ecology and new areas where research or monitoring might be needed.

For Delta Smelt physical habitat, the relationship of outflow with area of low-salinity zone has been previously examined (e.g., Brown et al. 2014, IEP-MAST 2015) and has been extensively modeled (Kimmerer et al. 2013, MacWilliams et al. 2015). Significant work has been done on sediment transport in the SFE (e.g., Schoellhamer 2011, Hestir et al. 2013, 2016), including studies focused on the deposition of fine sediments needed for resuspension and the processes producing summer/fall turbidity in various regions of the Delta (e.g., Morgan-King and Schoellhamer 2013). However, models

for estimating system-wide suspended sediment concentrations (i.e., turbidity) have only recently been developed (Bever and MacWilliams 2013, Achete et al. 2015) and have not yet been applied to ecological questions in the Delta. Further development of these models and application in the Delta will likely be useful in understanding the spatial distribution of suitable Delta Smelt habitat.

Water temperatures appear to have been a major factor limiting the success of Delta Smelt in summer and fall of 2017. Previous statistical analyses have been inconsistent regarding the importance of water temperature, but those studies were largely limited to statistical descriptions (e.g., mean) of water temperatures measured during limited periods of each month during daytime trawl surveys restricted to the geographic sampling frame of the specific survey. Those measurements are adequate to see differences in temperatures among years (Figures 17 and 18) but have a number of shortcomings, including not covering the full geographic range of the species, as already mentioned, and not providing the full range of water temperature the organism experiences in the field over a 24-h day or as daily water temperature changes across multiple days (Figure 114) within months and seasons. In this report we adopted an average of modeled daily temperature over the 2-week time period corresponding to the time between EDSM surveys as a variable of interest but we have access to the full output of the model (hourly including daily maximums and minimums). We based our conclusions on our assessment of available data, which suggested that extended exposure to temperatures above 22°C was stressful to the fish. We based that interpretation on several factors discussed earlier in several sections. First, as temperature increases above the upper boundary of the optimum range at 20°C, the metabolic rate of the fish increases and more energy (i.e., food) is needed for maintenance rather than growth, and if adequate food can't be found, the fish will begin to starve. This is consistent with reduced growth rates at higher temperatures (Figure 73). Thus, it seems likely that fish would avoid warm temperatures, except perhaps in areas where food is extremely abundant. Also, as the 2-week mean exceeds 22°C, variation in the daily mean and variation within a day around the daily mean could expose fish to extremely warm temperatures for several hours a day (Figure 114). Hobbs et al. (2019a,b) have linked multiple life history characteristics to temperature (see Life History Characteristics section) that will be useful in better understanding the effects of water temperature on Delta Smelt.

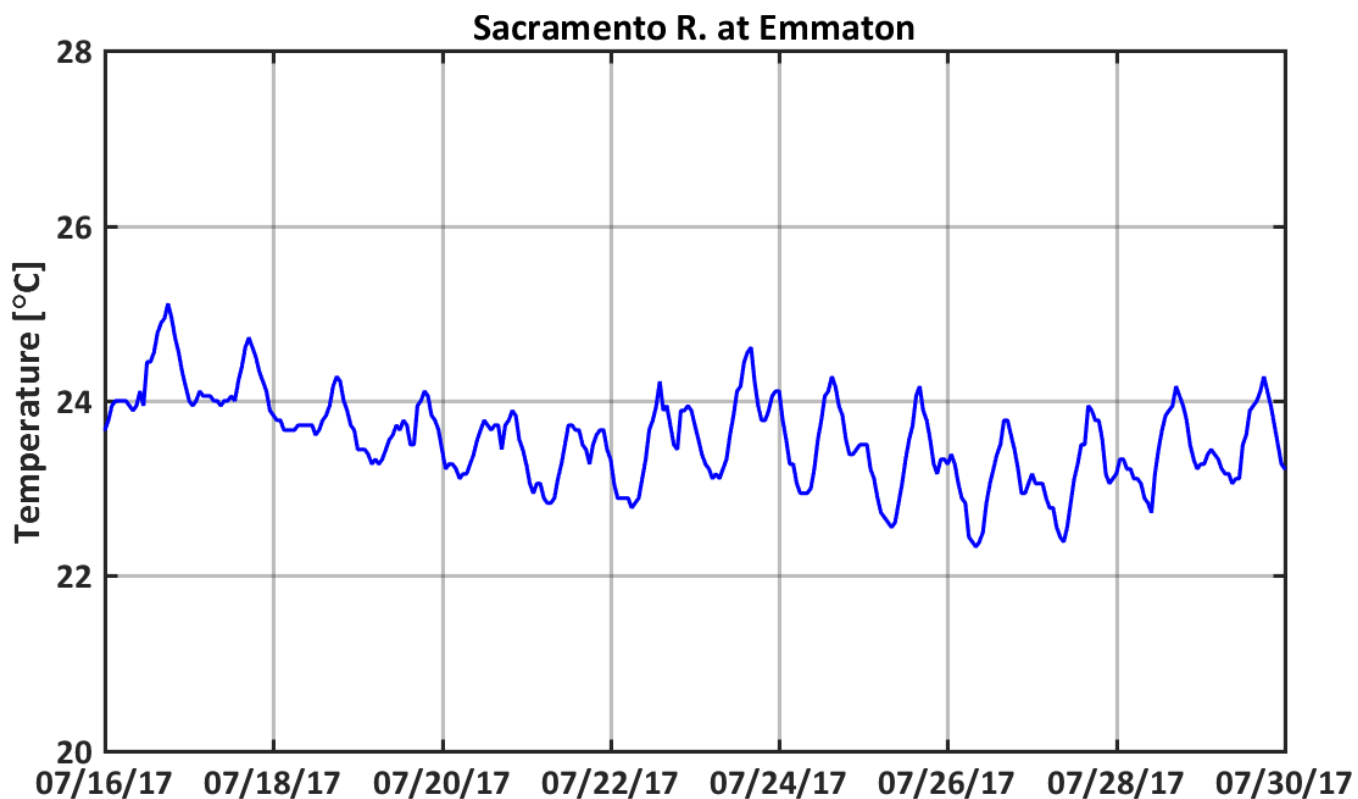


Figure 114. Variation in water temperature (hourly data) at Emmaton on the Sacramento River for a two-week period in July 2017, when the two-week average exceeded 22°C.

Water temperature was previously identified as potentially responsible for the differential response of Delta Smelt abundance in 2006 and 2011 (Figures 25 and 26). Given the long periods in July and August when water temperatures exceeded 22°C (Figure 17) we are confident that water temperature had a major negative effect on Delta Smelt in 2017 and is likely a primary factor in the lack of response of the Delta Smelt population to the high flows. It seems likely water temperatures may have also been important in 2006 (Figures 25 and 26). The duration of warm temperatures was shorter in 2006 but exceeded 24°C in some areas (Figures 26 and 27). The previously discussed failure of statistical models to consistently include temperature as a variable affecting Delta Smelt abundance could also be due to summer water temperatures only reaching levels of concern on an intermittent basis. In many cases, high temperatures occur during drier years and are considered a common companion to drought; however, during the post-POD era, 2 of 3 wet years have also been warm during the summer. Modeling of pre-POD years would be necessary to determine if temperature was an important factor affecting Delta Smelt abundance in earlier years.

Thus, freshwater and brackish-water rearing areas appear to have become extremely stressful and likely did not provide good conditions for growth or survival in 2006 or 2017 based on observed and modeled temperatures (Figures 17, 25 and 26, see Appendix 2 for additional detail). Overall, the data suggest that high flows set up salinity conditions predicted to be favorable for survival of Delta Smelt as observed in 2011, but the benefits of high flows may be contingent on other physical factors, particularly water temperature.

Within the group of wet years (2006, 2011, 2017), Delta Smelt physical habitat conditions were fairly comparable for salinity, turbidity, and the Delta Smelt habitat index (see Dynamic Abiotic Habitat section and Appendix 2). One clear difference was in summer-fall water temperatures, with only 2011 having relatively cool temperatures throughout the summer and fall (Figures 25 and 26). High water temperatures in 2006 and 2017 were not at lethal levels (based on laboratory studies) for any extended period of time but did reach levels where physiological stress was likely (2006) or where high metabolic requirements likely left little energy for growth and reproduction, possibly even leading to starvation and increased vulnerability to other stressors for fish rearing in the warmest areas.

Dynamic biotic habitat components were somewhat better in 2017; however, the lack of response of the Delta Smelt population suggests that any benefits of changes in the biotic habitat were minimal. Decreases in area occupied by Water Hyacinth were accompanied by increases in area occupied by Water Primrose, which is also invading tidal marshes. Thus, there was no net gain in open water habitat, which might have benefited Delta Smelt. It was also unclear if the decline of Water Hyacinth was more strongly related to outflow or control efforts. Harmful algal blooms have generally been responsive to flow, but nutrients and water temperature can also be important factors. In 2017, there was no large bloom of *Microcystis* and presumably there was minimal effect on the Delta Smelt population.

Phytoplankton biomass was somewhat greater in 2017 compared to other years, but there was no clear pattern associated with water year type. The phytoplankton biomass in the lower Sacramento and San Joaquin Rivers in the fall of 2017 was only marginally higher than previous post-POD years (2003-2016). This contrasted from the last high outflow year of 2011 in which a fall phytoplankton bloom (chlorophyll-*a* >10 µg/L¹) occurred in the lower Sacramento and San Joaquin Rivers (Figures 33B and 44A). There was a significant phytoplankton bloom in the summer of 2017 in the lower

Sacramento and San Joaquin Rivers (Figures 33C, 34, 36A,B) composed of the same dominant centric diatom *Aulacoseira* sp. as observed in fall 2011; however, the bloom was not sustained through the late summer and fall. It is not clear why bloom dynamics differed between the two years or if such intermittent bursts of productivity can move up through the food web to increase annual survival of Delta Smelt.

Similar to phytoplankton, zooplankton abundance, specifically herbivorous calanoid copepods, was higher in 2017 compared to other years, but there was no clear pattern related to water year type (Table 8, Figures 52). Abundance of mysid shrimp was also relatively high (Figure 53). However, the abundance of zooplankton was variable across regions and seasons. A portion of the high zooplankton abundance appears to have been a subsidy of *Pseudodiaptomus forbesi* from the central Delta (Kimmerer et al. 2018), which was too warm for Delta Smelt, to more seaward regions. Increased water temperatures in 2017 may have stimulated production of this copepod. Decreased clam biomass in 2017 (See Clam section) may have been a contributing factor in increased zooplankton because of reduced clam grazing on phytoplankton and young life stages of zooplankton.

Increased abundance of zooplankton, combined with the low biomass and grazing rates for clams and low incidence of harmful algal blooms (HABs) in 2017, would suggest more food available for planktivorous fishes. Indeed, biomass of planktivorous fishes did increase in 2017 and Delta Smelt stomach fullness was high in 2017. However, any response of Delta Smelt population was undetectable and survival in 2017 was poor. This suggests some mismatch of timing or geographic area, such that increased production of food or food of sufficient quality was unavailable to Delta Smelt. *Limnoithona* spp. is considered poor quality prey due to its small size and is selected against by Delta Smelt; however, it appeared regularly in diets likely as evidence of lower densities of larger prey. As mentioned above, *Pseudodiaptomus forbesi*, is a tropical species that reached high abundance in central areas of the Delta in 2017; however, these areas are too warm for Delta Smelt. *Pseudodiaptomus* is transported to the downstream areas of the Delta, providing a subsidy for downstream consumers (Kimmerer et al. 2018). Unfortunately, zooplankton abundance in Suisun Bay, which had suitable habitat and temperatures for Delta Smelt, only showed a small increase in zooplankton abundance (see Zooplankton section and Appendix 6). Given the general increase in zooplanktivorous fishes, it appears likely that the benefits of increased production of zooplankton

likely went to species better adapted to warm water, such as Threadfin Shad, American Shad, and Striped Bass.

The metrics of Delta Smelt response appear to be useful but were not necessarily responsive to flow. Growth appears to be more responsive to water temperature than to position of the low-salinity zone. There were no particularly strong patterns of life history diversity, as measured by hatch dates, natal origins, dispersal and life history phenotypes, with outflow and water year type (see Growth and Life History Diversity sections). Several temperature-related metrics, particularly the maturation window, were strongly associated with temperature rather than flow. The health metrics evaluated (gill and liver lesions) showed regional and annual differences; however, the meaning of those differences is not clear. In previous studies, the presence of fish with lesions was originally interpreted as indicating stress (Hammock et al. 2015); however, recent work has suggested the hypothesis that the presence of fish with lesions may indicate relatively benign conditions for fish survival, in that unhealthy fish (i.e., with lesions) are able to survive to be sampled. Under this hypothesis, in truly stressful conditions only the healthiest fish can survive. The spatial distribution of liver damage described by Hammock et al. (2015) persisted with the most damaged livers found in Cache Slough and Suisun Bay, while the healthiest fish occurred in Suisun Marsh. Fish collected from Suisun Marsh showed the most glycogen rich livers suggesting that Suisun Marsh provides excellent habitat when it is not too saline. The difficulty in interpreting health metrics, and lesions in particular, stems in part from lack of systematically collected data on contaminant concentrations and the lack of understanding of the variety of interactions among contaminants and with other stressors. There is evidence that fish are being exposed to contaminants at above-benchmark concentrations and that these contaminants are likely having important effects in the ecosystem (Brooks et al. 2012, Fong et al. 2016, De Parsia et al. 2019). Survival is the ultimate summation of all health metrics and is dependent on all of the factors affecting individual metrics.

Notably, quantitative modeling made significant contributions to the foregoing analysis. Physical models provided much more complete geographic and temporal representations of salinity, water temperature, and turbidity than were available from monitoring data (see Abiotic section). Modeling of the actual number of Delta Smelt in the system (Polansky et al. 2018) allowed more quantitative estimates of survival, and modeling of the *Pseudodiaptomus* population allowed for a

better understanding of food subsidies from one part of the system to another (Kimmerer et al. 2018). Other analyses have indicated the possible importance of geography to Delta Smelt (Manly et al. 2015, Bever et al. 2016, Hammock et al. 2015, 2017, 2019). Models can be designed to accommodate geographic and temporal variability in the importance of various factors on Delta Smelt (e.g., Rose et al. 2013 a,b), and it is possible that advances can be made in the near future with focused effort. It would be useful to bring physical, lower food web, and Delta Smelt (and other fishes) modelers together to establish commonalities among geographic and temporal modeling frames, encourage direct communication, and determine if adjustments in field surveys and monitoring could better inform existing or future models. Such an integrated approach could also form the basis for assessing future changes in the ecosystem and in Delta Smelt habitat (Cloern et al. 2011, Brown et al. 2013, 2016a,b, Dettinger et al. 2016)

As discussed earlier, the conclusion we draw from the year 2017 is that while high flow might be a critical component of Delta Smelt habitat in the estuary, an increase in freshwater flow alone is not sufficient to address the habitat needs of this endangered species. Delta Smelt has already experienced a long-term decline in years prior to fall of 2017. The lower baseline for Delta Smelt abundance was driven by multiple interacting large-scale ecosystem changes that have continued into 2017. Due to the multi-causal nature of Delta Smelt decline and the importance of preceding conditions (including the abundance of larval fishes in the spring prior to fall), it is rather difficult to isolate fall outflow from other factors. However, given the modest improvements to Delta Smelt habitat in 2017 with regards to salinity, turbidity, *Microcystis*, phytoplankton, and zooplankton, we conclude that warm summer temperature was likely the primary reason for the low Delta Smelt survival into the fall of 2017. As noted by Brown et al. (2014), it is important to consider prior conditions when evaluating the impact of a particular management change. In 2017, favorable conditions in the fall may have been overshadowed by stressful conditions during the preceding summer and lack of spawning adults in the prior spring. Future investigations should evaluate all seasons so flow alterations and other important interacting variables like water temperatures can be viewed in the appropriate context.

Similarly, we also note that productivity of the system is a key issue. As reviewed earlier, invasive clams have been identified as a key factor in the decline of phytoplankton and zooplankton in

the upper SFE and water quality may also have a role. The importance of tidal wetlands and tidal wetland restoration to pelagic fishes like Delta Smelt has been a topic of discussion (Herbold et al. 2014), and recent studies indicate that tidal wetlands may provide some benefit (Hammock et al. 2019).

Next Steps

The conclusion of this report that high fall outflow alone is not sufficient to provide favorable conditions for Delta Smelt poses difficult challenges for managers and policy makers. Regulating flow is straightforward in that we have appropriate tools (e.g., reservoir releases) for management. We do not currently have practical tools for significantly affecting turbidity, water temperature, or food production. Turbidity is controlled by interactions between sediment supply, wind, and hydrodynamics (Bever and MacWilliams, Bever et al. 2018, MacWilliams et al. 2015). In addition, aquatic vegetation can alter these relationships by trapping sediment (Hestir et al. 2016).

Water temperature in the upper SFE is largely controlled by air temperature, which varies seasonally and annually, but is also influenced by conditions in the cooler San Francisco Bay. Thus, water temperatures are cooler in Suisun Bay and become warmer in the Delta as the influence of cooler air diminishes. The direct management of these climatological factors is beyond the tools available to resource managers at this time. Water temperature models have been developed for the Delta, and it is clear that air temperature and insolation (i.e., cloud cover) are much stronger drivers of water temperature than flow, particularly in the summer and fall (Wagner et al. 2011, Vroom et al. 2017). Vroom et al. (2017) found that if flow had been reduced by 33% in 2011 (comparable to the change in peak discharge between WY2011 and WY2012), average water temperature in the Estuary throughout the year would rise about 1°C. If we assume that flow increases of this magnitude could cool the Delta by 1°C then some level of temperature management might be possible; however, adjusting flows for this purpose would have to be considered in the context of overall water management and maintenance of reservoir cold water pools for temperature management required by other species like Winter Run Chinook Salmon. Similar to Vroom et al. (2017), Wagner et al. (2011) noted that flow can have significant effects on water temperature over short-time scales, which may be key for managing water temperature in the Estuary. However, the most important effect of flow

was associated with short periods of coldwater runoff in the winter, when elevated temperature is less of a concern. These issues should be further explored by testing various scenarios of flow, insolation, and air temperature across seasons using temperature models and detailed examination of the potential spatial and temporal patterns of any changes in water temperature.

How can we make progress in understanding Delta Smelt ecology and formulating new management strategies? Here we make some fairly general suggestions in no particular order of priority with the understanding that numerous suggestions have been made as part of previous reports on Delta Smelt (e.g., Brown et al. 2014, IEP-MAST 2015).

1. Establish an adaptive-management group of scientists and managers dedicated to the development and implementation of a science plan for Delta Smelt. For agency biologists, making this a priority assignment rather than a volunteer effort would improve management outcomes. A dedicated and funded leader could provide consistent and important long-term leadership. Ad hoc efforts have been useful but have proven insufficient to provide rapid progress.
2. The Delta Smelt Science Plan should consider all aspects of Delta Smelt science from monitoring to modeling and should consider all factors and processes potentially affecting the species. Significant progress has been made in developing models for various aspects of Delta Smelt physical habitat, biotic habitat, and the Delta Smelt population. The groups developing these models need to be brought together to exchange information needs and model results. Data collection efforts need to be evaluated to determine if they meet the needs of models, and if not, the existing efforts need to be modified or new programs developed to better advance Delta Smelt Science.
3. This report clearly identifies water temperature as an important factor affecting the Delta Smelt population in warmer years, and previous studies suggest water temperature will become more important in the future (Brown et al. 2013, 2016a,b). Because the climatological factors driving water temperatures are beyond local adaptive-management control, we suggest an initial effort to better understand how water temperature varies across the Delta in different water year types. This effort could help management efforts in various ways. For example, it might identify

geographic areas that stay relatively cool or identify habitat features that promote cooling. This knowledge could help in the design and placement of habitat restoration projects. Modeling efforts could also consider future conditions and how water management can be used in the near term to mitigate high water temperatures. These efforts could be useful for other native species in addition to Delta Smelt (e.g., Chinook Salmon).

4. Food abundance has been a concern since the invasion of *Potamocorbula*. Additional studies of the lower trophic levels and development of models to better understand production of Delta Smelt food are needed to determine if management actions can improve conditions for Delta Smelt feeding.
5. Although not discussed directly in this report, much of the information on the physiology of Delta Smelt has been developed using hatchery-raised fish. Large mesocosm studies or field experiments using caged hatchery fish would likely be useful in understanding responses of Delta Smelt to ambient conditions. Such experiments are currently in development.

References Cited

- Achete, F.M., M. van der Wegen, D. Roelvink, and B. Jaffe 2015 A 2-D process-based model for suspended sediment dynamics: a first step towards ecological modeling. *Hydrology and Earth System Sciences* 19(6):2837.
- Acuña, S.C., D. Baxa, and S.J. Teh. 2012a. Sublethal dietary effects of microcystin producing *Microcystis* on threadfin shad, *Dorosoma petenense*. *Toxicon* 60:1191-1202.
- Acuña, S.C., D-F. Deng, P.W. Lehman, and S.J. Teh. 2012b. Dietary effects of *Microcystis* on Sacramento splittail, *Pogonichthys macrolepidotus*. *Aquatic Toxicology* 110-111:1-8.
- Acuña, S., D. Baxa, P. Lehman, F-C. Teh, D-F. Deng, and S. Teh. in press. Determining the exposure pathway and impacts of *Microcystis* on Threadfin shad, *Dorosoma petenense*, in San Francisco Estuary. *Environmental Toxicology and Chemistry*.

- Adams, S.M., W.D. Crumby, M.S. Greeley, M.G. Ryon, and E.M. Schilling. 1992. Relationships between physiological and fish population responses in a contaminated stream. *Environmental Toxicology and Chemistry* 11:1549–57.
- Alpine, A.E. and J.E. Cloern. 1992. Trophic interactions and direct physical effects control phytoplankton biomass and production in an estuary. *Limnology and Oceanography* 37:946-955.
- Anderson, J.T. 1988. A review of size dependent survival during pre-recruit stages of fishes in relation to recruitment. *Journal of Northwest Atlantic Fishery Science* 8:55-66.
- Baxter, R., R. Breuer, L. Brown, M. Chotkowski, F. Feyrer, M. Gingras, B. Herbold, A. Mueller-Solger, M. Nobriga, T. Sommer, and K. Souza. 2008. Pelagic organism decline progress report: 2007 synthesis of results. Stockton, Calif., Interagency Ecological Program for the San Francisco Estuary, Technical Report 227, 86 p., https://water.ca.gov/LegacyFiles/iep/docs/pod/synthesis_report_031408.pdf.
- Baxter, R., R. Breuer, L. Brown, L. Conrad, F. Feyrer, S. Fong, K. Gehrts, L. Grimaldo, B. Herbold, P. Hrodey, A. Mueller-Solger, T. Sommer, and K. Souza. 2010. Interagency Ecological Program 2010 Pelagic Organism Decline work plan and synthesis of results. Interagency Ecological Program for the San Francisco Estuary. 259 p. Available at: https://water.ca.gov/LegacyFiles/iep/docs/pod/2010_POD_Workplan.pdf.
- Bennett, W.A. 2005. Critical assessment of the delta smelt population in the San Francisco Estuary, California. *San Francisco Estuary and Watershed Science* 3(2).
- Bennett, W.A., and J.R. Burau. 2015. Riders on the storm: selective tidal movements facilitate the spawning migration of threatened Delta Smelt in the San Francisco Estuary. *Estuaries and Coasts*, 38:826-835.
- Bennett, W.A., and P.B. Moyle. 1996. Where have all the fishes gone? Interactive factors producing fish declines in the Sacramento San Joaquin Estuary, in Hollibaugh, J.T., ed., *San Francisco Bay: the ecosystem: San Francisco, Calif., Pacific Division American Association for the Advancement of Science*, p. 519–542.
- Bever, A.J., and M.L. MacWilliams. 2013. Simulating sediment transport processes in San Pablo Bay using coupled hydrodynamic, wave, and sediment transport models. *Marine Geology* 345: 235–253. <https://doi.org/10.1016/j.margeo.2013.06.012>.

- Bever, A.J., M.L. MacWilliams, and D.K. Fullerton. 2018. Influence of an observed decadal decline in wind speed on turbidity in the San Francisco Estuary. *Estuaries and Coasts*, 41:1943-1967.
- Bever, A.J., M.L. MacWilliams, B. Herbold, L.R. Brown, and F.V. Feyrer. 2016. Linking hydrodynamic complexity to Delta smelt (*Hypomesus transpacificus*) distribution in the San Francisco estuary, USA. *San Francisco Estuary and Watershed Science*, 14(1).
- Bowling, L., S. Egan, J. Holliday, and G. Honeyman. 2016. Did spatial and temporal variations in water quality influence cyanobacterial abundance, community composition and cell size in the Murray River, Australia during a drought affected low-flow summer? *Hydrobiologia* 765: 359–377.
- Boyer, K. and M. Sutula. 2015. Factors controlling submersed and floating macrophytes in the Sacramento-San Joaquin Delta. Southern California Coastal Water Research Project. Technical Report No. 870. Costa Mesa, CA.
- Brooks ML, E. Fleishman, L.R. Brown, P.W. Lehman, I. Werner, N. Scholz, C. Mitchelmore, J.R. Lovvorn, M.L. Johnson, D. Schlenk, S. van Drunick. 2012. Life histories, salinity zones, and sublethal contributions of contaminants to pelagic fish declines illustrated with a case study of San Francisco Estuary, California, USA. *Estuaries and Coasts* 35:603-621.
- Brown, L.R. and D. Michniuk. 2007. Littoral fish assemblages of the alien-dominated Sacramento-San Joaquin Delta, California, 1980–1983 and 2001–2003. *Estuaries and Coasts* 30:186-200.
- Brown, L.R., and P.B. Moyle. 2005. Native fish communities of the Sacramento-San Joaquin watershed, California: a history of decline. Pages 75-98 *in* F. Rinne, R. Hughes, and R. Calamusso, editors. *Fish Communities of Large Rivers of the United States*. American Fisheries Society, Bethesda, Maryland.
- Brown, L.R., W.A. Bennett, R.W. Wagner, T. Morgan-King, N. Knowles, F. Feyrer, D.H. Schoellhamer, M.T. Stacey, M. Dettinger. 2013. Implications for future survival of Delta Smelt from four climate change scenarios for the Sacramento-San Joaquin Delta, California. *Estuaries and Coasts* 36:754-774.
- Brown, L.R., R. Baxter, G. Castillo, L. Conrad, S. Culberson, G. Erickson, F. Feyrer, S. Fong, K. Gehrts, L. Grimaldo, B. Herbold, J. Kirsch, A. Mueller-Solger, S. Slater, K. Souza, and E. Van Nieuwenhuysse. 2014. Synthesis of studies in the fall low-salinity zone of the San Francisco Estuary, September–December 2011. U.S. Geological Survey Scientific Investigations Report 2014–5041. 136 p.

- Brown, L.R., W. Kimmerer, J.L. Conrad, S. Lesmeister, and A. Mueller–Solger. 2016a. Food webs of the Delta, Suisun Bay, and Suisun Marsh: an update on current understanding and possibilities for management. *San Francisco Estuary and Watershed Science*, 14(3).
- Brown, L.R., L.M. Komoroske, R.W. Wagner, T. Morgan-King, J.T. May, R.E. Connon, and N.A. Fangue. 2016b. Coupled downscaled climate models and ecophysiological metrics forecast habitat compression for an endangered estuarine fish. PLOS ONE DOI:10.1371/journal.pone.0146724.
- Brown, T. 2009. Phytoplankton community composition: the rise of the flagellates. *IEP Newsletter* 22(3):20–28.
- Bush, E.E. 2017. Migratory life histories and early growth of the endangered estuarine Delta Smelt (*Hypomesus transpacificus*). University of California, Davis. Available at: DOI: 10.13140/RG.2.2.19204.42888
- California Fish and Game Commission. 2009. Final statement of reasons for regulatory action, Amend Title 14, CCR, Section 670.5, Re: uplisting the delta smelt to endangered species status: Sacramento, Calif., California Fish and Game Commission. 11 p., http://www.fgc.ca.gov/regulations/2009/670_5dsfsor.pdf.
- California Natural Resources Agency. 2016. Delta Smelt Resiliency Strategy. California Natural Resources Agency, Sacramento, CA. Available at: <https://resources.ca.gov/CNRALegacyFiles/docs/Delta-Smelt-Resiliency-Strategy-FINAL070816.pdf>
- Carey, C.C., B.W. Ibelings, E.P. Hoffmann, D.P. Hamilton, and J.D. Brookes. 2012. Eco-physiological adaptations that favor freshwater cyanobacteria in a changing climate. *Water Research* 46:1394-1407.
- Castillo, G.C., L.J. Damon, and J.A. Hobbs. 2018. Community patterns and environmental associations for pelagic fishes in a highly modified estuary. *Marine and Coastal Fisheries: Dynamics, Management, and Ecosystem Science* 10:508–524.
- Casulli, V. 2009. A high-resolution wetting and drying algorithm for free-surface hydrodynamics. *International Journal for Numerical Methods in Fluids* 60:391-408.
- Clarke, K.R., and R.M. Warwick. 2001. Change in marine communities: an approach to statistical analysis and interpretation, 2nd edition. PRIMER-E, Plymouth, UK.

- Cloern, J.E., and R. Dufford. 2005. Phytoplankton community ecology: principles applied in San Francisco Bay. *Marine Ecology Progress Series* 285:11-28.
- Cloern, J.E., and A.D. Jassby. 2008. Complex seasonal patterns of primary producers at the land–sea interface. *Ecology Letters* 11:1294-1303.
- Cloern, J.E., N. Knowles, L.R. Brown, D. Cayan, M.D. Dettinger, T.L. Morgan, T.L., D.H. Schoellhamer, M.T. Stacey, M. van der Wegen, R.W. Wagner, and A.D. Jassby. 2011. Projected evolution of California's San Francisco Bay-Delta-River system in a century of climate change. *PloS one*, 6(9), p.e24465.
- Codd, G.A. 2000. Cyanobacterial toxins, the perception of water quality, and the prioritization of eutrophication control. *Ecological Engineering* 16:51-60.
- Cohen, R.R., P.V. Dresler, E.J. Phillips, and R.L. Cory. 1984. The effect of the Asiatic clam, *Corbicula fluminea*, on phytoplankton of the Potomac River, Maryland. *Limnology and Oceanography* 29:170-180.
- Conomos, T.J. ed., 1979, San Francisco Bay: the urbanized estuary. Investigation into the natural history of San Francisco Bay and Delta with reference to the influence of man: San Francisco, California, Pacific Division American Association for the Advancement of Science, 493 p.
- Conrad, J.L., A.J. Bibian, K.L. Weinersmith, D. De Carion, M.J. Young, P. Crain, E.L. Hestir, M.J. Santos, and A. Sih. 2016. Novel species interactions in a highly modified estuary: association of Largemouth Bass with Brazilian waterweed *Egeria densa*. *Transactions of the American Fisheries Society* 145:249-263.
- Cushing, D. 1990. Plankton production and year-class strength in fish populations: an update of the match/mismatch hypothesis. Pages 249-293 in *Advances in marine biology*, volume 26. Elsevier.
- Damon, L.J., S.B. Slater, R.D. Baxter, and R.W. Fujimura. 2016. Fecundity and reproductive potential of wild female Delta Smelt in the upper San Francisco Estuary, California. *California Fish and Game* 102:188-210.
- Davis, B.E., M.J. Hansen, D.E. Cocherell, T.X. Nguyen, T. Sommer, R.D. Baxter, N.A. Fangué, and A.E. Todgham. 2019. Consequences of temperature and temperature variability on swimming activity, group structure, and predation of endangered delta smelt. *Freshwater Biology* 64:2156-2175.

- Dege, M., and L.R. Brown. 2004. Effect of outflow on spring and summertime distribution and abundance of larval and juvenile fishes in the upper San Francisco Estuary. *American Fisheries Society Symposium* 39:49–65.
- Deng, D-F., K. Zheng, F-C. Teh, P.W. Lehman, and S.J. Teh. 2010. Toxic threshold of dietary microcystin (-LR) for quart medaka. *Toxicon* 55:787-794.
- De Parsia, M., Woodward, E.E., Orlando, J.L., and Hladik, M.L., 2019, Pesticide mixtures in the Sacramento–San Joaquin Delta, 2016–17: Results from year 2 of the Delta Regional Monitoring Program: U.S. Geological Survey Data Series 1120, 33 p., <https://doi.org/10.3133/ds1120>.
- Dettinger, M., J. Anderson, M. Anderson, L.R. Brown, D. Cayan, and E. Maurer. 2016. Climate change and the Delta. *San Francisco Estuary and Watershed Science* 14(3).
- Downing, S., S.A. Banack, J.S. Metcalf, P.A. Cox, and T.G. Downing. 2011. Nitrogen starvation of cyanobacteria results in the production of β -N-methylamino-L-alanine. *Toxicon* 58:187-194.
- Dugdale, R.C., F.P. Wilkerson, V.E. Hogue, and A. Marchi. 2007. The role of ammonium and nitrate in spring bloom development in San Francisco Bay. *Estuarine, Coastal, and Shelf Science* 73:17–29.
- Durand, J., W. Fleenor, R. McElreath, M.J. Santos, and P. Moyle. 2016. Physical controls on the distribution of the submersed aquatic weed *Egeria densa* in the Sacramento–San Joaquin Delta and implications for habitat restoration. *San Francisco Estuary and Watershed Science* 14(1).
- Erkkila, L.F., J.W. Moffett, O.B. Cope, B.R. Smith, and R.S. Nelson. 1950. Sacramento-San Joaquin Delta fishery resources: effects of Tracy pumping plant and delta cross channels. Special Scientific Report, Fisheries 56, U.S. Fish and Wildlife Service, 109 p. Available at: <https://spo.nmfs.noaa.gov/content/sacramento-san-joaquin-delta-fishery-resources-effects-tracy-pumping-plant-and-delta-cross>
- Feyrer, F., M.L. Nobriga, and T.R. Sommer. 2007. Multidecadal trends for three declining fish species: habitat patterns and mechanisms in the San Francisco Estuary, California, USA. *Canadian Journal of Fisheries and Aquatic Sciences* 64:723-734.
- Feyrer, F., T. Sommer, and W. Harrell. 2006. Managing floodplain inundation for native fish: production dynamics of age-0 splittail in California’s Yolo Bypass. *Hydrobiologia* 573:213–226.

- Feyrer, F., L.R. Brown, R.L. Brown, and J.J. Orsi, eds. 2004. Early life history of fishes in the San Francisco Estuary and Watershed. American Fisheries Society Symposium 39, Bethesda, Maryland, American Fisheries Society, 296 p.
- Feyrer, F., B. Herbold, S.A. Matern, and P.B. Moyle. 2003. Dietary shifts in a stressed fish assemblage: consequences of a bivalve invasion in the San Francisco Estuary. *Environmental Biology of Fishes* 67:277-288.
- Feyrer, F., K. Newman, M. Nobriga, and T. Sommer. 2011. Modeling the effects of future outflow on the abiotic habitat of an imperiled estuarine fish. *Estuaries Coasts* 34:120–128. doi: <http://dx.doi.org/10.1007/s12237-010-9343-9>
- Fisch, K.M., J.M. Henderson, R.S. Burton, and B. May Bernie. 2011. Population genetics and conservation implications for the endangered delta smelt in the San Francisco Bay-Delta. *Conservation Genetics* 12:1421–1434.
- FLaSH Panel (Fall Low Salinity Habitat (FLaSH) Study Review Panel). 2012. Fall low salinity habitat (FLaSH) study synthesis – Year one of the Delta Fall Outflow Adaptive Management Plan, review panel summary report. Delta Science Program, Sacramento, CA. available at: http://deltacouncil.ca.gov/sites/default/files/documents/files/FallOutflowReviewPanelSummaryReport_Final_9_11.pdf.
- Flombaum, P., J.L. Gallegos, R.A. Gordillo, J. Rincón, L.L. Zabala, N. Jiao, D.M. Karl, W.K.W. Li, M.W. Lomas, D. Veneziano, C.S. Vera, J.A. Vrugt, and A.C. Martiny. 2013. Present and future global distributions of the marine cyanobacteria *Prochlorococcus* and *Synechococcus*. *Proceedings of the National Academy of Sciences of the United States of America* 110, 9824–9829.
- Foe, C., and A. Knight. 1985. The effect of phytoplankton and suspended sediment on the growth of *Corbicula fluminea* (Bivalvia). *Hydrobiologia* 127:105-115.
- Fong, S., S. Louie, I. Werner, J. Davis, and R.E. Connon. 2016. Contaminant effects on California Bay–Delta species and human health. *San Francisco Estuary and Watershed Science* 14(4).
- Frantzich, J., T. Sommer, and B. Schreier. 2018. Physical and biological responses to flow in a tidal freshwater slough complex. *San Francisco Estuary and Watershed Science* 16(1) <https://escholarship.org/uc/item/6s50h3fb>

- Garrett, J.D. 2012. Concentrations, loads, and yields of select constituents from major tributaries of the Mississippi and Missouri Rivers in Iowa, water years 2004–2008. U.S. Geological Survey Scientific Investigations Report, 5240, 72.
- Ger, K.A., S.J. Teh, and C.R. Goldman. 2009. Microcystin-LR toxicity on dominant copepods *Eurytemora affinis* and *Pseudodiaptomus forbesi* of the upper San Francisco Estuary. *Science of the Total Environment* 407:4852-4857.
- Ger, K.A., S.J. Teh, D.V. Baxa, S.H. Lesmeister, and C.R. Goldman. 2010. The effects of dietary *Microcystis aeruginosa* and microcystin on the copepods of the upper San Francisco Estuary. *Freshwater Biology* 55:1548-1559.
- Glibert, P.M. 2010. Long-term changes in nutrient loading and stoichiometry and their relationships with changes in the food web and dominant pelagic fish species in the San Francisco Estuary, California. *Reviews in Fisheries Science* 18:211-232.
- Goertler, P.A.L., T.R. Sommer, W.H. Satterthwaite, and B.M. Schreier. 2018. Seasonal floodplain-tidal slough complex supports size variation for juvenile Chinook salmon (*Oncorhynchus tshawytscha*). *Ecology of Freshwater Fish* 27:580-593.
- Greene, V.E., L.J. Sullivan, J.K. Thompson, and W.J. Kimmerer. 2011. Grazing impact of the invasive clam *Corbula amurensis* on the microplankton assemblage of the northern San Francisco Estuary. *Marine Ecology Progress Series* 431:183–193. doi: <http://dx.doi.org/10.3354/meps09099>
- Greenfield, B.K., G.S. Siemering, J.C. Andrews, M. Rajan, S.P. Andrews, and D.F. Spencer. 2007. Mechanical shredding of water hyacinth (*Eichhornia crassipes*): Effects on water quality in the Sacramento-San Joaquin River Delta, California. *Estuaries and Coasts* 30:627-640.
- Grillas, P., L. Tan Ham, A. Dutartre, and F. Mesleard. 1992. Distribution de *Ludwigia* en France: étude des causes de l'expansion récente en Camargue. 15ème conférence du COLUMA journées internationales sur la lutte contre les mauvaises herbes, Versailles, 2-4 décembre 1992, 1083–1090.
- Grimaldo, L.F., T. Sommer, N. Van Ark, G. Jones, E. Holland, P.B. Moyle, B. Herbold, and P. Smith. 2009. Factors affecting fish entrainment into massive water diversions in a tidal freshwater estuary: can fish losses be managed? *North American Journal of Fisheries Management* 29:1253-1270.

- Ha, K., E. Cho, H. Kim, and G. Joo. 1999. *Microcystis* bloom formation in the lower Nakdong River, South Korea, importance of hydrodynamics and nutrient loading. *Marine and Freshwater Research* 50:89-94.
- Hamilton, S.A., and D.D. Murphy. 2018. Analysis of limiting factors across the life cycle of delta smelt (*Hypomesus transpacificus*). *Environmental Management* 62:365-382.
- Hammock, B.G., R. Hartman, S.B. Slater, A. Hennessy, and S.J. Teh. 2019. Tidal wetlands associated with foraging success of Delta Smelt. *Estuaries and Coasts* 42. Available at: <https://link.springer.com/article/10.1007/s12237-019-00521-5>
- Hammock, B.G., J.A. Hobbs, S.B. Slater, S. Acuña, and S.J. Teh. 2015. Contaminant and food limitation stress in an endangered estuarine fish. *Science of the Total Environment* 532:316-326.
- Hammock, B.G., S.B. Slater, R.D. Baxter, N.A. Fangué, D. Cocherell, A. Hennessy, T. Kurobe, C.Y. Tai, and S.J. Teh. 2017. Foraging and metabolic consequences of semi-anadromy for an endangered estuarine fish. *PloS one*, 12(3), p.e0173497.
- Hanna, G.D. 1966. Introduced mollusks of western North America. *California Academy of Sciences Occasional Papers* 48:1-108.
- Harke, M.J., M.M. Steffen, C.J. Gobler, T.G. Otten, S.W. Wilhelm, S.A. Wood, and H.W. Paerl. 2016. A review of the global ecology, genomics, and biogeography of the toxic cyanobacterium, *Microcystis* spp. *Harmful Algae* 54:4-20.
- Hasenbein, M., L.M. Komoroske, R.E. Connon, J. Geist, and N.A. Fangué. 2013. Turbidity and salinity affect feeding performance and physiological stress in the endangered delta smelt. *Integrative and Comparative Biology* 53:620-634.
- Herbold, B., Baltz, D. M, Brown, L., Grossinger, R., Kimmerer, W., Lehman, P., et al. (2014). The Role of Tidal Marsh Restoration in Fish Management in the San Francisco Estuary. *San Francisco Estuary and Watershed Science*, 12(1). doi:<https://doi.org/10.15447/sfews.2014v12iss1art1> Retrieved from <https://escholarship.org/uc/item/1147j4nz>
- Hestir, E.L., D.H. Schoellhamer, T. Morgan-King, and S.L. Ustin. 2013. A step decrease in sediment concentration in a highly modified tidal river delta following the 1983 El Niño floods. *Marine Geology* 345:304-313.

- Hestir, E.L., D.H. Schoellhamer, J. Greenberg, T. Morgan-King, and S.L. Ustin. 2016. The effect of submerged aquatic vegetation expansion on a declining turbidity trend in the Sacramento-San Joaquin River Delta. *Estuaries and Coasts* 39:1100-1112.
- Hinton, D.E., P.C. Baumann, G.R. Gardner, W.E. Hawkins, J.D. Hendricks, R.A. Murchelano, M.S. Okihiro. 1992. Histopathologic biomarkers. In: Hugget, R.J., R.A. Kimerle, P.M. Mehrle, and H.L. Bergman (eds) *Biomarkers, biochemical, physiological, and histologic markers of anthropogenic stress*. Lewis, Boca Raton, FL, pp 155–209
- Hjort, J. 1914. Fluctuations in the great fisheries of northern Europe viewed in the light of biological research. ICES. 228 p.
- Hobbs, J.A., W.A. Bennett, J.E. Burton, and B. Baskerville-Bridges. 2007. Modification of the biological intercept model to account for ontogenetic effects in laboratory-reared delta smelt (*Hypomesus transpacificus*). *Fishery Bulletin* 105:30-38.
- Hobbs, J.A., C. Denney, L. Lewis, M. Willmes, W. Xieu, A. Schultz, O. Burgess. 2019c. Environmental and ontogenetic drivers of growth in a critically endangered species. Pages 123-146 in A. A. Schultz, editor. *Directed Outflow Project: Technical Report 1*. U.S. Bureau of Reclamation, Bay-Delta Office, Mid-Pacific Region, Sacramento, CA. November 2019, 318 pp.
- Hobbs, J.A., L.S. Lewis, M. Willmes, C. Denney, and E. Bush. 2019a. Complex life histories discovered in a critically endangered fish. *Scientific Reports* 9:1-12.
- Hobbs, J.A., C. Denney, L. Lewis, M. Willmes, A. Schultz, O. Burgess. 2019b. Exploring life history diversity of Delta Smelt during a period of extreme environmental variability. Pages 79-122 in A. A. Schultz, editor. *Directed Outflow Project: Technical Report 1*. U.S. Bureau of Reclamation, Bay-Delta Office, Mid-Pacific Region, Sacramento, CA. November 2019, 318 pp.
- Hollibaugh, J.T., ed. 1996. *San Francisco Bay: the ecosystem*. San Francisco, California, Pacific Division American Association for the Advancement of Science, 542 p.
- Houde, E. 1989a. Subtleties and episodes in the early life of fishes. *Journal of Fish Biology* 35(sA):29-38.
- Houde, E.D. 1989b. Comparative growth, mortality, and energetics of marine fish larvae: temperature and implied latitudinal effects. *Fishery Bulletin* 87:471-495.

- ICES (International Council for the Exploration of the Sea), 1997. ICES review of the status of biological effects techniques relative to their potential application programmes. ICES Cooperative Research Report, No. 222, pp. 12–20.
- Ibelings, B.W., and K.E. Havens. 2008. Cyanobacterial toxins, a qualitative meta-analysis of concentrations, dosage and effects in freshwater estuarine and marine biota. Cyanobacterial harmful algal blooms, state of the science and research needs. *Advances in Experimental Medicine and Biology* 619:675–732.
- IEP-MAST. 2015. An updated conceptual model of Delta Smelt biology: our evolving understanding of an estuarine fish. Interagency Ecological Program: Management, Analysis and Synthesis Team, Sacramento, CA. 205 p.
- International Agency for Research on Cancer. 2006. Carcinogenicity of nitrate, nitrite and cyanobacterial peptide toxins. *The Lancet Oncology* 7:628-629.
- Jassby, A.D. 2008. Phytoplankton in the upper San Francisco Estuary: recent biomass trends, their causes and their trophic significance. *San Francisco Estuary and Watershed Science* 6(1).
- Jassby, A.D., J.E. Cloern, and B.E. Cole. 2002. Annual primary production: Patterns and mechanisms of change in a nutrient-rich tidal ecosystem. *Limnology and Oceanography* 47:698-712.
- Jassby, A.D., J.E. Cloern, and T.M. Powell. 1993. Organic carbon sources and sinks in San Francisco Bay: variability induced by river flow. *Marine Ecology Progress Series* 1993:39-54.
- Jassby, A.D., W.J. Kimmerer, S.G. Monismith, C. Armor, J.E. Cloern, T.M. Powell, J.R. Schubel, and T.J. Vendlinski. 1995. Isohaline position as a habitat indicator for estuarine populations. *Ecological Applications* 5:272-289.
- Jeffries, K.M., N.A. Fanguie, and R.E. Connon. 2018. Multiple sub-lethal thresholds for cellular responses to thermal stressors in an estuarine fish. *Comparative Biochemistry and Physiology Part A: Molecular & Integrative Physiology* 225:33-45.
- Jeffries, K.M., R.E. Connon, B.E. Davis, L.M. Komoroske, M.T. Britton, T. Sommer, A.E. Todgham, and N.A. Fanguie. 2016. Effects of high temperatures on threatened estuarine fishes during periods of extreme drought. *Journal of Experimental Biology* 219:1705-1716.
- Kayfetz, K., and W.J. Kimmerer. 2017. Abiotic and biotic controls on the copepod *Pseudodiaptomus forbesi* in the upper San Francisco Estuary. *Marine Ecology Progress Series* 581:85-101.

- Khanna, S., M.J. Santos, E.L. Hestir, and S.L. Ustin. 2012. Plant community dynamics relative to the changing distribution of a highly invasive species, *Eichhornia crassipes*: a remote sensing perspective. *Biological Invasions* 14:717-733.
- Khanna, S., M.J. Santos, J.D. Boyer, K.D. Shapiro, J. Bellvert, and S.L. Ustin. 2018. Water primrose invasion changes successional pathways in an estuarine ecosystem. *Ecosphere* 9(9):e02418 doi: 10.1002/ecs2.2418.
- Kim, Y., J. Jeon, M.S. Kwak, G.H. Kim, I. Koh, and M. Rho. 2018. Photosynthetic functions of *Synechococcus* in the ocean microbiomes of diverse salinity and seasons. *PLoS ONE* 13(1): e0190266. <https://doi.org/10.1371/journal.pone.0190266>
- Kimmerer, W.J. 2002. Effects of freshwater flow on abundance of estuarine organisms: physical effects or trophic linkages? *Marine Ecology Progress Series* 243:39-55.
- Kimmerer, W. 2005. Long-term changes in apparent uptake of silica in the San Francisco estuary. *Limnology and Oceanography* 50:793-798.
- Kimmerer, W.J. 2006. Response of anchovies dampens effects of the invasive bivalve *Corbula amurensis* on the San Francisco Estuary foodweb. *Marine Ecology Progress Series* 324:207-218.
- Kimmerer, W.J. and L. Lougee. 2015. Bivalve grazing causes substantial mortality to an estuarine copepod population. *Journal of Experimental Marine Biology and Ecology* 473:53-63.
- Kimmerer, W.J., E. Gartside, and J.J. Orsi. 1994. Predation by an introduced clam as the likely cause of substantial declines in zooplankton of San Francisco Bay. *Marine Ecology Progress Series* 113:81-93.
- Kimmerer, W.J., E.S. Gross, and M.L. MacWilliams. 2009. Is the response of estuarine nekton to freshwater flow in the San Francisco Estuary explained by variation in habitat volume? *Estuaries and Coasts* 32:375.
- Kimmerer, W.J., M.L. MacWilliams, and E. Gross. 2013. Variation of fish habitat and extent of the low-salinity zone with freshwater flow in the San Francisco Estuary. *San Francisco Estuary and Watershed Science*, 11(4). Available at: <http://escholarship.org/uc/item/3pz7x1x8>.
- Kimmerer, W.J., T.R. Ignoffo, K.R. Kayfetz, and A.M. Slaughter. 2018. Effects of freshwater flow and phytoplankton biomass on growth, reproduction, and spatial subsidies of the estuarine copepod *Pseudodiaptomus forbesi*. *Hydrobiologia* 807:113-30.

- Kimmerer, W.J., E.S. Gross, A.M. Slaughter, and J.R. Durand. 2019. Spatial subsidies and mortality of an estuarine copepod revealed using a box model. *Estuaries and Coasts*, 42:218-236.
- Kimmerer, W.J., and J.K. Thompson. 2014. Phytoplankton Growth Balanced by Clam and Zooplankton Grazing and Net Transport into the Low-Salinity Zone of the San Francisco Estuary. *Estuaries and Coasts* 37:1202-1218.
- Komoroske, L.M., R.E. Connon, K.M. Jeffries, and N.A. Fangué. 2015. Linking transcriptional responses to organismal tolerance reveals mechanisms of thermal sensitivity in a mesothermal endangered fish. *Molecular Ecology* 24:4960–4981.
- Komoroske, L.M., R.E. Connon, J. Lindberg, B.S. Cheng, G. Castillo, M. Hasenbein, and N.A. Fangué. 2014. Ontogeny influences sensitivity to climate change in an endangered fish. *Conservation Physiology* 2:cou008.
- Komoroske, L.M., K.M. Jeffries, R.E. Connon, J. Dexter, M. Hasenbein, C. Verhille, and N.A. Fangué. 2016. Sublethal salinity stress contributes to habitat limitation in an endangered estuarine fish. *Evolutionary Applications* 9:963-981.
- Kurobe, T., D.V. Baxa, C.E. Mioni, R.M. Kudela, T.R. Smythe, S. Waller, A.D. Chapman, and S.J. Teh. 2013. Identification of harmful cyanobacteria in the Sacramento-San Joaquin Delta and Clear Lake, California by DNA barcoding. *SpringerPlus* 2: 491.
- Kurobe, T., P.W. Lehman, M.E. Haque, T. Sedda, S. Lesmeister, and S. Teh. 2018. Evaluation of water quality during successive severe drought years within *Microcystis* blooms using fish embryo toxicity tests for the San Francisco Estuary. *Science of the Total Environment* 610-611:1029-1037.
- Kurobe, T., M.O. Park, A. Javidmehr, F. The, S. Acuna, C.J. Corbin, A.J. Conley, W.A. Bennett, and S.J. The. 2016. Assessing oocyte development and maturation in the threatened Delta Smelt, *Hypomesus transpacificus*. *Environmental Biology of Fishes* 99:423-432.
- Leggett, W., and E. Deblois. 1994. Recruitment in marine fishes: is it regulated by starvation and predation in the egg and larval stages? *Netherlands Journal of Sea Research* 32:119-134.
- Lehman, P.W. 1996. Changes in chlorophyll a concentration and phytoplankton community composition with water year type in the upper San Francisco Bay estuary. In J. T. Hollibaugh (ed.), *San Francisco Bay: The Ecosystem*. Pac. Div., Amer. Assoc. Adv. Sci.

- Lehman, P.W. 2000. The influence of climate on phytoplankton community carbon in San Francisco Bay Estuary. *Limnology and Oceanography* 45:580-590.
- Lehman, P. W. 2004. The influence of climate on mechanisms that affect lower food web production in estuaries. *Estuaries* 27:312-325.
- Lehman, P.W., T. Kurobe, S.J. Teh. In press. Impact of extreme wet and dry years on the persistence of *Microcystis* harmful algal blooms in San Francisco Estuary. *Quaternary International*.
- Lehman, P.W., G. Boyer, C. Hall, S. Waller, and K. Gehrts. 2005. Distribution and toxicity of a new colonial *Microcystis aeruginosa* bloom in the San Francisco Bay Estuary, California. *Hydrobiologia* 541: 87-90.
- Lehman, P. W., G. Boyer, M. Satchwell and S. Waller. 2008. The influence of environmental conditions on the seasonal variation of *Microcystis* cell density and microcystins concentration in San Francisco Estuary. *Hydrobiologia* 600:187-204.
- Lehman, P.W., T. Kurobe, S. Lesmeister, D. Baxa, A. Tung, S.J. Teh. 2017. Impacts of the 2014 severe drought on the *Microcystis* bloom in San Francisco Estuary. *Harmful Algae* 63:94-108.
- Lehman, P.W., T. Kurobe, S. Lesmeister, C. Lam, A. Tung, M. Xiong, and S.J. Teh. 2018. Strong differences characterize *Microcystis* blooms between successive severe drought years in the San Francisco Estuary, California, USA. *Aquatic Microbial Ecology* 81(3):293-299.
- Lehman, P.W., K. Marr, G.L. Boyer, S. Acuña, and S.J. Teh. 2013. Long-term trends and causal factors associated with *Microcystis* abundance and toxicity in San Francisco Estuary and implications for climate change impacts. *Hydrobiologia* 718: 141-158.
- Lehman, P.W., S.J. Teh, G.L. Boyer, M. Nobriga, E. Bass, and C. Hogle. 2010. Initial impacts of *Microcystis* on the aquatic food web in the San Francisco Estuary. *Hydrobiologia* 637: 229-248.
- Light, T., T. Grosholz, and P. Moyle. 2005. Delta ecological survey (Phase I): Non-indigenous aquatic species in the Sacramento–San Joaquin Delta, a literature review. Final report for agreement DCN 1113322J011. US Fish and Wildlife Service. Stockton, CA.
<https://www.anstaskforce.gov/EcoSurveys/DeltaSurveyFinalReport.pdf>
- Lindberg, J.C., G. Tigan, L. Ellison, T. Rettinghouse, M.M. Nagel, and K.M. Fisch. 2013. Aquaculture methods for a genetically managed population of endangered Delta Smelt. *North American Journal of Aquaculture* 75:186-196.

- Lopez, C.B., J.E. Cloern, T.S. Schraga, A.J. Little, L.V. Lucas, J.K. Thompson, and J.R. Burau. 2006. Ecological values of shallow-water habitats: implications for the restoration of disturbed ecosystems. *Ecosystems* 9:422-440.
- Lott J. 1998. Feeding habits of juvenile and adult delta smelt from the Sacramento–San Joaquin River Estuary. Interagency Ecological Program for the Sacramento–San Joaquin Estuary. IEP newsletter 11(1):14–19. Sacramento (CA): California Department of Water Resources. Available from: <http://www.water.ca.gov/iep/newsletters/1998/IEP-winter-1998.cfm>
- Lotze, H.K., H.S. Lenihan, B.J. Bourque, R.H. Bradbury, R.G. Cooke, M.C. Kay, S.M. Kidwell, M.X. Kirby, C.H. Peterson, and J.B.C. Jackson. 2006, Depletion, degradation, and recovery potential of estuaries and coastal seas. *Science* 312:1806–1809.
- Lucas, L.V. and J.K. Thompson. 2012. Changing restoration rules: exotic bivalves interact with residence time and depth to control phytoplankton productivity. *Ecosphere* 3:1-26.
- Lucas, L.V., J.E. Cloern, J.K. Thompson, and N.E. Monsen. 2002. Functional variability of habitats within the Sacramento-San Joaquin Delta: restoration implications. *Ecological Applications* 12:1528-1547.
- Lucas, L.V., J.K. Thompson, and L.R. Brown. 2009. Why are diverse relationships observed between phytoplankton biomass and transport time? *Limnology and Oceanography* 54:381-390.
- Lung W.-S, and H.W. Paerl. 1988. Modeling blue-green algal blooms in the lower Neuse River. *Water Research* 22:895–905.
- Mac Nally, R., J.R. Thompson, W.J. Kimmerer, F. Feyrer, K.B. Newman, A. Sih, W.A. Bennett, L. Brown, E. Fleishman, S.D. Culberson, and G. Castillo. 2010, An analysis of pelagic species decline in the upper San Francisco Estuary using multivariate autoregressive modeling (MAR). *Ecological Applications* 20:1417–1430.
- MacWilliams, M.L., and E.S. Gross. 2010. UnTRIM San Francisco Bay–Delta Model sea level rise scenario modeling report, Bay–Delta Conservation Plan. Prepared for Science Applications International Corporation and California Department of Water Resources. 562 p. Available at: https://www.waterboards.ca.gov/waterrights/water_issues/programs/bay_delta/california_waterfix/exhibits/exhibit4/docs/Public_Draft_BDCP_EIR-EIS_Appendix_5A_-_Section_D_-_Attachment_3.sflb.pdf

- MacWilliams, M.L., F.G. Salcedo, and E.S. Gross. 2008. San Francisco Bay-Delta UnTRIM Model Calibration Report, POD 3-D Particle Tracking Modeling Study. Prepared for the California Department of Water Resources. December 19, 2008. Available at:
http://www.snugharbor.net/images-2015/barriers/docs/2007UnTRIM_Calibration_Report.pdf
- MacWilliams, M.L., A.J. Bever, E.S. Gross, G.S. Ketefian, and W.J. Kimmerer. 2015. Three-dimensional modeling of hydrodynamics and salinity in the San Francisco estuary: An evaluation of model accuracy, X2, and the low-salinity zone. *San Francisco Estuary and Watershed Science* 13(1).
<https://doi.org/10.15447/sfews.2015v13iss1art2>.
- Mager, R.C., S.I. Doroshov, J.P. van Eenennaam, and R.L. Brown. 2004. Early life stages of delta smelt. In: Feyrer F, Brown LR, Orsi JJ, editors. Early life history of fishes in the San Francisco Estuary and watershed. Symposium 39. Bethesda (MD): American Fisheries Society. p. 169–180.
- Mahardja, B., Conrad, J.L., Lusher, L. and Schreier, B. 2016. Abundance trends, distribution, and habitat associations of the invasive Mississippi Silverside (*Menidia audens*) in the Sacramento–San Joaquin Delta, California, USA. *San Francisco Estuary and Watershed Science*, 14(1).
- Mahardja, B., M.J. Farruggia, B. Schreier, and T. Sommer. 2017. Evidence of a shift in the littoral fish community of the Sacramento-San Joaquin Delta. *PLoS ONE* 12(1): e0170683
- Mahardja, B., J.A. Hobbs, N. Ikemiyagi, A. Benjamin, and A.J. Finger. 2019. Role of freshwater floodplain-tidal slough complex in the persistence of the endangered delta smelt. *PLoS ONE* 14(1): e0208084
- Mallatt, J. 1985. Fish gill structural changes induced by toxicants and other irritants: a statistical review. *Can. J. Fish. Aquat. Sci.* 42:630-648.
- Manly, B.J.F., and M.A. Chotkowski, 2006. Two new methods for regime change analysis. *Archiv für Hydrobiologie* 167:593–607.
- Manly, B.F.J., D. Fullerton, A.N. Hendrix, and K.P. Burnham. 2015. Comments on Feyrer et al. “modeling the effects of future outflow on the abiotic habitat of an imperiled estuarine fish”. *Estuaries and Coasts* 38:1815-1820.
- Merz, J.E., S. Hamilton, P.S. Bergman, and B. Cavallo. 2011. Spatial perspective for delta smelt: a summary of contemporary survey data. *California Fish and Game* 97(4):164–189.

- Miller, W.J., B.F.J. Manly, D.D. Murphy, D. Fullerton, and R.R. Ramey. 2012. An investigation of factors affecting the decline of delta smelt (*Hyposmesus transpacificus*) in the Sacramento-San Joaquin Estuary. *Rev Fish Sci* 20:1–19. doi: <http://dx.doi.org/10.1080/10641262.2011.634930>
- Miller M.A., R.M. Kudela, A. Mekebri, D. Crane, S.C. Oates, M.T. Tinker, M. Staedler, W.A. Miller, S. Toy-Choutka, C. Dominik, D. Hardin, G. Langlois, M. Murray, K. Ward, and D.A. Jessup. 2010. Evidence for a novel marine harmful algal bloom, cyanotoxin (microcystin) transfer from land to sea otters. *PLoS ONE* 5: e12576.
- Morrongiello, J.R., and R.E. Thresher. 2015. A statistical framework to explore ontogenetic growth variation among individuals and populations: a marine fish example. *Ecological Monographs* 85:93-115.
- Morgan-King, T.L. and D.H. Schoellhamer. 2013. Suspended-sediment flux and retention in a backwater tidal slough complex near the landward boundary of an estuary. *Estuaries and Coasts* 36:300-318.
- Morris, T., and M. Civiello. 2013. *Microcystis aeruginosa* status and trends during the Fall Midwater Trawl Survey and a comparison to trends in the Summer Towntnet Survey. Interagency Ecological Program for the Sacramento-San Joaquin Estuary Newsletter 26(2): 33-39.
- Moyle, P.B., and W.A. Bennett. 2008. The future of the Delta ecosystem and its fish, Technical appendix D, in Lund, J., E. Hanak, W. Fleenor, W. Bennett, R. Howitt, J. Mount, and P. Moyle, eds., *Comparing Futures for the Sacramento-San Joaquin Delta: San Francisco, California*, Public Policy Institute of California, 46 p., http://www.ppic.org/content/pubs/other/708ehr_appendixd.pdf.
- Moyle, P.B., J.A. Hobbs, and J.R. Durand. 2018. Delta Smelt and water politics in California. *Fisheries* 43(1):42-50.
- Moyle, P.B., W.A. Bennett, W.E. Fleenor, and W.E. Lund, J.R. 2010, Habitat variability and complexity in the upper San Francisco Estuary. *San Francisco Estuary and Watershed Science* 8(3). available at <http://escholarship.org/uc/item/0kf0d32x>.
- Moyle, P.B., L.R. Brown, J.R. Durand, and J.A. Hobbs. 2016. Delta Smelt: life history and decline of a once-abundant species in the San Francisco Estuary. *San Francisco Estuary and Watershed Science* 14.

- Moyle, P.B., B. Herbold, D.E. Stevens, and L.W. Miller. 1992. Life-history and status of Delta Smelt in the Sacramento-San-Joaquin Estuary, California. *Transactions of the American Fisheries Society* 121:67-77.
- Munn, M.D., J.W. Frey, A.J. Tesoriero, R.W. Black, J.H. Duff, K. Lee, T.R. Maret, C.A. Mebane, I.R. Waite, and R.B. Zelt. 2018. Understanding the influence of nutrients on stream ecosystems in agricultural landscapes: U.S. Geological Survey Circular 1437, 80 p., <https://doi.org/10.3133/cir1437>.
- Mueller-Solger, A.B., A.D. Jassby, and D.C. Mueller-Navarra. 2002. Nutritional quality of food resources for zooplankton (*Daphnia*) in a tidal freshwater system (Sacramento-San Joaquin River Delta). *Limnology and Oceanography* 47:1468–1476.
- Murphy, D.D., and S.A. Hamilton. 2013. Eastward migration or marshward dispersal: Exercising survey data to elicit an understanding of seasonal movement of delta smelt. *San Francisco Estuary and Watershed Science* 11(3).
- Murphy, J.C., R.M. Hirsch, and L.A. Sprague. 2014. Antecedent flow conditions and nitrate concentrations in the Mississippi River Basin. *Hydrology and Earth System Sciences* 18:967-979.
- Myers, M.S., L.L. Johnson, O.P. Olson, C.M. Stehr, B.H. Horness, T.K. Collier, and B. McCain. 1998. Toxicopathic hepatic lesions as biomarkers of chemical contaminant exposure and effects in marine bottomfish species from the northeast and pacific coasts, USA. *Mar. Pollut. Bull.* 37:92–113.
- National Research Council. 2012. Sustainable water and environmental management in the California Bay-Delta. National Research Council, Washington, D.C., The National Academies Press, 280 p., http://www.nap.edu/catalog.php?record_id=13394.
- Neuheimer, A.B. 2019. The pace of life: Time, temperature, and a biological theory of relativity. [bioRxiv:609446](https://doi.org/10.1101/394446).
- Neuheimer, A., R. Thresher, J. Lyle, and J. Semmens. 2011. Tolerance limit for fish growth exceeded by warming waters. *Nature Climate Change* 1(2):110. 3364
- Nichols, F.H., J. K. Thompson, and L.E. Schemel. 1990. Remarkable invasion of San Francisco Bay (California, USA) by the Asian clam *Potamocorbula amurensis*. 2. Displacement of a former community. *Marine Ecology Progress Series* 66:95-101.
- Nichols, F.H., J.E. Cloern, S.N. Luoma, and D.H. Peterson. 1986. The modification of an estuary. *Science* 231(4738):567-573.

- Nobriga ML. 2002. Larval delta smelt diet composition and feeding incidence: environmental and ontogenetic influences. *Calif Fish Game* 88:149–164. Available from:
http://www.water.ca.gov/aes/docs/Nobriga_2002.pdf
- Nobriga, M.L., and F. Feyrer. 2007. Shallow-water piscivore-prey dynamics in California's Sacramento–San Joaquin Delta. *San Francisco Estuary and Watershed Science* 5(2).
- Nobriga, M.L., T.R. Sommer, F. Feyrer, and K. Fleming. 2008. Long-term trends in summertime habitat suitability for delta smelt, *Hypomesus transpacificus*. *San Francisco Estuary and Watershed Science* 6(1). <http://escholarship.org/uc/item/5xd3q8tx>.
- O’Neil, J.M., T.W. Davis, M.A. Burford, and C.J. Gobler. 2012. The rise of harmful cyanobacteria blooms: The potential roles of eutrophication and climate change. *Harmful Algae* 14:313–334.
- Orsi, J.J. and W.L. Mecum. 1996. Food limitation as the probable cause of a long-term decline in the abundance of *Neomysis mercedis* the opossum shrimp in the Sacramento-San Joaquin Estuary. In *San Francisco Bay: The ecosystem*, ed. J.T. Hollibaugh, 375-401. San Francisco: Pacific Division of the American Association for the Advancement of Science.
- Paganini, A., W.J. Kimmerer, and J.H. Stillman. 2010. Metabolic responses to environmental salinity in the invasive clam *Corbula amurensis*. *Aquatic Biology* 11:139–147. doi:
<http://dx.doi.org/10.3354/ab00304>
- Penfound, W.T. and T.T. Earle. 1948. The biology of the water hyacinth. *Ecological Monographs* 18(4):447-472.
- Peterson, M.S. 2003. Conceptual view of the environment-habitat-production linkages in tidal river estuaries. *Reviews in Fisheries Science* 11:291–313.
- Peterson, H.A. and M. Vayssières. 2010. Benthic assemblage variability in the upper San Francisco Estuary: A 27-year retrospective. *San Francisco Estuary and Watershed Science* 8(1).
- Polansky, L., K.B. Newman, M.L. Nobriga, and L. Mitchell. 2018. Spatiotemporal models of an estuarine fish species to identify patterns and factors impacting their distribution and abundance. *Estuaries and Coasts* 41:572-81.
- Poleksic, V. and V. Mitrovic-Tutundzic, 1994. Fish gills as a monitor of sublethal and chronic effects of pollution. In: *Sublethal and Chronic Effects of Pollutants on Freshwater Fish* (ed. by R. Muller & R. Lloyd), pp. 339-352. FAO, Fishing News Books, Oxford.

- Prokopovich, N.P. 1969. Deposition of clastic sediments by clams. *Journal of Sedimentary Petrology* 30:891-901.
- Radtke, L.D. 1966. Distribution of smelt, juvenile sturgeon, and starry flounder in the Sacramento-San Joaquin Delta. California Department of Fish and Game, Fish Bulletin 136:115–129.
- Robson, B.J., and D.P. Hamilton. 2003. Summer flow event induces a cyanobacterial bloom in a seasonal Western Australia estuary. *Marine and Freshwater Research* 54:139-151.
- Rocha, C., H. Galvão, and A. Barbosa. 2002. Role of transient silicon limitation in the development of cyanobacteria blooms in the Guadiana estuary, south-western Iberia. *Marine Ecology Progress Series* 228: 35-45.
- Rose, K.A., W.J. Kimmerer, K.P Edwards, and W.A. Bennett. 2013a. Individual-based modeling of Delta Smelt population dynamics in the upper San Francisco Estuary: I. Model description and baseline results. *Transactions of the American Fisheries Society* 142:1238-1259.
- Rose, K.A., W.J. Kimmerer, K.P Edwards, and W.A. Bennett. 2013b. Individual-based modeling of Delta Smelt population dynamics in the upper San Francisco Estuary: II. Alternative baselines and good versus bad years. *Transactions of the American Fisheries Society* 142:1260-1272.
- Ruhl, C.A., and D.H. Schoellhamer. 1999. Time series of suspended-solids concentration in Honker Bay during water year 1997 (pp. 82-92). San Francisco Estuary Regional Monitoring Program for Trace Substances.
- Ruhl, C.A. and D.H. Schoellhamer. 2004. Spatial and temporal variability of suspended-sediment concentrations in a shallow estuarine environment. *San Francisco Estuary and Watershed Science* 2(2).
- Sampson, S.J., J.H. Chick, and M.A. Pegg. 2009. Diet overlap among two Asian carp and three native fishes in backwater lakes on the Illinois and Mississippi rivers. *Biological Invasions* 11:483-496.
- Sansalone, J.J., and S.G. Buchberger. 1997. Partitioning and first flush of metals in urban roadway storm water. *Journal of Environmental Engineering* 123:134-143.
- Santos, M.J., S. Khanna, E.L. Hestir, M.E. Andrew, S.S. Rajapakse, J.A. Greenberg, L.W. Anderson, and S.L. Ustin. 2009. Use of hyperspectral remote sensing to evaluate efficacy of aquatic plant management. *Invasive Plant Science and Management* 2:216-229.

- Schoellhamer, D.H. 2011. Sudden clearing of estuarine waters upon crossing the threshold from transport to supply regulation of sediment transport as an erodible sediment pool is depleted: San Francisco Bay, 1999. *Estuaries and Coasts* 34:885–899.
- Schreier, B.M., M.R. Baerwald, J.L. Conrad, G. Schumer, and B. May. 2016. Examination of predation on early life stage Delta Smelt in the San Francisco estuary using DNA diet analysis. *Transactions of the American Fisheries Society* 145:723-733.
- Schultz, A. A., editor. 2019. Directed Outflow Project: Technical Report 1. U.S. Bureau of Reclamation, Bay-Delta Office, Mid-Pacific Region, Sacramento, CA. November 2019, 318 pp. Available at: <https://www.usbr.gov/mp/bdo/docs/directedoutflowproject-techreport1-final-121619.pdf>
- Schultz, A.A., L. Grimaldo, J. Hassrick, A. Kalmbach, A. Smith, O. Burges, D. Barnard, J. Brandon. 2019. Effect of isohaline (X2) and region on Delta Smelt habitat, prey and distribution during summer and fall: insights into managed flow actions in a highly modified estuary.. Pages 322-402 in A. A. Schultz, editor. Directed Outflow Project: Technical Report 1. U.S. Bureau of Reclamation, Bay-Delta Office, Mid-Pacific Region, Sacramento, CA. November 2019, 318 pp. Available at: <https://www.usbr.gov/mp/bdo/docs/directedoutflowproject-techreport1-final-121619.pdf>
- Schwaiger, J., R. Wanke, S. Adam, M. Pawert, W. Honnen, and R. Triebkorn. 1997. The use of histopathological indicators to evaluate contaminant-related stress in fish. *Journal of Aquatic Ecosystem Stress and Recovery* 6:75–86.
- Sellner K G, R.V. Lacouture, K.G. Parlish. 1988. Effect of increasing salinity on a cyanobacteria bloom in the Potomac River Estuary. *Journal of Plankton Research* 10:49–61.
- Slater, S.B., and R.D. Baxter. 2014. Diet, prey selection and body condition of age-0 Delta Smelt, *Hypomesus transpacificus*, in the upper San Francisco Estuary. *San Francisco Estuary and Watershed Science* 12(3).
- Slater, S.B., A. Schultz, B.G. Hammock, A. Hennessy, and C. Burdi. 2019. Patterns of zooplankton consumption by juvenile and adult Delta Smelt (*Hypomesus transpacificus*). Pages 9-54 in A. A. Schultz, editor. Directed Outflow Project: Technical Report 1. U.S. Bureau of Reclamation, Bay-Delta Office, Mid-Pacific Region, Sacramento, CA. November 2019, 318 pp.

- Sobczak, W.V., J.E. Cloern, A.D. Jassby, and A.B. Muller-Solger. 2002. Bioavailability of organic matter in a highly disturbed estuary: The role of detrital and algal resources. *Proceedings of the National Academy of Sciences of the United States of America* 99:8101–8105.
- Sommer, T., F. Mejia. 2013. A place to call home: a synthesis of Delta Smelt habitat in the upper San Francisco Estuary. *San Francisco Estuary and Watershed Science* 11(2).
- Sommer, T.R., W.C. Harrell, M.L. Nobriga, and R. Kurth. 2003. Floodplain as habitat for native fish: Lessons from California's Yolo Bypass, in Faber, P.M., ed., *California riparian systems: Processes and floodplain management, ecology, and restoration*, 2001 Riparian Habitat and Floodplains Conference Proceedings: Riparian Habitat Joint Venture, Sacramento, California, p. 81–87.
- Sommer, T., M.L. Nobriga, W.C. Harrell, W. Batham, and W.J. Kimmerer. 2001. Floodplain rearing of juvenile chinook salmon: evidence of enhanced growth and survival: *Canadian Journal of Fisheries and Aquatic Sciences* 58:325–333.
- Sommer, T., C. Armor, R. Baxter, R. Breuer, L. Brown, M. Chotkowski, S. Culberson, F. Feyrer, M. Gingras, B. Herbold, W. Kimmerer, A. Mueller-Solger, M. Nobriga, and K. Souza. 2007. The collapse of pelagic fishes in the upper San Francisco Estuary. *Fisheries* 32(6):270–277.
- Sommer, T., F.H. Mejia, M.L. Nobriga, F. Feyrer, and L. Grimaldo. 2011. The spawning migration of delta smelt in the upper San Francisco Estuary. *San Francisco Estuary and Watershed Science* 9(2). <http://www.escholarship.org/uc/item/86m0g5sz>.
- Stevens, D.E., and L.W. Miller. 1983. Effects of river flow on abundance of young Chinook salmon, American shad, longfin smelt, and delta smelt in the Sacramento-San Joaquin River system. *North American Journal of Fisheries Management* 3:425–437.
- Sullivan, L., T.R. Ignoffo, B. Baskerville-Bridges, D.J. Ostrach, and W. Kimmerer. 2016. Prey selection of larval and juvenile planktivorous fish: impacts of introduced prey. *Environmental Biology of Fishes* 99:633-646.
- Swanson, C., T. Reid, P.S. Young, and J.J. Cech, Jr. 2000. Comparative environmental tolerances of threatened delta smelt (*Hypomesus transpacificus*) and introduced wakasagi (*H. nipponensis*) in an altered California estuary. *Oecologia* 123:384–390.

- Teh, S., S. Adams, and D. Hinton. 1997. Histopathologic biomarkers of anthropogenic stress in resident redbreast sunfish (*Lepomis auritus*) and largemouth bass (*Micropterus salmoides* lacèpède) from contaminant impacted sites. *Aquatic Toxicology* 37:51-70.
- Teh, S. J., A.A. Schultz, W. Ramirez-Duarte, S. Acuña, D.M. Barnard, R.D. Baxter and B.H. Hammock. 2019. Histological analysis of 7 year-classes of Delta Smelt. Pages 55-78 in A.A. Schultz, editor. Directed Outflow Project: Technical Report 1. U.S. Bureau of Reclamation, Bay-Delta Office, Mid-Pacific Region, Sacramento, CA. November 2019, 318 pp.
- Tempel, T. 2017. Evaluation of adding index stations in calculating the 20-mm Survey Delta Smelt abundance index. IEP Newsletter 30(1):21-23.
<https://nrm.dfg.ca.gov/FileHandler.ashx?DocumentId=151850&inline>
- Tempel, T. 2018a. The 2018 20-mm Survey Delta Smelt Index. California Department of Fish and Wildlife memo to Gregg Erickson. 08/09/2018.
<https://www.wildlife.ca.gov/Conservation/Delta/20mm-Survey/Bibliography>
- Tempel, T. 2018b. 2018 20-mm Survey Delta Smelt Index of relative abundance supplemental documentation. California Department of Fish and Wildlife memo to Gregg Erickson. 10/09/2018.
<https://www.wildlife.ca.gov/Conservation/Delta/20mm-Survey/Bibliography>.
- The State of the Estuary Partnership. 2015. The State of the Estuary 2015: Status and trends updates on 33 indicators of ecosystem health. A report from the San Francisco Estuary Partnership. Available at: http://www.sfestuary.org/wp-content/uploads/2015/10/SOTER_2.pdf.
- Thomson, J.R., W.J. Kimmerer, L.R. Brown, K.B. Newman, R. Mac Nally, W.A. Bennett, F. Feyrer, and E. Fleishman. 2010. Bayesian change-point analysis of abundance trends for pelagic fishes in the upper San Francisco Estuary. *Ecological Applications* 20:1431–1448.
- Toft, J.D., C.A. Simenstad, J.R. Cordell, and L.F. Grimaldo. 2003. The effects of introduced water hyacinth on habitat structure, invertebrate assemblages, and fish diets. *Estuaries* 26:746-758.
- Tonk, L., K. Bosch, P.M. Visser, and J. Huisman. 2007. Salt tolerance of the harmful cyanobacterium *Microcystis aeruginosa*. *Aquatic Microbial Ecology* 46:117-123.
- U.S. Bureau of Reclamation. 2012. Adaptive management of fall outflow for delta smelt protection and water supply reliability. U.S. Bureau of Reclamation, Sacramento, Calif.,

- http://deltacouncil.ca.gov/sites/default/files/documents/files/Revised_fall_X2_Adaptive_MgmtPlan_EVN_06_29_2012_final.pdf.
- U.S. Fish and Wildlife Service. 1993. Endangered and threatened wildlife and plants; determination of threatened status for the delta smelt. Federal Register 58:12854–12864.
- U.S. Fish and Wildlife Service. 2008. Formal Endangered Species Act consultation on the proposed coordinated operations of the Central Valley Project and State Water Project. Sacramento, Calif., U.S. Fish and Wildlife Service, 410 p., http://www.fws.gov/sfbaydelta/documents/swp-cvp_ops_bo_12-15_final_ocr.pdf.
- U.S. Fish and Wildlife Service. 2010. Endangered and threatened wildlife and plants; 12-month finding on a petition to reclassify the delta smelt from threatened to endangered throughout its range. Federal Register 75:17677–17680.
- Van Metre, P.C., J.W. Frey, M. Musgrove, N. Nakagaki, S. Qi, B.J. Mahler, M.E. Wiczorek, and D.T. Button. 2016. High nitrate concentrations in some Midwest United States streams in 2013 after the 2012 drought. Journal of Environmental Quality 45:1696-1704.
- Vanderstukken, M., N. Mazzeo, W. Van Colen, S.A. Declerck, and K. Muylaert. 2011. Biological control of phytoplankton by the subtropical submerged macrophytes *Egeria densa* and *Potamogeton illinoensis*: a mesocosm study. Freshwater Biology 56:1837-1849.
- Vroom, J., M. van der Wegen, R.C. Martyr-Koller, and L.V. Lucas. 2017. What determines water temperature dynamics in the San Francisco Bay-Delta system? Water Resources Research 53:9901-9921. <https://agupubs.onlinelibrary.wiley.com/doi/full/10.1002/2016WR020062>
- Wagner, R.W., M. Stacey, L.R. Brown, M. Dettinger. 2011. Statistical models of temperature in the Sacramento-San Joaquin Delta under climate-change scenarios and ecological implications. Estuaries and Coasts 34:544-556. <https://link.springer.com/article/10.1007/s12237-010-9369-z>
- Wang, J. 2007. Spawning, early life stages, and early life histories of the osmerids found in the Sacramento-San Joaquin Delta of California. Tracy Fish Facility Studies. United States Bureau of Reclamation. Volume 38. http://deltarevision.com/2007_docs/TracyReportsVolume38.pdf
- Wenger, A.S., J. Whinney, B. Taylor, and F. Kroon. 2016. The impact of individual and combined abiotic factors on daily otolith growth in a coral reef fish. Scientific Reports 6:28875.

- Whipple, A., R. Grossinger, D. Rankin, B. Stanford, and R. Askevold. 2012. Sacramento-San Joaquin Delta historical ecology investigation: Exploring pattern and process. Richmond, Calif., San Francisco Estuary Institute, 225 p., available at: <http://www.sfei.org/DeltaHEStudy>.
- Wilcock, R.J., P.D. Champion, J.W. Nagels, and G.F. Croker. 1999. The influence of aquatic macrophytes on the hydraulic and physico-chemical properties of a New Zealand lowland stream. *Hydrobiologia* 416:203-214.
- Wilkerson F.P., R.C. Dugdale, V.E. Hogue, and A. Marchi. 2006. Phytoplankton blooms and nitrogen productivity in San Francisco Bay. *Estuaries and Coasts* 29:401–416.
- Winder, M. and A.D. Jassby. 2011. Shifts in zooplankton community structure: Implications for food web processes in the Upper San Francisco Estuary. *Estuaries and Coasts* 34:675-690.
- Yarrow, M., V.H. Marin, M. Finlayson, A. Tironi, L.E. Delgado, and F. Fischer. 2009. The ecology of *Egeria densa* Planchon (Liliopsida: alismatales): A wetland ecosystem engineer?. *Revista Chilena de Historia Natural* 82(2).
- Zanchett, G., and E. Oliveira-Filho. 2013. Cyanobacteria and cyanotoxins: From impacts on aquatic ecosystems and human health to anticarcinogenic effects. *Toxins* 5:1896.
- Zegura, B., A. Straser, and M. Filipic. 2011. Genotoxicity and potential carcinogenicity of cyanobacterial toxins – a review. *Mutation Research/Reviews in Mutation Research* 727:16-41.

Appendices

Appendix 1: Enhanced Delta Smelt Monitoring

Denise Barnard, U.S. Fish and Wildlife Service

Appendix 2: Modeling of Physical Habitat

Michael MacWilliams and Aaron Bever, Anchor QEA, LLC

Appendix 3: Environmental Variables

Steven Slater, California Department of Fish and Wildlife

Appendix 4: Phytoplankton

Jared Frantzich and Peggy Lehman, California Department of Water Resources

Appendix 5: Cyanobacteria Harmful Algal Blooms

Peggy Lehman, California Department of Water Resources

Appendix 6: Zooplankton

April Hennessy, California Department of Fish and Wildlife

Appendix 7: Clams

Janet Thompson, U.S. Geological Survey

Appendix 8: Aquatic Vegetation

Louise Conrad, Delta Science Program, and Shruti Khanna, California Department of Fish and Wildlife

Appendix 9: Fish Assemblages

Brian Mahardja, U.S. Fish and Wildlife Service

Appendix 10: Mississippi Silversides

Brian Mahardja, U.S. Fish and Wildlife Service

Appendix 11: Survival and Population Growth

Steven Slater, California Department of Fish and Wildlife and Gonzalo Castillo, U.S. Fish and Wildlife Service